THE HENRYK NIEWODNICZAŃSKI
INSTITUTE OF NUCLEAR PHYSICS
POLISH ACADEMY OF SCIENCES

TEMPORAL NONLOCALITY IN EVOLUTION EQUATIONS: CHARACTERIZATION OF WAVE AND DIFFUSION PROPERTIES

Author

mgr inż. Tobiasz Pietrzak

Supervisor

prof. dr hab. Katarzyna Górska

A thesis submitted for the degree of Doctor of Philosophy

September 2025

Acknowledgments

I want to express my deepest gratitude to my supervisor, Prof. Katarzyna Górska, for her exceptional guidance, unwavering support, and insightful discussions throughout my PhD journey. Her encouragement, dedication, and passion for mathematical physics have been a constant source of inspiration. Her constructive feedback has profoundly shaped both my research and my development as a scientist. I am truly grateful for her patience, mentorship, and for always motivating me to explore new ideas and perspectives in the field of mathematical physics. I also want to thank Prof. Andrzej Horzela for the fruitful collaboration in our joint research. His expertise, insightful suggestions, and inspiring discussions greatly enriched my work and made our scientific teamwork a truly rewarding experience.

I am grateful to Prof. Živorad Tomovski, Prof. Trifce Sandev, Prof. Ralf Metzler, and Prof. Ljupčo Kocarev, for their collaboration, valuable insights, and constructive feedback on our publications. I would like to give special thanks to Prof. Trifce Sandev for giving me the opportunity to undertake a research visit under his supervision, which was an immensely valuable and inspiring experience.

This research was made possible thanks to the financial support from the National Science Centre (NCN) and the National Agency for Academic Exchange (NAWA) within the Preludium Bis 2 program.

Finally, I am profoundly grateful to my family and loved ones for their unwavering support. My parents, Anna and Waldemar, my brother, Piotr, and my grandparents have always believed in me and supported me in following my path. I am also grateful to my friends for their support and for the positive moments we shared along the way. Above all, I am deeply thankful to my beloved Monika for her love, patience, and constant support. Her presence has been a source of strength and joy throughout this journey. I could not have completed this PhD without all of you. Thank you for always being there.

Abstract

In theoretical physics, many fundamental evolution equations assume temporal locality, meaning that a system's future state depends solely on its present state. However, numerous processes require modeling memory effects, where past states influence future evolution. The first approaches to such memory-dependent processes were introduced over 150 years ago. Over time, mathematical modeling of processes with memory has evolved, encompassing integro-differential equations and fractional calculus, whose nonlocal operators inherently account for the history of the system. Fractional-order models are often more accurate than integer-order counterparts due to their additional degrees of freedom, making them applicable across physics, chemistry, biology, control theory, and engineering. The core focus of this dissertation is the analysis of memory-dependent dynamical systems, with particular emphasis on the generalized telegraph equation subjected to an external moving harmonic source. The generalized telegraph equation incorporates nonlocal time derivatives through memory functions that modify both the first- and second-order time derivatives, allowing the description of hereditary effects in wave propagation. The research demonstrates the emergence of Doppler-like frequency shifts in the presence of moving sources, showing that the interaction between wave propagation and memory functions can generate velocity-dependent spectral modifications, even in the absence of a sharp wavefront. Three representative memory scenarios are analyzed: localized, power-law, and mixed, revealing that the presence of a wavefront amplifies the observable frequency shift, whereas purely power-law memory still induces subtle but measurable spectral changes. These results provide new insights into the interplay between wave propagation and nonlocal temporal behavior in generalized transport processes. In addition to the telegraph equation, the dissertation addresses the generalized Fokker-Planck equation with fading memory and the generalized Langevin equation. Analytical solutions using the distributed-order memory kernel and Volterra-Prabhakar memory kernel ensure physically meaningful results. Anomalous diffusion phenomena, such as subdiffusion, superdiffusion, and ultraslow diffusion, are analyzed under different internal noise and friction kernels, highlighting the role of memory in shaping complex dynamical behavior.

Streszczenie

W fizyce teoretycznej wiele podstawowych równań ewolucyjnych zakłada lokalność procesu w czasie, co oznacza, że przyszły stan układu zależy wyłącznie od jego stanu obecnego. Jednakże istnieją procesy wymagające modelowania efektów pamięciowych, w których przeszłe stany wpływają na przyszłą ewolucję. Pierwsze podejścia do tego typu procesów zależnych od pamięci zostało wprowadzone ponad 150 lat temu. Z biegiem czasu modelowanie matematyczne procesów z pamięcią ewoluowało, obejmując równania całkowo-różniczkowe i rachunek ułamkowy, których operatory nielokalne z natury uwzględniają historię układu. Modele rzędu ułamkowego są często dokładniejsze niż ich odpowiedniki rzędu całkowitego ze względu na dodatkowe stopnie swobody, dzięki czemu mają zastosowanie w fizyce, chemii, biologii, teorii sterowania czy inżynierii. Głównym przedmiotem niniejszej rozprawy jest analiza systemów dynamicznych zależnych od pamięci, ze szczególnym uwzględnieniem uogólnionego równania telegraficznego poddanego działaniu zewnętrznego ruchomego źródła harmonicznego. Uogólnione równanie telegraficzne uwzględnia nielokalne pochodne czasowe poprzez funkcje pamięci, które modyfikują zarówno pochodne czasowe pierwszego, jak i drugiego rzędu, umożliwiając opis efektów pamięci w propagacji fal. Badania wykazują pojawienie się przesunięć częstotliwości podobnych do efektu Dopplera w obecności ruchomych źródeł, pokazując, że interakcja między propagacją fal a funkcjami pamięci może generować modyfikacje spektralne zależne od prędkości, nawet przy braku ostrego czoła fali. Przeanalizowano trzy reprezentatywne scenariusze pamięci: zlokalizowany, potęgowy i mieszany, ujawniając, że obecność czoła fali wzmacnia obserwowalne przesunięcie częstotliwości, podczas gdy pamięć czysto potęgowa nadal wywołuje subtelne, ale mierzalne zmiany spektralne. Wyniki te dostarczają nowych informacji na temat wzajemnego oddziaływania między propagacją fal a nielokalnym zachowaniem czasowym w uogólnionych procesach transportu. Oprócz równania telegraficznego, rozprawa dotyczy uogólnionego równania Fokkera-Plancka z zanikającą pamięcią oraz uogólnionego równania Langevina. Rozwiązania analityczne wykorzystujące jądra pamięci o rozłożonym rzędzie i Volterra-Prabhakara zapewniają wyniki mające znaczenie fizyczne. Zjawiska dyfuzji anomalnej, takie jak subdyfuzja, superdyfuzja i ultrapowolna dyfuzja, są analizowane pod kątem różnych jąder szumu i tarcia, podkreślając rolę pamięci w kształtowaniu złożonych zachowań dynamicznych.

Contents

1. Introduction

In theoretical physics, many of the fundamental equations of evolution that describe changes in a dynamical system over time have a built-in assumption that the process they describe is local in time, i.e. that the future state of the system is independent of past states and is determined only by the present state of that system. However, it is possible to identify several processes for which creating a more realistic model requires denying the assumption of temporal locality and including past states of the system in the model. Moreover, in certain problems, it is essential to account for the dependence on past states. The first physical models that took into account the need to analyze the history of states of a given system in the context of predicting its future behavior appeared about 150 years ago. Pioneering in this field of research was the work of scientists such as Boltzmann [1], Meyer [2], and Wiechert [3]. The need to formulate a mathematical theory of heredity (processes with memory) was recognized by the prominent French mathematician Charles-Émile Picard, who wrote in the ICM conference proceedings [4] published in 1908,

"*Il ne faut pas cependant réduire à l'avance notre conception mathématique du monde, et nous pouvons rêver d'équations fonctionnelles plus compliquées que les précédentes parce qu'elles renfermeront en outre des intégrales prises entre un temps passé très éloigné et le temps actuel, intégrales qui apporteront la part de l'hérédité.*"[1]

This need was also recognized by the Italian mathematician and physicist Vito Volterra whose work [5, 6, 7] was a milestone in the mathematical theory of processes with memory. Over the past hundred and fifty years, there have been significant developments in theory describing phenomena

[1]However, we must not reduce our matematical conception of the world in advance, and we can dream of functional equations more complicated than the previous ones because they will also contain integrals taken between a very distant past time and the present time, integrals which will bring in the part of heredity.

with memory. The modeling of effects of this type has found wide application not only in physics but also in chemistry, control theory, medicine, biology, economics as well as information theory [8, 9, 10, 11, 12, 13, 14]. In contemporary scientific research, integro-differential equations are extensively utilized to characterize processes with memory. These equations encompass a significant category known as fractional calculus, which entails derivatives and integrals of non-integer orders. The implementation of fractional calculus has become an indispensable tool for the precise modeling of memory-dependent phenomena. The fractional calculus itself is almost as old as the classical differential calculus. The first mention of the derivative of non-integer order appears in correspondence between Leibniz and L'Hospital in 1695 [15]. The rapid development of the theory occurred in the nineteenth century. Today, the applications of fractional calculus are ubiquitous. It is fair to assert that virtually no discipline within modern engineering and science remains unaffected by the tools and techniques of fractional calculus [16, 17, 18, 19, 20, 21, 22, 23, 24, 25, 26, 27]. In fact, one could argue that real-world processes are generally fractional-order systems. The primary reason for the successful application of fractional calculus lies in the fact that fractional-order models often prove to be more accurate than their integer-order counterparts. This advantage stems from the additional degrees of freedom present in fractional-order models compared to classical models. One of the fascinating aspects of fractional calculus is that fractional derivatives are inherently nonlocal quantities. Fractional operators consider the entire history of the process under analysis, enabling the modeling of nonlocal and distributed effects that are commonly observed in nature and technology.

In the dissertation, I present my research on theoretical physics equations and mathematical objects that can be used to model physical processes with memory. The work is theoretical however, it is strongly motivated by practical applications of such models. In my work, I considered the problem of frequency shift in the solutions of the generalized telegraph equation with an external moving point-wise harmonic source. I was also involved in the study of solutions to the generalized Fokker-Planck equation with fading memories. I also dealt with the generalized Langevin equation in the context of anomalous diffusion for a harmonic oscillator and a free particle driven by various internal noises. From a formal perspective, my dissertation comprises a collection of four interrelated research articles. These articles collectively contribute to a comprehensive understanding of the chosen research area, each addressing different facets and aspects crucial for a holistic analysis. The list of articles is presented below:

- T. Pietrzak, A. Horzela, K. Górska
  The generalized telegraph equation with moving harmonic source: Solvability using the integral decomposition technique and wave aspects
  International Journal of Heat and Mass Transfer **225**, 125373 (2024)

- T. Pietrzak, A. Horzela, K. Górska, L. Kocarev
  Can the Doppler be useful for a benchmark analysis of the wave-like properties of memory-dependent telegraphers' equation
  Chaos **35**, 023134 (2025)

- K. Górska, T. Pietrzak, T. Sandev, Z. Tomovski
  Volterra-Prabhakar function of distributed order and some applications
  Journal of Computational and Applied Mathematics **433**, 115306 (2023)

- Z. Tomovski, K. Górska, T. Pietrzak, R. Metzler, T. Sandev
  Anomalous and ultraslow diffusion of a particle driven by power-law-correlated and distributed-order noises
  Journal of Physics A: Mathematical and Theoretical **57**, 235004 (2024)

The first paper from the list above explored the frequency shift in the solution of the generalized telegraph equation with a moving point-wise harmonic source. The equation incorporates nonlocal time derivatives, represented by memory functions η and γ, where η modifies the second time-derivative, and γ alters the first one. By employing integral decomposition, we solve the generalized telegraph equation with an external source, allowing the solution to be written as the product of the solution to the telegrapher's equation with a harmonic source and a function $f_{\hat{\gamma}}$ depending on the Laplace transform of the memory function γ. The solution exhibits a frequency shift, demonstrated through three examples of memory functions: the localized case, a mixture with a power-law, and the power-law case alone. The results show that only the first two cases display a wavefront and a Doppler-like shift. The third example, although lacking wavefronts, also shows a frequency shift. This indicates that the frequency shift occurs regardless of the presence of a wavefront, but it is more pronounced when a wavefront exists. The second article also considers a generalized telegraph equation with the loss term included. The study investigates the telegraph equation perturbed by a uniformly moving external harmonic impact, seeking to distinguish properties of time evolution patterns in memoryless versus memory-dependent modeling of transport phenomena. This generalized telegraph equation is solved for initial conditions that determine the values of the solution and its time derivative at the initial moment, and boundary conditions that require the solution to vanish at spatial infinity or the boundaries of a finite interval. The key question is which solutions are classified as traveling or standing waves. To answer this, we consider the Doppler effect and investigate how the frequency and velocity of the external source influence the obtained solutions. Utilizing the short-time Fourier transform, we push the problem further, showing that solutions in the infinite domain to the generalized telegraph equation, illustrated by a model example involving Caputo fractional derivatives ${}^{C}D^{2\alpha}$ and ${}^{C}D^{\alpha}$ with $0 < \alpha \leq 1$, exhibit a velocity-dependent Doppler-like frequency shift if $\frac{1}{2} < \alpha \leq 1$. This effect remains unnoticed if $0 < \alpha \leq \frac{1}{2}$. The third paper examines the exact solution of two types of generalized Fokker-Planck equations, where the integral kernels are either the distributed-order function or the distributed-order Prabhakar function. Both integral kernels are referred to as fading memory functions and are classified as Stieltjes functions. It is demonstrated that their Stieltjes nature is sufficient to ensure the non-negativity of the mean-square values and higher even moments, while the odd moments vanish. Consequently, solutions to the generalized Fokker-Planck equations can be considered probability density functions. Additionally, the Volterra-Prabhakar function and its generalization were introduced. The final article examines an approach to anomalous diffusion based on a generalized Langevin equation for a harmonic oscillator and a free particle driven by various internal noises, such as power-law noise and diffuse order noise, that satisfy generalized versions of the fluctuation-dissipation theorem. In this work, the mean squared displacement and normalized displacement correlation function are determined for different forms of friction memory kernel. In addition, the corresponding damped generalized Langevin equation for these scenarios is studied. The results of this work demonstrate that such models effectively describe anomalous diffusion in complex media, leading to subdiffusion, superdiffusion, ultraslow diffusion, strong anomalies, and other intricate diffusive behaviors. More detailed information on the problems analyzed in the above papers, as well as the mathematical tools used, will be provided later in this dissertation.

2. Basic aspects of diffusion theory

2.1 Historical outline on diffusion

The results that are the basis of my doctoral thesis mainly concern the description of the anomalous diffusion process and its properties. The term diffusion in physics is derived from the Latin word *diffusio* which can be translated as *spreading* and refers to molecular diffusion. This process involves the random motion of molecules, which leads to the transport of matter from regions of higher concentration to regions of lower concentration. At a temperature above absolute zero, the molecules of a substance move continuously and randomly, independently of each other. There are frequent collisions between particles, making the path of a single particle zigzag. Yet a collection of diffusing particles exhibits an observable drift from areas of higher concentration to areas of lower concentration. This justifies calling diffusion a transport process [28]. The first systematic experimental examination of diffusion was conducted by Thomas Graham [29]. He measured the rate of gases diffusing through gypsum plugs, through very thin pipes and through small holes. With these types of experiments, he was able to slow down the process and study it quantitatively. Based on the results, he was able to formulate a law for the rate of gas effusion known today as Graham's law. In 1855, German physician Adolf Fick published a paper [30] in which he proposed laws describing diffusion. Fick's first law introduces the relation between the diffusion flux $\mathbf{j}$[1] and the concentration gradient. This law can be written as

$$\mathbf{j} = -D\nabla\varphi \tag{2.1}$$

where D is the diffusion coefficient and φ is the concentration. This general law applies to both gases and liquids, as well as solids. Fick's second law predicts how diffusion causes concentration to change locally over time. This

[1] In the text, symbols describing vector quantities will be marked in bold.

law can be derived from Fick's first law and the law of conservation of mass and takes the form of the diffusion equation, which, assuming a constant diffusion coefficient, is of the form

$$\frac{\partial \varphi}{\partial t} = D\nabla^2\varphi. \tag{2.2}$$

In formulating his laws, Fick was inspired by the work of the French mathematician Jean-Baptiste Joseph Fourier on thermal conductivity. The extension of diffusion studies to solids was done by British metallurgist and former Graham's assistant William Roberts-Austen [31]. His work involved measuring the diffusivity of precious metals such as gold and platinum in liquid lead. The modern atomistic theory of diffusion and Brownian motion was developed after 1900 and will be described in more detail below.

2.2 Description of Brownian motion

The observation of zigzag paths that are the tracks of particles suspended in a liquid so characteristic of the diffusion process was probably first described by the Roman poet Titus Lucretius Carus in his work *The Nature of Things* [32]. The phenomenon described by Lucretius was later named Brownian motion after the Scottish biologist Robert Brown who described it accurately [33] in 1827. Observing pollen in an aqueous suspension through a microscope, he noticed that it was in constant, chaotic motion. Later studies showed that the nature of Brownian motion is independent of the properties of the substance of which the particles suspended in a liquid or gas are composed, while it is dependent on the properties of the medium (liquid or gas) in which the phenomenon occurs. It has been noted that the velocity of particles performing Brownian motion increases with increasing temperature and decreasing size of the particles. The properties of Brownian motion can be explained by assuming that the movements of suspended particles occur because of the impacts they receive from moving liquid or gas molecules. The obvious assumption is that each particle of the suspension is subjected to the impact of the molecules of the medium in which it is suspended from all sides. It is worth noting that in the case of disordered movement of the medium molecules, it can be expected that the number of hits of these molecules on the suspension particle from different sides should compensate and the particle should remain motionless. This is indeed the case when we are dealing with large suspension particles - when the size of the suspension particles is too large compared to the size of the medium particles, then the fluctuations in the liquid density on different sides of the suspension particle are too small to set the particles in motion. When the suspension particles are small, fluctuations in the density of the medium cause them to move. Since fluctuations are usually short-lived, the direction of the net force acting on the particle changes very quickly, and with it the direction of motion of the particles changes.

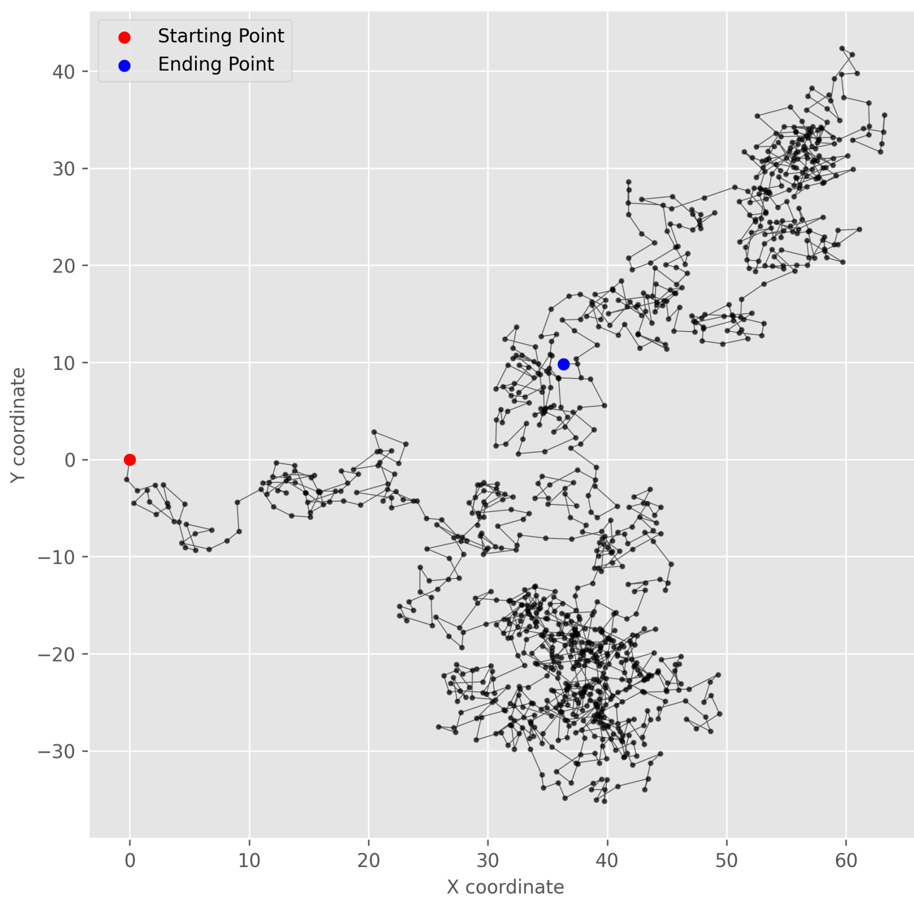

Figure 2.1: Simulation of 2D Brownian motion for a single particle

Although Brown described the phenomenon he observed, he did not explain it quantitatively. The quantitative theory was developed independently by Albert Einstein, Marian Smoluchowski, and Paul Langevin [34, 35, 36, 37]. Einstein's theory contains the derivation of the diffusion equation for Brownian particles, in which the resulting diffusion coefficient is related to the mean square displacement. In his approach to explaining Brownian motion, he considered an equation that we can write as

$$\varrho(x, t+\varepsilon) = \int_{-\infty}^{\infty} \varrho(x - x', t)\phi(x', \varepsilon)\,\mathrm{d}x', \tag{2.3}$$

where $\varrho(x, t)$ is the number of particles per unit volume with $x \in \mathbb{R}$ and $t > 0$ and $\phi(x', \varepsilon)\,\mathrm{d}x'$ is the probability of a particle moving from x' to $x' + \mathrm{d}x'$ during the time interval ε, and this is the so-called jumping probability. The function ϕ satisfies the conditions:

$$\int_{-\infty}^{\infty} \phi(x', \varepsilon)\,\mathrm{d}x' = 1 \quad \text{and} \quad \phi(x', \varepsilon) = \phi(-x', \varepsilon). \tag{2.4}$$

Using Taylor series expansion, for a sufficiently small ε the term $\varrho(x, t+\varepsilon)$ can be approximated as follows

$$\varrho(x, t+\varepsilon) = \varrho(x, t) + \frac{\partial \varrho(x, t)}{\partial t}\varepsilon. \tag{2.5}$$

Expanding the function $\varrho(x - x', t)$ to second-order terms and substituting into the right-hand side of equation (2.3), one gets the following

$$\begin{aligned}\int_{-\infty}^{\infty} \varrho(x - x', t)\phi(x', \varepsilon)\,\mathrm{d}x' = \varrho(x, t) &\int_{-\infty}^{\infty} \phi(x', \varepsilon)\,\mathrm{d}x' + \\ - \frac{\partial \varrho(x, t)}{\partial x} &\int_{-\infty}^{\infty} \phi(x', \varepsilon)x'\,\mathrm{d}x' + \\ + \frac{\partial^2 \varrho(x, t)}{\partial x^2} &\int_{-\infty}^{\infty} \phi(x', \varepsilon)\frac{x'^2}{2}\,\mathrm{d}x'.\end{aligned} \tag{2.6}$$

Using the conditions of (2.4), it can be seen that the term $\int_{-\infty}^{\infty} \phi(x', \varepsilon)x'\,\mathrm{d}x'$ vanishes, and the above expression can be simplified to the form

$$\int_{-\infty}^{\infty} \varrho(x - x', t)\phi(x', \varepsilon)\,\mathrm{d}x' = \varrho(x, t) + \frac{\partial^2 \varrho(x, t)}{\partial x^2} \int_{-\infty}^{\infty} \phi(x', \varepsilon)\frac{x'^2}{2}\,\mathrm{d}x'. \tag{2.7}$$

Substituting expressions (2.5) and (2.7) into equation (2.3) one gets

$$\frac{\partial \varrho(x, t)}{\partial t} = D\frac{\partial^2 \varrho(x, t)}{\partial x^2}, \tag{2.8}$$

and

$$D = \frac{1}{2\varepsilon}\int_{-\infty}^{\infty}\phi(x',\varepsilon)x'^2\,\mathrm{d}x'. \tag{2.9}$$

Equation (2.8) is a diffusion equation with the coefficient D defined as the second moment of the probability distribution. Assuming that $\varrho(x,0)=\delta(x)$ and the solution vanishes at $\pm\infty$, then the solution to equation (2.8) takes the form of

$$\varrho(x,t) = \frac{1}{\sqrt{4\pi Dt}}\exp\Big(\frac{-x^2}{4Dt}\Big), \quad x\in\mathbb{R} \quad \text{and} \quad t>0. \tag{2.10}$$

The obtained solution made it possible to calculate the moments of the distribution directly. The first moment is zero, which means that the particle is just as likely to move one way as the other. The second moment does not vanish and is defined as

$$\langle x^2\rangle = 2Dt. \tag{2.11}$$

Equation (2.11) expresses the mean squared displacement with time and diffusion coefficient. Based on the result obtained, Einstein concluded that the mean squared displacement is not proportional to the elapsed time, but rather to its square root. Moreover, in his work he obtained a relationship linking the diffusion coefficient to other measurable physical quantities. The result he obtained makes it possible to experimentally determine the Avogadro number and thus the size of the particles. The theory of Brownian motion proposed by Smoluchowski starts from the same assumption as the theory described above and introduces the same probability distribution (2.3) leading to the same expression for mean squared displacement as in Einstein's theory. Both Smoluchowski's and Einstein's theories assume independence of displacement, the process is considered Markovian.

The approach used by Langevin to describe Brownian motion was significantly different from that proposed by Smoluchowski and Einstein, see [37]. He applied Newton's second law of motion to a single Brownian particle. This equation can be written in the following form

$$m\frac{d^2\mathbf{r}}{dt^2} = \mathbf{F} - 6\pi\eta R\mathbf{v}, \tag{2.12}$$

where $\mathbf{F}$ is the force occurring due to the chance difference between the number of impacts of the particles on the suspension particle from different directions, and a viscous resistance is given by $-6\pi\eta R\mathbf{v}$ with $\mathbf{v}$ is the velocity of the particle of radius R. The internal friction coefficient of the medium is denoted by η. For an arbitrary axis of the rectangular coordinate system (let it be the x-axis), equation (2.12) can be written as

$$m\frac{d^2x}{dt^2} = F_x - 6\pi\eta R\frac{dx}{dt}. \tag{2.13}$$

Multiplying the above equation by x and applying elementary transformations, one can write it in the form of

$$\frac{1}{2}m\frac{d^2x^2}{dt^2} - m\Big(\frac{dx}{dt}\Big)^2 = xF_x - 3\pi\eta R\frac{d}{dt}x^2. \tag{2.14}$$

Equation (2.14) will also apply to mean values as long as averaging is performed for a sufficiently large number of particles. For mean values it will take the form

$$\frac{1}{2}m\frac{d^2\langle x^2\rangle}{dt^2} - m\Big\langle\Big(\frac{dx}{dt}\Big)^2\Big\rangle = \langle xF_x\rangle - 3\pi\eta R\frac{d}{dt}\langle x^2\rangle. \tag{2.15}$$

Assuming that there is

$$\Big\langle\Big(\frac{dx}{dt}\Big)^2\Big\rangle = \frac{1}{3}\langle v^2\rangle \quad \text{and} \quad \langle xF_x\rangle = 0 \tag{2.16}$$

one can rewrite equation (2.15) in the form

$$\frac{1}{2}m\frac{d^2\langle x^2\rangle}{dt^2} - \frac{1}{3}m\langle v^2\rangle = -3\pi\eta R\frac{d}{dt}\langle x^2\rangle. \tag{2.17}$$

Using the equipartition theorem, the above equation can be transformed to the following form

$$\frac{1}{2}m\frac{d\xi}{dt} + 3\pi\eta R\xi = k_BT \tag{2.18}$$

where

$$\xi = \frac{d\langle x^2\rangle}{dt}, \tag{2.19}$$

and k_B is the Boltzmann constant, and T is the temperature. The solution to equation (2.18) with the condition $\xi(0) = 0$ is

$$\xi = \frac{k_BT}{3\pi\eta R}\Big[1 - \exp\Big(-\frac{6\pi\eta R}{m}t\Big)\Big]. \tag{2.20}$$

Although the time interval between two consecutive observations of the suspended particle is rather small, based on an analysis of the actual values of the quantities η, R and m, the exponential expression in the solution of (2.20) can be neglected. Then (2.20) reduces to

$$\xi = \frac{k_B T}{3\pi\eta R} \quad \text{which leads to} \quad \langle x^2 \rangle = \frac{k_B T}{3\pi\eta R} t, \tag{2.21}$$

which is the same result as that obtained by Einstein. This result indicates the normal diffusion behavior of the process considered.

2.3 Anomalous diffusion

The diffusion equation (2.8) implies a linear dependence of the mean squared displacement on time. One may ask whether such a relation is always satisfied. The first experiment that showed that this relationship is not always linear was performed in 1926 by Levis Fry Richardson [38]. He studied diffusion in turbulent flow, for which he observed a nonlinear increase in mean squared displacement. Based on the results obtained, he concluded that

$$\langle x^2 \rangle \propto t^3. \tag{2.22}$$

Introducing the general dependence of mean squared displacement on time in the form

$$\langle x^2 \rangle \propto t^\alpha, \tag{2.23}$$

where α is a positive real number, allows the classification of the diffusion process. We say that diffusion is normal if $\alpha = 1$ and anomalous when $\alpha \neq 1$. Moreover, in the case when $\alpha < 1$, then the process is called subdiffusion and in the case when $\alpha \in (1, 2)$ then such a process is called superdiffusion. For $\alpha = 2$ the process is called ballistic motion and for $\alpha > 2$ it is called superballistic motion. Since the experiment conducted by Richardson, examples of the occurrence of anomalous diffusion have been found in various scientific fields like: quantum optics [39], astrophysics [40], biophysics [41], materials science [42], or soft matter physics [43].

One of the ways to describe anomalous diffusion is to use the so-called generalized diffusion equation [44]. This equation can be derived from the Continuous-Time Random Walk (CTRW) theory proposed in 1965 by Elliott Montroll and George Weiss [45]. The theory introduces a stochastic process in which important aspects are waiting time g and jump length λ distributions defined as follows:

$$g(t) = \int_{-\infty}^{\infty} \psi(x,t)\,\mathrm{d}x, \tag{2.24}$$

$$\lambda(x) = \int_{0}^{\infty} \psi(x,t)\,\mathrm{d}t, \tag{2.25}$$

where ψ is a joint probability distribution of jump length and waiting time. Let's introduce the probability p that the particle will reach position x in the time between t and $t + \mathrm{d}t$

$$p(x,t) = \delta(x)\delta(t) + \int_{-\infty}^{\infty} \left[\int_{0}^{t} p(x',t')\psi(x-x',t-t')\,\mathrm{d}t' \right] \mathrm{d}x', \tag{2.26}$$

where the first term of the expression on the right-hand side refers to the initial conditions of the random walk. The distribution of the probability that a particle at time t will be at position x is given by the expression

$$\varrho(x,t) = \int_{0}^{t} p(x,t')\Phi(t-t')\,\mathrm{d}t', \tag{2.27}$$

where Φ is the probability that the particle will remain in the same position after a given waiting time. Substituting $p(x,t)$ from equation (2.26) into equation (2.27), we get

$$\varrho(x,t) = \delta(x)\Phi(t) + \int_{-\infty}^{\infty} \left[\int_{0}^{t} p(x',t')\psi(x-x',t-t')\,\mathrm{d}t' \right] \mathrm{d}x'. \tag{2.28}$$

Applying the joint Laplace-Fourier transform[2] to equation (2.28), one gets

$$\tilde{\hat{\varrho}}(k,s) = \frac{\hat{\Phi}(s)}{1 - \tilde{\hat{\psi}}(k,s)}. \tag{2.29}$$

[2]The joint Laplace-Fourier transform of the f function is defined as

$$\mathfrak{LF}[f(x,t)] = \tilde{\hat{f}}(k,s) = \int_{-\infty}^{\infty} \mathrm{e}^{-\,\mathrm{i}kx} \left[\int_{0}^{\infty} f(x,t)\,\mathrm{e}^{-st}\,\mathrm{d}t \right] \mathrm{d}x.$$

If one considers the probability that a particle makes a jump of length x during the time interval t to $t + dt$, then the following relation holds

$$\Phi(t) = 1 - \int_0^t g(t')\,\mathrm{d}t'. \tag{2.30}$$

Determining the Laplace transform from (2.30) and substituting the result into expression (2.29), one obtains

$$\tilde{\hat{\varrho}}(k,s) = \frac{1-\hat{g}(s)}{s}\frac{1}{1-\tilde{\hat{\psi}}(k,s)}. \tag{2.31}$$

Consider the case when g and λ are independent random variables. In this situation, the joint probability distribution factorizes as:

$$\tilde{\hat{\psi}}(k,s) = \hat{g}(s)\tilde{\lambda}(k). \tag{2.32}$$

Introducing a generalized waiting time probability density function whose Laplace transform is of the form

$$\hat{g}(s) = \frac{1}{1+s\hat{\gamma}(s)} \tag{2.33}$$

with the conditions:

$$\lim_{t\to\infty}\gamma(t) = \lim_{s\to 0} s\hat{\gamma}(s) = 0 \tag{2.34}$$

and Gaussian probability density function for the distribution of jump lengths whose Fourier transform for small values of k and $\langle x^2(t)\rangle = 2$ can be taken as [46]

$$\tilde{\lambda}(k) = 1 - k^2. \tag{2.35}$$

Using (2.33) and (2.35), we can write the expression (2.31) in the form

$$\tilde{\hat{\varrho}}(k,s) = \frac{\hat{\gamma}(s)}{s\hat{\gamma}(s)+k^2}, \tag{2.36}$$

which is equivalent to the equation

$$\hat{\gamma}(s)[s\tilde{\hat{\varrho}}(k,s) - 1] = -k^2\tilde{\hat{\varrho}}(k,s). \tag{2.37}$$

Applying the inverse Laplace-Fourier transform to (2.37), we get the generalized diffusion equation

$$\int_0^t \gamma(t-\chi)\frac{\partial\varrho(x,\chi)}{\partial\chi}\,\mathrm{d}\chi = \frac{\partial^2\varrho(x,t)}{\partial x^2}, \tag{2.38}$$

where the integral kernel γ encodes time nonlocality, which can be interpreted as a memory.

It is worth mentioning that from a mathematical point of view, to guarantee a well-posed Cauchy problem [47] for (2.38), the function γ should be a Sonin function [48]. Thus, there should be a function ζ called Sonin's partner such that the convolution of these two functions satisfies the condition $(\gamma * \zeta)(t) = 1$. Furthermore, it is then possible to write an equation equivalent to equation (2.38) in the form

$$\frac{\partial \varrho(x,t)}{\partial t} = \frac{\mathrm{d}}{\mathrm{d}t} \int_0^t \zeta(t-\chi) \frac{\partial^2 \varrho(x,\chi)}{\partial x^2} \, \mathrm{d}\chi. \tag{2.39}$$

It can be shown [49] that the mean squared displacement associated with (2.38) depends on the memory kernel γ as follows

$$\langle x^2(t) \rangle = 2\mathfrak{L}^{-1}\left[\frac{s^{-2}}{\hat{\gamma}(s)}\right]. \tag{2.40}$$

Using relation (2.40), one can analyze the diffusion behavior for a given type of memory kernel. If one takes the memory kernel as $\gamma(t) = \delta(t)$, one gets the standard diffusion equation and the relation $\langle x^2(t) \rangle \propto t$. Another important case is the selection of a memory kernel in the form of a power-law

$$\gamma(t) = \frac{t^{-\alpha}}{\Gamma(1-\alpha)}, \tag{2.41}$$

where $\alpha \in (0,1)$ and Γ is the gamma function[3]. For such a choice of memory kernel, equation (2.38) can be written in the form

$${}^{C}D_t^{\alpha} \varrho(x,t) = \frac{\partial^2 \varrho(x,t)}{\partial x^2}, \tag{2.42}$$

where

$${}^{C}D_t^{\alpha} f(t) = \frac{1}{\Gamma(n-\alpha)} \int_0^t \frac{f^{(n)}(\xi)}{(t-\xi)^{\alpha+1-n}} \, \mathrm{d}\xi, \quad n-1 < \alpha < n \tag{2.43}$$

[3]The gamma function is defined by a convergent improper integral for complex numbers with a positive real part

$$\Gamma(z) = \int_0^{\infty} t^{z-1} \, \mathrm{e}^{-t} \, \mathrm{d}t.$$

is the Caputo fractional derivative [50]. The corresponding mean squared displacement shows subdiffusive behavior, namely $\langle x^2(t)\rangle \propto t^\alpha$.

Superdiffusive behavior arises when the particle's jump lengths are drawn from a stable Lévy distribution with a power-law tail and a divergent second moment [51]. The resulting stochastic process is known as Lévy flights. Various other types of memory kernels can also be considered, allowing for the modeling of anomalous diffusion behavior [44].

The other way to describe anomalous diffusion that is worth mentioning is to use the generalized Langevin equation. This equation can be written in the form [52]

$$m\ddot{x}(t) + m\int_0^t \mathfrak{z}(t-\chi)\dot{x}(\chi)\,\mathrm{d}\tau + \frac{dV(x)}{dx} = \xi(t), \quad \dot{x}(t) = v(t), \tag{2.44}$$

where $x(t)$ and $v(t)$ are the displacement of the particle and its velocity, respectively. In (2.44), $\mathfrak{z}$ stands for a friction kernel, V is the position-dependent external potential, and ξ is the time-dependent stochastically varying force. By using various forms of the $\mathfrak{z}$ memory kernel, in particular, the power-law type [53] and Mittag-Leffler[4] [54], it is possible to model anomalous diffusion for which, as already mentioned, mean squared displacement scales nonlinearly in time.

The solution (2.10) of the standard diffusion equation (2.8) shows that for $t > 0$ the value of this solution is positive and nonvanishing for any real value of x. In the context of particle transport, this means that the diffusion model allows for the possibility of particles traveling at arbitrarily high speeds [55]. One way to overcome this unphysical feature of the diffusion equation is to modify it to the so-called telegraph equation, which still preserves the essential diffusion properties, but which is also characterized by a limited propagation speed. The equation was first introduced by Oliver Heaviside in 1880 in the context of understanding of the physics of electrical impulse propagation in long cables [56]. On the ground of circuit theory, the telegraph equation can be obtained by analyzing an infinitesimally small section of

[4] The one-parameter Mittag-Leffler function is a complex-valued functions of a complex argument and can be defined as

$$E_\alpha(z) = \sum_{n=0}^{\infty} \frac{z^n}{\Gamma(\alpha n + 1)},$$

where α is a complex parameter with a positive real part.

telegraph wire (Fig. 2.2), which can be modeled as an electrical circuit consisting of a resistor of a given resistance $R\,\mathrm{d}x$ and an inductor of a given inductance $L\,\mathrm{d}x$. Let $I(x,t)$ and $U(x,t)$ denote the current through the circuit and the voltage, respectively. The change in voltage between the ends

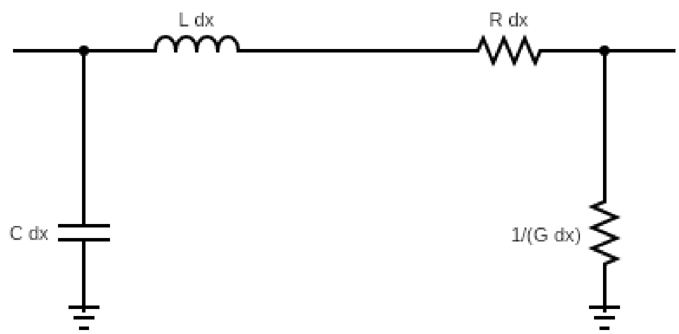

Figure 2.2: Infinitesimal piece of telegraph wire

of the piece of wire under consideration is

$$\mathrm{d}U = -IR\,\mathrm{d}x - \frac{\partial I}{\partial t}L\,\mathrm{d}x. \tag{2.45}$$

Let us additionally assume the possibility of losses, i.e., that current can escape from the wire to ground either through a resistor with a given conductivity $G\,\mathrm{d}x$ or through a capacitor with capacitance $C\,\mathrm{d}x$. The amount of current that escapes through the resistor is $UG\,\mathrm{d}x$, while through the capacitor is $(\partial_t U)C\,\mathrm{d}x$. In total, we have

$$\mathrm{d}I = -UG\,\mathrm{d}x - \frac{\partial U}{\partial t}C\,\mathrm{d}x. \tag{2.46}$$

Equations (2.45) and (2.46) can be written as

$$\begin{cases} \frac{\partial U(x,t)}{\partial x} + L\frac{\partial I(x,t)}{\partial t} + RI(x,t) = 0 \\ \frac{\partial I(x,t)}{\partial x} + C\frac{\partial U(x,t)}{\partial t} + GU(x,t) = 0. \end{cases} \tag{2.47}$$

Applying simple transformations to the above system, we obtain the telegraph equation (an analogous equation can be obtained for $I(x,t)$)

$$\frac{\partial^2 U(x,t)}{\partial t^2} + \left(\frac{G}{C} + \frac{R}{L}\right)\frac{\partial U(x,t)}{\partial t} + \frac{RG}{CL}U(x,t) = \frac{1}{LC}\frac{\partial^2 U(x,t)}{\partial x^2}. \tag{2.48}$$

The problem of infinite speed of propagation on the ground of transport theory was dealt with by Carlo Cattaneo [57] and Pierre Vernotte [58], who proposed a different constitutive equation for heat conduction in the form

$$\mathbf{j} + \tau \partial_t \mathbf{j} = -k \nabla T, \tag{2.49}$$

where $\tau > 0$ is called a thermal relaxation time and k is a thermal conductivity. Using (2.49) and the continuity equation, one gets the Cattaneo-Vernotte equation in the form

$$\partial_t^2 T + \tau^{-1} \partial_t T = a^2 \nabla T, \tag{2.50}$$

where a is a signal propagation speed. The form of this equation is the same as the form of the telegraph equation without leakage.

The Cattaneo-Vernotte equation can also be derived from the theory of Correlated Random Walk (CRW) [59]. In this process, also known as Persistent Random Walk (PRW), the transition probability depends on the direction of the previous step. Let $P(x,t)$ denote the probability that a particle subjected to a one-dimensional CRW starting at 0 will reach x at time t. Let $P_L(x,t)$ denote the probability that a particle will reach x from the left while $P_R(x,t)$ denotes the probability that a particle will reach x from the right. The relation

$$P(x,t) = P_L(x,t) + P_R(x,t) \tag{2.51}$$

is satisfied. In addition, let p_R denote the probability that the particle's next move will be to the right if the last move was also to the right, while $q_R = 1 - p_R$ denotes the probability that the particle's next move will be to the left if the last move was to the right. Similarly, let p_L denote the probability that the particle's next move will be to the left if the last move was also to the left, while $q_L = 1 - p_L$ denotes the probability that the particle's next move will be to the right if the last move was to the left. In addition, we assume that the particle takes steps of length Δx, and the time between two consecutive steps is Δt. Based on the above, one can write:

$$\begin{aligned} P_L(x, t+\Delta t) &= p_L P_L(x+\Delta x, t) + q_R P_R(x+\Delta x, t) \\ &= p_L[P(x+\Delta x, t) - P_R(x+\Delta x, t)] + q_R P_R(x+\Delta x, t) \\ &= p_L P(x+\Delta x, t) + (p_R - q_L) P_R(x+\Delta x, t), \end{aligned} \tag{2.52}$$

$$
\begin{aligned}
P_R(x, t+\Delta t) &= p_R P_R(x-\Delta x, t) + q_L P_L(x-\Delta x, t) \\
&= p_R[P(x-\Delta x, t) - P_L(x-\Delta x, t)] + q_L P_L(x-\Delta x, t) \\
&= p_R P(x-\Delta x, t) + (p_R - q_L) P_L(x-\Delta x, t).
\end{aligned}
\tag{2.53}
$$

In addition, there is a relation

$$
P_R(x+\Delta x, t) + P_L(x-\Delta x, t) = P(x, t-\Delta t). \tag{2.54}
$$

From (2.51), (2.52), (2.53), and (2.54) we have that

$$
P(x, t+\Delta t) = p_R P(x-\Delta x, t) + p_L P(x+\Delta x, t) - (p_R - q_L) P(x, t-\Delta t). \tag{2.55}
$$

Using the Taylor series expansion, one obtains:

$$
P(x, t+\Delta t) = P(x, t) + \Delta t \frac{\partial P}{\partial t} + \frac{1}{2}(\Delta t)^2 \frac{\partial^2 P}{\partial t^2} + o([\Delta t]^3), \tag{2.56}
$$

$$
P(x, t-\Delta t) = P(x, t) - \Delta t \frac{\partial P}{\partial t} + \frac{1}{2}(\Delta t)^2 \frac{\partial^2 P}{\partial t^2} + o([\Delta t]^3), \tag{2.57}
$$

$$
P(x+\Delta x, t) = P(x, t) + \Delta x \frac{\partial P}{\partial x} + \frac{1}{2}(\Delta x)^2 \frac{\partial^2 P}{\partial x^2} + o([\Delta x]^3), \tag{2.58}
$$

$$
P(x-\Delta x, t) = P(x, t) - \Delta x \frac{\partial P}{\partial x} + \frac{1}{2}(\Delta x)^2 \frac{\partial^2 P}{\partial x^2} + o([\Delta x]^3). \tag{2.59}
$$

Substituting the above into (2.55) and simplifying, we get

$$
\begin{aligned}
\frac{\partial^2 P}{\partial t^2} + \frac{2(q_R + q_L)}{(p_R + p_L)\Delta t} \frac{\partial P}{\partial t} = &\left(\frac{\Delta x}{\Delta t}\right)^2 \left[\frac{\partial^2 P}{\partial x^2} - \frac{2(p_R - p_L)}{(p_R + p_L)\Delta x} \frac{\partial P}{\partial x}\right] + \\
&+ o([\Delta t]) + o\left(\frac{[\Delta x]^3}{[\Delta t]^2}\right).
\end{aligned}
\tag{2.60}
$$

Assuming that $p_R = p_L = p$ and for $\Delta t, \Delta x \to 0$ we get

$$
\frac{\partial^2 P}{\partial t^2} + \frac{1}{\tau} \frac{\partial P}{\partial t} = a^2 \frac{\partial^2 P}{\partial x^2}, \tag{2.61}
$$

where a is the velocity of the particle and the constant τ is defined as

$$
\tau = \lim_{\Delta t \to 0} \frac{p \Delta t}{2(1-p)}. \tag{2.62}
$$

The obtained equation (2.61) is the Cattaneo-Vernotte equation in one spatial dimension.

It is known [55] that the mean squared displacement associated with the telegraph equation in the short time limit is proportional to the square of time, i.e., it describes ballistic motion. In contrast, in the long time limit, it depends linearly on time, which corresponds to normal diffusion. Obtaining a description of anomalous diffusion behavior using the Cattaneo-Vernotte equation requires its generalization. This can be done [60] by smearing the time derivatives in the standard equation as follows

$$\int_0^t \eta(t-\xi)\partial_\xi^2\varrho(x,\xi)\,\mathrm{d}\xi + \tau^{-1}\int_0^t \gamma(t-\xi)\partial_\xi\varrho(x,\xi)\,\mathrm{d}\xi = a^2\partial_x^2\varrho(x,t), \quad (2.63)$$

where η and γ are memory kernels. From a general point of view, the functions η and γ appearing in (2.63) could be any mutually independent well-behaved functions, however, as shown in [61], these functions must be coupled as follows

$$\eta(t) = \int_0^t \gamma(\xi)\gamma(t-\xi)d\xi. \quad (2.64)$$

The rationale for the above condition goes as follows. For a function f, of class at least C^2, whose derivative at zero vanishes, the smearing of its first derivative, denoted by ${}^{\mathfrak{s}}\partial$, is given by

$${}^{\mathfrak{s}}\partial_t f(t) = \int_0^t \gamma(t-\xi)\partial_\xi f(\xi)d\xi. \quad (2.65)$$

The smearing of the second derivative of this function is going to be given by

$$\begin{aligned}
&{}^{\mathfrak{s}}\partial_t\big({}^{\mathfrak{s}}\partial_t f\big)(t) = \int_0^t \gamma(t-t_1)\partial_{t_1}[{}^{\mathfrak{s}}\partial_{t_1} f(t_1)]dt_1 \\
&= \int_0^t \gamma(t-t_1)\partial_{t_1}\Big[\int_0^{t_1} \gamma(t_1-t_2)\partial_{t_2} f(t_2)dt_2\Big]dt_1 \\
&= \int_0^t \gamma(t-t_1)\Big[\gamma(0)\partial_{t_1} f(t_1) + \int_0^{t_1} \partial_{t_1}\Big(\gamma(t_1-t_2)\partial_{t_2} f(t_2)\Big)dt_2\Big]dt_1 \qquad (2.66)\\
&= \int_0^t \Big[\gamma(t-t_1)\gamma(t_1)f'(0) + \int_0^{t_1} \gamma(t-t_1)\gamma(t_1-t_2)\partial_{t_2}^2 f(t_2)dt_2\Big]dt_1 \\
&= \int_0^t \Big[\int_0^{t_1} \gamma(t-t_1)\gamma(t_1-t_2)\partial_{t_2}^2 f(t_2)dt_2\Big]dt_1.
\end{aligned}$$

Introducing the variable $\xi = t - t_1$ we obtain the following

$$ {}^{\mathfrak{s}}\partial_t\big({}^{\mathfrak{s}}\partial_t f\big)(t) = \int_0^t \Big[\int_0^{t-t_2} \gamma(\xi)\gamma(t - t_2 - \xi)d\xi\Big]\partial^2_{t_2} f(t_2)dt_2. \tag{2.67} $$

from which the relation (2.64) arises. The generalized telegraph equation is not only used in describing anomalous diffusion [62, 63, 64, 65] but can also be used in modeling thermoelasticity [20], describing chemical reactions [66, 67], and biological phenomena [68].

The next section will present details of the results of my research work, which can be found in the papers mentioned in the introduction.

3. Generalized evolution equations with memory

3.1 Wave properties and the Doppler-like effect in the Generalized Telegraph Equations

The telegraph equation is classified as a dissipative wave equation, i.e. a wave equation with damping. Accordingly, its solutions are expected to exhibit fundamental characteristics of mechanical wave phenomena, including the formation of wave fronts and the manifestation of the Doppler effect. This has been rigorously demonstrated in [69]. In [70, 71], the same authors investigated the effects of incorporating fractional time derivatives into the telegraph equation in (1+1)- and (2+1)-dimensional spacetime under the action of a moving time-harmonic source. They examined two specific classes of models: the so-called *wave-type* case, which involves fractional time derivatives of order $1 \leq \alpha < 2$ in addition to the classical second-order time derivative, and the *heat-type* case, which includes only fractional time derivatives of order $1 \leq \alpha < 2$. Their analysis revealed that the *wave-type* formulation retains the classical wave properties mentioned earlier, whereas the *heat-type* formulation does not.

In the paper *The generalized telegraph equation with moving harmonic source: Solvability using the integral decomposition technique and wave aspects* [60], a generalized telegraph equation (GTE) with a uniformly moving point-wise harmonic source was proposed in the form

$$\int_0^t \Big[\eta(t-\xi)\partial_\xi^2 + \tau^{-1}\gamma(t-\xi)\partial_\xi\Big]u(x,\xi)\,\mathrm{d}\xi - a^2\partial_x^2 u(x,t) = S(x,t), \tag{3.1}$$

where

$$S(x,t) = Q\int_0^\infty f_{\hat{\gamma}}(\xi,t)\delta(x-v\xi)\,\mathrm{e}^{\mathrm{i}\omega\xi}\,\mathrm{d}\xi, \tag{3.2}$$

with initial conditions given by

$$u(x,0) = u_0(x) \geq 0 \quad \text{and} \quad \partial_t u(x,t)|_{t=0} = 0.$$

The functions $f_{\hat{\gamma}}$ describe the relationship between the irregularly ticking internal time ξ - for example, the randomly distributed waiting times experienced by a diffusing walker at particular spatial locations and the regularly ticking laboratory time which is measured with respect to periodic phenomena. These functions are assumed to provide a mapping between the internal time ξ and the physical time t such that the correspondence $\xi \leftrightarrow t$ satisfies all the conditions required of probability distributions. It is important to note that in the equation under consideration, the smearing of time derivatives was performed in such a way that the smeared second derivative gives the action of the smeared derivative on the smeared first derivative. This means that the time derivatives appearing in the equation under consideration are coupled and that the model under analysis does not fit into the class of fractional generalizations of the telegraph equation, which allow independent extensions of first- and second-order derivatives to their fractional counterparts. This means that the memory functions η and γ appearing in equation (3.1) satisfy relation (2.64). Furthermore, in this case, we can express the Laplace transform of the function $f_{\hat{\gamma}}$ as

$$\hat{f}_{\hat{\gamma}}(\xi, s) = \hat{\gamma}(s)\, \mathrm{e}^{-\xi s \hat{\gamma}(s)}\,.$$

With [70, 71] in view, and being convinced that the most natural memory-dependent extension of the telegraph equation is given by (3.1), we are led to pose the following question: do the classical wave properties persist for solutions of the proposed generalized telegraph equation? In particular, does the incorporation of temporal nonlocality, manifested through memory effects, preserve the existence of wavefronts and velocity-dependent frequency shifts? Paper [60] is devoted to addressing this problem.

The crucial phenomenon considered in [60] is the signal frequency shift effect. A commonly encountered example of a velocity-dependent frequency shift in everyday life is the longitudinal Doppler effect, manifested in acoustic waves. In its idealized form, the effect is explained in introductory physics courses purely on the basis of kinematical properties of wave motion. It arises from the observation that the detected pitch depends on the relative velocity between the emitter and the detector. More precisely, the analysis of the Doppler effect requires three essential elements: an observer capable of moving with velocity w, a source (emitter) of the signal, capable of moving with velocity v, and the propagation speed of the signal, denoted by a, which is determined by the physical properties of the medium. The characteristic signature of the Doppler effect occurs when a stationary observer detects a signal emitted by a moving source and finds that the received frequency Ω differs, for any $v \neq 0$, from the emitted frequency ω: it is higher during approach, identical at the instant of passage, and lower during recession. For a periodic sinusoidal signal, it is straightforward to derive the relation

$$\Omega_{\pm} = \frac{\omega a}{a \pm v} \tag{3.3}$$

where the positive sign corresponds to approach and the negative to recession, thus providing a quantitative connection between the emitted and observed frequencies. In the regime $\frac{v}{a} \ll 1$, typical of acoustic phenomena, this reduces to the commonly used approximation

$$\Omega_{\mp} \approx \omega\left(1 \pm \frac{v}{a}\right) \tag{3.4}$$

which directly relates the frequency shift to the relative velocity. Within this idealized picture, a defining feature of the Doppler effect is the sudden and discontinuous change in the observed frequency given by

$$\Delta\Omega_{\pm} = \Omega_{+} - \Omega_{-} = \frac{\omega a}{1 - (a/v)^2}, \tag{3.5}$$

which occurs at the instant when the source and observer pass each other. When the wave-like nature of the signal is emphasized, the phenomenon becomes even more apparent: the distances between successive wave crests effectively distorted wavelengths are shorter during approach and abruptly lengthen at the moment the source and observer begin to recede. This qualitative behavior is not confined to simple periodic signals but can also be observed in more complex wave-like phenomena encountered in the natural environment, even when a full theoretical description requires models beyond those of idealized harmonic waves. Consequently, the direct visual detection of such wavelength changes provides evidence of the Doppler effect.

The solution method adopted in [60] originates from the integral decomposition approach, which is closely connected to operator methods [72] and to analytic subordination techniques [61, 73]. Integral decompositions constitute an effective analytical tool for addressing a wide range of problems in transport phenomena, particularly those associated with anomalous diffusion and non-Debye relaxation. Building on the probabilistic and stochastic-process framework for anomalous kinetics introduced in [74], the method was subsequently advanced in [75, 76]. A complementary line of inquiry, situated more firmly within the theory of evolution equations, was pursued in [77], where the interplay between Markovian and non-Markovian descriptions of anomalous diffusion and non-Debye relaxation was examined in detail. More recently, the theoretical foundations of integral decompositions have been significantly clarified through the rediscovery and novel application of the Efros theorem, which has situated the method within the domain of rigorous mathematical analysis [73]. The Efros theorem [78] generalizes the convolution theorem for the Laplace transform. It can be stated as follows: if $\hat{G}(s)$ and $\hat{q}(s)$ are analytic functions, and

$$\mathscr{L}[h(x,\xi)] = \hat{h}(x,s) \tag{3.6}$$

as well as

$$\mathscr{L}[f(\xi,t)] = \hat{G}(s)\,\mathrm{e}^{-\xi\hat{q}(s)}, \tag{3.7}$$

exist, then

$$\hat{G}(s)\hat{h}(x,\hat{q}(s)) = \int_0^\infty \Big[\int_0^\infty h(x,\xi)f(\xi,t)\,\mathrm{d}\xi\Big]\,\mathrm{e}^{-st}\,\mathrm{d}t. \tag{3.8}$$

An immediate consequence of the Efros theorem is the inversion formula

$$\mathscr{L}^{-1}[\hat{G}(s)\hat{h}(x,\hat{q}(s))] = \int_0^\infty h(x,\xi)f(\xi,t)\,\mathrm{d}\xi. \tag{3.9}$$

The Efros theorem not only furnishes operational rules for the inversion of Laplace–Fourier transforms arising in the study of evolution equations, but also elucidates the mathematical structure of integral decompositions, thereby providing a framework for their physical interpretation [73]. Within this formalism, physically admissible solutions to memory-dependent equations emerge naturally as convolution-type integrals.

The integral decomposition provided by Efros' theorem can be reduced to the subordination approach when h and f are the nonnegative and normalized functions. Moreover, the Laplace transform of f is an infinitely divisible function. From a probabilistic perspective, subordination corresponds to the composition of two independent stochastic processes, each characterized by its own probability density function. The first is the parent process, which describes the intrinsic dynamics of the system. This process evolves in terms of an auxiliary random variable known as operational time (or internal time). The second is the leading process, which specifies how physical (laboratory) time is mapped into the operational time. This time-change process is itself random and must satisfy certain general mathematical conditions, but it can be selected with some flexibility depending on the specific physical problem under consideration.

In paper [60], we investigated solutions to the (1+1)-dimensional generalized telegraph equation, introduced here as a modification of the classical telegraph equation in which both time derivatives are replaced by integro-differential linear operators. These operators involve memory kernels that are assumed to depend nonlocally on time and are not identified with the kernels underlying the commonly employed fractional derivatives. The proposed formulation thus extends previous studies based on standard fractional generalizations of the telegraph equation. Our methodological framework combines the Laplace-Fourier transform with operational calculus, integrated within the technique of integral decompositions. This approach enables the construction of solutions to memory-dependent evolution equations from the corresponding solutions of their time-local counterparts. Based on this approach, the solution to equation (3.1) can be sought in the form

$$u(x,t) = \int_0^\infty \mathfrak{u}(x,\xi) f_{\hat{\gamma}}(\xi,t)\,\mathrm{d}\xi, \tag{3.10}$$

where $\mathfrak{u}(x,t)$ is the solution to (3.1) with $\gamma(t) = \delta(t)$ while $f_{\hat{\gamma}}(\xi,t)$ has been described above. The integral decomposition method has been successfully employed in the analysis of anomalous diffusion and non-exponential relaxation.

The solution $u(x,t)$ to (3.1) is the sum of $u_{\mathrm{hom}}(x,t)$, which solves the homogeneous equation (i.e., (3.1) without $S(x,t)$), and $u_{\mathrm{inhom}}(x,t)$, which represents the particular solution of the inhomogeneous (3.1). The homogeneous and inhomogeneous solutions mentioned above can be obtained using expression (3.10). The solution $\mathfrak{u}_{\mathrm{hom}}(x,t)$ of the homogeneous equation for $\gamma(t) = \delta(t)$ required for this purpose is given by the formula [69]

$$\mathfrak{u}_{\mathrm{hom}}(x,t) = \frac{1}{2}\,\mathrm{e}^{-\frac{t}{2\tau}}[u_0(x-at) + u_0(x+at)] + \frac{1}{4\tau a}\,\mathrm{e}^{-\frac{t}{2\tau}} \int_{x-at}^{x+at} \mathfrak{y}(y) u_0(y)\,\mathrm{d}y \tag{3.11}$$

where

$$\mathfrak{y}(y) = \frac{ta}{\sqrt{a^2t^2 - |y-x|^2}} I_1\Big(\frac{\sqrt{a^2t^2 - |y-x|^2}}{2a\tau}\Big) + I_0\Big(\frac{\sqrt{a^2t^2 - |y-x|^2}}{2a\tau}\Big) \tag{3.12}$$

while I_0 and I_1 are the modified Bessel functions of the first kind. A particular solution of the inhomogeneous equation (3.1) with the same memory kernel as above is expressed by the formula [69]

$$\mathfrak{u}_{\text{inhom}}(x,t) = \mathfrak{h}_1(x,t)\Big[\mathfrak{h}_2(x,t) + \int_{|x|/a}^{t} h(t-y)\mathfrak{h}_3(x,y)\,\mathrm{d}y\Big] + \mathfrak{h}_4(x,t), \tag{3.13}$$

where:

$$\mathfrak{h}_1(x,t) = \frac{Q\,\mathrm{e}^{\frac{-t}{2\tau}}}{4a\lambda(\tau,\omega)}\Theta\Big(t - \frac{|x|}{a}\Big),$$

$$\mathfrak{h}_2(x,t) = \frac{1+\beta\,\mathrm{sign}x}{1-\beta^2} h\Big(t - \frac{|x|}{a}\Big),$$

$$\mathfrak{h}_3(x,y) = \frac{ay + \beta|x|\,\mathrm{sign}x}{2\tau(1-\beta^2)\sqrt{a^2y^2 - x^2}} + I_1\Big(\frac{\sqrt{a^2y^2-x^2}}{2\tau a}\Big) - A(\tau,\omega)I_0\Big(\frac{\sqrt{a^2y^2-x^2}}{2\tau a}\Big),$$

$$\mathfrak{h}_4(x,t) = -\frac{Q\,\mathrm{e}^{\mathrm{i}\omega\frac{|x|}{v}}}{4a\lambda(\tau,\omega)}\Theta\Big(t - \frac{|x|}{v}\Big)\frac{\beta(1+\mathrm{sign}x)}{1-\beta^2} k\Big(t - \frac{|x|}{v}\Big).$$

The additional auxiliary functions appearing in the above expressions are defined as follows:

$$h(\sigma) = 2\exp[A(\tau,\omega)\sigma]\sinh[\lambda(\tau,\omega)\sigma],$$

$$k(\sigma) = 2\exp[B(\tau,\omega)\sigma]\sinh[\lambda(\tau,\omega)\sigma],$$

$$A(\tau,\omega) = \frac{\mathrm{i}\omega + \frac{1}{2\tau}}{1-\beta^2}, \quad B(\tau,\omega) = \frac{\mathrm{i}\omega + \frac{\beta^2}{2\tau}}{1-\beta^2}, \quad \lambda(\tau,\omega) = \frac{\mathrm{i}\omega\beta}{1-\beta^2}\Big(1 - \frac{\mathrm{i}}{\tau\omega} - \frac{\beta^2}{4\tau^2\omega^2}\Big)^{1/2},$$

with

$$\beta = \frac{v}{a}.$$

This is part of the solution that serves as a source of information about the effects of frequency shifting. Based on expressions (3.10) and (3.13), we examined solutions associated with three distinct memory kernels: the localized case, the mixed localized-power-law case, and the purely power-law case. The analysis indicates that wavefronts accompanied by Doppler-like frequency shifts arise only in the first two cases. In the third case, despite the absence of wavefronts, a frequency shift is nevertheless present. These findings establish that the emergence of frequency shifts is not conditioned upon the existence of a wavefront, although their manifestation is more pronounced when a wavefront is present.

Recapitulating, the paper sheds light on the wave-like properties of heat transport as modeled by the Cattaneo-Vernotte equation, the close analogue of the telegraph equation, and its nonlocal-in-time generalization. As a testbed for probing the wave character of heat transport, we analyzed whether solutions to the generalized equations exhibit phenomena analogous to those of the standard telegraph equation, in particular, the Doppler effect and the existence of wavefronts. Our results demonstrate that the Doppler effect, albeit in a smeared form, persists in the presence of nontrivial memory effects. By contrast, the existence of wavefronts is not preserved, as it crucially depends on the presence of the second-order time derivative in the governing evolution equation.

The paper *Can the Doppler be useful for a benchmark analysis of the wave-like properties of memory-dependent telegraphers' equation* [79] presents a continuation of research on the telegraph equation in the context of the wave properties of the solutions to this equation. This paper considers the telegraph equation in the form:

$$\int_0^t \Big[\eta(t-\xi)\partial_\xi^2 + \tau^{-1}\gamma(t-\xi)\partial_\xi\Big] u(x,\xi)\,\mathrm{d}\xi + [b^2 - a^2\partial_x^2]u(x,t) = S(x,t) \quad (3.14)$$

where

$$S(x,t) = Q\delta(x - vt)\cos(\omega_0 t) \quad (3.15)$$

and is equipped with initial conditions:

$$u(x,0) = u_0(x) \in \mathbb{R} \quad \text{and} \quad \partial_t u(x,t)\Big|_{t=0} = v_0(x) \in \mathbb{R}. \quad (3.16)$$

In equation (3.14), compared to equation (3.1), an additional term $b^2 u(x,t)$ has been included, which causes extra damping. Both equations contain the term $S(x,t)$ describing a uniformly moving point-wise harmonic signal source, in which $Q > 0$ and $\omega_0 > 0$ are the amplitude and frequency of the signal generated by this source, while $v > 0$ is the speed of the source. We recall that the functions η and γ, appearing in (3.14), represent the memory kernels associated with the smearing of the first- and second-order time derivatives, respectively. These memory effects, introduced through the kernels η and γ, imply a nonlocal temporal evolution scheme in which the present state of the system depends not only on its instantaneous values but also on its history. As in [60], it is also assumed here that memory functions satisfy condition (2.64). The objective of this paper was to determine, based on two types of boundary conditions, namely:

$$\lim_{x\to\pm\infty} u(x,t) = 0, \tag{3.17}$$

and

$$u(-l,t) = u(l,t) = 0 \tag{3.18}$$

whether the solutions to (3.14) could be classified as traveling or standing waves. To address this question, we examined the possible occurrence of a velocity-dependent frequency shift commonly referred to as the Doppler or Doppler-like effect in the solution $u(x,t)$ for both types of boundary conditions. The GTE (3.14) is an inhomogeneous integrodifferential equation in which the inhomogeneity is determined by the external source information encoded in $S(x,t)$. As in the case of equation (3.1), the solution $u(x,t)$ to (3.14) is the sum of $u_{\text{hom}}(x,t)$, and $u_{\text{inhom}}(x,t)$ which are the solution of the homogeneous and the particular solution of the inhomogeneous equation (3.14), respectively. The information on the initial conditions (3.16) is incorporated into u_{hom}, whereas u_{inhom} contains the contribution from the external source. Since the u_{hom} is independent of the external harmonic impact, the analysis was performed for the inhomogeneous part of the solution to equation (3.14). In the case of the infinite domain, i.e., solutions to GTE satisfying the boundary condition (3.17), the particular solution of the inhomogeneous equation (3.14) can be written as:

$$u_{\text{inhom}}(x,t) = \frac{Q}{\pi a}\int_0^t \cos\big(\omega_0(t-\xi)\big)\left[\mathfrak{J}_1(x,t,\xi) + \mathfrak{J}_2(x,t,\xi)\right] \mathrm{d}\xi, \tag{3.19}$$

where

$$\mathfrak{J}_1(x,t,\xi) = \int_0^\sigma \frac{\mathfrak{S}_1(p,\xi)}{\sqrt{\sigma^2-p^2}} \cos\left[\frac{p}{2a\tau}\big(x+v[t-\xi]\big)\right] \mathrm{d}p, \tag{3.20}$$

and

$$\mathfrak{J}_2(x,t,\xi) = \int_\sigma^\infty \frac{\mathfrak{S}_2(p,\xi)}{\sqrt{p^2-\sigma^2}} \cos\left[\frac{p}{2a\tau}\big(x+v[t-\xi]\big)\right] \mathrm{d}p, \tag{3.21}$$

with

$$g_{\hat{\gamma}}(y,\xi) = \mathscr{L}^{-1}\big[e^{-ys\hat{\gamma}(s)};\xi\big] \quad \text{and} \quad \sigma = \sqrt{1-4\tau^2 b^2}. \tag{3.22}$$

The auxiliary functions $\mathfrak{S}_1$ and $\mathfrak{S}_2$ appearing in expressions (3.20) and (3.21) are given by:

$$\mathfrak{S}_1(p,\xi) = \int_0^\infty e^{-\frac{y}{2\tau}} \sinh\Big(\frac{\sqrt{\sigma^2-p^2}}{2\tau}y\Big) g_{\hat{\gamma}}(y,\xi)\,\mathrm{d}y, \tag{3.23}$$

$$\mathfrak{S}_2(p,\xi) = \int_0^\infty e^{-\frac{y}{2\tau}} \sin\Big(\frac{\sqrt{p^2-\sigma^2}}{2\tau}y\Big) g_{\hat{\gamma}}(y,\xi)\,\mathrm{d}y. \tag{3.24}$$

A solution $u_{\mathrm{hom}}(x,t)$ to a homogeneous equation (i.e., (3.14) without $S(x,t)$) can be found in [79]. It is worth emphasizing that, according to the conjecture formulated in [61, 60] for a memory function γ containing the Dirac-δ distribution, the solution (3.19) is nonzero only within the confined domain. To construct the inhomogeneous solution of (3.14) subject to the Dirichlet boundary and initial conditions given by (3.18) and (3.16), respectively, we first considered the corresponding homogeneous equation and assumed a separable solution of the form

$$u_{\mathrm{hom}}(x,t) = X(x)T(t). \tag{3.25}$$

Substituting this ansatz into the homogeneous equation and applying the separation of variables method yields a Sturm-Liouville problem for the spatial component $X(x)$, given by

$$\frac{d^2X(x)}{dx^2} + \frac{\lambda}{a^2}X(x) = 0 \tag{3.26}$$

with Dirichlet boundary conditions $X(-l) = X(l) = 0$. The resulting eigenvalues

$$\lambda_n = \frac{\pi^2 a^2 (2n+1)^2}{4l^2} \tag{3.27}$$

and eigenfunctions

$$X_n(x) = \cos\Big[\frac{\pi(2n+1)x}{2l}\Big], \quad n \in \mathbb{N}_0, \tag{3.28}$$

form a complete basis for the spatial domain. The solution of the inhomogeneous equation is then expressed as a series expansion

$$u(x,t) = \sum_{n=0}^{\infty} c_n(t) X_n(x). \tag{3.29}$$

Using Efros' theorem and Laplace convolution, one can determine the coefficients $c_n(t)$ and write down the form of a particular solution to the inhomogeneous equation as

$$u_{\text{inhom}}(x,t) = \sum_{n=0}^{\infty} X_n(x) \left[\int_0^t \mathscr{L}^{-1}\big[\hat{\nu}_1(\Lambda_n; s\hat{\gamma}(s)); r\big] I_n(t-r)dr \right], \quad (3.30)$$

where:

$$\hat{\nu}_1(\Lambda_n; s\gamma(s)) = \frac{1}{[s\gamma(s)]^2 + \tau^{-1}s\gamma(s) + \Lambda_n}, \quad (3.31)$$

$$I_n(t) = \frac{Q}{2l}\Big[\cos(\Omega_+ t) + \cos(\Omega_- t)\Big] \quad \text{with} \quad \Omega_\pm = \pi(2n+1)\frac{v}{2l} \pm \omega_0. \quad (3.32)$$

The quantity Λ_n appearing in the above expressions is defined as $\Lambda_n = b^2 + \lambda_n$. In paper [79], examples of equations describing various models of temporal evolution were analyzed for both cases presented above, specifically the memoryless telegrapher equation (i.e., the standard one) and its fractional counterpart in Caputo's sense, which incorporates power-law memory functions.

To assess the influence of the source velocity on the signal frequency spectrum, a numerical time-frequency analysis was conducted. The analysis was performed using the short-time Fourier transform (STFT), which can be formally expressed in the time and frequency domains as

$$STFT_s^T(t,f) = \int_{-\infty}^{\infty} s(\tau)h^*(\tau - t)e^{-i2\pi f\tau}\, \mathrm{d}\tau, \quad (3.33)$$

$$STFT_s^F(t,f) = e^{-i2\pi ft}\int_{-\infty}^{\infty} \tilde{s}(\nu)\tilde{h}^*(\nu - f)e^{i2\pi\nu t}\, \mathrm{d}\nu, \quad (3.34)$$

where $s(t)$ denotes the analyzed signal, $\tilde{s}(\nu)$ its Fourier transform, and $h(t)$ the temporal analysis window with Fourier spectrum $\tilde{h}(\nu)$. The squared magnitude of the STFT, $|STFT_s(t,f)|^2$, defines the spectrogram, providing a quantitative representation of the signal's energy distribution in the joint time-frequency domain. In the temporal formulation, the STFT is obtained by applying the Fourier transform to successive segments of the signal selected by a sliding window $h(t)$. In contrast, the frequency-domain formulation involves computing the inverse Fourier transform of a windowed portion of the signal spectrum, shifted by f. These dual perspectives underscore the STFT's role as a localized time-frequency representation, capturing both transient and stationary components of the signal. A fundamental feature of

STFT-based analysis is the intrinsic trade-off between temporal and spectral resolution: a wider window enhances frequency resolution at the expense of temporal precision, whereas a narrower window improves temporal localization while broadening the spectral response. In the present study, a wide Tukey window was employed, defined by

$$\begin{cases} h[n] = \frac{1}{2}\left[1 - \cos\left(\frac{2\pi n}{\alpha_T N}\right)\right], & 0 \leq n < \frac{\alpha_T N}{2}, \\ h[n] = 1, & \frac{\alpha_T N}{2} \leq n < \frac{N}{2}, \end{cases} \tag{3.35}$$

with the symmetry condition

$$h[N-n] = h[n], \quad 0 \leq n \leq \frac{N}{2}. \tag{3.36}$$

The Tukey window can be interpreted as the convolution of a cosine lobe of width $\frac{\alpha_T N}{2}$ with a rectangular window of width $N(1 - \frac{\alpha_T}{2})$, where N denotes the number of samples of the signal under analysis. Spectrograms are extensively utilized in diverse disciplines, including audio and speech processing, biomedical signal analysis, and environmental monitoring. They enable the identification of transient phenomena, harmonic components, modulation patterns, and anomalies within complex signals. Examination of spectrograms thus facilitates a detailed characterization of signal dynamics in both time and frequency, providing critical insights into underlying processes and temporal evolution [80].

In the infinite-domain scenario, which can be intuitively associated with the physical concept of a traveling wave, based on the analysis conducted, it can be concluded that the signature of velocity-dependent frequency shifts observed in the memoryless case persists in the memory-dependent case for $\alpha \in (\frac{1}{2}, 1)$, whereas it remains absent for $\alpha \in (0, \frac{1}{2})$. Comparing this result with those previously reported in [69, 70] and, as mentioned in Sect. 3.1, discussing so-called wave-like and heat-like extensions of the telegraph equation, we recall that our study explores the generalized telegraph equation involving nonlocal time derivatives whose blurring is interrelated according to (2.64). This distinguishes our approach from that in references [69, 70], but it is worth noting that in both schemes the standard wave properties accompany the presence of the second time derivative, which is equivalent to the presence of the Dirac delta in the memory function. Our results indicate that manifestations of the velocity-dependent frequency shifts may arise even in the absence of wavefronts, a behavior consistent with the typical characteristics of nonlocal temporal evolution. For a bounded domain, the solutions are necessarily of standing-wave character. In this setting, and in accordance with the reasoning developed for the unbounded case, any Doppler-type effect that might appear transiently is not expected to persist in the long-time limit. While certain solution profiles may mimic features conventionally attributed to traveling waves, we contend that such instances should not be interpreted as genuine manifestations of Doppler shifts. Rather, they represent artifacts whose origin lies outside the present scope of understanding. The standing-wave nature of the solutions becomes particularly evident as α approaches unity, corresponding to the near-telegrapher regime, where the Doppler effect is rigorously absent under bounded-domain conditions.

3.2 Memory-driven diffusion: Fokker-Planck and Langevin perspectives

The paper *Volterra-Prabhakar function of distributed order and some applications* [81] considers a different approach to diffusion modeling than that proposed in the papers described above, namely the generalized Fokker-Planck equation. This equation is of the form

$$\int_0^t k(t-\xi)\partial_\xi p(x,\xi)\,\mathrm{d}\xi = \partial_x^2[B(x,t)p(x,t)] - \partial_x[\lambda(x,t)p(x,t)], \tag{3.37}$$

whereby $B(x,t)$ is the diffusion and $\lambda(x,t)$ is the drift coefficiants, respectively. In this paper, it is assumed that the diffusion coefficient is a positive constant, while the drift coefficient vanishes. It is worth noting that this type of equation is a limiting case of the homogeneous telegraph equation (3.1) when τ approaches zero. The paper presents the exact solution to the generalized Fokker-Planck equation, whose integral kernel $k(t)$ determines the form of smearing the first-time derivative, and is referred to as a memory function. With regard to the structure of the memory function, two formulations of the generalized Fokker-Planck equation are considered. In the first formulation, the memory kernel is of distributed order and is of the form

$$k_1(t) = \int_0^1 \frac{t^{-\mu}}{\Gamma(1-\mu)}\,\mathrm{d}\mu \quad \text{and} \quad \hat{k}_1(s) = \int_0^1 s^{\mu-1}\,\mathrm{d}\mu = \frac{s-1}{s\ln s}. \tag{3.38}$$

In the second example, the generalized Fokker-Planck equation with a distributed-order Prabhakar kernel is considered. In this example, the memory kernel is given by

$$k_2(t) = \int_0^1 e^{-\gamma}_{\alpha,1-\mu}(\lambda;t)\,\mathrm{d}\mu \quad \text{and} \quad \hat{k}_2(s) = \hat{k}_1(s)\left(1+\frac{\lambda}{s^\alpha}\right)^\gamma, \tag{3.39}$$

where $\alpha,\gamma,\mu \in (0,1)$ and $\lambda > 0$. The values of the Prabhakar function $e^{\gamma}_{\alpha,\beta}(\lambda;t)$ are defined as

$$e^{\gamma}_{\alpha,\beta}(\lambda;t) = t^{\beta-1}E^{\gamma}_{\alpha,\beta}(-\lambda t^\alpha), \quad \text{where} \quad E^{\gamma}_{\alpha,\beta}(z) = \sum_{r=0}^{\infty}\frac{(\gamma)_r z^r}{r!\Gamma(\beta+\alpha r)} \tag{3.40}$$

is the three parameters Mittag-Leffler functions and $(\gamma)_r = \Gamma(\gamma+r)/\Gamma(\gamma)$ is the Pochhammer (raising) symbol. It is worth emphasizing that the distributed order kernel $k_1(t)$ and the distributed order Prabhakar kernel $k_2(t)$

satisfy Kochubei's limits given in [47]. From these limits, it follows that $[s\hat{k}_1(s)]^{-1}$ and $[s\hat{k}_2(s)]^{-1}$ vanishes at $s \gg 1$. Therefore, both kernels can be classified as fading memory functions [82]. In [83] it is shown that $\hat{k}_1(s)$ and $\hat{k}_2(s)$ are Stieltjes functions (SFs). They can be expressed in the form $\frac{s\hat{k}_1(s)}{s}$ and $\frac{s\hat{k}_2(s)}{s}$, where $s\hat{k}_1(s)$ and $s\hat{k}_2(s)$ are completely Bernstein functions (CBFs). This implies the existence of the Sonin partners of $\hat{k}_1(s)$ and $\hat{k}_2(s)$. Namely:

$$\hat{M}_1(s) = \frac{\ln s}{s-1} \quad \text{and} \quad \hat{M}_2(s) = \hat{M}_1(s)\left(1 + \frac{\lambda}{s^\alpha}\right)^{-\gamma}, \tag{3.41}$$

and $\alpha, \gamma \in (0,1)$ with $\lambda > 0$. Sonin partners are important because they provide a mathematical tool for analyzing and inverting convolution-type relations, which frequently appear in fractional calculus, viscoelasticity, and anomalous diffusion. It has been shown that the fundamental solution to (3.37) for $B > 0$ and in the absence of the drift term, i.e., for $\lambda(x,t) = 0$, in the Laplace space is given by

$$\hat{p}(x,s) = \frac{1}{2s}\sqrt{\frac{s\hat{k}(s)}{B}}\, \mathrm{e}^{-|x|\sqrt{\frac{s\hat{k}(s)}{B}}}. \tag{3.42}$$

By Bernstein's theorem [84], it follows that $p(x,t)$ represents a probability density function (PDF) if (3.42) is a completely monotone function (CMF), that is, a non-negative function in C^∞ whose derivatives alternate in sign. This condition can be satisfied in two ways: when $\sqrt{s^{-1}\hat{k}(s)}$ is a CMF and $\sqrt{s\hat{k}(s)}$ is a Bernstein function (BF), or when $\sqrt{s\hat{k}(s)}$ being CBF. For both memory kernels under consideration, it has been shown that the solutions of equation (3.37) associated with them are PDFs. These solutions for $k_1(t)$ and $k_2(t)$ are as follows:

$$p_1(x,t) = \frac{1}{2\sqrt{B}}\sum_{r=0}^{\infty}\left(\frac{-|x|}{\sqrt{B}}\right)^r \frac{1}{r!\,\Gamma(b_r)}\, \epsilon^{-b_r}_{1,b_r-1,-b_r}(t), \tag{3.43}$$

$$p_2(x,t) = \sum_{r=0}^{\infty}\int_0^\infty p_1(x,t-\xi)\, e^{-\gamma b_r}_{1,0}(\lambda,\xi)\,\mathrm{d}\xi, \tag{3.44}$$

where $b_r = (r+1)/2$, and ϵ is a new mathematical object called the Volterra-Prabhakar function introduced in the paper. The values of this function depend on (3.40) and are given by

$$\epsilon^{\gamma}_{\alpha,\,p}(\lambda;t) = \int_0^{\infty} e^{\gamma}_{\alpha,u+p+1}(\lambda;t)\,\mathrm{d}u. \tag{3.45}$$

The paper also analyzes a number of mathematical properties of the introduced function. Furthermore, in [81], the mean squared displacements (MSDs) were determined for both memory kernels. The asymptotic behavior for short and long times is described by the following expressions:

$$\langle x^2(t)\rangle_{\hat{k}_1} \simeq 2B \begin{cases} \ln t, & \text{for} \quad t \to \infty, \\ t\ln(1/t), & \text{for} \quad t \to 0, \end{cases} \tag{3.46}$$

$$\langle x^2(t)\rangle_{\hat{k}_1} \simeq 2B \begin{cases} \lambda^{-\gamma}\frac{t^{-\alpha\gamma}}{\Gamma(1-\alpha\gamma)}\ln t, & \text{for} \quad t \to \infty, \\ t\ln(1/t), & \text{for} \quad t \to 0. \end{cases} \tag{3.47}$$

The coincidence of the MSD for both kernels in the short-time regime can be interpreted physically as a manifestation of a universal pre-asymptotic diffusion stage. In this regime, the particle has performed only a few random displacements, so the process is dominated by the immediate stochastic fluctuations rather than by the long-term memory encoded in the kernel. From the perspective of stochastic modeling, this means that the distributed-order kernel and the distributed-order Prabhakar kernel are indistinguishable at early times: both generate the same statistical spreading of the probability density. Only when the observation time increases does the system begin to accumulate the long-range memory contributions that are specific to the Prabhakar kernel. This leads to a qualitative divergence of transport laws in the long-time limit: while both models generate ultraslow diffusion, the Prabhakar kernel introduces additional algebraic modulation controlled by its parameters α, γ, and λ. Thus, the short-time universality emphasizes that the memory effects are emergent phenomena: they require a sufficiently long observation window to become visible. In practical terms, this implies that experimental measurements confined to short times may not provide sufficient information to discriminate between different distributed-order models of anomalous diffusion, whereas long-time data are essential for revealing the true memory structure of the system.

In the paper, the exact solution of the generalized Fokker-Planck equation is presented, with the integral kernel $k(t)$ referred to as the memory function, specifying the form of the smeared first-order time derivative. Two forms of the memory function are examined. The first corresponds to the distributed-order kernel, denoted by $k_1(t)$, while the second involves the distributed-order Prabhakar kernel, $k_2(t)$. It is demonstrated that $k_1(t)$ and $k_2(t)$ can be represented, respectively, as differences of Volterra functions[1] and Volterra-Prabhakar functions, the latter introduced in this work. On this basis, the mean squared displacements (MSDs), fourth moments, and probability density functions (PDFs) are computed. The non-negativity of these quantities follows from the Stieltjes character of the memory kernels.

The dynamics of a test particle of mass m, coupled to a thermal bath at temperature T, can be described using Newton's second law in the presence of a deterministic external potential $V(x)$ and a stochastic force $\xi(t)$. When the particle experiences a constant friction $\mathfrak{z}_0$, its motion is governed by the standard Langevin equation for a Brownian particle:

$$m\ddot{x}(t) + m\mathfrak{z}_0\dot{x}(t) + \frac{\mathrm{d}V(x)}{\mathrm{d}x} = \xi(t), \quad \dot{x}(t) = v(t), \tag{3.48}$$

where $x(t)$ and $v(t)$ denote the particle's displacement and velocity, respectively. The stochastic force $\xi(t)$, representing thermal noise, is Gaussian with zero mean and delta-correlated in time:

$$\langle \xi(t+t')\,\xi(t)\rangle = mk_BT\mathfrak{z}_0\,\delta(t'), \tag{3.49}$$

where k_BT is the thermal energy. The MSD predicted by (3.48) exhibits a short-time quadratic growth reflecting inertial, ballistic motion and crosses over to a linear, diffusive regime at times longer than the characteristic friction timescale $1/\mathfrak{z}_0$. In the paper *Anomalous and ultraslow diffusion of a particle driven by power-law-correlated and distributed-order noises* [86], generalizations of the stochastic equation (3.48) are considered that incorporate memory effects, i.e., temporal nonlocalities. For a general friction kernel $\mathfrak{z}(t)$, the dynamics of a stochastic process is described by the generalized Langevin equation (GLE) [52]:

$$m\ddot{x}(t) + m\int_0^t \mathfrak{z}(t-t')\dot{x}(t')\,\mathrm{d}t' + \frac{\mathrm{d}V(x)}{\mathrm{d}x} = \xi(t), \quad \dot{x}(t) = v(t). \tag{3.50}$$

[1]Volterra's function is defined as follows [85]

$$\mu(t,\beta,\alpha) = \frac{1}{\Gamma(1+\beta)}\int_0^\infty \frac{t^{u+\alpha}\,u^\beta}{\Gamma(u+\alpha+1)}\,\mathrm{d}u, \qquad \mathfrak{Re}(\beta) > -1 \quad \text{and} \quad t>0.$$

The second fluctuation-dissipation theorem (FDT) establishes a relation between the friction kernel $\mathfrak{z}(t)$ and the autocorrelation of the stochastic force $\xi(t)$ [87]:

$$\langle \xi(t+t')\,\xi(t')\rangle = C(t) = k_B T\,\mathfrak{z}(t). \tag{3.51}$$

The friction kernel is assumed to satisfy [88]:

$$\lim_{t\to\infty} \mathfrak{z}(t) = \lim_{s\to 0} s\hat{\mathfrak{z}}(s) = 0. \tag{3.52}$$

In the case of external noise, as defined by Klimontovich [89], where the stochastic force does not originate from a thermal bath in a non-equilibrium system, the relation in (3.51) does not hold, and the correlation function is written as $\langle \xi(t)\,\xi(t')\rangle = C(t-t')$ instead. Considering the harmonic oscillator with unit mass $m=1$, i.e., $V(x) = \omega^2 x^2/2$, (3.50) can be expressed as:

$$x(t) = \langle x(t)\rangle + \int_0^t G(t-t')\,\xi(t')\,\mathrm{d}t', \quad v(t) = \langle v(t)\rangle + \int_0^t g(t-t')\,\xi(t')\,\mathrm{d}t', \tag{3.53}$$

where the mean displacement and velocity are given by (with the initial conditions $x_0 = x(0)$ and $v_0 = v(0)$):

$$\langle x(t)\rangle = x_0\left[1-\omega^2 I(t)\right] + v_0 G(t), \quad \langle v(t)\rangle = v_0 g(t) - \omega^2 x_0 G(t). \tag{3.54}$$

The relaxation functions $G(t)$, $I(t) = \int_0^t G(\chi)\,\mathrm{d}\chi$, and $g(t) = \frac{\mathrm{d}G(t)}{\mathrm{d}t}$ are introduced, with Laplace-space representations:

$$\hat{G}(s) = \frac{1}{s^2 + s\hat{\mathfrak{z}}(s) + \omega^2}, \quad \hat{g}(s) = s\hat{G}(s), \quad \hat{I}(s) = \frac{\hat{G}(s)}{s}. \tag{3.55}$$

These functions were used to define the following four basic quantities:

- The mean squared displacement (MSD)

$$\langle x^2(t)\rangle = 2k_B T I(t) = 2k_B T \int_0^t G(\chi)\,\mathrm{d}\chi,$$

- The diffusion coefficient

$$D(t) = k_B T G(t) = k_B T \frac{\mathrm{d}I(t)}{\mathrm{d}t},$$

■ The normalized displacement autocorrelation function (DACF)[2]

$$C_X(t) = \frac{\langle x(t)x_0 \rangle}{\langle x_0^2 \rangle} = 1 - \omega^2 I(t) = 1 - \omega^2 \int_0^t G(\chi)\, \mathrm{d}\chi,$$

■ The normalized velocity autocorrelation function (VACF)

$$C_V(t) = \frac{\langle v(t)v_0 \rangle}{\langle v_0^2 \rangle} = g(t) = \frac{\mathrm{d}G(t)}{\mathrm{d}t}.$$

Based on the above-defined quantities, the case for the GLE under white and power-law noises was explored. For additive white noise, the model recovers familiar diffusive behaviors, with ballistic scaling at short times and linear growth of the mean squared displacement (MSD) at long times. When power-law noises are introduced, the memory kernel produces fractional-order dynamics. Depending on the exponent, the motion ranges from subdiffusive to superdiffusive. The analysis extends to multiple simultaneous power-law noises and to mixtures of white and power-law components, where complex crossovers appear. The overdamped limit is also derived, simplifying the dynamics for long times or high friction. The paper introduces distributed-order Langevin equations, in which the friction kernel is given by

$$\mathfrak{z}(t) = (k_B T)^{-1} \int_0^1 p(\lambda) \frac{t^{-\lambda}}{\Gamma(1-\lambda)}\, \mathrm{d}\lambda \tag{3.56}$$

where $p(\lambda)$ is a weight function, which is a dimensionless, non-negative function with $\int_0^1 p(\lambda)\mathrm{d}\lambda = c$, where c is a constant. This formulation generalizes the finite-sum case and naturally produces ultraslow diffusion regimes, with MSDs growing logarithmically or as powers of logarithms. Two cases are studied in detail: the free particle, where diffusion laws reflect the weighting function of the distributed order, and the overdamped harmonic oscillator, where relaxation and correlations display ultraslow and nontrivial behaviors. This approach captures diffusive regimes not accessible through single-order fractional models. The paper also develops further generalizations by considering alternative distributed order noise models. Examples include Langevin equations with power-logarithmic distributed orders, distributed-order Mittag-Leffler kernels, Caputo-Prabhakar derivatives, and

[2]The above formula is valid under the initial conditions $\langle x_0^2 \rangle = k_B T/\omega^2$, $\langle x_0 v_0 \rangle = 0$, and $\langle \xi(t) x_0 \rangle = 0$.

Volterra functions. Each case introduces new asymptotic forms for the relaxation function I, enriching the taxonomy of anomalous diffusion. These extensions reveal that small modifications of the kernel's functional form can drastically alter long-time dynamics, enabling the modelling of strong anomalies and multiple crossovers between diffusive regimes.

In the paper, the generalized Langevin equation was analyzed for both an external harmonic potential and its free-particle limit under various forms of the friction kernel. In particular, the corresponding mean squared displacement (MSD) and displacement autocorrelation function (DACF) were derived for kernels of Dirac delta, power-law, and distributed-order types. The results reveal a wide range of anomalous diffusive behaviors, including subdiffusion, superdiffusion, ultraslow diffusion, and strong anomalies. Particular emphasis was placed on distributed-order GLEs and the associated distributed-order diffusion equations. Depending on the choice of weight functions, the analysis yielded ultraslow diffusion, strong anomalies, and further complex diffusive regimes.

4. Summary

The research explores the dynamics of transport and diffusion processes by examining generalized equations incorporating memory effects, offering significant theoretical insights and practical applications. The generalized telegraph equation (GTE), a pivotal focus, extends the classical telegraph equation by introducing memory effects through integral-differential operators. This modification allows the equation to account for nonlocal temporal influences, reflecting the persistence of past states in the evolution of the system. A critical question addressed is whether these memory effects preserve classical wave properties, such as wavefronts and the Doppler effect, which are hallmarks of wave-like behavior in memoryless systems. Analytical methods, including integral decomposition, Laplace-Fourier techniques, and the application of Efros' theorem, have been employed to investigate wavefronts and frequency shift in these models. It has been demonstrated that the presence of memory kernels modifies, but does not necessarily suppress, fundamental wave characteristics. The analysis highlights that the specific nature of the memory functions plays a crucial role in determining these behaviors. For instance, the Doppler effect's visibility depends on the parameter α in memory functions with a power-law distribution. When $\alpha \in (\frac{1}{2}, 1)$, speed-dependent frequency shifts are observable, whereas for $\alpha \in (0, \frac{1}{2})$, they are not. A complementary line of research has addressed generalized Fokker-Planck equations in which the standard first-order time derivative is replaced by a smeared derivative defined through distributed-order memory functions. Two formulations have been analyzed: one involving a distributed-order kernel and another incorporating a distributed-order Prabhakar kernel. The latter necessitated the introduction of a new mathematical object, the Volterra-Prabhakar function. Exact solutions have been obtained, along with explicit expressions for probability density functions, moments, and mean squared displacements. A universal short-time behavior has been identified, whereas long-time asymptotics reveal qualitative differences between kernels, leading to ultraslow diffusion and algebraically modulated transport. The non-negativity of solutions has been ensured through the Stieltjes character of the kernels. Further extending the scope, the research examines the generalized Langevin equation (GLE), focusing on its application to anomalous diffusion in systems driven by memory-dependent noise. The GLE framework is applied to both harmonic oscillators and free particles subjected to various forms of noise, including power-law and distributed-order noise. This approach enables the characterization of a wide spectrum of diffusive behaviors, including subdiffusion, superdiffusion, ultraslow diffusion, and strong anomalies. These findings underscore the versatility of the GLE in modeling real-world systems where traditional diffusion models are insufficient. Collectively, these studies challenge traditional classifications of transport processes into rigid categories such as wave-like and diffusion-like phenomena. They reveal that the presence of memory effects introduces a spectrum of behaviors that blend features of both categories. For example, while classical wavefronts vanish in memory-dependent systems, the Doppler effect remains, albeit in a modified form. In a broader context, these works advance the mathematical tools available for studying systems with memory effects, bridging theoretical approaches like fractional calculus with practical applications. By unifying diverse phenomena under a common framework, the research provides methods to analyze transport and diffusion in fields ranging from heat transfer and viscoelasticity to biological processes and materials science. This interdisciplinary relevance emphasizes the importance of understanding memory effects, not only as a mathematical curiosity but as a fundamental aspect of real-world systems. The work sets the stage for future investigations, including clarifying the role of signal velocity in memory-dependent evolution equations and further exploring the interplay between wave-like and diffusion-like behaviors in complex systems.

Bibliography

[1] L. Boltzmann, Zur theorie der elastischen nachwirkung, Wiener Berichte 70 (1874) 275–306.

[2] O. Meyer, Theorie der elastischen nachwirkung, Ann. der Phys. und Chemie CLI (1874) 108–119.

[3] E. Wiechert, Gesetze der elastischen für konstante temperatur, Ann. der Phys. und Chemie L (1893) 275–306.

[4] C.-E. Picard, La mathématique dans ses rapports avec la physique, ICM Proceedings 1 (1908) 183–195.

[5] V. Volterra, Sulle equazioni integro-differenziali, Opere Matematiche 3 (1909) 269–275.

[6] V. Volterra, Sur les équations intégro-différentielles et leurs applications, Acta Math. 35 (1912) 295–356.

[7] V. Volterra, Sur la theorie mathematique des phenomenes heneditaires, J. Math. Pures Appl. 7 (1928) 249–298.

[8] V. M. Bogdan, Existence of solutions to differential equations of relativistic mechanics involving Lorentzian time delays, J. Math. Anal. Appl. 118 (1986) 561–573.

[9] I. Epstein, Delay effects and differential delay equations in chemical kinetics, Int. Rev. Phys. Chem. 11 (1992) 135–160.

[10] J. Bansal, K. S. Chang, Optimal control of dispersion type distributed-parameter systems with time-delay in interacting two-point boundary conditions, Int. J. Control 16 (1972) 481–500.

[11] F. Grodins, J. Buell, A. Bart, Mathematical analysis and digital simulation of the respiratory control system, J. Appl. Physiol. 22 (1967) 260–276.

[12] J. M. Cushing, Integro-differential equations and delay models in population dynamics, Springer, Berlin, 1977.

[13] I. Belair, M. C. Mackey, Consumer memory and price fluctuations in commodity markets: an integrodifferential model, J. Dyn. Diff. Equ. 1 (1989) 299–325.

[14] C. M. Marcus, R. M. Westervelt, Stability of analog networks with delay, Phys. Rev. A 39 (1989) 347–359.

[15] G. H. Pertz, C. J. Gerhardt, Leibnizens gesammelte Werke, Lebinizens mathematische Schriften, Erste Abtheilung, Band II, A. Asher Co, Berlin, 1849.

[16] R. Metzler, J.-H. Jeon, A. G. Cherstvy, E. Barkai, Anomalous diffusion models and their properties: Non-stationarity, non-ergodicity, and ageing at the centenary of single particle tracking, Phys. Chem. Chem. Phys. 16 (2014) 24128–24164.

[17] S. Holm, R. Sinkus, A unifying fractional wave equation for compressional and shear waves, J. Acoust. Soc. Am. 127 (2010) 542–559.

[18] X. Wu, W. Deng, E. Barkai, Tempered fractional Feynman-Kac equation: Theory and examples, Phys. Rev. E 93 (2016) 032151.

[19] V. Pandey, S. Holm, Connecting the grain-shearing mechanism of wave propagation in marine sediments to fractional order wave equations, J. Acoust. Soc. Am. 140 (2016) 4225–4236.

[20] Y. Povstenko, Fractional Thermoelasticity, Springer, New York, 2015.

[21] P. D. Mandić, T. B. Šekara, M. P. Lazarević, B. M., Dominant pole placement with fractional order PID controllers: D-decomposition approach, ISA Transactions 67 (2017) 76–86.

[22] R. R. Nigmatullin, C. Ceglie, G. Maione, et al., Reduced fractional modeling of 3D video streams: the FERMA approach, Nonlinear Dyn. 80 (2015) 1869–1882.

[23] D. S. Grebenkov, Use, misuse, and abuse of apparent diffusion coefficients, Conc. Magn. Reson. 36A (2010) 24–25.

[24] C. M. A. Pinto, A. R. M. Carvalho, A latency fractional order model for HIV dynamics, J. Comput. Appl. Math. 312 (2017) 240–256.

[25] Y. Zhang, J. Qian, C. Papelis, P. Sun, Improved understanding of bimolecular reactions in deceptively simple homogeneous media: from laboratory experiments to Lagrangian quantification, Water Resour. Res. 50(2) (2014) 1704–1715.

[26] Z. Li, H. Wang, R. Xiao, S. Yang, A variable-order fractional differential equation model of shape memory polymers, Chaos, Solitons & Fract. 102 (2017) 473–485.

[27] V. V. Tarasova, V. E. Tarasov, Logistic map with memory from economic model, Chaos, Solitons & Fract. 95 (2017) 84–91.

[28] L. Evangelista, E. K. Lenzi, Fractional Diffusion Equations and Anomalous Diffusion, Cambridge University Press, Cambridge, 2018.

[29] T. Graham, A short account of experimental researches on the diffusion of gas through each other, and their separation by mechanical means, Quart. J. Sci. 2 (1829) 74.

[30] A. Fick, Über diffusion, Poggendorff's Annalen der Physik und Chemie 94 (1855) 59–86.

[31] W. Roberts-Austen, On the diffusion of gold in solid lead at the ordinary temperature, Proc. R. Soc. Lond. 67 (1901) 435–441.

[32] Lucretius, The Nature of Things (Penguin Classics), Penguin Books, London, 2007.

[33] R. Brown, A brief account of microscopical observations on the particles contained in the pollen of plants and the general existence of active molecules in organic and inorganic bodies, Edinburgh New Philos. J. (1828) 358–371.

[34] A. Einstein, Über die von der molekularkinetischen theorie der wärme geforderte bewegung von in ruhenden flüssigkeiten suspendierten teilchen, Ann. Phys. 17 (1905) 549–560.

[35] M. Smoluchowski, Sur le chemin moyen parcouru par les molécules d'un gaz et son rapport avec la théorie de la diffusion, Bull. Int. Acad. Sci. Cracovie (1906) 202–213.

[36] P. Langevin, Sur la théorie du mouvement brownien, C. R. Acad. Sci. 146 (1908) 530–533.

[37] D. S. Lemons, A. Gythiel, Paul Langevin's 1908 paper "On the theory of brownian motion" ["Sur la théorie du mouvement brownien", C. R. Acad. Sci. (Paris) 146, 530-533 (1908)], Am. J. Phys. 65 (1997) 1080–1081.

[38] L. Richardson, Atmospheric diffusion shown on a distance-neighbour graph, Proc. R. Soc. Lond. 110 (1926) 709.

[39] Y. Sagi, M. Brook, I. Almog, N. Davidson, Observation of anomalous diffusion and fractional self-similarity in one dimension, Phys. Rev. Lett. 108 (2012) 093002.

[40] M. J. Colbrook, X. Ma, P. F. Hopkins, J. Squire, Scaling laws of passive-scalar diffusion in the interstellar medium, Monthly Notices of the Royal Astronomical Society 467 (2017) 2421–2429.

[41] B. M. Regner, et al., Anomalous diffusion of single particles in cytoplasm, Biophys. J. 104 (2013) 1652–1660.

[42] Z. Zhang, U. Angst, A dual-permeability approach to study anomalous moisture transport properties of cement-based materials, Transport in Porous Media 135 (2020) 59–78.

[43] J.-H. Jeon, N. Leijnse, L. B. Oddershede, R. Metzler, Anomalous diffusion and power-law relaxation of the time averaged mean squared displacement in worm-like micellar solutions, New J. Phys. 15 (2013) 045011.

[44] T. Sandev, A. Chechkin, H. Kantz, R. Metzler, Diffusion and Fokker-Planck-Smoluchowski equations with generalized memory kernel, Fract. Calc. Appl. Anal. 18 (2015) 1006–1038.

[45] E. Montroll, G. Weiss, Random walks on lattices. II, J. Math. Phys. 6 (1965) 167–181.

[46] R. Metzler, J. Klafter, The random walk's guide to anomalous diffusion: a fractional dynamics approach, Phys. Rep. 339 (2000) 1–77.

[47] A. Kochubei, General fractional calculus, evolution equations, and renewal processes, Integer. Equ. Oper. Theory 71 (2011) 583–600.

[48] A. Hanyga, A comment on a controversial issue: A generalized fractional derivative cannot have a regular kernel, Fract. Calc. Appl. Anal. 23 (2020) 211–223.

[49] T. Sandev, R. Metzler, A. Chechkin, From continuous time random walks to the generalized diffusion equation, Fract. Calc. Appl. Anal. 21 (2018) 10–28.

[50] F. Mainardi, Fractional Calculus and Waves in Linear Viscoelesticity: An introduction to Mathematical Models, Imperial College Press, London, 2010.

[51] M. F. Shlesinger, G. M. Zaslavsky, U. Frisch, Lévy Flights and Related Topics, Springer-Verlag, Berlin, 1995.

[52] R. Zwanzig, Nonequilibrium Statistical Mechanics, Oxford Univ. Press, New York, 2001.

[53] E. Lutz, Fractional Langevin equation, Phys. Rev. E 64 (2001) 051106.

[54] T. Sandev, Z. Tomovski, Fractional Equations and Models, Springer Cham, 2019.

[55] J. Masoliver, G. H. Weiss, Finite-velocity diffusion, Eur. J. Phys. 17 (1996) 190.

[56] O. Heaviside, On induction between parallel wires, J. Soc. Telegraph Eng. 9 (1880) 427–458.

[57] C. Cattaneo, Sulla conduzione del calore, Atti del Seminario Matematico e Fisico dell'Università di Modena 3 (1948) 3–21.

[58] P. Vernotte, Les paradoxes de la théorie continue de l'équation de la chaleur, Comptes Rendus de l'Académie des Sciences 246 (1958) 3154–3155.

[59] G. H. Weiss, Some applications of persistent random walks and the telegrapher's equation, Physica A 311 (2002) 381–410.

[60] T. Pietrzak, A. Horzela, K. Górska, The generalized telegraph equation with moving harmonic source: Solvability using the integral decomposition technique and wave aspects, Int. J. Heat Mass Transf. 225 (2024) 125373.

[61] K. Górska, Integral decomposition for the solutions of the generalized Cattaneo equation, Phys. Rev. E 104 (2021) 024113.

[62] K. Górska, A. Horzela, E. K. Lenzi, G. Pagnini, T. Sandev, General Cattaneo (telegrapher's) equation in modeling anomalous diffusion phenomena, Phys. Rev. E 102 (2020) 022128.

[63] A. Compte, R. Metzler, The generalized Cattaneo equation for the description of anomalous transport processes, J. Phys. A: Math. Gen. 30 (1997) 7277.

[64] E. Orsingher, L. Beghin, Time-fractional telegraph equations and telegraph process with Brownian time, Probab. Theory Relat. Fields 128 (2004) 141.

[65] E. Awad, On the time-fractional Cattaneo equation of distributed order, Physica A 518 (2019) 210.

[66] T. Kosztołowicz, Cattaneo-type subdiffusion-reaction equation, Phys. Rev. E 90 (2014) 042151.

[67] K. D. Lewandowska, T. Kosztołowicz, Application of generalized Cattaneo equation to model subdiffusion impedance, Acta Phys. Pol. B 39 (5), (2008) 1211.

[68] A. Madhukar, Y. Park, W. Kim, H. J. Sunaryanto, R. Berlin, L. P. Chamorro, J. Bentsman, M. Ostoja-Starzewski, Heat conduction in porcine muscle and blood: experiments and time-fractional telegraph equation model, J. R. Soc. Interface 16 (2019) 20190726.

[69] Y. Povstenko, M. Ostoja-Staszewski, Doppler effect described by the solutions of the Cattaneo telegrapher's equation, Acta Mech. 232 (2021) 725.

[70] Y. Povstenko, M. Ostoja-Staszewski, Fractional telegraph equation under moving time-harmonic impact, Int. J. Heat and Mass Transfer 182 (2022) 121958.

[71] Y. Povstenko, M. Ostoja-Staszewski, T. Kyrylych, Fractional telegraph equation under moving time-harmonic impact, Int. J. Heat and Mass Transfer (2023) 121958.

[72] E. Bazhlekova, Subordination principle for space-time fractional evolution equations and some applications, Integr. Transf. Spec. Funct. 30 (2019) 431–452.

[73] K. Górska, A. Horzela, Subordination and memory dependent kinetics in diffusion and relaxation phenomena, Fract. Calc. Appl. Anal. 26 (2023) 480–512.

[74] H. Fogedby, Langevin equations for continuous time Lévy flights, Phys. Rev. E 50 (1994) 1657–1660.

[75] R. Gorenflo, F. Mainardi, A. Vivoli, Continuous time random walk and parametric subordination in fractional diffusion, Chaos, Solitons & Fractals 34 (2007) 87–103.

[76] R. Gorenflo, F. Mainardi, Subordination pathways to fractional diffusion, Eur. Phys. J. Spec. Top. 193 (2011) 119–132.

[77] I. Sokolov, Solution of a class of non-Markovian Fokker-Planck equation, Phys. Rev. E 66 (2002) 041101.

[78] A. Efros, The application of the operational calculus to the analysis, Mat. Sb. 42 (1935) 699–706.

[79] T. Pietrzak, K. Górska, A. Horzela, L. Kocarev, Can the Doppler be useful for a benchmark analysis of the wave-like properties of memory-dependent telegraphers' equation, Chaos 35 (2025) 023134.

[80] B. Boashash, Time-Frequency Analysis: Theory and Applications, Elsevier Science, San Diego, 2003.

[81] K. Górska, T. Pietrzak, T. Sandev, Z. Tomovski, Volterra-Prabhakar function of distributed order and some applications, J. Comput. Appl. Math. 433 (2023) 115306.

[82] D. Zhao, S. HoangGuang, Anomalous relaxation model based on the fractional derivative with a Prabhakar like kernel, Z. Angew. Math. Phys. 70 (2019) 42.

[83] T. Sandev, Z. Tomovski, J. Dubbeldam, A. Chechkin, Generalized diffusion-wave equation with memory kernel, J. Phys. A: Math. Theor. 52 (2019) 015201.

[84] R. Schilling, R. Song, Z. Vondracek, Bernstein Functions. Theory and Applications, De Gruyter, Berlin/Boston, 2012.

[85] A. Ansari, On the Volterra μ-functions and m-wright functions as kernels and eigenfunctions of Volterra type integral operators, Fract. Calc. Appl. Anal. 19 (2) (2016) 567–572.

[86] Z. Tomovski, K. Górska, T. Pietrzak, R. Metzler, T. Sandev, Anomalous and ultraslow diffusion of a particle driven by power-law-correlated and distributed-order noises, J. Phys. A: Math. Theor. 57 (2024) 235004.

[87] F. Mainardi, P. Pironi, The fractional Langevin equation: Brownian motion revisited, Extr. Math. 10 (1996) 140.

[88] M. Despósito, A. Viñales, Memory effects in the asymptotic diffusive behavior of a classical oscillator described by a generalized Langevin equation, Phys. Rev. E 77 (2008) 031123.

[89] Y. Klimontovich, Turbulent Motion and the Structure of Chaos, Kluwer, 1991.

5. Articles

The results presented in this PhD thesis are contained in the following articles:

- T. Pietrzak, A. Horzela, K. Górska
  The generalized telegraph equation with moving harmonic source: Solvability using the integral decomposition technique and wave aspects
  International Journal of Heat and Mass Transfer **225**, 125373 (2024)

- T. Pietrzak, A. Horzela, K. Górska, L. Kocarev
  Can the Doppler be useful for a benchmark analysis of the wave-like properties of memory-dependent telegraphers' equation
  Chaos **35**, 023134 (2025)

- K. Górska, T. Pietrzak, T. Sandev, Z. Tomovski
  Volterra-Prabhakar function of distributed order and some applications
  Journal of Computational and Applied Mathematics **433**, 115306 (2023)

- Z. Tomovski, K. Górska, T. Pietrzak, R. Metzler, T. Sandev
  Anomalous and ultraslow diffusion of a particle driven by power-law-correlated and distributed-order noises
  Journal of Physics A: Mathematical and Theoretical **57**, 235004 (2024)

International Journal of Heat and Mass Transfer 225 (2024) 125373

Contents lists available at ScienceDirect

International Journal of Heat and Mass Transfer

journal homepage: www.elsevier.com/locate/ijhmt

The generalized telegraph equation with moving harmonic source: Solvability using the integral decomposition technique and wave aspects

T. Pietrzak [a,b], A. Horzela [b], K. Górska [b,*]

[a] Kraków Interdisciplinary Doctoral School (KISD), ul. Eljasza-Radzikowskiego 152, PL 31342 Kraków, Poland

[b] H. Niewodniczański Institute of Nuclear Physics, Polish Academy of Sciences, ul. Eljasza-Radzikowskiego 152, PL 31342 Kraków, Poland

ARTICLE INFO

Keywords:
Generalized telegraph equation with moving harmonic source
Integral decomposition
Frequency shift
Doppler-like effects
Wave fronts

ABSTRACT

The paper is devoted to study the frequency shift in the solution of the generalized telegraph equation with a moving point-wise harmonic source. This equation contains the nonlocality in time derivatives which is expressed by the memory functions $\eta(t)$ and $\gamma(t)$, where $\eta(t)$ smears the second time-derivative and $\gamma(t)$ the first one. Moreover, in the Laplace domain we have $\hat{\eta}(s) = \hat{\gamma}^2(s)$. The generalized telegraph equation with an external source is solved by using the integral decomposition which allows us to write this solution as a product of the solution of the telegrapher equation with harmonic source and $f_{\hat{\gamma}}(\xi, t)$ which is a function of the Laplace transform of memory function γ. Such obtained solution manifests the frequency shift which is illustrated in three examples of the memory functions $\gamma(t)$: the localized case, its mixture with power-law, and the power-law case only. We show that only the first two cases have the wave front and the Doppler-like shift. The third example, despite the lack of wave fronts, also manifests the frequency shift. Thus it turns out that the frequency shift occurs regardless of the existence of a wave front, but it is more visible when such a front exists.

1. Introduction

The telegraph, called also telegrapher's, equation

$$\partial_x^2 u(x,t) = ck\partial_t u(x,t) + sc\partial_t^2 u(x,t) \tag{1.1}$$

was discovered in 1876 by O. Heaviside who, that time working on improving signaling along submarine cables, found it as the "fundamental equation of telegraphy". If Eq. (1.1) is used to solve signal transmission problems then $u(x,t)$ denotes the voltage at a line point x while c, k and s are capacitance, resistance and inductance, all taken per unit length, respectively.[1] It is also usually assumed that $u(x,t)$ is defined on $(x,t) \in \mathbb{R} \times \mathbb{R}_+$, vanishes for $x \to \pm\infty$ and satisfy initial conditions

$$u(x,0) = u_0(x) \quad \text{and} \quad \partial_t u(x,t)|_{t=0} = 0. \tag{1.2}$$

If compared with the diffusion-like propagation equation proposed 20 years earlier by Sir William Thompson to describe electric transmission line the essential novelty introduced by Heaviside was that he took into account self-inductance which Lord Kelvin had ignored in his model as negligible [1]. From the mathematical point of view Heaviside's discovery changed the type of sought equation from the first order parabolic into the second order hyperbolic one belonging to the class of dissipative wave equations. The latter was familiar to the physicists' community and successfully applied for modeling processes quantitatively different from diffusion-like spreading. So it was natural that during the next years the telegraph equation found applications whose utility went far beyond electrical engineering and provided physicists with a versatile tool to study a large variety of phenomena observed in the realm of physics, chemistry and life sciences. In 1948 Eq. (1.1) appeared in the theory of heat transfer along with the paper "Sulla conduzione del calore" by C. Cattaneo [2]. The paper went unnoticed for 10 years but gained growing attention after publication in 1958, one after the other, two short notes by P. Vernotte [3] and C. Cattaneo himself [4]. Motivated by the desire to avoid instantaneous propagation of the temperature field $\mathcal{T}(\tau; x,t)$ resulting in the Fourier-Kirchoff parabolic heat equation as a consequence of using the Fourier heat conduction law $j(x,t) = -\kappa \operatorname{grad} \mathcal{T}(x,t)$ linking the heat flux $j(x,t)$ and the temperature gradient $\operatorname{grad} \mathcal{T}(x,t)$ both

* Corresponding author.
E-mail addresses: tobiasz.pietrzak@ifj.edu.pl (T. Pietrzak), andrzej.horzela@ifj.edu.pl (A. Horzela), katarzyna.gorska@ifj.edu.pl (K. Górska).

[1] In general the RHS of Eq. (1.1) may be completed by adding the term $kg\,u(x,t)$ where g is the line conductance.

https://doi.org/10.1016/j.ijheatmasstransfer.2024.125373
Received 14 January 2024; Accepted 23 February 2024
Available online 12 March 2024

these authors independently proposed to replace the Fourier law by relation $j(\tau;x,t)+\partial_t j(\tau;x,t)/\tau=-\kappa\,\mathrm{grad}\,\mathcal{T}(\tau;x,t)$, nowadays known as the modified Fourier, or Maxwell-Cattaneo, constitutive relation. This, if merged with the energy conservation law, gave the hyperbolic equation

$$\partial_t^2\mathcal{T}(\tau;x,t)+\tau^{-1}\partial_t\mathcal{T}(\tau;x,t)=a^2\partial_x^2\mathcal{T}(\tau;x,t) \tag{1.3}$$

nowadays commonly known among physicists working in the field of kinetic phenomena as the Cattaneo-Vernotte (CV) equation of the heat transport. Completed with the initial conditions

$$\mathcal{T}(\tau;x,0)=\mathcal{T}_0(x) \quad \text{and} \quad \partial_t\mathcal{T}(\tau;x,t)|_{t=0}=0 \tag{1.4}$$

Eqs (1.3), (1.4) are nothing else than Eqs. (1.1) and (1.2), i.e., damped wave equation whose fundamental solution propagates with the velocity a. This naturally leads to questions concerning wave properties of the heat transport phenomena and their coexistence with typical diffusion-like effects. Despite of the fact that pairs of equations (1.1), (1.2) and (1.3), (1.4) are formally identical anyone who tries to answer just mentioned questions has to pay attention that physical meaning of the parameters sitting inside them as well as the requirements put on their solutions may be completely different. Parameters in Eq. (1.1) denote electromagnetic quantities which characterize the transmission line whilst a of Eq. (1.3) reflects a propagation velocity. The time constant $\tau>0$ meets different interpretations. Here we mention two of them: i.) τ denotes some time lag modifying the Fourier heat conduction law to the time nonlocal constitutive relation $j(x,t+\tau)=-\kappa\,\mathrm{grad}\,T(x,t)$ subsequently expanded as the Taylor series restricted to the first order in τ, ii.) τ is a relaxation parameter which enters the solution to the Maxwell-Cattaneo constitutive relation representing $j(x,t)$ as a memory dependent integrated history of $\mathrm{grad}\,T(x,t)$, namely $j(x,t)=-\int_0^t k(t-t')\mathrm{grad}\,T(x,t')\,\mathrm{d}t'$ with the memory kernel $k(t-t')=\tau^{-1}\kappa\exp(-t/\tau)$.[2] Here it should be mentioned that physicists' interest in the telegraph equation proposed as an equation describing transport phenomena started from theoretical investigation of problems related to the finite speed diffusion [11,12] and became much more extensive when it was found that understanding the finite speed diffusion and wave governed heat transfer is a key-tool for studies of exotic properties obeyed by the heat transport in liquid helium. This, the so-called "second sound" effect, was predicted by L. Tisza in 1938 [13], in a much detailed way elaborated by L. D. Landau in 1941 within his theory of superfluidity [14] and soon after confirmed experimentally for helium II in 1944 [15]. Further research showed that the second sound phenomena take place also in solids and may be much better understood if heat transport proceeds by wave propagation rather than by diffusion [16], see also [17] for more contemporary information.

Current applications of the telegraph equation cover a broad range of phenomena occurring in different branches of physics. Focusing attention on the transport processes we recall that its theoretical background, besides of previously quoted Refs. [9,10], has been studied for a plethora of microscopic and macroscopic models, among them those constructed to derive finite speed diffusion equation from the continuous time random walk approach [18], to describe phonon hydrodynamics [20,21] or viscous heat transfer [22] and to study the so-called bio-heat transport taking place in biological tissues [23,24]. Development of fractional dynamics, in particular progress achieved in modeling anomalous diffusion phenomena with fractional calculus, caused that generalized versions of the telegraph equation (GT) involving fractional derivatives have become more and more popular for characterizing diffusive processes [9,19,25,27,28], thermoelasticity [29], chemical reactions [30,31] and specific biological/medical problems such as heat conduction in muscles and blood [32]. Merged with the long-time known Pennes model [33] GT has appeared to be one of the most advantageous tools used in laser therapy to monitor the skin treatment, control the elimination of necrotic area and to minimize damage to the surrounding normal tissues [34,35].

In what follows we assume that the GT equation we are dealing with is a nonlocal in time, i.e., memory dependent, evolution equation. It generalizes the standard local telegraph equation by smearing the time derivatives and replacing them with integro-differential operators.[3] Under this assumption the evolution described by GT equation may be written down as

$$\int_0^t \eta(t-\xi)\partial_\xi^2 T_{\hat{\gamma}}(\tau;x,\xi)\,\mathrm{d}\xi+\tau^{-1}\int_0^t \gamma(t-\xi)\partial_\xi T_{\hat{\gamma}}(\tau;x,\xi)\,\mathrm{d}\xi = a^2\partial_x^2 T_{\hat{\gamma}}(\tau;x,t) \tag{1.5}$$

with initial conditions given by Eq. (1.4). The memory functions $\eta(t)$ and $\gamma(t)$ are coupled in such a way that if $\gamma(t)$ expresses the time smearing of the first derivative then the choice

$$\eta(t)=\int_0^t \gamma(u)\gamma(t-u)\,\mathrm{d}u \quad \text{and} \quad \hat{\eta}(s)=\hat{\gamma}^2(s) \tag{1.6}$$

consistently represents the smearing of the smeared second-time derivative, as discussed and explained in Refs. [19,36].

The telegraph equation itself belongs to the class of dissipative wave equations or, in other words, to the class of wave equations with damping. Thus, one can suspect that its solutions should manifest properties typical for wave phenomena, among them those characteristic for traveling waves. This way outlined goal of research distinguishes our efforts from those concentrated on the description and analysis of temperature oscillations induced in some medium when the classical diffusion equation is coupled to the external harmonic source. These oscillations are customarily named thermal or heat waves although it is known that they are subject to ongoing discussion concerning the comparison of their properties with those characterizing the standard wave motion [37–43].[4]

Treating the telegraph equation as a wave equation we shall focus our investigations on the existence of wave fronts and the Doppler effect which should be noted in solutions describing relevant physical situations. Both these effects have been studied in [45]. The authors of this paper solved, for $x\in\mathbb{R}$ and $t\in\mathbb{R}_+$, the (1+1) telegraph equation with uniformly moving harmonic source and demonstrated that its fundamental solution shares desirable properties, namely the existence of wave fronts and the Doppler effect, in the same manner as observed in solutions to the wave equation with an uniformly moving harmonic source (see Eqs. (13)–(15) and (20)–(23) in Ref. [45]). In the papers [46,47] the same authors looked for the consequences of introducing Caputo fractional time derivatives into the (1+1) and (2+1)

[2] Phenomenology and physical justification of adopting the modified Fourier conduction law as a constitutive relation has been the subject of a long-standing debate, repeatedly critical, see e.g. [5,6], while for other authors being fully justified and obeying fundamental physical meaning, see [7]; for comprehensive discussion and current list of references see [8]. We emphasize that independently from *à priori* postulated form of constitutive relations the CV equation is derivable from general considerations rooted in thermodynamics and kinetic theory [9,10].

[3] By smearing the time derivatives we understand convoluting them with some nonlocal time dependent kernels which are not *à priori* assumed to be connected with commonly used fractional derivatives. Thus the goal of our research does not repeat the goals of investigations performed e.g. in [25] where GT involving the Caputo-Djhershyan derivatives of orders α and 2α has been used to show the probability context of solutions to such an equation or applying the Riemann-Liouville derivatives to study modeling of transmission lines involving memory dependent (fractional) L and C elements [26].

[4] Doubts concerning the physical meaning of such class of solutions, analogical to steady waves, include e.g., lack of wave fronts, instantaneous propagation and null energy transport [37,44].

dimensional telegraph equation impacted by moving time-harmonic source. They considered cases of the so-called "wave-type" model involving time derivatives of the order $1 \le \alpha < 2$ and besides of that the usual second order time derivative and "heat-type" model involving time derivatives of the order $1 \le \alpha < 2$. Analysis of the solutions led them to the conclusion that the "wave-type" model exhibits previously mentioned "classical" wave properties while the "heat-type" does not. Having Refs. [45–47] in mind, and feeling convinced that the most natural memory dependent extension of the telegraph equation is Eq. (1.5), we ask the question: *Do the classical wave properties survive for solutions of such proposed GT, i.e., does compliance of the time non-locality reflected in memory effects leaves the wave fronts and velocity dependent frequency shifts (or their track(s)) existing and observable?*. Thus the main goal of our research is to look for the answer to this question.

1.1. Interlude - the Doppler effect

The best known example of velocity dependent frequency shift observed in everyday life is the longitudinal Doppler effect manifested by acoustic waves. For idealized physical situation the effect relies on the observation that detected pitch changes in dependence of the emitter *vs* detector relative velocity and is explained within the course of school physics using only kinematical properties of the wave motion. Considering more details we can state that in order to detect and analyze the Doppler effect three basic elements are needed: an observer who may move with a velocity V, an emitter, i.e., a signal (wave) source, which may move with a velocity v, and the signal propagation speed, denoted by a, known for the signal being observed and depending on properties of the medium in which the signal propagates. The signature of Doppler's effect appears if a stationary observer detects a signal emitted by a moving source and finds out that the received frequency Ω differs, for any $v \neq 0$, from the emitted frequency ω: it is higher during the approach, identical at the instant of passing by, and lower during the recession. For periodic sinusoidal signal it is easy to derive the relation $\Omega_\pm = \omega a/(a \pm v)$ which, if supplemented by + as the sign convention for approach and − for recession, quantitatively links both frequencies.[5] For $v/a \ll 1$, situation typically met in acoustics, $\Omega_\mp$ is estimated by $\omega(1 \pm v/a)$ commonly used to relate frequency shift and velocity in everyday life [48]. Within the above sketched idealized picture the characteristic feature of the Doppler effect is sudden and discontinuous change of the observed frequency $\Omega_+ - \Omega_- = \Delta\Omega_\pm = \omega a/\left[1-(v/a)^2\right]$. This occurs at the instant of time in which the observer and the source are passing each other. If the observer focuses attention on the wave-like behavior of the signal then the phenomenon would be visualized even more spectacularly. Observed distances separating subsequent wave crests, in fact representing more or less distorted wavelenghts, if compared with those of emitted waves are shorter if the observer and the source are approaching each other but suddenly become longer with the instant of time in which the signal source and observer start to move away. Qualitatively the same effect we notice when are watching wave-like phenomena taking place in our environment, even if they need modeling going far beyond consideration of simple periodic signals. This entitles us to make a statement that detection, even qualitatively, of just mentioned changes of the wavelengths shows the track of the Doppler effect.

2. Content of the paper, its goals and methods been used

Studies of the Doppler-like phenomena influencing solutions to the telegraph-like wave equations have appeared in physical literature quite recently. The research has been motivated by the desire to explain effects accompanying the heat transfer occurring during the laser-assisted surgery procedures [32] and relies on the theoretical background proposed and developed in [45–47]. To analyze the problem from the physical point of view the authors have extended either the telegraph equation or its fractional version by adding to it an external harmonic current, next have solved such obtained equations and analyzed their solutions in order to identify modulation and wave front terms. The signature of a Doppler-like shift has been looked for in the parts of solutions that contain the frequency ω characterizing the wave emitted by the source. Following Ref. [45] we begin with Eq. (1.1) modified by an external harmonic point-wise source $Q\delta(x - vt)\exp(i\omega t)$, $Q > 0$ moving with the speed $v < a$ along the line determined by the δ-Dirac distribution and joining the source and the observer. That leads to

$$\partial_t^2\, \mathfrak{T}_1(\tau, Q; x, t) + \tau^{-1}\partial_t\, \mathfrak{T}_1(\tau, Q; x, t) - a^2\partial_x^2\, \mathfrak{T}_1(\tau, Q; x, t) = Q\delta(x - vt)\, e^{i\omega t} \tag{2.1}$$

with the initial condition Eq. (1.4). For $Q = 0$ the source vanishes and we get Eq. (1.1) together with its τ-dependent limit cases, namely the wave (for $\tau \to \infty$) and diffusion (heat) (for $\tau \to 0$) equations. For further use note that the case $Q = 0$ corresponds the homogeneous equation (1.1) with its general solution $\mathfrak{T}_1(\tau, 0; x, t) = T(\tau; x, t)$ while the solution of the inhomogeneous equation with $Q > 0$, $\mathfrak{T}_1(\tau, Q; x, t)$ can be represented as the sum of $T(\tau; x, t)$ and some special solution of Eq. (2.1). To distinguish these cases in a more visible way we will use for $Q > 0$ gothic letters, e.g., $\mathfrak{T}$, and roman characters T, for $Q = 0$. Having at hands these remarks we shall organize the paper as follows. In Sect. 3 we explain how to construct the time-smeared, either memory dependent, telegraph equation with a moving point-wise harmonic source. The solution method applied by us stems from the integral decomposition approach [49] closely related to the operator methods [61,62] and analytic subordination [36,55]. The second pillar of our technique is the operational calculus, first of all application of the Laplace-Fourier (LF) transform merged with the Efros theorem (see Appendix A). Obtained GT equation, being an inhomogeneous integro-differential equation with external current, reads[6]

$$\int_0^t \eta(t-\xi)\partial_\xi^2 \mathfrak{T}_{\hat{\gamma}}(\tau; x, \xi)\, d\xi + \tau^{-1}\int_0^t \gamma(t-\xi)\partial_\xi \mathfrak{T}_{\hat{\gamma}}(\tau; x, \xi)\, d\xi - a^2\partial_x^2 \mathfrak{T}_{\hat{\gamma}}(\tau; x, t) = \left[Q\delta(x - vt)\, e^{i\omega t}\right]_{\mathcal{U}(\hat{\gamma})}. \tag{2.2}$$

Operation $\mathcal{U}(\hat{\gamma})$ and the solution to Eq. (2.2) are found in Sect. 4. Applications of the operational technique enable us to write down just the mentioned solution as a convolution-type integral whose integrand is the product of the solution to the memory-less equation (in our case Eq. (2.1)) and well-defined function, named the subordination function, depending solely on the memory. The analytic form of the solution to Eq. (2.1) is known [45,46] and thus we have at hands all elements needed for our construction to work. The solution $\mathfrak{T}_{\hat{\gamma}}(\tau, Q; x, t)$ is a sum of two parts: the solution $\mathfrak{T}_{\hat{\gamma};1}(\tau, 0; x, t) \equiv T_{\hat{\gamma}}(\tau; x, t)$ of the homogeneous equation and the special solution $\mathfrak{T}_{\hat{\gamma};2}(\tau, Q; x, t)$ of the inhomogeneous equation (2.1). Only the second part depends on Q and thus only it manifests the frequency shift, if any. In Sect. 4.4 we show that the shift observed in $\mathfrak{T}_{\hat{\gamma};2}(\tau, Q; x, t)$ is linked to the solution of the generalized diffusion-wave equation $\mathfrak{w}_{\hat{\gamma};2}(Q; x, t)$ and can be represented as an extra term which perturbs it. In Sect. 5 the Doppler-like effects are illustrated in three examples of evolution equations with the memory functions built in: i.) the localized one, ii.) the power-law memory function and iii.) the superposition of the previous cases. The results of the paper are

[5] If the observer is not at rest but moves with the uniform velocity V then instead of frequencies $\Omega_\pm$ it notes the frequencies $\Psi_\pm = \Omega_\pm\left(1 \mp V/a\right) = \omega(a \mp V)/(a \pm v)$ expected from $\Omega_\pm$ and the Galilean transformation rule for velocities.

[6] We recall once more that we do not postulate *á priori* any shape of the memory function. In this sense we go beyond the use of common fractional equations and thus prefer to call equations under study "memory dependent".

discussed and concluded in Sects 6 and 7. Four appendices contain brief information on mathematical tools used throughout the main text.

3. GT equation: memory dependence and subordination hidden behind it

As mentioned in the Introduction solution to the time local Eq. (2.1) is explicitly given in [45]. We shall use this result to get solutions of the memory dependent Eq. (1.5) by applying the methodology of integral decomposition and operational calculus without going into details of the subordination technique.

Integral decompositions are known to be an effective tool that makes solvable many problems of transport phenomena, in particular those related to the anomalous diffusion and non-Debye relaxation. They were introduced in [49] as stemming from the probability and stochastic processes-based analysis of anomalous kinetics and developed in [50–52]. An alternative approach, closer to the analysis of evolution equations, was highlighted and pushed forward in [53,54] where the relation between Markovian and non-Markovian descriptions of anomalous diffusion and non-Debye relaxation was extensively studied. Recently, new light has been shed on the mechanism of integral decomposition with the rediscovery and novel use of the Efros theorem (Appendix A) which has opened the possibility to put the integral decomposition in the framework of mathematical analysis [55]. The Efros theorem not only enables one to exploit well-defined operational rules in order to invert the LF transforms of evolution equations describing the system [19,36] but also explains the mathematical meaning of integral decompositions and provides us with a signpost toward physical interpretation of it [55]. According to that formalism physically acceptable solutions of the memory-dependent equations are represented by convolution-type integrals. Integrands that form integral decompositions appear to be products of solutions to the relevant time-local evolution equations considered to be governed by some time-like (positive and never decreasing but in general obeying a random character) variable ξ, called the internal time, and memory-dependent functions $f_{\hat{\gamma}}(\xi,t)$. The functions $f_{\hat{\gamma}}(\xi,t)$ determine the relation between irregularly ticking internal time ξ, e.g. randomly distributed waiting times spent by a diffusing walker at some locations x's and regularly ticking laboratory time measured using periodic phenomena. They are assumed to map the variable ξ onto physical (laboratory) time t in such a way that the map $\xi \leftrightarrow t$ obeys all properties required from the probability distributions. Supported by this general approach we will look for solutions to the time-smeared Eq. (2.1) in the form

$$\mathfrak{T}_{\hat{\gamma}}(\tau,Q;x,t) = \int_0^\infty \mathfrak{T}(\tau,Q;x,\xi) f_{\hat{\gamma}}(\xi,t)\,\mathrm{d}\xi, \tag{3.1}$$

where $\mathfrak{T}(\tau,Q;x,\xi)$ is the solution to Eq. (2.1) while $f_{\hat{\gamma}}(\xi,t)$ is just mentioned probability distribution $\xi \leftrightarrow t$ to be recovered from the knowledge of the memory function $\gamma(t)$ (cf. Eq. (1.6)).

Assuming that

$$f_{\hat{\gamma}}(\xi,t) = \mathscr{L}^{-1}[\hat{\gamma}(s)\,\mathrm{e}^{-\xi s\hat{\gamma}(s)};t], \tag{3.2}$$

we will show that the time-smeared version of Eq. (2.1) reads

$$\int_0^t \Big[\eta(t-\xi)\partial_\xi^2 + \tau^{-1}\gamma(t-\xi)\partial_\xi\Big]\,\mathfrak{T}_{\hat{\gamma}}(\tau,Q;x,\xi)\,\mathrm{d}\xi - a^2\partial_x^2\,\mathfrak{T}_{\hat{\gamma}}(\tau,Q;x,t) = Q\int_0^\infty f_{\hat{\gamma}}(\xi,t)\delta(x-\upsilon\xi)\,\mathrm{e}^{\mathrm{i}\omega\xi}\,\mathrm{d}\xi \tag{3.3}$$

with the initial conditions Eq. (1.2) and the memory functions $\eta(t)$ and $\gamma(t)$ related by Eq. (1.6). Performing the integration present in the right-hand side (RHS) of Eq. (3.3) with Eq. (3.2) put in we have

$$Q\int_0^\infty f_{\hat{\gamma}}(\xi,t)\delta(x-\upsilon\xi)\,\mathrm{e}^{\mathrm{i}\omega\xi}\,\mathrm{d}\xi = \frac{Q}{\upsilon}\mathscr{L}^{-1}\Big[\hat{\gamma}(s)\,\mathrm{e}^{-\frac{x}{\upsilon}s\hat{\gamma}(s)};t\Big]\,\mathrm{e}^{\mathrm{i}\omega\frac{x}{\upsilon}}\,\Theta\Big(\frac{x}{\upsilon}\Big) \tag{3.4}$$

Eq. (3.3) describes the memory-dependent answer of the system to the stimulus generated by the external time-local source. Note that the reaction of the system takes into account its previous history which depends on the internal properties of the system under investigation but does not affect the external source.

To demonstrate how to pass from Eq. (2.1) to Eq. (3.3) we will use the Efros theorem (see Appendix A). The proof goes in four steps. At first, we write down Eq. (2.1) in terms of ξ instead of t, multiply each of its terms by $f_{\hat{\gamma}}(\xi,t)$ and integrate the result over $\xi \in \mathbb{R}_+$. So we have

$$\int_0^\infty f_{\hat{\gamma}}(\xi,t)\Big[\partial_\xi^2\,\mathfrak{T}(\tau,Q;x,\xi) + \tau^{-1}\partial_\xi\,\mathfrak{T}(\tau,Q;x,\xi) - a^2\partial_x^2\,\mathfrak{T}(\tau,Q;x,\xi) - Q\delta(x-\upsilon\xi)\,\mathrm{e}^{\mathrm{i}\omega\xi}\Big]\,\mathrm{d}\xi = 0. \tag{3.5}$$

Next, we rewrite the square bracket in Eq. (3.5) as the inverse Laplace transform[7]

$$\mathscr{L}^{-1}\Big\{[s^2\hat{\mathfrak{T}}(\tau,Q;x,s) - sT_0(x)] + \tau^{-1}[s\hat{\mathfrak{T}}(\tau,Q;x,s) - T_0(x)] - a^2\partial_x^2\hat{\mathfrak{T}}(\tau,Q;x,s) - \frac{Q}{\upsilon}\,\mathrm{e}^{-\frac{x}{\upsilon}(s-\mathrm{i}\omega)}\,\Theta\Big(\frac{x}{\upsilon}\Big);\xi\Big\}, \tag{3.6}$$

where $\mathfrak{T}(\tau,Q;x,t=0)=T_0(x)$ and $\dot{\mathfrak{T}}(\tau,Q;x,t)|_{t=0}=0$. Thus, the integrand of Eq. (3.6) is the product of two inverse Laplace transforms. Using once again the Efros theorem allows us to express Eq. (3.6) as

$$\mathscr{L}^{-1}\Big\{\hat{\gamma}(s)\Big[s^2\hat{\gamma}^2(s)\hat{\mathfrak{T}}(\tau,Q;x,s\hat{\gamma}(s)) - s\hat{\gamma}(s)T_0(x)\Big] + \tau^{-1}\hat{\gamma}(s)\Big[s\hat{\gamma}(s)\hat{\mathfrak{T}}(\tau,Q;x,s\hat{\gamma}(s)) - T_0(x)\Big] - a^2\partial_x^2\Big[\hat{\gamma}(s)\hat{\mathfrak{T}}(\tau,Q;x,s\hat{\gamma}(s)\Big] - \hat{\gamma}(s)\frac{Q}{\upsilon}\,\mathrm{e}^{\frac{x}{\upsilon}(\mathrm{i}\omega-s\hat{\gamma}(s))}\,\Theta(x/\upsilon);t\Big\} = 0. \tag{3.7}$$

To proceed further we define

$$\hat{\mathfrak{T}}_{\hat{\gamma}}(\tau,Q;x,s) = \hat{\gamma}(s)\hat{\mathfrak{T}}(\tau,Q;x,s\hat{\gamma}(s)), \tag{3.8}$$

being the Laplace transform of Eq. (3.1). Notice that for $\hat{\gamma}(s)=1$ (i.e., $\gamma(t)=\delta(t)$) we get $\hat{\mathfrak{T}}_1(\tau,Q;x,s)\equiv\hat{\mathfrak{T}}(\tau,Q;x,s)$. The same equivalency appears in the t domain. As the third step of the proof we substitute Eq. (3.8) into Eq. (3.7). That gives

$$\mathscr{L}^{-1}\Big\{\hat{\gamma}^2(s)\Big[s^2\hat{\mathfrak{T}}_{\hat{\gamma}}(\tau,Q;x,s) - sT_0(x)\Big] + \tau^{-1}\hat{\gamma}(s) \times\Big[s\hat{\mathfrak{T}}_{\hat{\gamma}}(\tau,Q;x,s) - T_0(x)\Big] - a^2\partial_x^2\hat{\mathfrak{T}}_{\hat{\gamma}}(\tau,Q;x,s);t\Big\} = \mathscr{L}^{-1}[\hat{\gamma}(s)\frac{Q}{\upsilon}\,\mathrm{e}^{\frac{x}{\upsilon}(\mathrm{i}\omega-s\hat{\gamma}(s))}\,\Theta(x/\upsilon);t]. \tag{3.9}$$

The fourth step is based on using the Laplace convolution for the inverse Laplace transform sitting in Eq. (3.9). From the first component of its LHS, i.e. $\hat{\gamma}^2(s)[s^2\hat{\mathfrak{T}}_{\hat{\gamma}}(\tau,Q;x,s) - sT_0(x)]$ we get that it can be rewritten as

[7] The symbol '∧' denotes the Laplace transform of $f(t)$ such that $\hat{f}(s) = \mathscr{L}[f(t);s]$. The Laplace coordinates are given by $s \div t$.

$$\int_0^t \mathscr{L}^{-1}[\hat{\gamma}^2(s);t-\xi]\mathscr{L}^{-1}[s^2\hat{\mathfrak{T}}_{\hat{\gamma}}(\tau,Q;x,s)-sT_0(x);\xi]\,\mathrm{d}\xi$$

$$=\int_0^t \eta(t-\xi)\partial_\xi^2\,\mathfrak{T}_{\hat{\gamma}}(\tau,Q;x,\xi)\,\mathrm{d}\xi,$$

where $\mathfrak{T}_{\hat{\gamma}}(\tau,Q;x,t)=\mathscr{L}^{-1}[\hat{\mathfrak{T}}_{\hat{\gamma}}(\tau,Q;x,s);t]$ and $\eta(t)$ satisfies Eq. (1.6). The Laplace inverse of $\tau^{-1}\hat{\gamma}(s)\big[s\hat{\mathfrak{T}}_{\hat{\gamma}}(\tau,Q;x,s)-T_0(x)\big]$ gives

$$\tau^{-1}\int_0^t \mathscr{L}^{-1}[\hat{\gamma}(s);t-\xi]\mathscr{L}^{-1}[s\hat{\mathfrak{T}}_{\hat{\gamma}}(\tau,Q;x,s)-T_0(x);\xi]\,\mathrm{d}\xi$$

$$=\tau^{-1}\int_0^t \gamma(t-\xi)\partial_\xi\,\mathfrak{T}_{\hat{\gamma}}(\tau,Q;x,\xi)\,\mathrm{d}\xi.$$

Obviously, the Laplace inverse of the third component produces $-a^2\partial_x^2\hat{\mathfrak{T}}_{\hat{\gamma}}(\tau,Q;x,t)$. Thus, we obtain the LHS of Eq. (3.3). Taking the inverse Laplace transform of the RHS of Eq. (3.9) and employing the Efros theorem once more we arrive at the RHS of Eq. (3.3). This completes the proof.

4. Remarks on solutions to the telegraph and GT equations with moving harmonic impact

4.1. Telegraph equation with a moving harmonic source

Eq. (3.3) is an inhomogeneous equation with the heterogeneity introduced by the external source Eq. (3.4). Recall that its solution $\mathfrak{T}_{\hat{\gamma}}(\tau,Q;x,t)$ can be represented as the sum of the general solution to its homogeneous, still memory dependent, counterpart (i.e., Eq. (3.3) with $Q=0$) and a special solution of inhomogeneous equation (3.3) for $Q>0$. This may be written down as

$$\mathfrak{T}_{\hat{\gamma}}(\tau,Q;x,t)=\mathfrak{T}_{\hat{\gamma};1}(\tau,0;x,t)+\mathfrak{T}_{\hat{\gamma};2}(\tau,Q;x,t), \tag{4.1}$$

where according to the rules of the integral decomposition method elucidated in the previous section

$$\mathfrak{T}_{\hat{\gamma};j}(\tau,Q;x,t)=\int_0^\infty \mathfrak{T}_{\hat{\gamma}=1;j}(\tau,Q;x,\xi)f_{\hat{\gamma}}(\xi,t)\,\mathrm{d}\xi \tag{4.2}$$

and the second subscript j distinguishes the cases $Q=0$ for $j=1$ and $Q>0$ for $j=2$. Notice that the initial condition for $\mathfrak{T}_{\hat{\gamma}}(\tau,Q;x,0)$, denoted $T_0(x)$, may be shared between the functions sitting in Eq. (4.1) as follows: $\mathfrak{T}_{\hat{\gamma};1}(\tau,Q;x,t)$ contains all information on $T_0(x)$ whereas $\mathfrak{T}_{\hat{\gamma};2}(\tau,Q;x,t)$ does not depend on $T_0(x)$ and we can assume that it is obtained from Eq. (3.3) for $T_0(x)=0$. To make the notation introduced in Eq. (4.2) less heavy we denote solutions to the homogeneous equations as $\mathfrak{T}_{\hat{\gamma}=1;1}(\tau,0;x,t)\equiv T(\tau;x,t)$ and $\mathfrak{T}_{\hat{\gamma};1}(\tau,0;x,t)\equiv T_{\hat{\gamma}}(\tau;x,t)$. Both functions $T(\tau;x,t)$ and $T_{\hat{\gamma}}(\tau;x,t)$ do not contain the frequency ω and as such will not give a contribution to the frequency shift. Nevertheless the knowledge of their properties is needed for our further considerations. We recall required information following Refs. [19,36,45–47] as well as the literature quoted therein.

The function $\mathfrak{T}_{1;1}(\tau,0;x,t)$ which solves the homogeneous telegraph equation (2.1) (or Eq. (1.5) with $\eta(t)=\gamma(t)=\delta(t)$) if written down in the LF space reads

$$\tilde{\hat{\mathfrak{T}}}_{1;1}(\tau,0;\kappa,s)\equiv\tilde{\hat{T}}(\tau;\kappa,s)=\frac{(s+1/\tau)\tilde{T}_0(\kappa)}{a^2\kappa^2+s^2+s/\tau}. \tag{4.3}$$

The general form of $T(\tau;x,t)$ can be found in [56, Eq. (102) on p. 300] and/or [57, Eq. (7.4.28)]. Taking into account Eq. (1.2) (see Appendix B for details) it figures out

$$T(\tau;x,t)=\frac{1}{2}\,\mathrm{e}^{-\frac{t}{2\tau}}[T_0(x-at)+T_0(x+at)]+\frac{1}{4\tau a}\,\mathrm{e}^{-\frac{t}{2\tau}}$$
$$\times\int_{x-at}^{x+at}\Big[\frac{ta}{\sqrt{a^2t^2-|y-x|^2}}I_1\Big(\frac{1}{2a\tau}\sqrt{a^2t^2-|y-x|^2}\Big)$$
$$+I_0\Big(\frac{1}{2a\tau}\sqrt{a^2t^2-|y-x|^2}\Big)\Big]T_0(y)\,\mathrm{d}y \tag{4.4}$$

where $I_\nu(\cdot)$ for $\nu=0,1$ are the modified Bessel functions of the first kind. Note that $T(\tau;x,t)$ inherits behavior of $T_0(x)$ in the sense that if $T_0(x)\neq 0$ for $x\in\Delta(t)$ and $T_0(x)=0$ outside this region then $T(\tau;x,t)$ also will be nonzero only inside a finite region. For the localized (δ-like) initial conditions, $T(\tau;x,t)$ can be found in, e.g., [12,36,58,59].

The function $\mathfrak{T}_{1;2}(\tau,Q;x,t)$ solves Eq. (2.1) in the presence of the point-wise source, i.e. with $Q>0$. In the LF domain it figures out

$$\tilde{\hat{\mathfrak{T}}}_{1;2}(\tau,Q;\kappa,s)=\frac{Q}{s-\mathrm{i}(\omega+\kappa v)}\,\frac{1}{a^2\kappa^2+s^2+s/\tau}, \tag{4.5}$$

which explicitly depends on ω and v. Thus, it is the part of solution which serves as a source of information about the frequency shift effects. Eq. (4.5) can be used to solve the inhomogeneous telegrapher equation (2.1). Its solution for $x\in\mathbb{R}$ and $t\in\mathbb{R}_+$ is explicitly given by [45, Eq. (13)]. We quote it in the form

$$\mathfrak{T}_{1;2}(\tau,Q;x,t)=\frac{Q\,\mathrm{e}^{-t/(2\tau)}}{4a\lambda(\tau,\omega)}\Theta\Big(t-\frac{|x|}{a}\Big)\Big\{\frac{1+\beta\,\mathrm{sign}\,x}{1-\beta^2}$$
$$\times h\Big(\tau,\omega;t-\frac{|x|}{a}\Big)+\int_{|x|/a}^t h(\tau,\omega;t-y)\Big[\frac{ay+\beta|x|\,\mathrm{sign}\,x}{1-\beta^2}$$
$$\times\frac{1/(2\tau)}{\sqrt{a^2y^2-x^2}}I_1\Big(\frac{1}{2\tau a}\sqrt{a^2y^2-x^2}\Big)-A(\tau,\omega)$$
$$\times I_0\Big(\frac{1}{2\tau a}\sqrt{a^2y^2-x^2}\Big)\Big]\,\mathrm{d}y\Big\}-\frac{Q\,\mathrm{e}^{\mathrm{i}\omega|x|/v}}{4a\lambda(\tau,\omega)}\Theta\Big(t-\frac{|x|}{v}\Big)$$
$$\times\frac{\beta(1+\mathrm{sign}\,x)}{1-\beta^2}k\Big(\tau,\omega;t-\frac{|x|}{v}\Big), \tag{4.6}$$

where auxiliary functions read

$$h(\tau,\omega;\sigma)=2\exp[A(\tau,\omega)\sigma]\sinh[\lambda(\tau,\omega)\sigma],\ \text{ and}$$
$$k(\tau,\omega;\sigma)=2\exp[B(\tau,\omega)\sigma]\sinh[\lambda(\tau,\omega)\sigma] \tag{4.7}$$

with $\beta=v/a$ and

$$A(\tau,\omega)=\frac{\mathrm{i}\,\omega+1/(2\tau)}{1-\beta^2},\quad B(\tau,\omega)=\frac{\mathrm{i}\,\omega+\beta^2/(2\tau)}{1-\beta^2}$$
$$\text{and}\quad \lambda(\tau,\omega)=\frac{\mathrm{i}\,\omega\beta}{1-\beta^2}\Big(1-\frac{\mathrm{i}}{\tau\omega}-\frac{\beta^2}{4\tau^2\omega^2}\Big)^{1/2}. \tag{4.8}$$

For $\tau\to\infty$, i.e., the case of the wave equation, $A(\tau,\omega)$, $B(\tau,\omega)$, and $\lambda(\tau,\omega)/\beta$ are equal to $\mathrm{i}\,\omega/(1-\beta^2)$. According to [45, Eq. (15)] it allows for the isolation of the modulation term and confirms the existence of the Doppler effect. Notice that $\mathfrak{T}_{1;2}(\tau,Q;x,t)$ is nonzero inside the finite region $x\in\Delta(t)$ and vanishes outside it. This means the existence of wave fronts.

For $v=0$ Eq. (4.6) reduces to the solution [45, Eq. (28)] of the telegraph equation with a non-moving time-harmonic source. That is seen if we use

$$\lim_{v\to 0}\frac{h(\tau,\omega;\sigma)}{\lambda(\tau,\omega)}=2\,\mathrm{e}^{(\mathrm{i}\omega+\frac{1}{2\tau})\sigma}\lim_{\lambda\to 0}\frac{\sinh(\sigma\lambda)}{\lambda}=2\sigma\,\mathrm{e}^{(\mathrm{i}\omega+\frac{1}{2\tau})\sigma}$$

and notice that $\Theta(t-|x|/v)$ tends to zero for large v. Hence, the last term in Eq. (4.6) vanishes and we consider only the terms in the curly bracket with $\Theta(t-|x|/a)$.

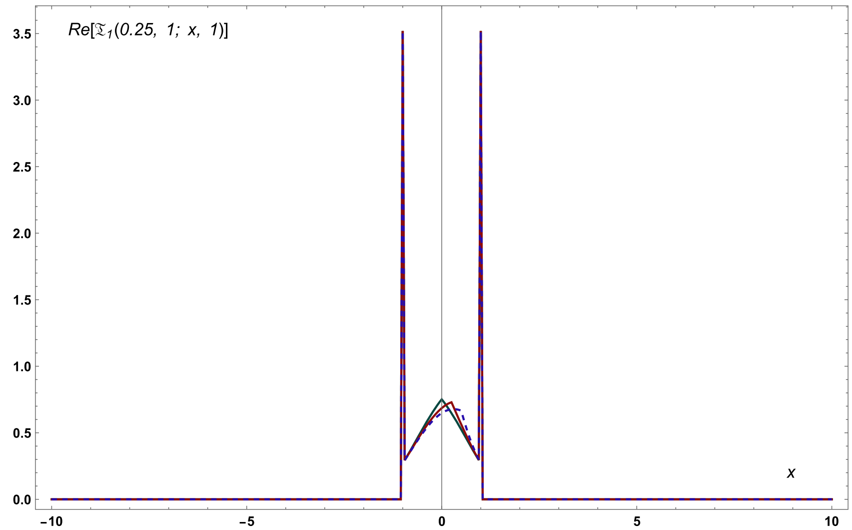

Fig. 1. The plot of $\Re[\mathfrak{T}_1(0.25, 1; x, t)]$ for $\omega = \pi/4$, $a = 1$, $t = 1$ with respect to $\beta = 0$ (the green solid curve), $\beta = 0.25$ (the red solid curve), and $\beta = 0.5$ (the blue dashed curve), where $\beta = v/a$. (For interpretation of the colors in the figure(s), the reader is referred to the web version of this article.)

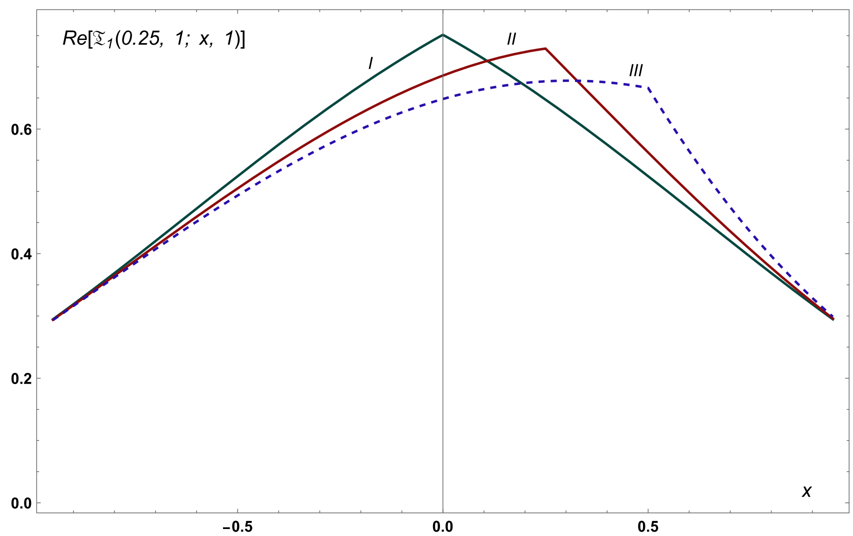

Fig. 2. Blow-up of the region $x \in (-1, 1)$ of $\mathfrak{Re}[\mathfrak{T}_1(0.25, 1; x, t)]$ for $\omega = \pi/4$ and $t = 1$ presented in Fig. 1. The green solid curve no. I is plotted for $\beta = 0$; the red solid curve no. II is for $\beta = 0.25$; and the blue dashed curve no. III is for $\beta = 0.5$; where $\beta = v/a$, and we take $a = 1$.

4.2. *The first hint - a few plots for the telegraph equation*

As explained in Sect. 4.1 $\mathfrak{T}_1(\tau, Q; x, t)$ represents solution to the Eq. (2.1), i.e., the telegraph equation with moving external harmonic source. Moreover, from Eq. (4.1) we learn that $\mathfrak{T}_1(\tau, Q; x, t)$ is the sum of $T(\tau; x, t)$ and $\mathfrak{T}_{1;2}(\tau, Q; x, t)$. Both of them are explicitly known but appear too much complex to be reliably studied using simple by-hands done analysis. So, to recognize, identify and interpret its properties we have calculated numerically $\mathfrak{Re}[\mathfrak{T}_1(\tau, Q; x, t)]$ and plotted it for the initial condition postulated as a narrow (base width equal to 0.03) smoothed rectangular-like signal with the area normalized to 1. The first group of results is presented in Figs. 1, 3, and 4. These are snapshots of $\mathfrak{Re}[\mathfrak{T}_1(\tau = 0.25, Q = 1; x, t)]$ taken for $\omega = \pi/4$ and different instants of time: $t = 1$ (Fig. 1); $t = 5$ (Fig. 3); $t = 9$ (Fig. 4). The plots exhibit also how the solutions depend on the values of $\beta = v/a$ chosen to be $0.0, 0.25, 0, 5$. To distinguish curves relevant for different values of β (difficult to be separated in Fig. 1) we have added Fig. 2 which magnifies the region $x \in (-1, 1)$. It should be noted here that Figs. 1, 3 and 4 have been plotted with different scales being used and it may lead to an erroneous and confusing impression that the wave fronts at $x = \pm at$, exhibited in Fig. 1, disappear. For $t \gg \tau$ the first part of $\mathfrak{Re}[\mathfrak{T}_1(\tau, Q; x, t)]$ is strongly damped by the factor $\exp[-t/(2\tau)]$ (cf. three upper lines of Eq. (4.6) with $\tau = 0.25$ taken into account) so numerically calculated bounds restricting its support remain graphically unnoticed. However, the velocity dependent oscillations survive, their magnitude weakly depends on time and the shape agrees with the Doppler-like form. Plots Figs. 5 and 6 obtained for $\tau = 1$ show the coexistence of wave fronts and oscillations obeying the Doppler-like pattern giving the propagation of distorted wave crests and throughs. Comparing Figs. 3, 4 with 5, 6 we see that, as expected, wave-like/oscillatory effects become more visible with growing value of τ. Qualitative information concerning the Doppler effect is read from snapshots Figs. 5 and 6 of the solution taken for growing source velocities directed towards positive x. Plots that are symmetric for $v = 0$ become asymmetric, shifted to the right, first becoming more and more shrank but next more and more stretched along the velocity direction. This behavior pattern changes instantly at the point $x = vt$. The spatial distance separating successive crests and troughs, in a rough sense related to the wavelength, decreases with x approaching vt from the left and begins to grow for $x > vt$. Such properties of $\mathfrak{Re}[\mathfrak{T}_1(\tau, Q; x, t)]$, if translated into frequency picture agree

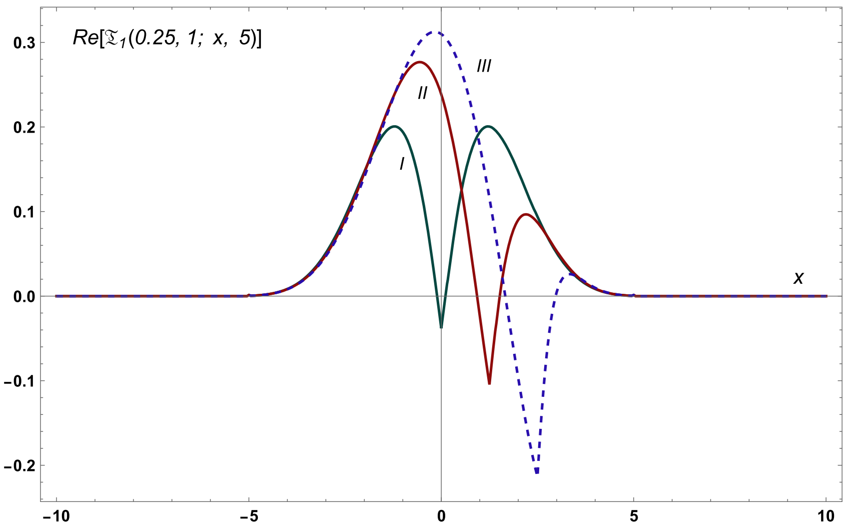

Fig. 3. The plot of $\Re\mathfrak{e}[\mathfrak{T}_1(0.25, 1; x, t)]$ for $\omega = \pi/4$, $a = 1$, $t = 5$, and $x \in [-10, 10]$. The description of curves is the same as is for Fig. 2. See that at $x = \pm 5$ is the initial peak which is more visible in Fig. 5 where $\tau = 1$.

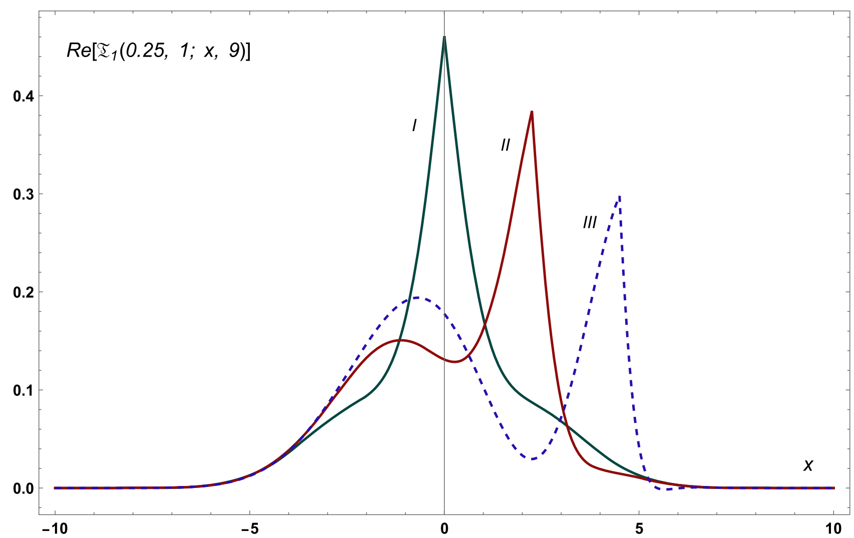

Fig. 4. The plot of $\Re\mathfrak{e}[\mathfrak{T}_1(0.25, 1; x, t)]$ for $\omega = \pi/4$, $a = 1$, $t = 9$ and $x \in [-10, 10]$. The description of curves is the same as is for Fig. 2. See that at $x = \pm 9$ is the initial peak which can be noticed for $\tau = 1$ as in Fig. 6.

with the Doppler effect analysis advocated in Sect. 1. Namely, it means that the observed signal frequency grows with decreasing distance between the source and the observer, achieves maximal pitch for $x = vt$ and becomes smaller and smaller when the source and the observer are moving away from each other. Effect has an universal meaning because the dependence of $\Re\mathfrak{e}[\mathfrak{T}_1(\tau, Q; x, t)]$ on the frequency ω does not touch significantly its characteristic Doppler-like properties (cf. Figs. 6 and 7). The above analysis becomes more complete if takes into account also the time evolution of the signal observed in a fixed point x, see Fig. 8. The observer begins to detect the signal at an instant of time $t = x/a$ when the wave front reaches its location and notes that the shape and frequency of oscillations changes when $t = x/v$: it grows as the source approaches the observer, achieves a maximum and starts to decrease when the source and the observer are passing each other. This confirms our previous arguments that when considering the telegraph equation with moving harmonic impact we are dealing with the Doppler-like effect. We also claim that for identifying the Doppler effect one should not be focused on the existence/non-existence of the wave fronts but rather on careful analysis of the solution in the neighborhood of singular point $x = vt$.

4.3. *The second hint: what can be learned from the limit $\tau \to \infty$?*

Considerations in Sect. 4.2 have enabled us to claim that we have at hands criteria that allow us to judge and point out the existence of the Doppler-like effect for solutions to the telegraph equation. Thus in the next step we can investigate the same problem for GT, i.e., its memory dependent counterpart. As was shown in Ref. [36] the solutions $T(\tau; x, t)$ of the telegraph equation as well as the solutions $T_{\hat{\gamma}}(\tau; x, t)$ of the GT equation tend for large τ to the solution $w(x, t)$ of the wave equation and the solution of diffusion-wave equation $w_{\hat{\gamma}}(x, t)$, respectively. Neither equations investigated in Ref. [36] nor their solutions depend on external sources and we must extend our further considerations to $\mathfrak{T}_{1;2}(\tau, Q; x, t)$ given by Eq. (4.6). As read out from Sect. 4.1, see Eqs. (4.8), in the limit $\tau \to \infty$ all functions $A(\tau, \omega)$, $B(\tau, \omega)$, and $\lambda(\tau, \omega)/\beta$ are equal to $\exp[\mathrm{i}\omega/(1-\beta^2)]$. Then

$$\lim_{\tau\to\infty} h(\tau, \omega; \sigma) = \lim_{\tau\to\infty} k(\tau, \omega; \sigma) = \exp(\mathrm{i}\Omega_{-}\sigma) - \exp(\mathrm{i}\Omega_{+}\sigma)$$

and $\lim_{\tau\to\infty} \mathfrak{T}_{1;2}(\tau, Q; x, t) = \mathfrak{w}_{1;2}(Q; x, t)$, where

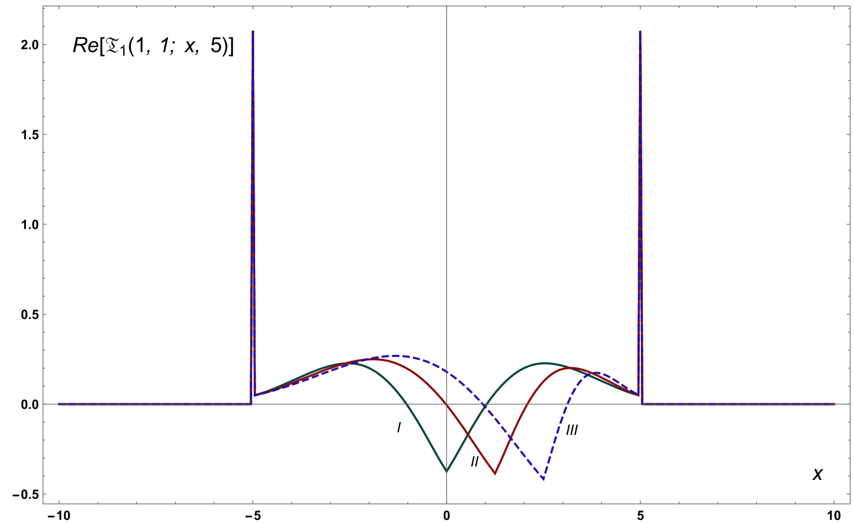

Fig. 5. The plot of $\mathfrak{Re}[\mathfrak{T}_1(1,1;x,t)]$ for $\omega = \pi/4$, $t = 5$ and $x \in [-10, 10]$. The description of curves is the same as is for Fig. 2.

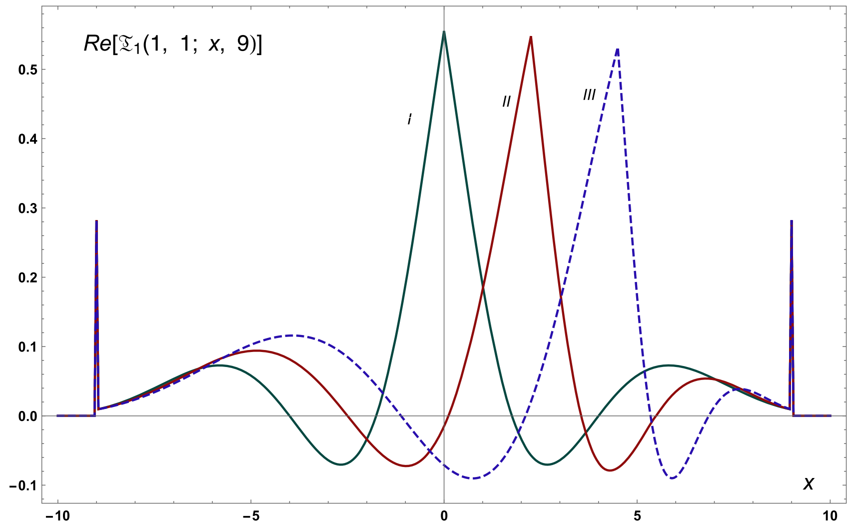

Fig. 6. The plot of $\mathfrak{Re}[\mathfrak{T}_1(1,1;x,t)]$ for $\omega = \pi/4$, $t = 9$ and $x \in [-10, 10]$. The description of curves is the same as is for Fig. 2.

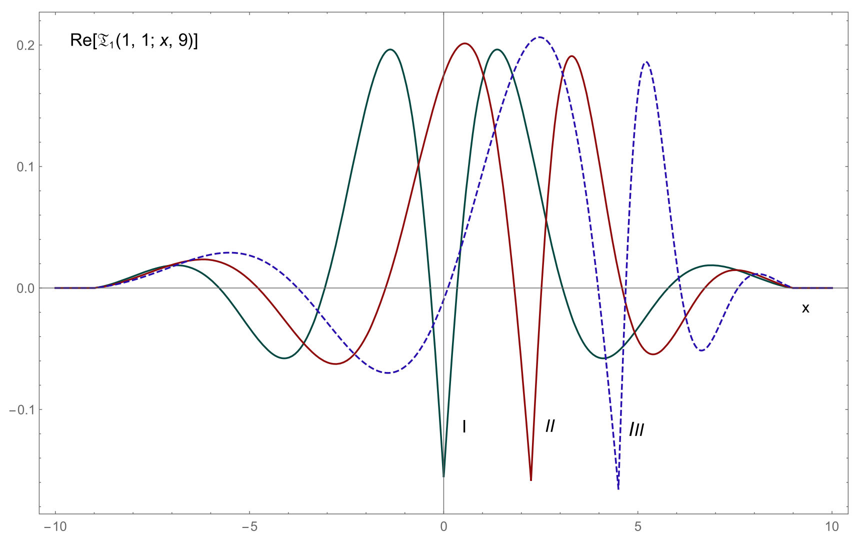

Fig. 7. The plot of $\mathfrak{Re}[\mathfrak{T}_1(1,1;x,t)]$ for $\omega = \pi/3$, $t = 9$ and $x \in [-10, 10]$. The description of curves is the same as is for Fig. 2.

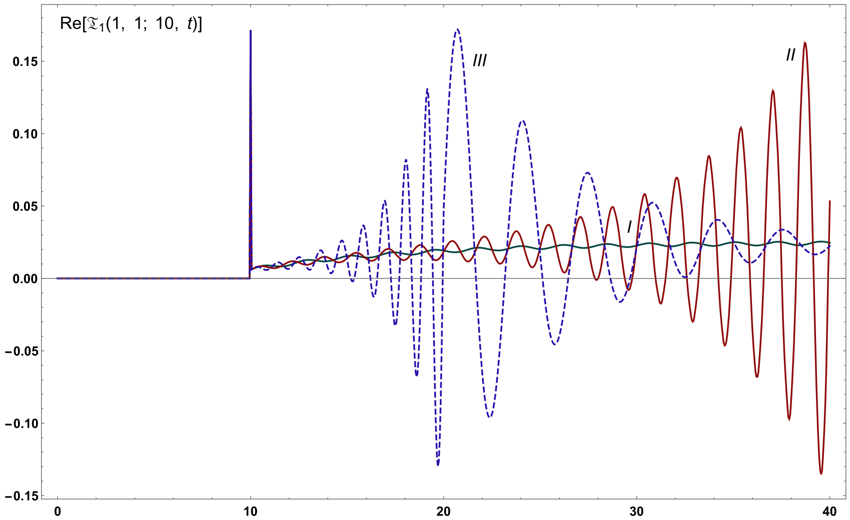

Fig. 8. The plot of $\Re\mathfrak{e}[\mathfrak{T}_1(1,1;x,t)]$ for $\omega=\pi/4$, $x=10$ and $t\in[0,20]$. The description of curves is the same as is for Fig. 2.

$$\begin{aligned}\mathfrak{w}_{1;2}(Q;x,t) &= \frac{Q}{2\,\mathrm{i}\,\omega a}\Big[\Theta(-x)\Theta(t+\frac{x}{a})\,\mathrm{e}^{\mathrm{i}\,\Omega_+(t+\frac{x}{a})} \\ &+\Theta(x)\big\{[\Theta(t-\frac{x}{a})-\Theta(t-\frac{x}{v})]\,\mathrm{e}^{\mathrm{i}\,\Omega_-(t-\frac{x}{a})} \\ &+\Theta(t-\frac{x}{v})\,\mathrm{e}^{\mathrm{i}\,\Omega_+(t+\frac{x}{a})}\big\}-\Theta(t-\frac{x}{a})\Big].\end{aligned}\tag{4.9}$$

Its real part quoted in [45, Eq. (21)] reads

$$\Re\mathfrak{e}[\mathfrak{w}_{1;2}(Q;x,t)]=\frac{Q}{2a\omega}\begin{cases}\sin[\Omega_+(t+x/a)], & x\in[-at,vt) \\ \sin[\Omega_-(t-x/a)], & x\in(vt,at]\end{cases}\tag{4.10}$$

and vanishes outside the sector $\Delta(t)=[-at,at]$. Obviously, Eq. (4.10) provides us with an explicit manifestation of the Doppler effect for the wave equation. Using the integral decomposition Eq. (3.1) we arrive at

$$\begin{aligned}&\int_0^\infty \lim_{\tau\to\infty}\mathfrak{T}_{1;2}(\tau,Q;x,t)f_{\hat{\gamma}}(\xi,t)\,\mathrm{d}\xi \\ &=\int_0^\infty \mathfrak{w}_{1;2}(Q;x,\xi)f_{\hat{\gamma}}(\xi,t)\,\mathrm{d}\xi=\mathfrak{w}_{\hat{\gamma};2}(Q;x,t),\end{aligned}\tag{4.11}$$

where $\mathfrak{w}_{\hat{\gamma};2}(Q;x,t)$ is the solution of the diffusion-wave equation under external harmonic impact. Having this in mind we are ready to demonstrate how to use just found limit behavior in order to restore properties that characterize GT solutions for finite τ.

4.4. *The third hint: relation between $\mathfrak{T}_{\hat{\gamma};2}(\tau,Q;x,t)$ and $\mathfrak{w}_{\hat{\gamma};2}(Q;x,t)$ for positive a and finite τ*

Pursuant to the rules of the integral decomposition approach we demonstrated in Sect. 4.3 that for large τ the solution of GT equation with an external source $\mathfrak{T}_{\hat{\gamma};2}(\tau,Q;x,t)$ tends to the solution $\mathfrak{w}_{\hat{\gamma};2}(\tau,Q;x,t)$ of the diffusion-wave equation with the same external impact. We will use this limit property to show that for arbitrary positive τ we can relate $\mathfrak{T}_{\hat{\gamma};2}(\tau,Q;x,t)$ to a combination of $\mathfrak{w}_{\hat{\gamma};2}(\tau,Q;x,t)$ with an auxiliary function $\mathfrak{p}_{\hat{\gamma}}(\tau,Q;x,t)$ vanishing for $\tau\to\infty$. If the above holds then for $\tau>0$ we should have

$$\mathfrak{T}_{\hat{\gamma};2}(\tau,Q;x,t)=\mathfrak{w}_{\hat{\gamma};2}(Q;x,t)-\mathfrak{p}_{\hat{\gamma}}(\tau,Q;x,t),\tag{4.12}$$

where

$$\mathfrak{p}_{\hat{\gamma}}(\tau,Q;x,t)=\int_0^\infty \mathfrak{p}(\tau,Q;x,\xi)f_{\hat{\gamma}}(\xi,t)\,\mathrm{d}\xi\tag{4.13}$$

with $\mathfrak{p}(\tau,Q;x,t)$ defined a few lines later, see Eq. (4.16).

To prove the above statements we begin with Eq. (4.2) for $j=2$. It contains functions $\mathfrak{T}_{1;2}(\tau,Q;x,\xi)$ and $f_{\hat{\gamma}}(\xi,t)$. The first of them solves the telegraph equation with moving source, see Eq. (2.1). The second one is defined by Eq. (3.2) and depends on the memory function $\gamma(t)$ which expresses the time non-locality present in GT equation. Support of $f_{\hat{\gamma}}(\xi,t)$ is unbounded on $\mathbb{R}_+$ and the procedure leads to smearing the wave front of $\mathfrak{T}_{\hat{\gamma};2}(\tau,Q;x,\xi)$ even for localized initial conditions [36]. To push our construction further we shall find the relation between $\mathfrak{T}_{1;2}(\tau,Q;x,\xi)$ and $\mathfrak{w}_{1;2}(Q;x,\xi)$ for $\tau>0$. First, rewrite Eq. (4.5) as

$$\tilde{\hat{\mathfrak{T}}}_{1;2}(\tau,Q;\kappa,s)=\Big(1-\frac{s/\tau}{a^2\kappa^2+s^2+s/\tau}\Big)\tilde{\hat{\mathfrak{w}}}_{1;2}(Q;\kappa,s),\tag{4.14}$$

where

$$\tilde{\hat{\mathfrak{w}}}_{1;2}(Q;\kappa,s)=\frac{Q}{s-\mathrm{i}(\omega+\kappa v)}\,\frac{1}{a^2\kappa^2+s^2}$$

and recall that $\tilde{\hat{\mathfrak{w}}}_{1;2}(Q;\kappa,s)$ in (x,t)-space equals to $\mathfrak{w}_{1;2}(Q;x,t)$ given by Eq. (4.9). Eq. (4.14) involves two functions: $\mathfrak{w}_{1;2}(Q;x,t)$ and up to now undefined function $\mathfrak{p}(\tau,Q;x,t)$ which is the only source corresponding to the corrections dependent on τ. Calculating the inverse LF transform of Eq. (4.14) we obtain

$$\mathfrak{T}_{1;2}(\tau,Q;x,t)=\mathfrak{w}_{1;2}(Q;x,t)-\mathfrak{p}(\tau,Q;x,t)\tag{4.15}$$

where

$$\mathfrak{p}(\tau,Q;x,t)=\frac{1}{\tau}\mathscr{L}^{-1}\left[\mathscr{F}^{-1}\Big[\frac{s\,\tilde{\hat{\mathfrak{w}}}_{1;2}(Q;\kappa,s)}{a^2\kappa^2+s^2+s/\tau};x\Big];t\right]\tag{4.16}$$

and vanishes in the limit $\tau\to\infty$. The inverse LF transforms in Eq. (4.16) are calculated in Appendix C. Additionally, it can be shown that $\Re\mathfrak{e}[\mathfrak{p}(\tau,Q;x,t)]$ does not cancel $\Re\mathfrak{e}[\mathfrak{w}_{1;2}(Q;x,t)]$ for $t>0$ and $x\in\Delta(t)$ but to prove that requires lengthy and laborious calculations. Instead we represent both these functions graphically being convinced that curves plotted in Fig. 9 may serve as a justification for the above made statement. We point out that from Eq. (4.15) it appears

$$\Re\mathfrak{e}[\mathfrak{p}(\tau,Q;x,t)]=\Re\mathfrak{e}[\mathfrak{w}_{1;2}(Q;x,t)]-\Re\mathfrak{e}[\mathfrak{T}_{1;2}(\tau,Q;x,t)]\tag{4.17}$$

which together with Fig. 9 shows that the frequency shift noticed for $\mathfrak{T}_{1;2}(\tau,Q;x,t)$ comes from two sources, namely $\mathfrak{w}_{1;2}(Q;x,t)$ and $\mathfrak{p}(\tau,Q;x,t)$. In view of that one can formulate the hypothesis that the Doppler-like effects if are observed for $\mathfrak{w}_{\hat{\gamma};2}(Q;x,t)$ then the solutions of the GT equation with the same external source also should manifest the Doppler-like effect. We will verify this hypothesis on examples presented in the next section.

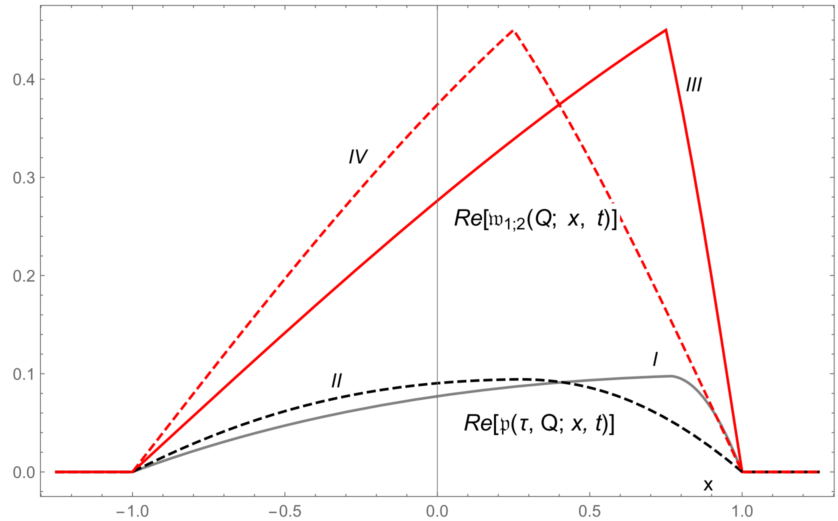

Fig. 9. Plot of the real parts of $\mathfrak{w}_{1;2}(Q;x,t)$ and $\mathfrak{p}(\tau,Q;x,t)$ for $t=1$, $Q=\tau=1$, $\omega=\pi/4$, $a=1$, $v=0.75$ or $v=0.25$. For $v=0.75$ we have the black solid curve no. I for $\mathfrak{Re}[\mathfrak{p}(1,1;x,1)]$ and the red solid curve no. II for $\mathfrak{Re}[\mathfrak{w}(1;x,1)]$. For $v=0.25$ we have the black dashed curve no. II for $\mathfrak{Re}[\mathfrak{p}(1,1;x,1)]$ and the red dashed curve no. IV for $\mathfrak{Re}[\mathfrak{w}(1;x,1)]$. These functions were plotted by using Eqs. (4.10) and (4.16) partially calculated in Appendix C.

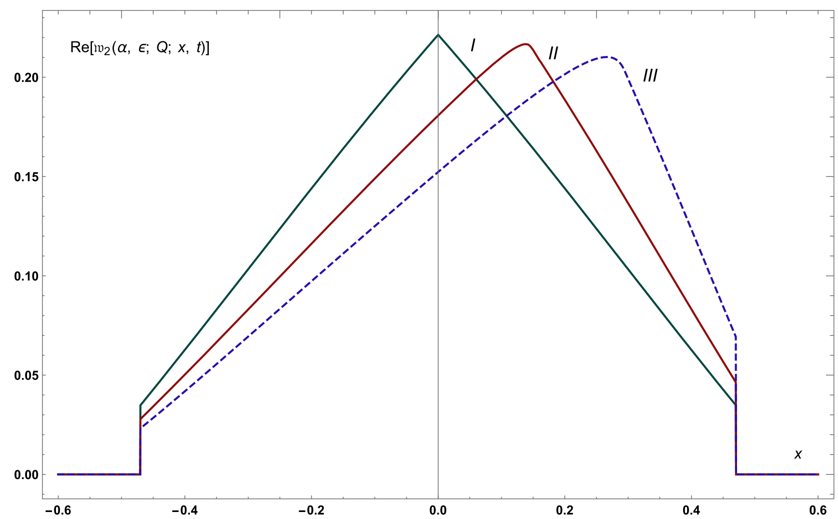

Fig. 10. The plot of $\mathfrak{w}_2(\alpha,\epsilon;Q;x,t)$ for $\alpha=2/3$, $\epsilon=10$, $\omega=\pi/3$, $Q=1$, $a=1$, and $t=6$. The green solid curve no. I is for $\beta=0$, the red solid curve no. II is for $\beta=0.25$, and the blue dashed curve no. III is for $\beta=0.5$.

5. GT equation: memory functions and the Doppler-like effects

In what follows we shall discuss the appearance of the Doppler-like effects for the case of stationary observer and moving source on three examples distinguished by different choices of the memory kernel $\gamma(t)$. Recall that $\mathfrak{T}_{\hat{\gamma}}(\tau,Q;x,t)$ is a sum of $T_{\hat{\gamma}}(\tau;x,t)$ and $\mathfrak{T}_{\hat{\gamma};2}(\tau,Q;x,t)$ and only the second component exhibits the Doppler-like effects.

Based on results presented in Ref. [36, Exs. (a), (b), and (c)] we shall analyze the solutions of GT equation involving three types of memory functions, namely:

(i) the localized memory $\gamma(t)$ for which we have $T_{\hat{\gamma}}(\tau;x,t)\neq 0$ for $x\in\Delta(t)$,
(ii) the sum of δ-Dirac function and a power-law memory kernel. That implies that $T_{\hat{\gamma}}(\tau;x,t)\neq 0$ for $x\in\Delta(t/\epsilon)$,
(iii) a power-law memory kernel which leads to $T_{\hat{\gamma}}(\tau;x,t)\neq 0$ for $x\in\mathbb{R}$,

Our task is to check for which aforementioned cases the signature of the Doppler-like effect is observed for $\mathfrak{w}_{\hat{\gamma};2}(Q;x,t)$.

(i) In the first case of localized memory function $\gamma(t)=\delta(t)$ ($\hat{\gamma}(s)=1$), we know that $f_1(\xi,t)$, given by Eq. (3.2), equals to $\mathscr{L}^{-1}[\exp(-\xi s);t]=\delta(t-\xi)$. Thus, $\mathfrak{T}_{\hat{\gamma};2}(\tau,Q;x,t)$ reduces to $\mathfrak{T}_{1;2}(\tau,Q;x,t)$ presented via Eq. (4.6) and for $\tau\to\infty$ approaches $\mathfrak{w}_{1;2}(Q;x,t)$ given by Eq. (4.9). Both of these functions, namely $\mathfrak{T}_{1;2}(\tau,Q;x,t)$ and $\mathfrak{w}_{1;2}(Q;x,t)$, manifest the existence of the Doppler frequency shift as well as the wave front, see Sect. 4.

(ii) The memory function equals to $\gamma(t)=\epsilon\delta(t)+t^{-\alpha}/\Gamma(1-\alpha)$ ($\hat{\gamma}(s)=\epsilon+s^{\alpha-1}$), where $\alpha\in(0,1)$ and $\epsilon>0$. For such $\gamma(t)$ we have $f_{\hat{\gamma}}(\xi,t)\equiv f(\alpha,\epsilon;\xi,t)$ found in [36, Eq. (35)], namely

$$f(\alpha,\epsilon;\xi,t)=\mathscr{L}^{-1}[(s^{\alpha-1}+\epsilon)\,\mathrm{e}^{-\xi s^{\alpha}}\,\mathrm{e}^{-\xi\epsilon s};t]$$
$$=\Theta(t-\epsilon\xi)\Big(\frac{t-\epsilon\xi}{\alpha\xi}+\epsilon\Big)\Phi_\alpha(\xi,t-\epsilon\xi), \tag{5.1}$$

where $\Phi_\alpha(\xi,y)$ is the two argument one-sided Lévy stable distribution $\Phi_\alpha(\xi,y)=\mathscr{L}^{-1}[\exp(-\xi s^{\alpha});y]$, being an example of the Wright-Mainardi M function [60,62]. It can be written in terms of the one argument one-sided Lévy stable distribution $\Phi_\alpha(\xi,y)=\xi^{-1/\alpha}\Phi_\alpha(y\xi^{-1/\alpha})$. We recall that the one-sided Lévy distribution $\Phi_\alpha(\sigma)$ vanishes for $\sigma\leq 0$ and is nonzero for $\sigma>0$. That can be obtained either from its Mikusin-

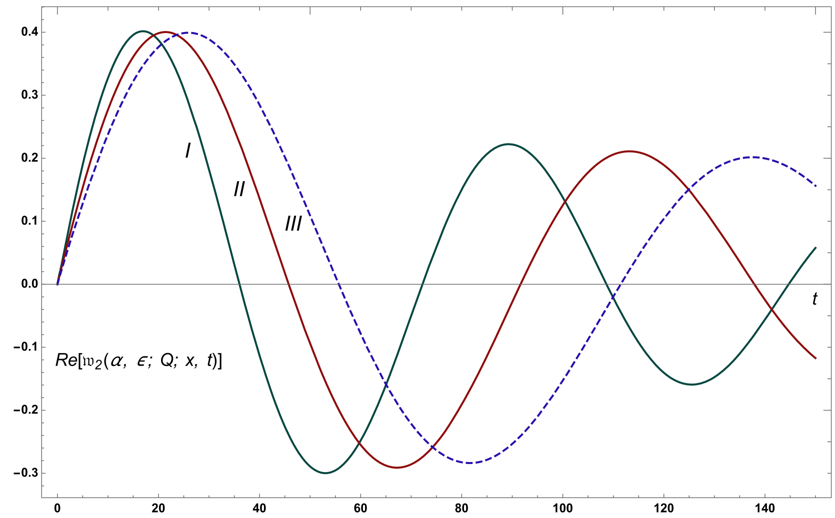

Fig. 11. The plot of $\mathfrak{Re}[\mathfrak{w}_2(\alpha,\epsilon;Q;x,t)]$ for $\alpha = 2/3$, $\epsilon = 10$, $\omega = \pi/3$, $Q = 1$, $a = 1$, and $x = 0$. The green solid curve no. I is for $\beta = 0$, the red solid curve no. II is for $\beta = 0.25$, and the blue dashed curve no. III is for $\beta = 0.5$.

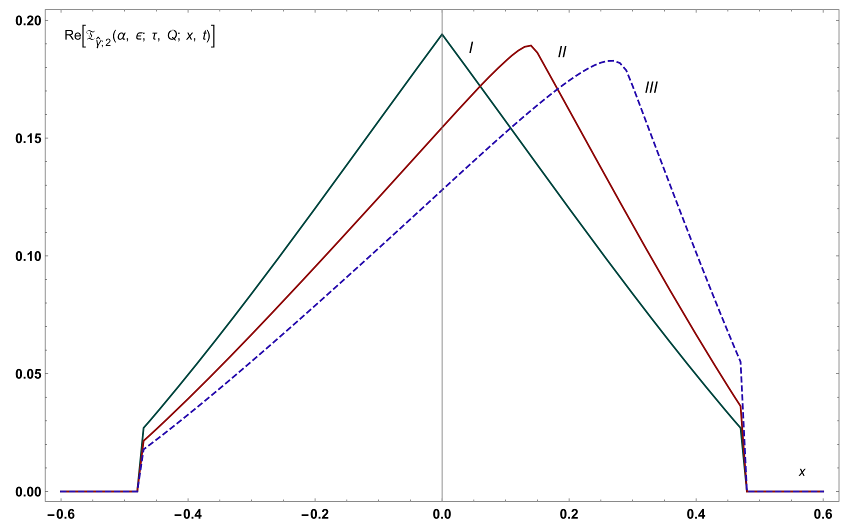

Fig. 12. The plot of $\mathfrak{T}_{\hat{\gamma};2}(\alpha,\epsilon;\tau,Q;x,t)$ for $\alpha = 2/3$, $\epsilon = 10$, $\omega = \pi/3$, $\tau = 1$, $Q = 1$, $a = 1$, and $t = 6$. The description of curves is the same as in Fig. 10.

ski's asymptotics or from Meijer G representation, see in Appendix D. Numerical calculations usually use the asymptotics form of the one-sided Lévy given by Eq. (D.3). Note also that the calculation of the inverse Laplace transform given by Eq. (5.1) is based on the formula $\mathscr{L}^{-1}[\exp(-bs)\hat{f}(s);t] = \Theta(t-b)f(t-b)$, and the definition of one-sided Lévy stable distribution.

Referring to Sect. 4.4, the Doppler-like effect observed in $\mathfrak{w}_{\epsilon+s^{\alpha-1};2}(Q;x,t) = \mathfrak{w}(\alpha,\epsilon,Q;x,t)$ and plotted in Figs. 10 and 11 should be quantitatively noticed in

$$\mathfrak{T}_{s^{\alpha-1}+\epsilon;2}(\tau,Q;x,t) \equiv \mathfrak{T}_{\hat{\gamma};2}(\alpha,\epsilon;\tau,Q;x,t) = \int_0^\infty \mathfrak{T}_{1;2}(\tau,Q;x,\xi) f(\alpha,\epsilon;\xi,t)\,\mathrm{d}\xi \tag{5.2}$$

illustrated in Figs. 12 and 13 for the same value of parameters as in Figs. 10 and 11, respectively. In Fig. 12 we see that the memory function $\gamma(t) = \epsilon\delta(t) + t^{-\alpha}/\Gamma(1-\alpha)$ smoothes out the cusps appearing in "pure" Doppler-like effect. Nevertheless the trails of this effect do survive. Moreover, Fig. 12 demonstrates the existence of wave front for $\mathfrak{T}_{\hat{\gamma};2}(2/3,10;1,1;x,t)$ which can be deduced analogically as it was done in [36] from the fact that $f(\alpha,\epsilon;\xi,t)$ contains the Heaviside step function $\Theta(t-\epsilon\xi)$ as well. This Heaviside step function ensures that the second argument of $\Phi_\alpha(\xi,t-\epsilon\xi)$ is non-negative and makes the integral defining $\mathfrak{T}_{\hat{\gamma};2}(\alpha,\epsilon;\tau,Q;x,t)$ non-vanishing on the bounded domain of ξ, namely $\xi \in (0,t/\epsilon)$. Thus, $\mathfrak{T}_{\hat{\gamma};2}(\alpha,\epsilon;\tau,Q;x,t)$ is nonzero for $x \in \Delta(t/\epsilon)$ which implies the existence of the wave front. The Doppler-like effect presented in Fig. 13 is also illustrated in Fig. 13, where $\mathfrak{T}(2/3,10;1,1;x=0,t)$ is presented as a function of t. We see here the fading oscillations which are stretched as the speed v increases.

(iii) As the last example we quote the power-law memory function, $\gamma(t) = t^{-\alpha}/\Gamma(1-\alpha)$ for $\alpha \in (0,1)$ studied in Ref. [36]. In the Laplace domain it reads $\hat{\gamma}(s) = s^{\alpha-1}$ and gives

$$f_{s^{\alpha-1}}(\xi,t) \equiv f(\alpha;\xi,t) = \mathscr{L}^{-1}[s^{\alpha-1}\,\mathrm{e}^{-\xi s^\alpha};t] = \frac{t}{\alpha\xi}\Phi_\alpha(\xi,t), \tag{5.3}$$

where $\Phi_\alpha(\xi,t)$ is the two arguments Lévy stable distribution. $f(\alpha;\xi,t)$ does not contain any Heaviside step function. Hence, using the considerations analogical to those presented in [36] it can be concluded that $\mathfrak{T}_{s^{\alpha-1};2}(\tau,Q;x,t) \equiv \mathfrak{T}_{\hat{\gamma};2}(\alpha;\tau,Q;x,t)$ does not have the wave front. However, from Fig. 14 it can be suspected that some frequency shift occurs similarly as for the real part of $\mathfrak{w}_{s^{\alpha-1};2}(Q;x,t) \equiv \mathfrak{w}_2(\alpha;Q;x,t)$ given by Eq. (4.11). With the help of Eq. (4.9) we get that Eq. (4.11) for $x=0$ reads

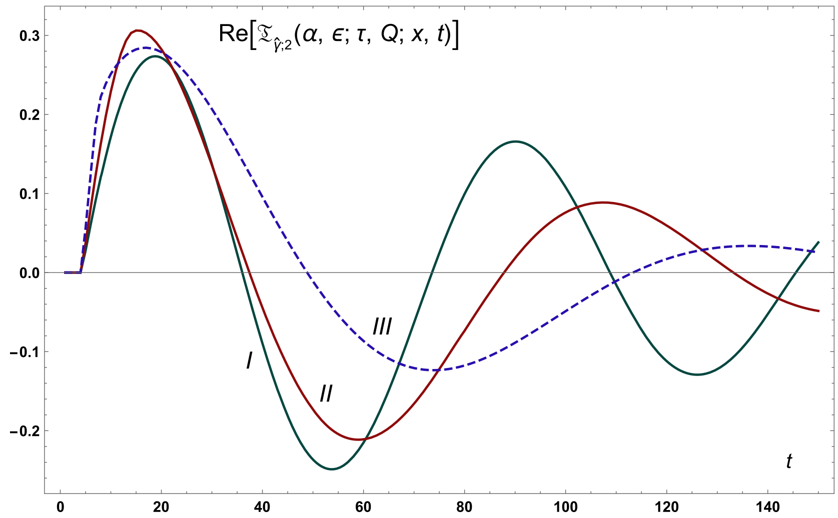

Fig. 13. The plot of $\mathfrak{T}_{\hat{\gamma};2}(\alpha, \epsilon; \tau, Q; x, t)$ for $\alpha = 2/3$, $\epsilon = 10$, $\omega = \pi/3$, $\tau = 1$, $Q = 1$, $a = 1$, and $x = 0.3$. The green solid curve no. I is for $\beta = 0$, the red solid curve no. II is for $\beta = 0.25$, and the blue dashed curve no. III is for $\beta = 0.5$.

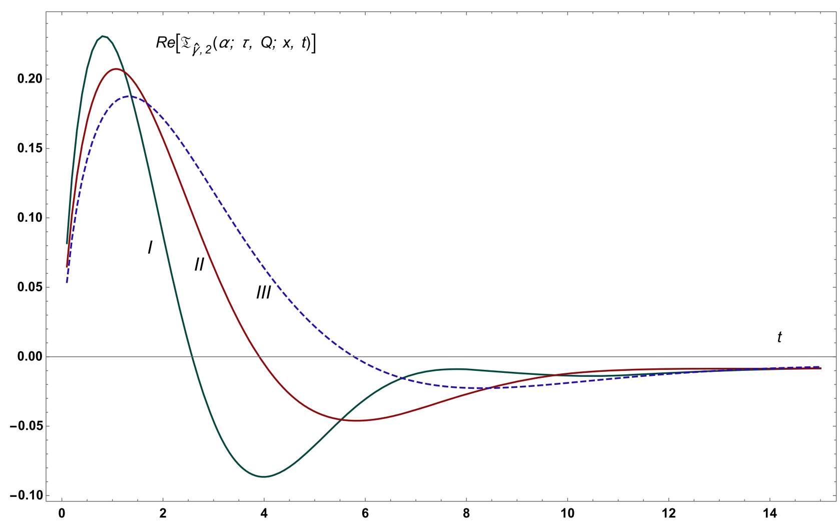

Fig. 14. The plot of $\mathfrak{T}_{\hat{\gamma};2}(\alpha; \tau, Q; x, t)$ for $\alpha = 0.75$, $\omega = \pi/3$, $\tau = 1$, $Q = 1$, $a = 1$, and $x = 0$. The green solid curve no. I is for $\beta = 0$, the red solid curve no. II is for $\beta = 0.25$, and the blue dashed curve no. III is for $\beta = 0.5$.

$$\begin{aligned}\mathfrak{Re}[\mathfrak{w}_2(\alpha; Q; x, t)] &= \frac{Q}{2a\omega}\int_0^\infty \sin(\Omega_+\xi) f(\alpha; \xi, t) \\ &= \frac{Q}{2a\omega}\sin_\alpha(\Omega_+ t)\end{aligned} \tag{5.4}$$

and it is illustrated in Fig. 15 for $\alpha = 3/4$. There can be seen that despite the lack of a wave front, we observe the frequency shift.

6. Discussion

In the Introduction we noticed that the telegraph equation, besides of using to describe the transmission lines, has been for many years proposed to serve as an equation which may govern the heat and/or mass transport phenomena. Physicists, when applying it to this class of problems, are used to name it the Cattaneo-Vernotte (CV) equation and consider it as a bridge between the wave-like and the diffusion-like description of the system. The telegraph equation, because of the hyperbolic character, admits solutions obeying wave properties. Compared with the commonly accepted diffusive nature of the heat transfer this leads to the dilemma concerning the existence and properties of the thermal/heat waves and the equation used to describe them, chosen either diffusion or wave-like. Diffusive modeling of the heat transfer works well in a vast majority of typical situations [6] but phenomena related to the second sound effects are much better explained when the wave-like evolution pattern stemming from the CV equation is used [7]. The CV equation is local in time but it should be remembered that its frequently quoted derivation is based on the constitutive relation which hides the time nonlocality. Also it is known that many kinetic phenomena taking place in media of complex structure, to mention anomalous diffusion and non-Debye relaxation, exhibit properties indicating the nonlocal time evolution and memory dependent modeling. This motivated us to focus on the time-smeared telegraph equation Eq. (1.5) as we are convinced that similarly to the results obtained in the framework of diffusion and relaxation theories also in this case the time smearing of the time-local evolution equations will provide us with better understanding of the heat transport problems. In favor of investigating GT we emphasize the fact that by using the integral decomposition procedure and having at hands solutions to the standard, time-local telegraph equation we are able to construct solutions relevant to the memory dependent counterparts of this equation and to analyze them with respect to “classical” wave properties, namely the existence of wave fronts and the Doppler effect. Comparing the wave-like pattern given by the standard telegraph equation with two examples of the

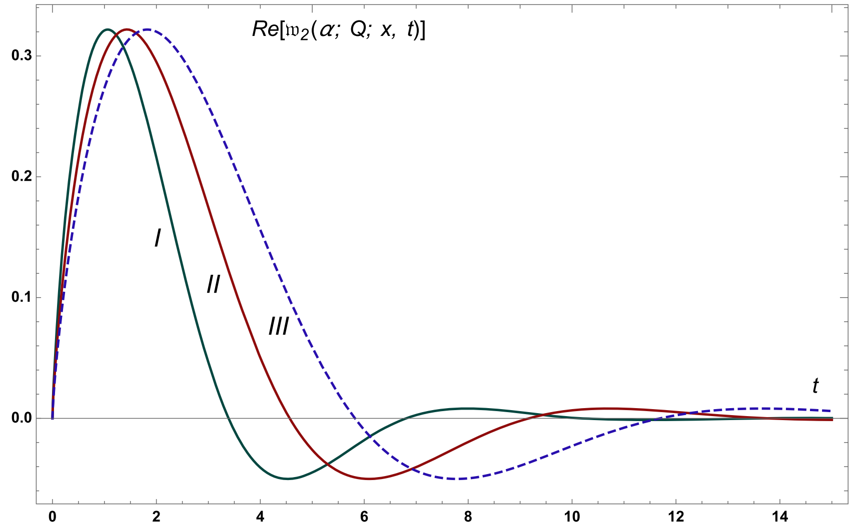

Fig. 15. Plot of Eq. (5.4) for $x = 0$, $\alpha = 0.75$, $\omega = \pi/3$, $Q = 1$, and $a = 1$. The green solid curve no. I is for $v = 0$, the red solid curve no. II is for $v = 0.25$, and the blue dashed curve no. III is for $v = 0.5$.

memory functions (see Sect. 5) we have concluded that the existence of wave fronts and "pure" Doppler effect accompanies the presence of the second time derivative independently from possible (power-like) memory terms have been added. The wave fronts disappear if the equation involves only the time-nonlocal operators, however smeared traces of the Doppler effect survive and may be observable, especially that in realistic physical situations we do not observe sharply manifested changes but rather more or less smoothed behavior.

We will mention here as a digression that basic physical literature does not provide us with a precise definition of the Doppler effect. In the Introduction we recalled the simplest approach leading to the statement that the Doppler effect appears if a stationary observer notes the change of pitch heard when a sound source approaches and recedes from it. More generally the Doppler effect occurs if the wave manifests the frequency shift related to the relative motion of the source, observer and medium in which the wave propagates. For specifically chosen physical situations this definition may lead to some quantitative criteria - if the observer is able to determine the signal frequency and the observer and the source move along the line which joins them then the observer may check that the measured frequency changes with respect to the emitted one ω according to the relation $\Omega_{\mp} = \omega/(1 \mp v/a)$ with $\mp$ signs adopted respectively for approach and moving away. If such a factor is identified within the solution then one can claim that deals with the Doppler effect. We would like to pay attention that Sect. 4.4 and examples in Sect. 5 show that if the frequency shift can be noticed for $\mathfrak{w}_{\hat{\gamma}}(Q; x, t)$ then it is also observed for the solution $\mathfrak{T}_{\gamma}(\tau, Q; x, t)$. A similar situation is with the wavef ronts. Thus, if we only need qualitative information about the appearance of the Doppler-like effect it is enough to study the behavior $\mathfrak{w}_{\hat{\gamma}}(Q; x, t)$ which is much friendly to analytical and numerical applications.

7. Conclusions

Throughout the paper we investigated solutions to the $(1 + 1)$-dim generalized telegraph equation introduced as a modification of the classical telegraph equation in which both time derivatives are replaced by integro-differential linear operators involving memory kernels given by functions assumed to be nonlocally depending on time and *à priori* not identified with kernels which define commonly used fractional derivatives. The proposed approach extends investigations based on the standard fractional generalizations of the telegraph equation. Methodology rooted in use of the Laplace-Fourier transforms and operational calculus merged in the framework of the integral decomposition technique allows us to construct solutions to the memory dependent evolution equations from the solutions to their time-local counterparts. In a broader mathematical context this is closely related to the subordination procedure successfully adopted to solve problems of anomalous diffusion and non-exponential relaxation. Going beyond the range of just mentioned physical phenomena we shed light on wave properties obeyed by the heat transport supposed to be described by the Cattaneo-Vernotte equation, the twin brother of the telegraph equation, and its time nonlocal generalization. As a training ground to test the wave nature of the heat transport phenomena we decided to check whether solutions to the generalized equations meet the Doppler effect and the existence of the wave fronts known to be exhibited by solutions to the standard telegraph equation. We found that the Doppler effect, at least in its smeared form, survives introducing non-trivial memory effects. Such a statement does not remain true for the wave fronts whose existence is conditioned by the presence of the second time derivative in the evolution equation under consideration.

CRediT authorship contribution statement

T. Pietrzak: Methodology, Software, Writing – original draft, Writing – review & editing. **A. Horzela:** Conceptualization, Methodology, Writing – original draft, Writing – review & editing. **K. Górska:** Conceptualization, Methodology, Supervision, Writing – original draft, Writing – review & editing.

Declaration of competing interest

The authors declare that they have no competing interests.

Data availability

No data was used for the research described in the article.

Acknowledgements

T.P. and K.G. acknowledge the National Science Centre (NCN) Grant Preludium Bis 2 No. UMO-2020/39/O/ST2/01563.

Appendix A. The Efros theorem

The Efros theorem [66–70] generalizes the convolution theorem for the Laplace transform. It states as follows:

Theorem A.1. *If $\hat{G}(s)$ and $\hat{q}(s)$ are analytic functions, and*

$$\mathscr{L}[h(x,\xi);s] = \hat{h}(x,s) \tag{A.1}$$

as well as

$$\mathscr{L}[f(\xi,t);s] = \int_0^\infty f(\xi,t)\,\mathrm{e}^{-st}\,\mathrm{d}t = \hat{G}(s)\,\mathrm{e}^{-\xi\hat{q}(s)}, \tag{A.2}$$

exist, then

$$\hat{G}(s)\hat{h}(x,\hat{q}(s)) = \int_0^\infty \Big[\int_0^\infty h(x,\xi)f(\xi,t)\,\mathrm{d}\xi\Big]\,\mathrm{e}^{-st}\,\mathrm{d}t.$$

From Efros theorem appears that

$$\mathscr{L}^{-1}[\hat{G}(s)\hat{h}(x,\hat{q}(s));t] = \int_0^\infty h(x,\xi)f(\xi,t)\,\mathrm{d}\xi. \tag{A.3}$$

Appendix B. Derivation of $T(\tau;x,t)$

Consider the homogeneous telegraph equation (1.1) with the initial conditions (1.4). We are using the LF transform method which lead to the nonnegative solution $T(\tau;x,t)$. The first step in solving the above equation is to perform the joint LF transform

$$\tilde{\hat{T}}(\tau;\kappa,s) = \frac{1}{\sqrt{2\pi}}\int_{-\infty}^{\infty}\mathrm{e}^{\mathrm{i}\kappa x}\Big[\int_0^\infty T(\tau;x,t)\,\mathrm{e}^{-st}\,\mathrm{d}t\Big]\,\mathrm{d}x,$$

which turns the initial-value problems (1.3) into an algebraic equation, whose solution is given by Eq. (4.3). Taking into account the convolution theorem which states that the Fourier transform of the convolution of two functions is the product of their corresponding Fourier transforms and the following integral [45]

$$\int_0^\infty \frac{1}{x^2+c^2}\cos(bx)\,\mathrm{d}x = \frac{\pi}{2c}\,\mathrm{e}^{-|b|c}, \qquad \mathfrak{Re}\,c > 0$$

we find the inverse Fourier transform of expression (1.2)

$$\hat{T}(\tau;x,s) = \frac{s+\tau^{-1}}{\sqrt{s^2+\tau^{-1}s}}\int_{-\infty}^{\infty}\mathrm{e}^{-\frac{|y-x|}{a}\sqrt{s^2+\frac{s}{\tau}}}\,T_0(y)\frac{\mathrm{d}y}{2a} \tag{B.1}$$

The solution to Eq. (1.3) will be the inverse Laplace transform of expression (B.1). In order to find it, we used the following equations for the inverse transform [45,71]

$$\mathscr{L}^{-1}\Big[\frac{\mathrm{e}^{-b\sqrt{s^2-c^2}}}{\sqrt{s^2-c^2}}\Big] = I_0(c\sqrt{t^2-b^2})\Theta(t-b), \tag{B.2}$$

$$\mathscr{L}^{-1}\Big[\frac{s\,\mathrm{e}^{-b\sqrt{s^2-c^2}}}{\sqrt{s^2-c^2}}\Big] = \delta(t-b) + \frac{ctI_1(c\sqrt{t^2-b^2})\Theta(t-b)}{\sqrt{t^2-b^2}}. \tag{B.3}$$

The obtained solution is of the form Eq. (4.4), which is obtained from [56, Eq. (102) on p. 300] and/or [57, Eq. (7.4.28)] by vanishing $\dot{T}(\tau;x,t)$ at $t=0$.

Appendix C. The inverse Laplace transform placed in Eq. (4.16)

The auxiliary function $\mathfrak{p}(\tau,Q;x,t)$ given by Eq. (4.16) can be calculated by making the Laplace and Fourier convolutions:

$$\mathfrak{p}(\tau,Q;x,t) = \frac{1}{\tau}\int_{\mathbb{R}}\Bigg\{\int_0^t \mathfrak{w}_{1;2}(Q;x-y,u)$$

$$\times\,\mathscr{L}^{-1}\Big[\frac{s\,\mathrm{e}^{-\frac{|y|}{a}\sqrt{s^2+s/\tau}}}{\sqrt{s^2+s/\tau}};t-u\Big]\,\mathrm{d}u\Bigg\}\frac{\mathrm{d}y}{2a} \tag{C.1}$$

To calculate the inverse Laplace transform sitting in Eq. (4.15) we use the well-know property of the inverse Laplace transform, i.e. $\mathscr{L}^{-1}[\hat{f}(s+\lambda);t] = \exp(-\lambda t)\mathscr{L}^{-1}[\hat{f}(s);t]$. It allows us to write

$$\begin{aligned}\mathscr{L}^{-1}\Big[\frac{s}{\sqrt{s^2+s/\tau}}\exp\big(-\frac{|y|}{\tau}\sqrt{s^2+s/\tau}\big);u\Big]\\ = \mathrm{e}^{-u/(2\tau)}\,\mathscr{L}^{-1}\Big[\frac{s\,\mathrm{e}^{-\frac{|y|}{\tau}\sqrt{s^2-1/(4\tau^2)}}}{\sqrt{s^2-1/(4\tau^2)}};u\Big]\\ - \frac{\mathrm{e}^{-u/(2\tau)}}{2\tau}\mathscr{L}^{-1}\Big[\frac{\mathrm{e}^{-\frac{|y|}{\tau}\sqrt{s^2-1/(4\tau^2)}}}{\sqrt{s^2-1/(4\tau^2)}};u\Big].\end{aligned} \tag{C.2}$$

The inverse Laplace transform sitting in Eq. (C.2) are calculated with the help of Eqs. (B.2) and (B.3). They imply

$$\begin{aligned}\text{LHS of Eq. (C.2)} &= \frac{a}{2}\,\mathrm{e}^{-u/(2\tau)}[\delta(au-y)+\delta(au+y)]\\ &- \frac{a}{2\tau}\,\mathrm{e}^{-u/(2\tau)}\Big[\frac{1}{a}I_0(\frac{1}{2\tau a}\sqrt{a^2u^2-y^2})\\ &- \frac{u}{\sqrt{a^2u^2-y^2}}I_1(\frac{1}{2\tau a}\sqrt{a^2u^2-y^2})\Big].\end{aligned} \tag{C.3}$$

Next, we numerically calculate the integral over y in Eq. (4.16). For values of parameters Q, τ, a, v, ω, and t indicated in Fig. 9 we obtained presented there curves.

Appendix D. One-sided Lévy stable distribution

The one-sided Lévy stable distribution is defined through the inverse Laplace transform as follows

$$\Phi_\alpha(\sigma) = \mathscr{L}^{-1}[\mathrm{e}^{-s^\alpha};s] = \int_L \mathrm{e}^{s\sigma}\,\mathrm{e}^{-s^\alpha}\,\frac{\mathrm{d}\sigma}{2\pi\mathrm{i}}, \tag{D.1}$$

where the integral contour is described in [64]. For rational $\alpha = l/k$, the one-sided Lévy stable distribution can be expressed by the Meijer G-function and/or the finite sum of hypergeometric function, see [63, Eqs. (2) and/or (3)] and [36, Eq. (31)], respectively. The exact and explicit form of $\Phi_{l/k}(\sigma)$ reads

$$\Phi_{l/k}(\sigma) = \frac{\sqrt{kl}}{(2\pi)^{(k-l)/2}}\frac{1}{\sigma}G^{k,0}_{l,k}\left(\frac{l^l}{k^k\sigma^l}\Big|{}^{\Delta(l,0)}_{\Delta(k,0)}\right), \tag{D.2}$$

where $\alpha = l/k$ such that $l<k$ and $l,k = 1,2,\ldots$. According to common convention the special list of n elements is equal to $\Delta(n,a) = a/n,(a+1)/n,\ldots,(a+n-1)/n$ which is placed in upper (it is $\Delta(l,0)$) and lower (it is $\Delta(k,0)$) list of parameters. The asymptotic behavior of $\Phi_\alpha(\sigma)$ is given by Mikusiński in Ref. [65] and figures out

$$\Phi_\alpha(\sigma) \overset{\sigma\to0+}{\simeq} \frac{(\alpha/\sigma)^{\frac{1}{2(1-\alpha)}}}{\sqrt{2\pi(1-\alpha)\sigma}}\exp\big[-(1-\alpha)(\alpha/\sigma)^{\frac{\alpha}{1-\alpha}}\big] \tag{D.3}$$

and

$$\Phi_\alpha(\sigma) \overset{\sigma\to\infty}{\simeq} -\frac{\sigma^{-1-\alpha}}{\Gamma(-\alpha)}. \tag{D.4}$$

Eq. (D.3) is usually use in numerical calculation with one-sided Lévy stable distribution.

References

[1] B.J. Hunt, The Maxwellians, Cornell University Press, Ithaca, NY, 2005.
[2] C.R. Cattaneo, Sulla conduzione del calore, Atti Semin. Mat. Fis. Univ. Modena 3 (1948) 83–101.
[3] P. Vernotte, Les paradoxes de la théories continue de l'equation de la chaleur, C. R. Acad. Sci., Paris 246 (1958) 3154–3155.

[4] C.R. Cattaneo, Sur une forme de l'equation de la chaleur eliminant le paradoxe d'une propagation instantanee, C. R. Acad. Sci. 247 (1958) 431–432.
[5] G. Fichera, Is the Fourier theory of heat propagation paradoxical?, Rend. Circ. Mat. Palermo (2) Suppl. XLI (1992) 5–28.
[6] D. Maillet, A review of the models using the Cattaneo-Vernotte hyperbolic heat equation and their experimental validation, Int. J. Therm. Sci. 139 (2019) 424–432.
[7] D.D. Joseph, L. Preziosi, Heat waves, Rev. Mod. Phys. 61 (1989) 41–73.
[8] A.I. Zhmakin, Non-Fourier Heat Conduction. From Phase-Lag Models to Relativistic and Quantum Transport, Springer Nature Switzerland AG, 2023.
[9] A. Compte, R. Metzler, The generalized Cattaneo equation for the description of anomalous transport processes, J. Phys. A, Math. Gen. 30 (1997) 7277–7289.
[10] J. Fort, V. Méndez, Wavefronts in time-delayed reaction-diffusion systems. Theory and comparison to experiment, Rep. Prog. Phys. 65 (2002) 895–954.
[11] S. Goldstein, On diffusion by discontinuous movements, and on the telegraph equation, Q. J. Mech. Appl. Math. 4 (2) (1951) 129–156.
[12] H.D. Weymann, Finite speed of propagation in heat conduction, diffusion, and viscous shear motion, Am. J. Phys. 35 (1967) 488–496.
[13] L. Tisza, Sur la supraconductabilité thermique de l'helium II liquide et la statistique de Bose-Einstein, C. R. Acad. Sci. 207 (1938) 1035.
[14] L.D. Landau, The theory of superfluidity of helium II, J. Phys. USSR 5 (1941) 71–104, Ch. 8.
[15] V.P. Peshkov, Second sound in helium II, J. Phys. USSR 8 (1944) 381.
[16] M. Chester, Second sound in solids, Phys. Rev. 131 (3) (1963) 2013–2015.
[17] L. Secia, T. Ruggeri, A. Muracchini, Second sound and multiple shocks in superfluid helium, Z. Angew. Math. Phys. 60 (2009) 1074–1094.
[18] M. Kac, A stochastic model related to the telegrapher's equation, Rocky Mt. J. Math. 4 (3) (1974) 497–509.
[19] K. Górska, A. Horzela, E.K. Lenzi, G. Pagnini, T. Sandev, General Cattaneo (telegrapher's) equation in modelling anomalous diffusion phenomena, Phys. Rev. E 102 (2020) 022128.
[20] Z. Ding, J. Zhou, B. Song, V. Chiloyan, M. Li, T.-H. Liu, G. Chen, Phonon hydrodynamic heat conduction and Knudsen minimum in graphite, Nano Lett. 18 (2018) 638–649.
[21] L. Lindsay, A. Katre, A. Cepellotti, N. Mingo, Perspective on ab initio phonon thermal transport, J. Appl. Phys. 126 (2019) 050902.
[22] M. Simoncelli, N. Marzari, A. Cepellotti, Generalization of Fourier's law into viscous heat equations, Phys. Rev. X 10 (2020) 011019.
[23] W. Dai, H. Wang, P.M. Jordan, R.E. Mickens, A. Bejan, A mathematical model for skin burn injury induced by radiation heating, Int. J. Heat Mass Transf. 51 (2008) 5497–5510.
[24] Y. Zhang, Generalized dual-phase lag bioheat equations based on nonequilibrium heat transfer in living biological tissues, Int. J. Heat Mass Transf. 52 (2009) 4829–4834.
[25] E. Orsinher, L. Beghin, Time-fractional telegraph equations and telegraph process with Brownian time, Probab. Theory Relat. Fields 128 (2004) 141–160.
[26] S.M. Cvetičanin, D. Zorica, M.R. Rapaić, Generalized time-fractional telegrapher's equation in transmission line modeling, Nonlinear Dyn. 88 (2017) 1453–1472.
[27] E. Awad, On the time-fractional Cattaneo equation of distributed order, Physica A 518 (2019) 210–233.
[28] J. Masoliver, Fractional telegrapher's equation from fractional persistent random walks, Phys. Rev. E 93 (2016) 052107.
[29] Yu. Povstenko, Fractional Thermoelasticity, Springer, New York, 2015.
[30] T. Kosztołowicz, Cattaneo-type subdiffusion-reaction equation, Phys. Rev. E 90 (2014) 042151.
[31] K.D. Lewandowska, T. Kosztołowicz, Application of generalized Cattaneo equation to model subdiffusion impedance, Acta Phys. Pol. B 39 (5) (2008) 1211–1220.
[32] A. Madhukar, Y. Park, W. Kim, H.J. Sunaryanto, R. Berlin, L.P. Chamorro, J. Bentsman, M. Ostoja-Starzewski, Heat conduction in porcine muscle and blood: experiments and time-fractional telegraph equation model, J. R. Soc. Interface 16 (2019) 20190726.
[33] H.H. Pennes, Analysis of tissue and arterial blood temperatures in the resting human forearm, J. Appl. Physiol. 1 (1948) 93–122.
[34] Qiao Zhang, Yuxin Sun, Jialing Yang, Thermoelastic responses of biological tissue under thermal shock based on three phase lag model, Case Stud. Therm. Eng. 28 (2021) 101376.
[35] Ying Hu, Xue-Yang Zhang, Xian-Fang Li, Thermoelastic response of skin using time-fractional dual-phase-lag bioheat heat transfer equation, J. Therm. Stresses 45 (2022) 597–615.
[36] K. Górska, Integral decomposition for the solutions of the generalized Cattaneo equation, Phys. Rev. E 104 (2021) 024113.
[37] A. Mandelis, Diffusion waves and their uses, Phys. Today 53 (2000) 29–34.
[38] R. Li Voti, G.L. Liakhou, S. Paoloni, C. Sibilia, M. Bertolotti, Thermal waves physics, J. Optoelectron. Adv. Mater. 3 (2001) 779–816.
[39] E. Marin, J. Marin, P. Diaz, On the wave treatment of the conduction of heat in photothermal experiments with solids, Eur. J. Phys. 23 (2002) 523–532.
[40] E. Marin, J. Marin, R. Hechavarria, Hyperbolic heat equation in photothermal experiments with solids, J. Phys. IV France 125 (2005) 365–368.
[41] E. Marin, L.S. Vaca-Oyola, O. Delgado-Vasallo, On thermal waves' velocity: some open questions in thermal waves' physics, Rev. Mex. Fís. E 62 (2016) 1–4.
[42] A. Mandelis, X. Guo, Fourier-Laplace spectral theory for non-steady-state thermal fields with applications to problems in steady-state photothermal linear frequency modulation, Phys. Rev. Appl. 14 (2020) 024058.
[43] R. Li Voti, M. Bertolotti, Thermal waves emitted by moving sources and the Doppler effect, Int. J. Heat Mass Transf. 176 (2021) 121098.
[44] A. Salazar, Energy propagation of thermal waves, Eur. J. Phys. 27 (2006) 1349–1355.
[45] Yu. Povstenko, M. Ostoja-Starzewski, Doppler effect described by the solutions of the Cattaneo telegraph equation, Acta Mech. 232 (2021) 725–740.
[46] Yu. Povstenko, M. Ostoja-Starzewski, Fractional telegraph equation under moving time-harmonic impact, Int. J. Heat Mass Transf. 182 (2022) 121958.
[47] Yu. Povstenko, M. Ostoja-Starzewski, T. Kyrylych, Fractional telegraph equation under moving time-harmonic impact, Int. J. Heat Mass Transf. 207 (2023) 124013.
[48] A.K. Wróblewski, J.A. Zakrzewski, Introduction to Physics. vol. 1 (Wstęp do Fizyki. Tom 1), Państwowe Wydawnictwo Naukowe, Warsaw, 1984, in Polish.
[49] H.C. Fogedby, Langevin equations for continuous time Lévy flights, Phys. Rev. E 50 (1994) 1657–1660.
[50] A. Baule, R. Friedrich, Joint probability distribution for a class of non-Markovian processes, Phys. Rev. E 71 (2003) 026101.
[51] R. Gorenflo, F. Mainardi, A. Vivoli, Continuous time random walk and parametric subordination in fractional diffusion, Chaos Solitons Fractals 34 (2007) 87–103.
[52] R. Gorenflo, F. Mainardi, Subordination pathways to fractional diffusion, Eur. Phys. J. Spec. Top. 193 (2011) 119–132.
[53] I.M. Sokolov, Solution of a class of non-Markovian Fokker-Planck equation, Phys. Rev. E 66 (2002) 041101.
[54] A.V. Chechkin, I.M. Sokolov, On relation between generalized diffusion and subordination schemes, Phys. Rev. E 103 (2021) 032133.
[55] K. Górska, A. Horzela, Subordination and memory dependent kinetics in diffusion and relaxation phenomena, Fract. Calc. Appl. Anal. 26 (2023) 480–512.
[56] J.A. Stratton, Electromagnetic Theory, McGraw-Hill Book Co., New York, 1941.
[57] P.M. Morse, H. Feshbach, Methods of Theoretical Physics, Mac Grow-Hill Book Company, New York/Toronto/London, 1953, Ch. 7.4.
[58] J. Masoliver, G.H. Weiss, Finite-velocity diffusion, Eur. J. Phys. 17 (1996) 190–196.
[59] M.A. Olivares-Robles, L.S. Garcia-Colin, On different derivations of telegrapher's type kinetic equations, J. Non-Equilib. Thermodyn. 21 (1996) 361–379.
[60] F. Mainardi, G. Pagnini, R. Gorenflo, Mellin transform and subordination laws in fractional diffusion processes, Fract. Calc. Appl. Anal. 6 (2003) 441–459.
[61] J. Prüss, Evolutionary Integral Equations and Applications, 2 ed., Birkhäuser, Basel, 2003.
[62] E. Bazhlekova, Subordination principle for space-time fractional evolution equations and some applications, Integral Transforms Spec. Funct. 30 (2019) 431–452.
[63] K.A. Penson, K. Górska, Exact and explicit probability densities for one-sided Lévy stable distributions, Phys. Rev. Lett. 105 (2010) 210604.
[64] H. Pollard, The representation of $e^{-x^{\alpha}}$ as a Laplace integral, Bull. Am. Math. Soc. 52 (1946) 908–910.
[65] J. Mikusiński, On the function whose Laplace-transform in $e^{-s^{\alpha}}$, Stud. Math. XVIII (1959) 191–198.
[66] A.M. Efros, The application of the operational calculus to the analysis, Mat. Sb. 42 (1935) 699–706, in Russian.
[67] Ł. Włodarski, Sur une formule de Efros, Stud. Math. 13 (1952) 183–187.
[68] U. Graf, Applied Laplace Transforms and z-Transforms for Sciences and Engineers, Birkhäuser, Basel, 2004.
[69] K. Górska, K.A. Penson, Lévy stable distributions via associated integral transform, J. Math. Phys. 53 (2012) 053302.
[70] A. Apelblat, F. Mainardi, Application of the Efros theorem to the function represented by the inverse Laplace transform of $s^{-\mu}\exp(-s^{\nu})$, Symmetry 13 (2021) 354–369.
[71] J. Masoliver, Telegraphic processes with stochastic resetting, Phys. Rev. E 99 (2019) 012121.

Chaos ARTICLE pubs.aip.org/aip/cha

Can the Doppler be useful for a benchmark analysis of the wave-like properties of memory-dependent telegraphers' equation

Cite as: Chaos 35, 0231 34 (2025); doi: 1 0.1 063/5.0251 227
Submitted: 30 November 2024 · Accepted: 22 January 2025 ·
Published Online: 1 0 February 2025

View Online Export Citation CrossMark

Tobiasz Pietrzak,[1,2,a)] Katarzyna Górska,[1,b)] Andrzej Horzela,[1,c)] and Ljupco Kocarev[3,4,d)]

AFFILIATIONS

[1] H. Niewodniczański Institute of Nuclear Physics, Polish Academy of Sciences, Division of Theoretical Physics, ul. Radzikowskiego 152, Kraków PL 31-342, Poland
[2] Krakow School of Interdisciplinary PhD Studies, H. Niewodniczanski Institute of Nuclear Physics, Polish Academy of Sciences, ul. Radzikowskiego 152, Kraków PL 31-342, Poland
[3] Macedonian Academy of Sciences and Arts, Bul. Krste Misirkov 2, Skopje 1000, Macedonia
[4] Faculty of Computer Science and Engineering, Ss. Cyril and Methodius University in Skopje, Arhimedova 3, Skopje 1000, Macedonia

Note: This paper is part of the Focus Issue on Anomalous Diffusion and Fluctuations in Complex Systems and Networks.

[a)] **Electronic mail:** tobiasz.pietrzak@ifj.edu.pl
[b)] **Author to whom correspondence should be addressed:** katarzyna.gorska@ifj.edu.pl
[c)] **Electronic mail:** andrzej.horzela@ifj.edu.pl
[d)] **Electronic mail:** lkocarev@manu.edu.mk

ABSTRACT

Telegraphers' equation perturbed by a uniformly moving external harmonic impact is investigated to uncover information useful for distinguishing properties of the time evolution patterns that describe either memoryless or memory-dependent modeling of transport phenomena. Memory effects are incorporated into telegraphers' equation by smearing the first- and second-order time derivatives so that the memory kernel smearing the second-order time derivative acts as the smeared derivative of the smeared first-order time derivative. Such a generalized telegraphers' equation (abbreviated as GTE) is solved under initial conditions that specify the values of the solutions and their time derivatives taken at the initial time and boundary conditions that require the sought solutions to vanish either at the x space infinity or the $(+l)/(-l)$ boundaries of a compact domain. The question is which solutions would be classified as traveling or standing waves. To answer this, we consider the Doppler effect and investigate how the frequency and velocity of external sources influence the obtained solutions. Using the short-time Fourier transform allows us to advance the problem and shows that infinite domain solutions to the GTEs, provided by a model example involving the Caputo fractional derivatives ${}^{C}D_t^{2\alpha}$ and ${}^{C}D_t^{\alpha}$ with $0 < \alpha \leq 1$, exhibit a kind of velocity-dependent Doppler-like frequency shift if $\frac{1}{2} < \alpha \leq 1$. The effect remains unnoticed if $0 < \alpha \leq \frac{1}{2}$. This confirms our previous hypothesis that the emergence of wave-like effects in solutions of fractional equations is related to the occurrence of fractional time derivatives of the order greater than 1.

It is well known that the Fourier equation, being a first-order parabolic equation, is used to describe transport processes such as diffusion or heat transport, which propagate with infinite velocity. Such a property contradicts the locality principle of the special relativity theory and thus is difficult to recognize in contemporary physics. Efforts to find a way out of this problematic situation led C. Cattaneo in the mid-20th century to propose replacing the Fourier equation with a second-order hyperbolic equation that describes propagation proceeding with a finite speed, the latter known and used in signal transmission as the Heaviside telegraphers' equation since the 1870s. Telegraphers' equation shares all the properties of the wave equations describing damped oscillations and immediately raises questions about their wave nature when applied to describe transport processes. This focused our interest on telegraphers' equation and its non-local generalizations, such as fractional ones, as mathematical tools that

could allow us to separate diffusion and wave-like properties of memory-dependent hyperbolic evolution equations (like the generalized telegraphers' equation is) used in studies of anomalous diffusion. As a test phenomenon, we considered the Doppler effect for two reasons: namely, it is known how to identify signatures of the Doppler effect present in the solutions to the standard telegraphers' equation, and this effect may also be sought in the $(1+1)$-dimensional case, in contradistinction to phenomena such as diffraction and refraction seen at least in two space dimensions. Assuming that the generalized telegraphers' equation in consideration is its fractional version with Caputo fractional time derivatives of the order 2α and α with $\alpha \in (0, 1]$, we studied it perturbed by a uniformly moving harmonic impact. For this equation, we found and compared solutions for two kinds of boundary conditions: either those vanishing at $+/-$ space infinity or those equal to 0 at $+l/-l$ bounds of a finite domain. Using the short-time Fourier transform, we investigated the possible dependence of the solution frequency on the velocity of the external source. We showed that for the infinite domain, the Doppler effect is observable for $\alpha \in (1/2, 1]$, i.e., for memory-dependent generalized telegraphers' equations with at least one fractional derivative of order greater than 1 and the standard memoryless telegraphers' equation. This means that the occurrence of the Doppler effect is not necessarily related to the existence of a wavefront. Solutions to the equation under consideration with $\alpha \in (0, 1/2]$ lead to standing wave-type solutions that do not exhibit the Doppler effect.

I. INTRODUCTION

The event that undoubtedly influenced the development of telegraphers' equation was the deployment of the first transatlantic telegraph cable in August 1858. The cable was laid between Foilhommerum on Valentia Island (western Ireland) and Heart's Content on the east coast of Newfoundland. The project was a huge engineering challenge for the time, both in terms of the manufacturing itself and the subsequent cable laying. However, from an electrical point of view, the circuit used was rather simple. It consisted of a pair of 3000 km long wires with a DC voltage source at one end and a mirror galvanometer at the other end used to detect changes in current on the line. Messages were sent by an operator using the Morse alphabet, which is a series of dots and dashes. This very expensive project, unfortunately, did not yield good results. It took up to two minutes to send a single character, which translates into a speed of about one-tenth of a word per minute. It took more than 17 h to send the first dispatch.[1] To overcome the problem of long information transmission times, scientists such as James Clerk Maxwell, Lord Kelvin, and Oliver Heaviside began working on a profound understanding of the physics of electrical impulse propagation in long cables. One of the most important results of this work was Heaviside's paper, published in 1880, in which he presented his analysis of signal propagation in cables using telegraphers' equation that he derived.[2] Heaviside's work gave us the first conceptual understanding of the transmission line and a set of mathematical tools still used today in transmission line analysis. Telegraphers' equation, originally used for transmission line analysis, also has other unexpected, versatile, far-reaching, and by no means less important applications, such as the description of heat transport in liquid helium[3] or the description of the so-called bioheat transfer occurring in biological tissues.[4,5] As for the theoretical relevance of telegraphers' equation, it is worth recalling that this equation has been extensively studied within the framework of microscopic models related to phonon hydrodynamics and the viscous heat transfer equation[6–8] and is used to describe heat transport[9–11] as well as diffusion processes in a confined domain.[12] It can be derived using the persistent time random walk model considered in Refs. 13–16. Telegraphers' equation has also been generalized using the concept of fractional derivative. An equation of this type (commonly called the generalized telegraphers' equation, GTE) has been used to describe anomalous diffusion,[17–21] thermoelasticity,[22] and chemical reactions,[23,24] as well as biological phenomena such as heat conduction in muscles and blood.[25]

In this paper, we will consider the GTE of the Volterra type with smeared time derivatives and an external harmonic point-wise source. $S_R(x, t) = Q\delta(x - vt)\cos(\omega_0 t)$ where $Q > 0$ and $\omega_0 > 0$ are the amplitude and frequency of the signal generated by this source, while $v > 0$ is the speed of the source. The GTE equation takes the following form:[26]

$$\int_0^t \eta(t-\xi)\partial_\xi^2 u(\hat{\gamma}; x, \xi)d\xi + \frac{1}{\tau}\int_0^t \gamma(t-\xi)\partial_\xi u(\hat{\gamma}; x, \xi)d\xi + [b^2 - a^2\partial_x^2]u(\hat{\gamma}; x, t) = S_R(x, t), \tag{1}$$

for $t \in \mathbb{R}_+$ and is equipped with initial conditions

$$u(\hat{\gamma}; x, 0) = u_0(x) \quad \text{and} \quad \partial_t u(\hat{\gamma}; x, t)\Big|_{t=0} = w_0(x). \tag{2}$$

Equation (1) will be solved using two kinds of Dirichlet boundary conditions, namely,

$$\lim_{x\to\pm\infty} u(\hat{\gamma}; x, t) = 0 \tag{3}$$

and

$$u(\hat{\gamma}; -l, t) = u(\hat{\gamma}; l, t) = 0. \tag{4}$$

We recall that the $\gamma(t)$ and $\eta(t)$ functions, appearing in Eq. (1), denote the memory kernels responsible for the smearing of the first- and second-order time derivatives, respectively. Memory effects coming from smearing the time derivatives and realized by introducing functions γ and η, mean considering a non-local temporal evolution scheme in which the current state of the system depends on its previous history. For the case $\gamma(t) = \eta(t) = \delta(t)$, where $\delta(t)$ is the Dirac distribution, evolution is local and Eq. (1) becomes the standard telegraphers' equation.

The goal of this paper is to determine [based on the boundary conditions given by Eqs. (3) and/or (4)] whether we can classify solutions to Eq. (1) as traveling or standing waves. To judge this challenging problem, we aim to investigate whether we can observe a velocity-dependent frequency shift (aka the Doppler, or Doppler-like effect) in the solution $u(\hat{\gamma}; x, t)$ when considering both types of solutions. To achieve this goal, we will compare the solution $u(\hat{\gamma}; x, t)$ with the reference source provided by the standard, time-local telegraphers' equation with external harmonic impact, whose solution is known to exhibit properties characteristic of the Doppler effect.[27,28] Thus, the paper is organized as follows. In Sec. II, we study the GTE in which the time derivatives are smeared by the memory functions related to one another. Next, we solve this equation under two kinds of boundary conditions. We assume that the solution vanishes either at $+/-$ space infinity or at the boundaries $+l/-l$ of the solution domain. In Sec. III, both types of solutions are illustrated for local and fractional cases. Section IV presents the numerical analysis of the frequency spectrum that characterizes the solutions obtained so far. The results of our investigation are summarized and discussed in Sec. V. Four appendices devoted to lesser-known mathematical details supplement the main text of the paper.

II. SOLUTION TO THE GTE WITH A MOVING SOURCE

The GTE (1) is an inhomogeneous integrodifferential equation in which the inhomogeneity is constituted by the external source information, which is encoded in $S_R(x,t)$. Its solution $u(\hat{\gamma};x,t)$ is the sum of $u_{\rm hom}(\hat{\gamma};x,t)$ solving the homogeneous equation, i.e., Eq. (1) without $S_R(x,t)$, and $u_{\rm inhom}(\hat{\gamma};x,t)$ being the special solution of inhomogeneous Eq. (1). The information on the initial conditions (2) is moved to $u_{\rm hom}(\hat{\gamma};x,t)$, whereas $u_{\rm inhom}(\hat{\gamma};x,t)$ contains the knowledge about external source. The solution of the analyzed equation, this is

$$u(\hat{\gamma};x,t) = u_{\rm hom}(\hat{\gamma};x,t) + u_{\rm inhom}(\hat{\gamma};x,t), \tag{5}$$

significantly depends on the assumed shape of memory functions η and γ. Details of considerations focused on the choice of the above-mentioned memory functions were presented in Refs. 17, 29, and 30. From a general point of view, the functions η and γ appearing in Eq. (1) could be any mutually independent well-behaved functions; however, as shown in the above-cited papers, these functions must be coupled as follows:

$$\eta(t) = \int_0^t \gamma(\xi)\gamma(t-\xi)d\xi. \tag{6}$$

The justification for the above condition is as follows. For a function f, of class at least C^2, for which the derivative at zero vanishes the smearing of its first derivative denoted by ${}^s\partial$ is given by the expression

$${}^s\partial_t f(t) = \int_0^t \gamma(t-\xi)\partial_\xi f(\xi)d\xi.$$

The smearing of the second derivative of this function will be given by

$$\begin{aligned}
{}^s\partial_t\left({}^s\partial_t f\right)(t) &= \int_0^t \gamma(t-t_1)\partial_{t_1}[{}^s\partial_{t_1} f(t_1)]dt_1 \\
&= \int_0^t \gamma(t-t_1)\partial_{t_1}\left[\int_0^{t_1}\gamma(t_1-t_2)\partial_{t_2}f(t_2)dt_2\right]dt_1 \\
&= \int_0^t \gamma(t-t_1)\left[\gamma(0)\partial_{t_1}f(t_1) + \int_0^{t_1}\partial_{t_1}\left(\gamma(t_1-t_2)\partial_{t_2}f(t_2)\right)dt_2\right]dt_1 \\
&= \int_0^t \left[\gamma(t-t_1)\gamma(t_1)f'(0) + \int_0^{t_1}\gamma(t-t_1)\gamma(t_1-t_2)\partial_{t_2}^2 f(t_2)dt_2\right]dt_1 \\
&= \int_0^t \left[\int_0^{t_1}\gamma(t-t_1)\gamma(t_1-t_2)\partial_{t_2}^2 f(t_2)dt_2\right]dt_1.
\end{aligned}$$

By introducing the variable $\xi = t - t_1$, we get

$${}^s\partial_t\left({}^s\partial_t f\right)(t) = \int_0^t\left[\int_0^{t-t_2}\gamma(\xi)\gamma(t-t_2-\xi)d\xi\right]\partial_{t_2}^2 f(t_2)dt_2,$$

from which the relation (6) follows.

A. The case of the infinite domain, i.e., solutions to GTE satisfying the boundary condition (3)

With the above in mind, the first step toward the solution of Eq. (1) with the boundary conditions given by Eq. (3) uses the joint Laplace–Fourier (LF) transform.[31] It turns the initial-value problem into an algebraic equation, whose solution is given by the LF transform of Eq. (5). From Eq. (1), we find that

$$\begin{aligned}\tilde{\tilde{u}}_{\rm hom}(\hat{\gamma};\kappa,s) &= \hat{\gamma}(s)\tilde{\tilde{v}}_0\left(b^2;\kappa,s\hat{\gamma}(s)\right)\tilde{u}_0(\kappa) \\ &\quad + \hat{\gamma}^2(s)\tilde{\tilde{v}}_1\left(b^2;\kappa,s\hat{\gamma}(s)\right)\tilde{w}_0(\kappa)\end{aligned} \tag{7}$$

and

$$\tilde{\tilde{u}}_{\rm inhom}(\hat{\gamma};\kappa,s) = \tilde{\tilde{v}}_1\left(b^2;\kappa,s\hat{\gamma}(s)\right)\tilde{\tilde{S}}_R(\kappa,s). \tag{8}$$

The auxiliary functions present in Eqs. (7) and (8) read

$$\tilde{\tilde{v}}_0\left(b^2;\kappa,s\right) = \frac{s+1/\tau}{s^2+s/\tau+b^2+a^2\kappa^2} \quad \text{and}$$
$$\tilde{\tilde{v}}_1\left(b^2;\kappa,s\right) = \frac{1}{s^2+s/\tau+b^2+a^2\kappa^2}. \tag{9}$$

The inversion of the LF transform in Eq. (7) obtained by using the Efros theorem[29,30,32–35] reads

$$u_{\rm hom}(\hat{\gamma};x,t) = \int_0^\infty u_{\rm hom}(1;x,\xi) f_{\hat{\gamma}}(\xi,t)d\xi, \tag{10}$$

in which

$$\begin{aligned} u_{\rm hom}(1;x,\xi) = {} & \frac{1}{2}e^{-\frac{\xi}{2\tau}}\left[u_0(x-a\xi)+u_0(x+a\xi)\right] + \frac{1}{4a\tau}e^{-\frac{\xi}{2\tau}}\int_{x-a\xi}^{x+a\xi} u_0(r)\left[I_0\left(\frac{\sigma}{2a\tau}\sqrt{a^2\xi^2-(x-r)^2}\right)\right. \\ & \left. + \frac{a\xi\sigma}{\sqrt{a^2\xi^2-(x-r)^2}} I_1\left(\frac{\sigma}{2a\tau}\sqrt{a^2\xi^2-(x-r)^2}\right)\right]dr + \frac{1}{2a}e^{-\frac{t}{2\tau}}\int_{x-at}^{x+at} I_0\left(\frac{\sigma}{2a\tau}\sqrt{a^2\xi^2-(x-r)^2}\right) w_0(r)dr, \end{aligned} \tag{11}$$

where

$$\sigma = \sqrt{1-4\tau^2 b^2}, \quad \text{and} \tag{12}$$

$$f_{\hat{\gamma}}(\xi,t) = \mathscr{L}^{-1}\left[\hat{\gamma}(s)e^{-\xi s\hat{\gamma}(s)};t\right]. \tag{13}$$

It is known that $u_{\rm hom}(1;x,\xi)$ is nonzero inside the compact region $x \in \Delta(\xi) = [-a\xi, a\xi]$. Furthermore, it is the solution of the homogeneous telegraphers' equation, i.e., Eq. (1) for $S_R(x,t) = 0$, which in (x,t)-space for $b = 0$ can be found in Ref. 36 ([Eq. (102) on p. 303]) and/or Ref. 37 [Eq. (7.4.28)]. We point out that Eq. (11) for $b = 0$ is also in Ref. 27 [Eq. (4.4)]. The derivation of Eq. (11) by using the integral transform method is shifted to Appendix A.

Since $u_{\rm hom}(\hat{\gamma};x,\xi)$ is independent of external harmonic impact, we concentrate on the special solution of the inhomogeneous equation denoted as $u_{\rm inhom}(\hat{\gamma};x,\xi)$ and given by Eq. (8). First, we take into account the convolution theorem, which states that the Laplace transform of the convolution of two functions is the product of their corresponding Laplace transforms. Next, we find the inverse Laplace transform of Eq. (8) to be given as

$$\tilde{u}_{\rm inhom}(\hat{\gamma};\kappa,t) = \int_0^t \mathscr{L}^{-1}\left[\tilde{v}_1\left(b^2;\kappa,s\hat{\gamma}(s)\right);\xi\right]\tilde{S}_R(\kappa,t-\xi)d\xi, \tag{14}$$

where

$$\tilde{S}_R(\kappa,t) = \mathscr{F}[S_R(x,t);\kappa] = Qe^{i\kappa v t}\cos\omega_0 t. \tag{15}$$

Thereafter, we proceed analogously as in the derivation of Eq. (11), i.e., employ Efros' theorem and the inverse LF transform. For $u_{\rm inhom}(\hat{\gamma};x,t)$, it results as

$$u_{\rm inhom}(\hat{\gamma};x,t) = \frac{Q}{\pi a}\int_0^t \cos\left(\omega_0(t-\xi)\right)\left[\mathfrak{J}_1(x,t,\xi)+\mathfrak{J}_2(x,t,\xi)\right]d\xi, \tag{16}$$

where

$$\begin{aligned} \mathfrak{J}_1(x,t,\xi) &= \int_0^\sigma \frac{\mathfrak{S}_1(p,\xi)}{\sqrt{\sigma^2-p^2}}\cos\left[\frac{p}{2a\tau}\left(x+v[t-\xi]\right)\right]dp, \\ \mathfrak{S}_1(p,\xi) &= \int_0^\infty e^{-\frac{y}{2\tau}}\sinh\left(\frac{\sqrt{\sigma^2-p^2}}{2\tau}y\right)g_{\hat{\gamma}}(y,\xi)dy \end{aligned} \tag{17}$$

and

$$\begin{aligned} \mathfrak{J}_2(x,t,\xi) &= \int_\sigma^\infty \frac{\mathfrak{S}_2(p,\xi)}{\sqrt{p^2-\sigma^2}}\cos\left[\frac{p}{2a\tau}\left(x+v[t-\xi]\right)\right]dp, \\ \mathfrak{S}_2(p,\xi) &= \int_0^\infty e^{-\frac{y}{2\tau}}\sin\left(\frac{\sqrt{p^2-\sigma^2}}{2\tau}y\right)g_{\hat{\gamma}}(y,\xi)dy \end{aligned} \tag{18}$$

with σ defined by Eq. (12) and

$$g_{\hat{\gamma}}(y,\xi) = \mathscr{L}^{-1}\left[e^{-ys\hat{\gamma}(s)};\xi\right]. \tag{19}$$

The derivation of Eq. (16) is presented in Appendix B. Note that from the conjecture formulated in Refs. 29 and 27 and proved in Appendix C of this paper, we know that for the memory function $\gamma(t)$ containing the Dirac-δ distribution, the solution (16) is nonzero in the compact domain $\Delta(t)$.

B. The case of the bounded domain, i.e., solutions to the GTE satisfying the boundary conditions (4)

Requiring the Dirichlet boundary and initial conditions given by Eqs. (2) and (4) we can solve Eq. (1) utilizing the separation of variables method. To do this, we analyze a homogeneous equation, namely, Eq. (1) with $Q = 0$, and assume that it has a solution of the form

$$u_{\rm hom}(\hat{\gamma};x,t) = X(x)T(t). \tag{20}$$

Substituting this expression into Eq. (1) without $S_R(x,t)$ and using the separation of variables method, we obtain two equations for the unknown functions X and T. For the first of them, the relevant equation is

$$\frac{d^2X(x)}{dx^2} + \frac{\lambda}{a^2}X(x) = 0, \tag{21}$$

with boundary conditions $X(-l) = 0$ and $X(l) = 0$. The Sturm–Liouville problem related to Eq. (21) has eigenvalues λ_n and corresponding eigenfunctions $X_n(x)$ that are, respectively, equal to

$$\lambda_n = \frac{\pi^2a^2(2n+1)^2}{4l^2} \quad \text{and} \quad X_n(x) = \cos\left[\frac{\pi(2n+1)x}{2l}\right], \tag{22}$$

where $n \in \mathbb{N}_0$. Using the obtained eigenfunctions $X_n(x)$, we look for the solution of the inhomogeneous Eq. (1) in the following series form:

$$u(\hat{\gamma};x,t)=\sum_{n=0}^{\infty}c_n(\hat{\gamma};t)X_n(x). \tag{23}$$

By substituting Eq. (23) into Eq. (1), we obtain the following equations for the coefficients $c_n(\hat{\gamma};t)$:

$$\int_0^t \eta(t-\xi)\partial_\xi^2 c_n(\hat{\gamma};\xi)d\xi + \frac{1}{\tau}\int_0^t \gamma(t-\xi)\partial_\xi c_n(\hat{\gamma};\xi)d\xi + \Lambda_n c_n(\hat{\gamma};t) = I_n(t), \tag{24}$$

where $\Lambda_n = b^2+\lambda_n$ and

$$I_n(t)=\frac{Q}{2l}\left[\cos(\Omega_+ t)+\cos(\Omega_- t)\right] \quad \text{with } \Omega_\pm = \pi(2n+1)\frac{v}{2l}\pm\omega_0 \tag{25}$$

being the coefficients of the point-wise source $S_R(x,t)$ in the space spanned by $X_n(x)$. Equation (24) can be solved by taking its Laplace transform. This leads to

$$\begin{aligned}\widehat{c}_n(\hat{\gamma};s) &= \hat{\gamma}(s)\hat{\nu}_0\left(\Lambda_n;s\hat{\gamma}(s)\right)c_n(\hat{\gamma};0)\\ &\quad+\hat{\gamma}^2(s)\hat{\nu}_1\left(\Lambda_n;s\hat{\gamma}(s)\right)\frac{d}{dt}c_n(\hat{\gamma};t)\Big|_{t=0}\\ &\quad+\hat{\nu}_1\left(\Lambda_n;s\hat{\gamma}(s)\right)\hat{I}_n(s).\end{aligned} \tag{26}$$

Formally, $\hat{\nu}_0(\Lambda_n;s)$ and $\hat{\nu}_1(\Lambda_n;s)$ have forms of $\tilde{\hat{\nu}}_0(\Lambda_n;\kappa,s)$ and $\tilde{\hat{\nu}}_1(\Lambda_n;\kappa,s)$ given by Eq. (9) for $\kappa=0$ and $b^2=\Lambda_n$, respectively. Nevertheless, it should be noted that there is a significant difference between these pairs of functions. Namely, $\hat{\nu}_0(\Lambda_n;s)$ and $\hat{\nu}_1(\Lambda_n;s)$ are defined only in s-space whereas the members of the second pair $\tilde{\hat{\nu}}_0(\Lambda_n;\kappa,s)$ and $\tilde{\hat{\nu}}_1(\Lambda_n;\kappa,s)$ are given in (s,κ)-space. Further, we can rewrite $\hat{\gamma}(s)\hat{\nu}_0\left(\Lambda_n;s\hat{\gamma}(s)\right)$ and $\hat{\gamma}^2(s)\hat{\nu}_1\left(\Lambda_n;s\hat{\gamma}(s)\right)$ in the following forms:

$$\hat{\gamma}(s)\hat{\nu}_0\left(\Lambda_n;s\hat{\gamma}(s)\right)=s^{-1}-\Lambda_n s^{-1}\hat{\nu}_1\left(\Lambda_n;s\hat{\gamma}(s)\right) \tag{27}$$

$$\begin{aligned}\hat{\gamma}^2(s)\hat{\nu}_1\left(\Lambda_n;s\hat{\gamma}(s)\right) &= s^{-2}-\tau^{-1}s^{-1}\hat{\gamma}(s)\hat{\nu}_1\left(\Lambda_n;s\hat{\gamma}(s)\right)\\ &\quad-\Lambda_n s^{-2}\hat{\nu}_1\left(\Lambda_n;s\hat{\gamma}(s)\right)\end{aligned} \tag{28}$$

and, then, calculate its inverse Laplace transform, remembering that $\mathscr{L}^{-1}[s^{-1};t]=1$ and $\mathscr{L}^{-1}[s^{-2};t]=t$. Using the properties of the Laplace transform, i.e., $\mathscr{L}^{-1}[s^{-n}\hat{f}(s);t]=\int_0^t(t-\xi)^{n-1}f(\xi)d\xi/(n-1)!$ for $n\geq 1$, and Efros' theorem, we have

$$\nu_0(\hat{\gamma};\Lambda_n;t)=1-\Lambda_n\int_0^t\left\{\int_0^\infty \nu_1(\Lambda_n;\xi)g_{\hat{\gamma}}(\xi,r)d\xi\right\}dr \tag{29}$$

and

$$\begin{aligned}\nu_1(\hat{\gamma};\Lambda_n;t) &= t-\tau^{-1}\int_0^t\left\{\int_0^\infty \nu_1(\Lambda_n;\xi)f_{\hat{\gamma}}(\xi,r)d\xi\right\}dr\\ &\quad-\Lambda_n\int_0^t\left\{\int_0^\infty \nu_1(\Lambda_n;\xi)g_{\hat{\gamma}}(\xi,r)d\xi\right\}(t-r)dr\end{aligned} \tag{30}$$

with $g_{\hat{\gamma}}(\sigma;r)$ given by Eq. (19), $f_{\hat{\gamma}}(\sigma;r)$ given by Eq. (13), and

$$\nu_1(\Lambda_n;t)=2\tau e^{-t/(2\tau)}\frac{\sinh\left(\frac{t}{2\tau}\sqrt{1-4\Lambda_n\tau^2}\right)}{\sqrt{1-4\Lambda_n\tau^2}}. \tag{31}$$

The coefficients $c_n(\hat{\gamma};0)$ and $\dot{c}_n(\hat{\gamma};t)|_{t=0}$ expressed in terms of the initial conditions (2) and in the basis $X_n(x)$ read

$$\begin{aligned}c_n(\hat{\gamma};0) &= \frac{1}{l}\int_{-l}^{l}u_0(x)X_n(x)dx \quad \text{and}\\ \frac{d}{dt}c_n(\hat{\gamma};t)\Big|_{t=0} &= \frac{1}{l}\int_{-l}^{l}w_0(x)X_n(x)dx,\end{aligned} \tag{32}$$

and it turns out that they do not depend on the memory function $\gamma(t)$. Thus, we will rename them as $c_n(0)\equiv c_n(\hat{\gamma};0)$ and $\dot{c}_n(t)|_{t=0}\equiv\dot{c}_n(\hat{\gamma};t)|_{t=0}$. For example, for the fundamental initial conditions, i.e., $u_0(x)=\delta(x)$ and $w_0(x)=0$, we have $c_n(0)=l^{-1}$ and vanishing $\dot{c}_n(t)|_{t=0}$.

Applying the Laplace convolution, as well as the Efros theorem, the inverse Laplace transform of the last term in Eq. (26) figures out

$$\mathscr{L}^{-1}\left[\hat{\nu}_1(\Lambda_n;s\hat{\gamma}(s))\hat{I}_n(s);t\right]=\int_0^t\mathscr{L}^{-1}\left[\hat{\nu}_1(\Lambda_n;s\hat{\gamma}(s));r\right]I_n(t-r)dr. \tag{33}$$

In analogy to Sec. II, we can also present $u(\hat{\gamma};x,t)$ as the sum of the homogeneous solution given by

$$\begin{aligned}&u_{\text{hom}}(\hat{\gamma};x,t)\\ &=\sum_{n=0}^{\infty}X_n(x)\left[\nu_0(\hat{\gamma};\Lambda_n;t)c_n(0)+\nu_1(\hat{\gamma};\Lambda_n;t)\frac{d}{dt}c_n(t)\Big|_{t=0}\right]\end{aligned} \tag{34}$$

and the inhomogeneous solution that figures out

$$\begin{aligned}&u_{\text{inhom}}(\hat{\gamma};x,t)\\ &=\sum_{n=0}^{\infty}X_n(x)\left[\int_0^t\mathscr{L}^{-1}\left[\hat{\nu}_1(\Lambda_n;s\hat{\gamma}(s));r\right]I_n(t-r)dr\right].\end{aligned} \tag{35}$$

III. SOLUTIONS TO GTES FOR CHOSEN EXAMPLES OF MEMORY FUNCTIONS: MEMORYLESS, I.E., TIME-LOCAL, VS MEMORY-DEPENDENT CASES

In this section, we shall discuss solutions to the GTEs for the case of a moving source and a stationary observer located at some point x. To illustrate the problem, we will concentrate on two examples that differ by the choice of the memory kernel γ and, in the first case, we consider a localized memory kernel while in the next case, we investigate a power-law kernel. Since the frequency shift is suspected to be noted only in the inhomogeneous solution, we focus solely on this part of the solution.

A. Memoryless, i.e., the time-local evolution

1. Time localized memory function: Solutions with boundary conditions Eq. (3)

When $\gamma(t) = \delta(t)$, then we arrive at the standard telegraphers' equation

$$\partial_t^2 u(1;x,t) + \frac{1}{\tau}\partial_t u(1;x,t) + [b^2 - a^2\partial_x^2]u(1;x,t) = S_R(x,t). \quad (36)$$

The homogeneous solution $u_{\mathrm{hom}}(1;x,t)$ of this equation under the boundary conditions (3) is given by Eq. (11), whereas its inhomogeneous solution $u_{\mathrm{inhom}}(1;x,t)$ can be obtained by using expression (16). It yields

$$u_{\mathrm{inhom}}(1;x,t) = \frac{Qt}{\pi a}\int_0^1 e^{-\frac{ut}{2\tau}}\cos[\omega_0 t(1-u)] \times (\mathfrak{J}_1(x,t,u) + \mathfrak{J}_2(x,t,u))\,du, \quad (37)$$

where Eqs. (17) and (18) reduce to

$$\mathfrak{J}_1(x,t,u) = \int_0^\sigma \frac{\sinh\left(\frac{ut}{2\tau}\sqrt{\sigma^2-p^2}\right)}{\sqrt{\sigma^2-p^2}}\cos\left[\frac{p}{2a\tau}(x+vt[1-u])\right]dp$$

and

$$\mathfrak{J}_2(x,t,u) = \int_\sigma^\infty \frac{\sin\left(\frac{ut}{2\tau}\sqrt{p^2-\sigma^2}\right)}{\sqrt{p^2-\sigma^2}}\cos\left[\frac{p}{2a\tau}(x+vt[1-u])\right]dp.$$

We recall that σ is defined by Eq. (12) which for $b = 0$ is equal to one, and Eq. (37) goes to Ref. 28 [Eq. (24)].

Taking first the Fourier transform and then the Laplace inverse transform, we obtain an alternative form of Eq. (37), namely,

$$u_{\mathrm{inhom}}(1;x,t) = \upsilon(1,\omega_0;x,t) + \upsilon(1,-\omega_0;x,t), \quad (38)$$

where

$$\upsilon(1,\omega_0;x,t) = \frac{Qe^{-t/(2\tau)}}{4C(\tau,\omega_0)}\Theta\left(t-\frac{|x|}{a}\right)\left\{\frac{1+\beta\,\mathrm{sign}x}{1-\beta^2}h\left(\tau,\omega_0;t-\frac{|x|}{a}\right) + \int_{|x|/a}^t h(\tau,\omega_0;t-\xi)\left[-A(\tau,\omega_0)I_0\left(\sqrt{a^2\xi^2-x^2}\right) + \frac{a\xi+\beta x}{2\tau(1-\beta^2)}\frac{\sigma I_1\left(\sqrt{a^2\xi^2-x^2}\right)}{\sqrt{a^2\xi^2-x^2}}\right]d\xi\right\} - \frac{Qe^{i\omega_0|x|/v}}{4C(\tau,\omega_0)}\Theta\left(t-\frac{|x|}{v}\right)k\left(\tau,\omega_0;t-\frac{|x|}{v}\right). \quad (39)$$

The auxiliary functions read

$$h(\tau,\omega_0;y) = \exp[A(\tau,\omega_0)y]\sinh[C(\tau,\omega_0)y], \quad \text{and}$$
$$k(\tau,\omega_0;y) = \exp[B(\tau,\omega_0)y]\sinh[C(\tau,\omega_0)y] \quad (40)$$

with $\beta = v/a$, and

$$A(\tau,\omega_0) = \frac{\mathrm{i}\omega_0 + 1/(2\tau)}{1-\beta^2}, \quad B(\tau,\omega_0) = \frac{\mathrm{i}\omega_0 + \beta^2/(2\tau)}{1-\beta^2},$$
$$C(\tau,\omega_0) = \frac{\mathrm{i}\omega_0\beta}{1-\beta^2}\left(1 - \frac{\mathrm{i}}{\tau\omega_0} - \frac{b^2}{\omega_0^2} - \frac{\beta^2\sigma^2}{4\tau^2\omega_0^2}\right)^{1/2}. \quad (41)$$

Notice that for $b = 0$, the right-hand side of Eq. (39) is proportional, as it should be, to Ref. 27 [Eq. (4.6)] and/or Ref. 28 [Eq. (13)]. Recall also that to derive Eq. (39), we proceed similarly as in the case of deriving Eqs. (7)–(12) presented in Ref. 28.

2. Time localized memory function: Solutions with boundary conditions Eq. (4)

The solution of the standard telegraphers' equation under the boundary conditions Eq. (4) is given by Eqs. (34) and (35). In the homogeneous part the auxiliary functions $\nu_0(\hat{\gamma};\Lambda_n;t)$ and $\nu_1(\hat{\gamma};\Lambda_n;t)$ for $\hat{\gamma}(s) = 1$ read

$$\nu_0(1;\Lambda_n;t) \equiv \nu_0(\Lambda_n;t) = \mathscr{L}^{-1}\left[\frac{s+1/\tau}{s^2+s/\tau+\Lambda_n};t\right]$$
$$= e^{-\frac{t}{2\tau}}\left[\cosh\left(\frac{t}{2\tau}\sqrt{1-4\Lambda_n\tau^2}\right) + \frac{1}{\sqrt{1-4\Lambda_n\tau^2}}\sinh\left(\frac{t}{2\tau}\sqrt{1-4\Lambda_n\tau^2}\right)\right] \quad (42)$$

and $\nu_1(1;\Lambda_n;t) \equiv \nu_1(\Lambda_n;t)$ given by Eq. (31). The inhomogeneous solution (35) can be presented as

$$u_{\mathrm{inhom}}(1;x,t) = \sum_{n=0}^\infty[\mathrm{Int}_+(n;t) + \mathrm{Int}_-(n;t)]X_n(x). \quad (43)$$

The integrals $\mathrm{Int}_\pm(n;t)$ are equal to

$$\mathrm{Int}_\pm(n;t) = \frac{Q\tau^2}{2l}\frac{\Lambda_n - \Omega_\pm^2}{\tau^2(\Lambda_n-\Omega_\pm^2)^2 + \Omega_\pm^2} \times\left[\cos(\Omega_\pm t) - e^{-\frac{t}{2\tau}}\cosh\left(\frac{t}{2\tau}\sqrt{1-4\Lambda_n\tau^2}\right)\right] + \frac{Q\tau}{2l}\frac{1}{\tau^2(\Lambda_n-\Omega_\pm^2)^2+\Omega_\pm^2}\left[\Omega_\pm\sin(\Omega_\pm t) - \frac{\tau(\Lambda_n+\Omega_\pm^2)}{\sqrt{1-4\Lambda_n\tau^2}}e^{-\frac{t}{2\tau}}\sinh\left(\frac{t}{2\tau}\sqrt{1-4\Lambda_n\tau^2}\right)\right], \quad (44)$$

where $\Omega_\pm$ are defined in Eq. (25).

B. Evolution dependent on power-law memory function

As the second example of the evolution pattern, we consider Eq. (1) with the memory kernel whose Laplace transform is given by $\hat{\gamma}(s) = s^{\alpha-1}$, where $\alpha \in (0,1)$. In this case, Eq. (1) takes the form of a fractional equation

$$^{C}D_t^{2\alpha} u(x,t) + \frac{1}{\tau}\, {}^{C}D_t^{\alpha} u(x,t) + [b^2 - a^2\partial_x^2]u(x,t) = S_R(x,t), \quad (45)$$

with

$$\left({}^{C}D_t^{\beta} h\right)(t) = \frac{1}{\Gamma(m-\beta)} \int_0^t \frac{h^{(m)}(\xi)}{(t-\xi)^{1+\beta-m}} d\xi$$

denoting for $m-1 < \beta < m$ the Caputo fractional derivative of order β.

1. Evolution governed by the power-law memory function: Solutions with boundary conditions Eq. (3)

The general method of solving GTE based on applying the joint Laplace–Fourier transform was presented in Sec. II A. For the case of Eq. (45), it boils down to using the functions $g_{s^{\alpha-1}}(y,\xi)$ and $f_{\hat{\gamma}}(y,\xi)$, previously introduced by Eqs. (19) and (13), and here given as

$$g_{s^{\alpha-1}}(y,\xi) = \Phi_\alpha(y,\xi) \quad \text{and} \quad f_{s^{\alpha-1}}(y,\xi) = \frac{\xi}{\alpha y}\Phi_\alpha(y,\xi), \quad (46)$$

in which $\Phi_\alpha(y,\xi) = y^{-1/\alpha}\Phi_\alpha(\xi y^{-1/\alpha})$ is the one-sided Lévy stable distribution.[29,38]

To find the solution satisfying the boundary conditions given by Eq. (3), we use expression (16) and, as in the previous example, we set $\eta = \xi/t$ and determine $\mathfrak{S}_1(p,\eta)$ and $\mathfrak{S}_2(p,\eta)$ defined by Eqs. (17) and (18), respectively. Then, we remove the parts depending on t and u shifting them to the final expression $u_{\text{inhom}}(s^{\alpha-1};x,t)$. That gives

$$u_{\text{inhom}}(s^{\alpha-1};x,t) = \frac{Qt^\alpha}{2\pi a}\int_0^1 \eta^{\alpha-1}\cos[\omega_0 t(1-\eta)] \times (\mathfrak{J}_1(x,t,\eta) + i\,\mathfrak{J}_2(x,t,\eta))\, d\eta \quad (47)$$

where

$$\mathfrak{J}_1(x,t,\eta) = \int_0^\sigma \frac{\mathfrak{S}_1(p,\eta)}{\sqrt{\sigma^2-p^2}} \cos\left[\frac{p}{2a\tau}(x+vt[1-\eta])\right] dp, \quad (48)$$

$$\mathfrak{S}_1(p,\eta) = E_{\alpha,\alpha}\left[\left(-1+\sqrt{\sigma^2-p^2}\right)\frac{\eta^\alpha t^\alpha}{2\tau}\right] - E_{\alpha,\alpha}\left[\left(-1-\sqrt{\sigma^2-p^2}\right)\frac{\eta^\alpha t^\alpha}{2\tau}\right],$$

and

$$\mathfrak{J}_2(x,t,\eta) = \int_\sigma^\infty \frac{\mathfrak{S}_2(p,\xi)}{\sqrt{p^2-\sigma^2}} \cos\left[\frac{p}{2a\tau}(x+vt[1-\eta])\right] dp, \quad (49)$$

$$\mathfrak{S}_2(p,\eta) = E_{\alpha,\alpha}\left[\left(-1-i\sqrt{p^2-\sigma^2}\right)\frac{\eta^\alpha t^\alpha}{2\tau}\right] - E_{\alpha,\alpha}\left[\left(-1+i\sqrt{p^2-\sigma^2}\right)\frac{\eta^\alpha t^\alpha}{2\tau}\right].$$

The two-parameter Mittag–Leffler function $E_{\alpha,\alpha}$ was obtained with the help of the Euler formula for the sinus hyperbolic function and the integral representation of $E_{\alpha,\alpha}$ presented in Ref. 30 [Example 2 for $\beta = 1$] or Eq. (D4) for $\mu = \alpha$.

2. Evolution governed by the power-law memory function: Solutions with boundary conditions Eq. (4)

To find the solution of Eq. (45) with boundary conditions Eq. (4), we incorporate the method and results presented in Sec. II B. The solution of Eq. (45) is equal to the sum of Eqs. (34) and (35), where $X_n(x)$ is defined by Eq. (22). At first, we calculate $u_{\text{hom}}(s^{\alpha-1};x,t)$, which contains the coefficients $v_0(s^{\alpha-1};\Lambda_n;t)$ and $v_1(s^{\alpha-1};\Lambda_n;t)$. They are the inverse Laplace transforms of $s^{\alpha-1}\hat{v}_0(\Lambda_n;s^\alpha)$ and $\hat{v}_1(\Lambda_n;s^\alpha)$ defined by Eqs. (27) and (28), respectively. We calculate them with the help of (D1) which gives

$$v_0(s^{\alpha-1};\Lambda_n;t) = 1 - \Lambda_n t^{2\alpha} E_{(\alpha,2\alpha);2\alpha+1}\left(-t^\alpha/\tau, -\Lambda_n t^{2\alpha}\right) \quad (50)$$

and

$$v_1(s^{\alpha-1};\Lambda_n;t) = t - \tau^{-1}t^{\alpha+1}E_{(\alpha,2\alpha),\alpha+2}\left(-t^\alpha/\tau, -\Lambda_n t^{2\alpha}\right) - \Lambda_n t^{2\alpha+1}E_{(\alpha,2\alpha),2\alpha+2}\left(-t^\alpha/\tau, -\Lambda_n t^{2\alpha}\right). \quad (51)$$

Equation (34) contains also $c_n(0)$ and $\dot{c}_n(t)|_{t=0}$ for $n \in \mathbb{N}_0$ which are given by Eq. (32) and depend on the initial conditions $u_0(x)$ and $w_0(x)$, respectively.

The solution $u_{\text{inhom}}(s^{\alpha-1}x,t)$ contains Eq. (33) which, after applying (D1), becomes

$$\mathscr{L}^{-1}\left[\hat{v}_1(\Lambda_n;s^\alpha);r\right] = \mathscr{L}^{-1}\left[\frac{s^{-2\alpha}}{1+s^{-\alpha}/\tau+\Lambda_n s^{-2\alpha}};r\right] = r^{2\alpha-1}E_{(\alpha,2\alpha),2\alpha}\left(-r^\alpha/\tau, -\Lambda_n r^{2\alpha}\right). \quad (52)$$

Inserting Eqs. (50) and (51) into Eq. (34) as well as Eq. (52) into Eq. (35) we reconstruct the results obtained by using Ref. 39 [Theorem 2.4] or Ref. 40 for the Cattaneo–Vernotte equation. The inhomogeneous solution figures out

$$u_{\text{inhom}}\left(s^{\alpha-1};x,t\right) = \sum_{n=0}^\infty X_n(x)\left\{\int_0^t r^{2\alpha-1}E_{(\alpha,2\alpha),2\alpha}\left(-\tau^{-1}r^\alpha, -\Lambda_n r^{2\alpha}\right) I_n(t-r)dr\right\}. \quad (53)$$

IV. THE TIME-FREQUENCY ANALYSIS: NUMERICAL STUDY USING THE SHORT-TIME FOURIER TRANSFORM

In this section, we present the results of the time-frequency analysis of the signals derived from the memoryless telegraph and fractional telegraph equations discussed in the previous section. These results will be illustrated using spectrograms. The analysis was conducted using the short-time Fourier transform (STFT), defined in both the time and frequency domains as

$$STFT_s^T(t,f) = \int_{-\infty}^{\infty} s(\tau)h^*(\tau - t)e^{-i2\pi f\tau}\, d\tau, \tag{54}$$

$$STFT_s^F(t,f) = e^{-i2\pi ft}\int_{-\infty}^{\infty} \tilde{s}(\nu)\tilde{h}^*(\nu - f)e^{i2\pi\nu t} d\nu, \tag{55}$$

respectively. In the above formulas, s denotes the analyzed signal, whose Fourier spectrum is denoted by $\tilde{s}$. The h function is the so-called temporal observation window with the Fourier spectrum denoted by $\tilde{h}$. The square of the modulus of the short-time Fourier transform is called a spectrogram. STFT in the time domain involves performing a Fourier transform on successive fragments of the signal that are selected by a sliding window. In the frequency domain, on the other hand, STFT involves the inverse Fourier transformation of a fragment of the signal spectrum selected by a frequency-shifted window spectrum. In time-frequency analysis based on the short-time Fourier transform, the selection of a wide window h results in high resolution on the frequency axis while lower resolution on the time axis. Choosing a narrow window produces the opposite effect described above. In all the results shown below, a wide Tukey window was used to generate the spectrograms. This window is defined

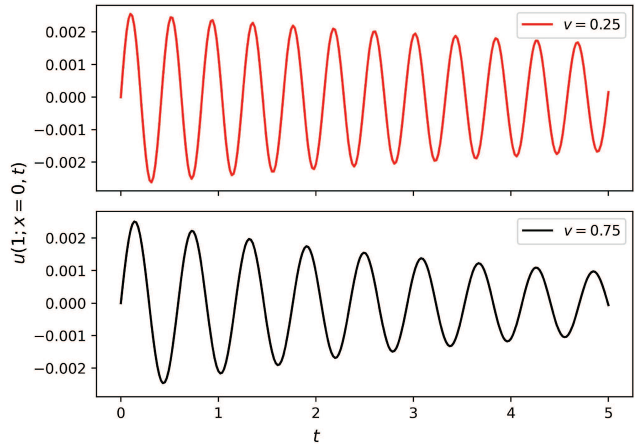

FIG. 2. The signals (37) used for generating Fig. 1 for $v = 0.25$ and $v = 0.75$. The remaining values of parameters are equal to $x = 0$, $Q = 0.1$, $\tau = 1.0$, $a = 1.0$, $b = 0.2$, and $\omega_0 = 6\pi$.

as follows:

$$\begin{cases} h[n] = \dfrac{1}{2}\left[1 - \cos\left(\dfrac{2\pi n}{\alpha_T N}\right)\right], & 0 \le n < \dfrac{\alpha_T N}{2}, \\ h[n] = 1, & \dfrac{\alpha_T N}{2} \le n < \dfrac{N}{2}. \end{cases} \tag{56}$$

In addition, for $0 \le n \le \frac{N}{2}$, the condition $h[N-n] = h[n]$ is satisfied. Tukey's window can be viewed as a convolution of a cosine lobe of width $\frac{N\alpha_T}{2}$ with a rectangular window of width $N\left(1 - \frac{\alpha_T}{2}\right)$. The

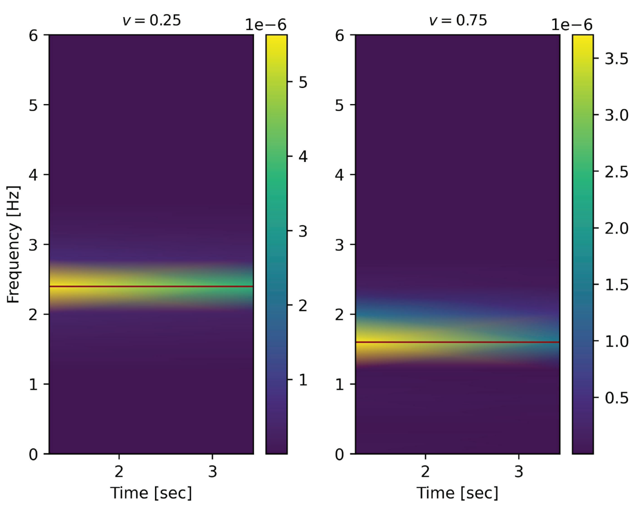

FIG. 1. Spectrograms of the signal (37) being the solution of standard telegraphers' equation for $x = 0$, $Q = 0.1$, $\tau = 1.0$, $a = 1.0$, $b = 0.2$, and $\omega_0 = 6\pi$.

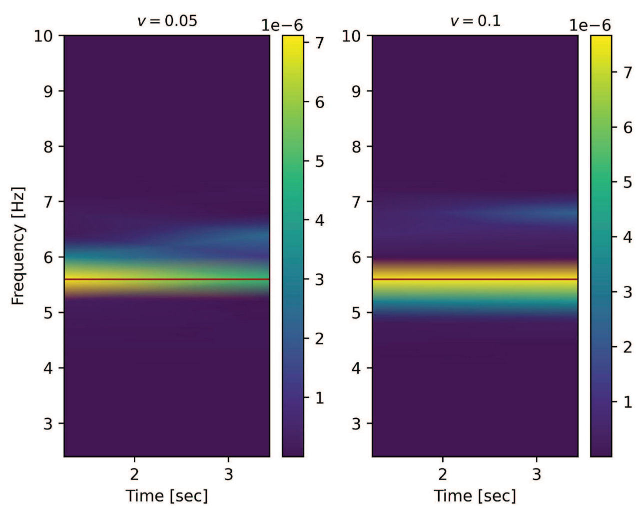

FIG. 3. Spectrograms of the signal (43) being the solution of standard telegraphers' equation for $x = 0$, $Q = 0.1$, $\tau = 1.0$, $a = 1.0$, $b = 0.2$, $\omega_0 = 6\pi$, and $l = 1.0$.

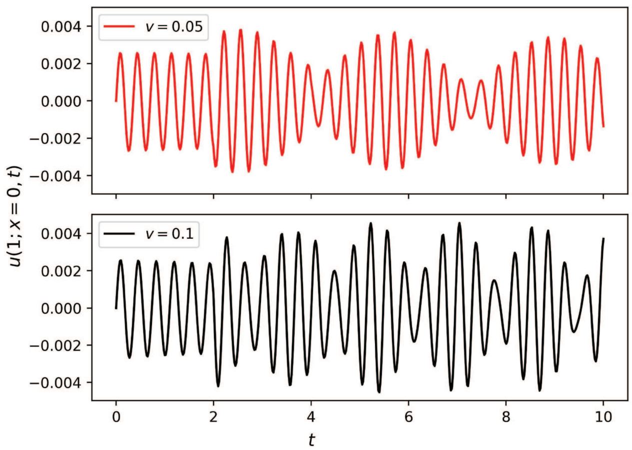

FIG. 4. The signals (43) used for generating Fig. 3 for $v = 0.05$ and $v = 0.1$. The remaining values of parameters are equal to $x = 0$, $Q = 0.1$, $\tau = 1.0$, $a = 1.0$, $b = 0.2$, $\omega_0 = 6\pi$, and $l = 1.0$.

parameter N is related to the number of samples of the analyzed signal. Spectrograms are widely used in various fields, including audio processing, speech analysis, biomedical signal processing, and environmental monitoring. They help identify patterns, features, and anomalies in complex signals. By examining the spectrogram, one can observe transient events, harmonic structures, and modulation effects.[41]

A. Memory independent evolution

The results of time-frequency analysis for the signal solving telegraphers' equation for two distinct boundary regimes are defined by Eqs. (37) and (43). Their spectrograms, calculated using two different values of velocity v each, are presented in Figs. 1 and 3, respectively. Here, the horizontal red line indicates the frequency at which the maximum value of the spectrogram occurs. Note that

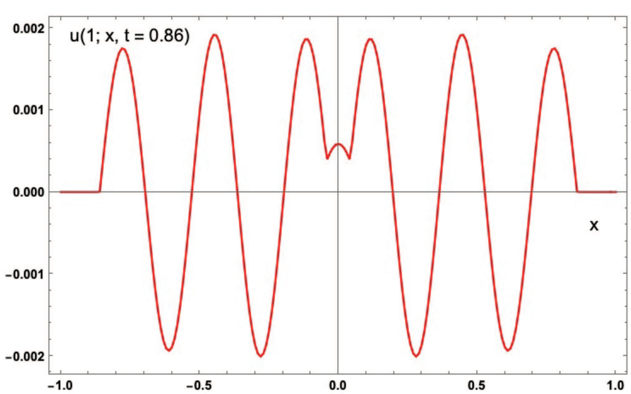

FIG. 5. The signal (43) for $v = 0.05$. The values of parameters and initial position x is the same as in Fig. 4.

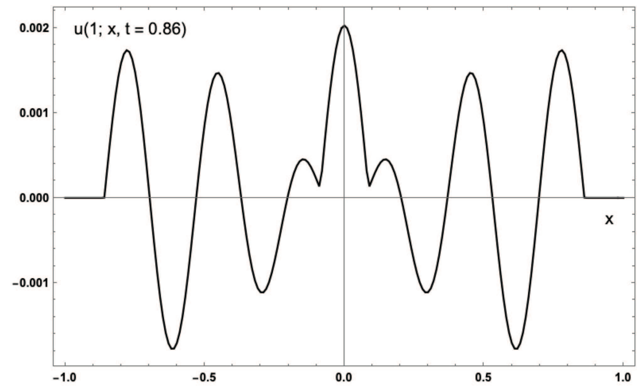

FIG. 6. The signal (43) for $v = 0.1$. The values of parameters and initial position x is the same as in Fig. 4.

Figs. 2 and 4, which show the signals for which respective spectrograms were generated in both cases, concern the case when observers remain at rest at the origin of the coordinate system ($x = 0$), and the parameters $Q = 0.1$, $\tau = 1.0$, $a = 1.0$, $b = 0.2$ and $\omega_0 = 6\pi$ are used. However, they were obtained for different ranges of the source velocity and, additionally, for the signal (43) restricted to the boundary domain $|l| = 1.0$. Differences seen at first glance in the shape of plots and their possible explanation/interpretation will be addressed below.

For the solution of the memoryless telegraphers' equation in the case of an infinite area of signal propagation (in fact, the equation is equivalent to the one that describes damped oscillations), we observe on the spectrogram Fig. 1 a shift in the signal frequency that

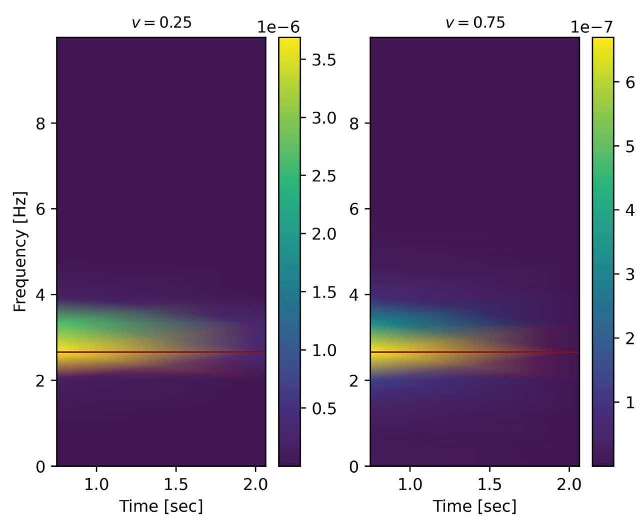

FIG. 7. Spectrograms of the signal (47) solving the fractional telegraphers' equation for $\alpha = 0.25$. The values of parameters and initial position x is the same as in Fig. 1.

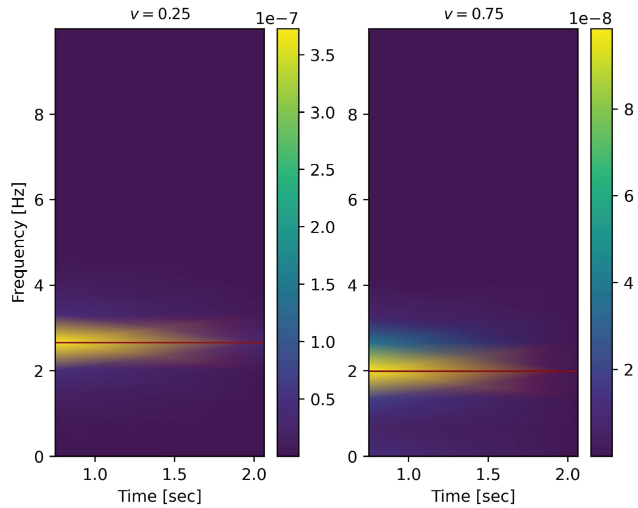

FIG. 8. Spectrograms of the signal (47) solving the fractional telegraphers' equation for $\alpha = 0.75$. The values of parameters and initial position x is the same as in Fig. 1.

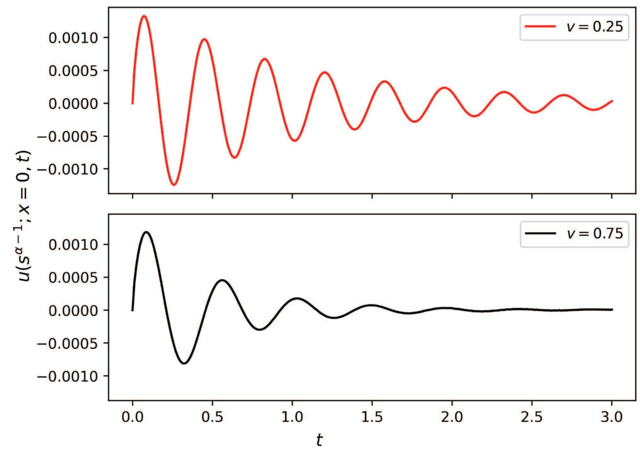

FIG. 10. The signals (47) used for generating Fig. 8 for $v = 0.25$ and $v = 0.75$. The remaining values of parameters are equal to $x = 0$, $Q = 0.1$, $\tau = 1.0$, $a = 1.0$, $b = 0.2$, $\omega_0 = 6\pi$, and $\alpha = 0.75$.

depends on the external source velocity. On the other hand, for the solution of the same equation restricted to the finite area, i.e., with boundary conditions (4), we do not observe any significant shift in the frequency of the signal associated with changing the velocity of the external source, see the spectrogram Fig. 3. But here, it is important to note that the observation is made over a sufficiently long period for the signal moving with the velocity $a = 1.0$ to reach the area boundary, reflect off it, and go backward to meet and interfere with much slower waves emitted by the external source. It comes into play for time lapses approximately equal to 2 and larger, as seen in Fig. 4. Such a scenario, if it happens, leads to the formation of periodic oscillations interpreted as standing waves that have neither wavefronts nor well-defined propagation velocities, and because of that, do not manifest the existence of phenomena more or less identifiable with the common Doppler effect. However, for lapses of time during which the signal does not yet reach the area boundary, the solution Eq. (43) is the same as the solution Eq. (37). This encourages one to ask for some deeply hidden traces of the Doppler effect, which could be found if one studies the solution for a short, or very short, time. To support these efforts, we present Figs. 5 and 6, in which, for a sufficiently short time, one may observe a cusp in the

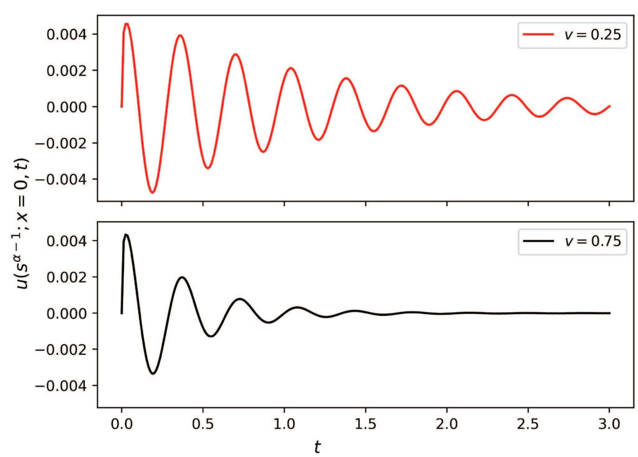

FIG. 9. The signals (47) used for generating Fig. 7 for $v = 0.25$ and $v = 0.75$ The remaining values of parameters are equal to $x = 0$, $Q = 0.1$, $\tau = 1.0$, $a = 1.0$, $b = 0.2$, $\omega_0 = 6\pi$ and $\alpha = 0.25$.

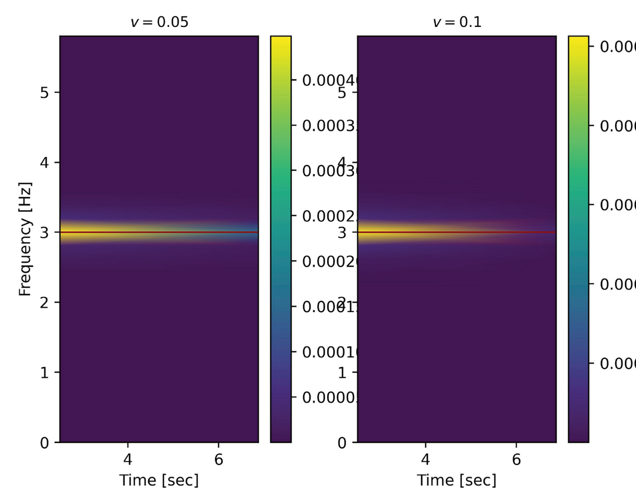

FIG. 11. Spectrograms of the signal (53) solving the fractional telegraphers' equation for $\alpha = 0.25$. The values of parameters and initial position x are the same as in Fig. 1.

snapshot of the solution $u(1; x, t)$, here plotted as a function of x. According to the arguments given in Ref. 27, the occurrence of such a cusp comes from the sudden change in the observed frequency, which happens when the moving source passes by the observer's location. The effect may be considered a shadow of the Doppler, or Doppler-like, effect. A similar conclusion, however, formulated only qualitatively, may be deduced from the behavior exhibited by the envelope of standing waves, as seen in Fig. 4. The time distance that separates subsequent antinodes decreases with growing velocity v, which may be translated into the increased frequency at which antinodes appear. Nevertheless, the frequency of component waves that altogether form the standing waves does not change. Summing up the considerations made so far, we remark that manifestations of the existence/non-existence of the Doppler effect sought for solutions to Eq. (1) with boundary conditions Eq. (4) put on are also obscured by the fact that in our analysis we did not touch the question of periodic boundary conditions and the problem how to incorporate the external current into Eq. (1) in such a case.

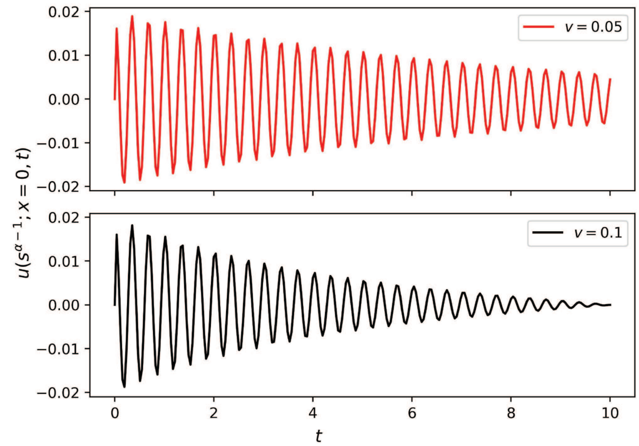

FIG. 13. The signals (53) used for generating Fig. 11 for $\alpha = 0.25$.

B. Memory-dependent evolution I

Figures 7 and 8 show the results of the time-frequency analysis for the solution of Eq. (1) for power-law memory for two different values of the alpha parameter, namely, $\alpha = 0.25$ and $\alpha = 0.75$. Recall that these values of the α parameter characterize, respectively, the so-called "heat (diffusion)-type" or "wave-type" regimes of the fractional diffusion-wave equation. The solution, defined in an unbounded domain, is given by Eq. (47). For just mentioned values of α, they are shown in Figs. 9 and 10. The spectrograms reveal a frequency shift for α set to 3/4. In contrast for α at 1/4, we do not observe any significant frequency change despite variations in the speed of the signal source. The insertion of power-law memory into Eq. (1) causes a faster decay of the signal that is the solution of the equation compared to the solution described by Eq. (37) and for this reason numerical results presented in Figs. 5 and 6 are limited to the time interval [0, 3]. Based on our previous numerical and analytical investigations, we can conjecture that a signal frequency change in response to source speed variations will occur for the solution (47) when the alpha parameter exceeds 1/2. Conversely, no such change is expected for alpha values at or below 1/2.

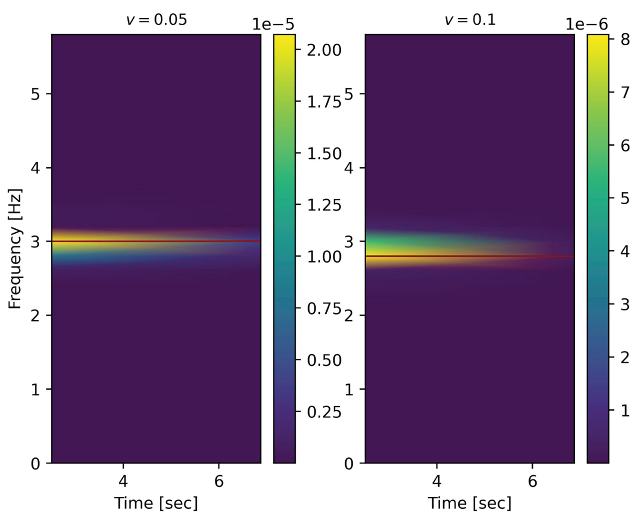

FIG. 12. Spectrograms of the signal (53) solving the fractional telegraphers' equation for $\alpha = 0.75$. The values of parameters and initial position x is the same as in Fig. 1.

C. Memory-dependent evolution II

Comparing solutions to the GTE given by Eq. (1) with two distinct variants of boundary conditions put on we paid attention that interpretation of our results in terms of the Doppler effect is clear

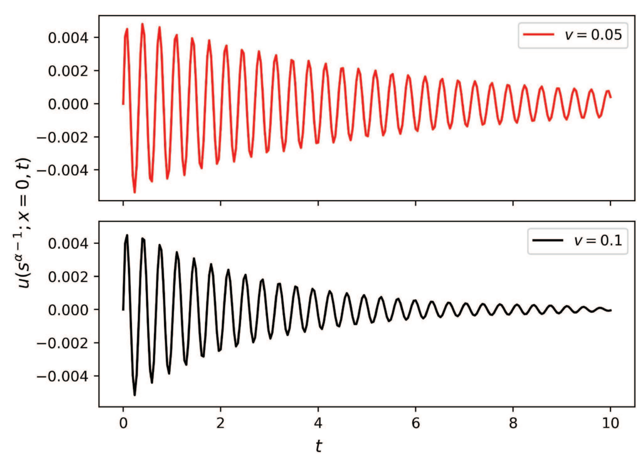

FIG. 14. The signals (53) used for generating Fig. 12 for $\alpha = 0.75$.

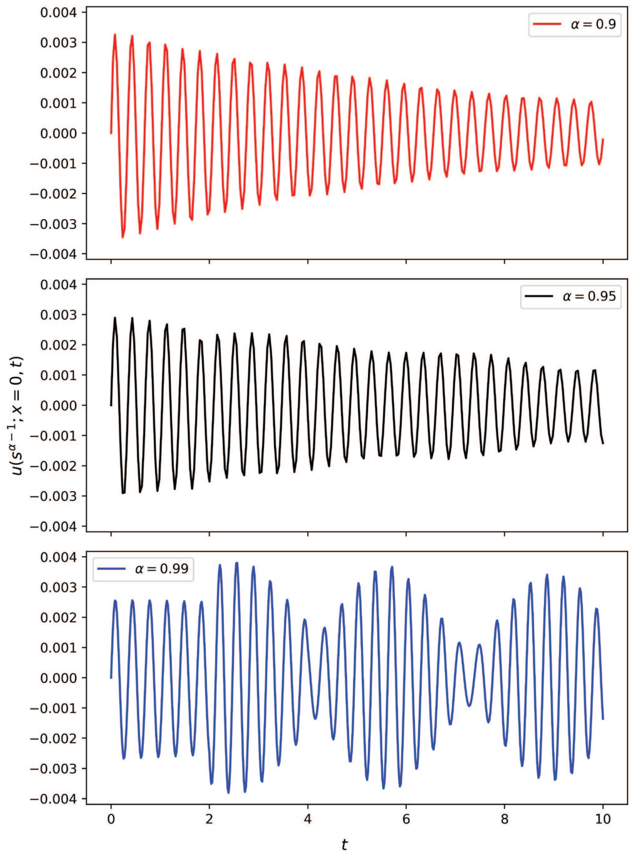

FIG. 15. The signals (53) for $v = 0.05$ and different values of alpha.

for the standard telegraphers' equation and highly suggestive for its memory-dependent extension with $\alpha > 1/2$ if infinite domain boundary conditions are taken into account. Physically, adopting such conditions means that we deal with waves that may travel all the space and can be identified with traveling waves. For the bounded domain, we face the situation in which standing waves have to appear, and we can repeat arguments given in Sec. IV A—the Doppler effect, if observed for longer lapses of time, should not be seen. Figure 11 confirms this statement, but Fig. 12 does not. Moreover, the plots exhibited in Figs. 13 and 14 do not show similarities with those of Fig. 4, they are of the type relevant for traveling waves. Nevertheless, we keep claiming that solutions to Eq. (1) with boundary conditions reducing its domain to be finite have the nature of standing waves which do not exhibit the Doppler effect and that signals of the form given by Figs. 13 and 14 are artifacts whose causes lie beyond our current knowledge—e.g., looking at Fig. 15 we note that the signal is starting to show the standing wave properties only for $\alpha = 0.99$, i.e., for an equation which being almost telegraphers' equation does not exhibit the Doppler effect if solved in the bounded domain, see Fig. 3.

V. SUMMARY

Throughout the paper, we considered the generalized telegraphers' equation of the Volterra type, abbreviated as GTE, in which the first- and second-time derivatives are replaced by non-local time integrodifferential operators modeled by smearing the usual time derivatives with some memory functions. According to the composition rules and causality arguments, these memory functions are mutually related to one another in such a way that the smeared second derivative gives the action of the smeared derivative on the smeared first derivative. This means that the time derivatives involved in the equations under consideration are coupled and that our model does not fit the class of fractional generalizations of telegraphers' equation, which admit independent extensions of the first- and second-time derivatives to their fractional counterparts. Interested in exploring wave properties of this type of memory-dependent equation, especially regarding possible manifestations of the Doppler effect, we considered GTE perturbed by a uniformly moving external harmonic source. We solved this equation for the $(1 + 1)$-dimensional case under the initial conditions stating that the solution and its time derivative at the initial time are given by two functions that depend only on the space variable x. Additionally, for the choice of boundary conditions, we assumed that the solution of the GTE under study vanishes either at $x \to \pm\infty$ (infinite domain case) or at $x = \pm l$ (bounded domain case). Depending on the boundary conditions considered, the solutions were found to represent either traveling or standing waves. In both cases, we illustrated examples of equations describing distinct models of evolution, namely, the memoryless, i.e., standard, telegraphers' equation or its Caputo sense fractional version involving power-law memory functions. $t^{-2\alpha}$ with $0 < \alpha \leq 1$. To recover whether the velocity at which the source moves influences the signal frequency spectrum, we performed the numerical time-frequency analysis using the short-time Fourier transform. For the infinite domain case, intuitively identified with the physical picture of "traveling wave," it enabled us to state that a signature of the velocity-dependent frequency shift seen for the memoryless case emerges in the memory-dependent case if $\alpha \in (\frac{1}{2}, 2)$ but remains unnoticed if $\alpha \in (0, \frac{1}{2})$. Our results differ from previous findings[28,42] according to which postulated generalizations of telegraphers' equation to the fractional ones in the Caputo sense split into two subclasses, called the "wave-like" and "heat (diffusion)-like," for which the basis of differentiation is the existence or non-existence of a wave-front, equivalent to the occurrence or absence of the Doppler effect. Within the results coming from our considerations, manifestations of the Doppler effect, or (more precisely) velocity-dependent frequency shifts, may also be observed if wavefronts are lacking, which is known to be true for typical non-local time evolution patterns. Nevertheless, a full explanation of these phenomena remains an open problem that, first of all, requires clarification of the notion of signal velocity for memory-dependent time evolution.

ACKNOWLEDGMENTS

T.P. and K.G. acknowledge support from the National Science Center (Narodowe Centrum Nauki, NCN) Research Grant Preludium Bis 2 No. UMO-2020/39/O/ST2/01563. T.P. acknowledges support from the Polish National Agency for Academic Exchange (Narodowa Agencja Wymiany Akademickiej, NAWA) Program NAWA Preludium Bis 2 Sig. BPN/PRE/2022/1/00082. L.K. acknowledges financial support from the German Science Foundation (DFG, Grant No. ME 1535/12-1) and the Alliance of International Science Organizations (Project No. ANSO-CR-PP-2022-05).

AUTHOR DECLARATIONS

Conflict of Interest

The authors have no conflicts to disclose.

Author Contributions

Tobiasz Pietrzak: Conceptualization (equal); Formal analysis (equal); Investigation (equal); Methodology (equal); Software (equal); Validation (equal); Writing – original draft (equal); Writing – review & editing (equal). **Katarzyna Górska:** Conceptualization (equal); Formal analysis (equal); Funding acquisition (equal); Investigation (equal); Methodology (equal); Supervision (equal); Validation (equal); Writing – original draft (equal); Writing – review & editing (equal). **Andrzej Horzela:** Conceptualization (equal); Formal analysis (equal); Investigation (equal); Methodology (equal); Supervision (equal); Writing – original draft (equal); Writing – review & editing (equal). **Ljupco Kocarev:** Conceptualization (equal); Formal analysis (equal); Investigation (equal); Methodology (equal); Software (equal); Writing – original draft (equal); Writing – review & editing (equal).

DATA AVAILABILITY

Data sharing is not applicable to this article as no new data were created or analyzed in this study.

APPENDIX A: DERIVATION OF EQ. (11)

To calculate the inverse Fourier transform of $\widetilde{u}_{\text{hom}}(\hat{\gamma};\kappa,t)$, $j=0,1$, we use the Fourier convolution of $\tilde{\hat{v}}_0(\kappa,s)\,\tilde{u}_0(\kappa)$ and $\tilde{\hat{v}}_1(\kappa,s)\,\tilde{w}_0(\kappa)$. Hence, we obtain

$$\int_{-\infty}^{\infty}\mathscr{F}^{-1}\left[\tilde{\hat{v}}_0(\kappa,s);x-y\right]u_0(y)dy = \int_{-\infty}^{\infty}\frac{a}{2}\frac{s+1/\tau}{\sqrt{s^2+s/\tau+b^2}}e^{-\frac{|x-y|}{a}\sqrt{s^2+s/\tau+b^2}}u_0(y)dy \tag{A1}$$

and

$$\int_{-\infty}^{\infty}\mathscr{F}^{-1}\left[\tilde{\hat{v}}_1(\kappa,s);x-y\right]w_0(y)dy = \int_{-\infty}^{\infty}\frac{a}{2}\frac{1}{\sqrt{s^2+s/\tau+b^2}}e^{-\frac{|x-y|}{a}\sqrt{s^2+s/\tau+b^2}}w_0(y)dy. \tag{A2}$$

Finally, taking the inverse Laplace transforms of Eqs. (A1) and (A2) we get Eq. (11).

APPENDIX B: DERIVATION OF EQ. (16)

Since the order of Fourier and Laplace transform is arbitrary, first we take the Laplace and then Fourier transform. Let us start with rewriting $\tilde{\hat{v}}_1(\kappa,s)$ in the form

$$\tilde{\hat{v}}_1(b^2;\kappa,s) = \begin{cases} \dfrac{\tau}{\rho_1}\left[\dfrac{1}{s+\frac{1-\rho_1}{2\tau}} - \dfrac{1}{s+\frac{1+\rho_1}{2\tau}}\right] & \text{if } \kappa\in(-2a\tau\sigma,2a\tau\sigma),\\ \dfrac{i\tau}{\rho_2}\left[\dfrac{1}{s+\frac{1+i\rho_2}{2\tau}} - \dfrac{1}{s+\frac{1-i\rho_2}{2\tau}}\right] & \text{otherwise,}\end{cases} \tag{B1}$$

where

$$\begin{aligned}\rho_1 &\equiv \rho_1(\kappa) = \sqrt{\sigma^2-4\tau^2a^2\kappa^2},\\ \rho_2 &\equiv \rho_2(\kappa) = \sqrt{4\tau^2a^2\kappa^2-\sigma^2},\end{aligned} \tag{B2}$$

and σ is given by Eq. (12). For both of the above cases (B1), using Efros' theorem, we determine the inverse Laplace transform $\tilde{v}_1(b^2;\kappa,\xi) = \mathscr{L}^{-1}[\tilde{\hat{v}}_1(b^2;\kappa,s\hat{\gamma}(s));\xi]$ and get the following: if $\kappa\in(-2a\tau\sigma,2a\tau\sigma)$ then

$$\tilde{v}_1(b^2;\kappa,\xi) = \frac{2\tau}{\rho_1}\int_0^\infty e^{-\frac{y}{2\tau}}\sinh\left(\frac{\rho_1}{2\tau}y\right)g_{\hat{\gamma}}(y,\xi)dy, \tag{B3}$$

and otherwise

$$\tilde{v}_1(b^2;\kappa,\xi) = \frac{2\tau}{\rho_2}\int_0^\infty e^{-\frac{y}{2\tau}}\sin\left(\frac{\rho_2}{2\tau}y\right)g_{\hat{\gamma}}(y,\xi)dy. \tag{B4}$$

Taking into account the convolution theorem which states that the Laplace transform of the convolution of two functions is the product of their corresponding Laplace transforms, we find the inverse Laplace transform of expression (8) as

$$\tilde{u}_{\text{inhom}}(\hat{\gamma};\kappa,t) = \int_0^\xi \mathscr{L}^{-1}\left[\tilde{v}_1\left(\kappa,s\hat{\gamma}(s)\right);\xi\right]\tilde{S}_R(\kappa,t-\xi)d\xi, \tag{B5}$$

where $\tilde{S}_R(\kappa,t)$ is given by Eq. (15). Thus, we obtain Eq. (16) with Eqs. (17) and (18).

APPENDIX C: PROOF OF THE CONJECTURE PRESENTED IN REFS. 29 and 27

The solution of the generalized telegraphers' equation, in which the memory functions $\eta(t)$ and $\gamma(t)$ satisfy relation Eq. (6) and are obtained for the initial and boundary conditions given by Eqs. (2) and (3), is nonzero in a compact domain $\Delta(t)$ if the memory function $\eta(t)$ contains a δ-Dirac decomposition.

Proof. The proof is based on the use of the integral decomposition method to solve Eq. (1), where we take $\hat{\eta}(s) = \hat{\gamma}^2(s)$ where $\hat{\gamma}(s) = \epsilon + \hat{\mu}(s)$ and $\mu(t) = \mathscr{L}^{-1}[\hat{\mu}(s);t]$ is a Sonine function. In the homogeneous solution of Eq. (1), the key term is $f_{\hat{\gamma}}(\xi,t) > 0$ for positive arguments and $f_{\hat{\gamma}}(\xi,t) = 0$ for non-positive arguments. If it contains the Heaviside step function $\Theta(\cdot)$, then $u_{\text{hom}}(\hat{\gamma};x,t)$ is nonzero in a compact region, namely,

$$f_{\epsilon+\hat{\mu}(s)}(\xi,t) = \epsilon\mathscr{L}^{-1}\{e^{-\xi\epsilon s}e^{-\xi s\hat{\mu}(s)};t\} + \mathscr{L}^{-1}\{\hat{\mu}(s)e^{-\xi\epsilon s}e^{-\xi s\hat{\mu}(s)};t\}. \tag{C1}$$

After applying the inverse Laplace transform property, i.e., $\mathscr{L}^{-1}[e^{-bs}\hat{h}(as);t] = a^{-1}\Theta(t-b)\mathscr{L}^{-1}[\hat{h}(s);(t-b)/a]$ (see Ref. 43

[Eq. (1.1.2.1)]), we obtain

$$f_{\epsilon+\hat{\mu}(s)}(\xi,t)=\Theta(t-\epsilon\xi)\left[g_{\hat{\mu}}\left(\xi,\frac{t}{\epsilon}-\xi\right)+\epsilon^{-1}f_{\hat{\mu}}\left(\xi,\frac{t}{\epsilon}-\xi\right)\right], \tag{C2}$$

where $f_{\hat{\mu}}(\cdot,-)$ and $g_{\hat{\mu}}(\cdot,-)$ are given by Eqs. (13) and (19), respectively. In the case of an inhomogeneous equation, whose solution is given by Eq. (16), the same role is played by $g_{\epsilon+\hat{\mu}}(\xi,y)>0$ for positive arguments and $g_{\hat{\gamma}}(\xi,t)=0$ for non-positive arguments, which, with analogous arguments as before, contains the Heaviside step function. □

APPENDIX D: TWO-VARIABLE PRABHAKAR FUNCTION

In this paper, we use the two-variable Prabhakar function[44] defined by the inverse Laplace transform as follows:

$$\mathscr{L}^{-1}\left[\frac{a_1 s^{-1+\alpha-\mu}}{a_1 s^{2\alpha}+a_2 s^{\alpha}+a_3};t\right]=t^{\alpha+\mu}E_{(\alpha,2\alpha),\alpha+\mu+1}\left(-\frac{a_2}{a_1}t^{\alpha},-\frac{a_3}{a_1}t^{2\alpha}\right). \tag{D1}$$

Its integral representation can be found by using Efros' theorem due to which the left-hand-side (LHS) of Eq. (D1) reads

$$\begin{aligned}\text{LHS of Eq. (D1)}&=\int_0^t\mathscr{L}^{-1}\left[\frac{a_1 s^{\alpha-\mu}}{a_1 s^{2\alpha}+a_2 s^{\alpha}+a_3};u\right]du\\&=\int_0^t\left\{\int_0^{\infty}\mathscr{L}^{-1}\left[\frac{a_1}{a_1 s^2+a_2 s+a_3};\xi\right]\mathscr{L}^{-1}[s^{\alpha-\mu}e^{-\xi s^{\alpha}};u]d\xi\right\}du.\end{aligned} \tag{D2}$$

The first inverse Laplace transforms placed in Eq. (D2) is equal to

$$\mathscr{L}^{-1}\left[\frac{a_1}{a_1 s^2+a_2 s+a_3};\xi\right]=\frac{2a_1\exp\left(-\frac{a_2}{2a_1}\xi\right)}{\sqrt{a_2^2-4a_1a_3}}\sinh\left(\frac{\xi}{2a_1}\sqrt{a_2^2-4a_1a_3}\right), \tag{D3}$$

which for $a_1=\tau$, $a_2=1$, and $a_3=\tau\Lambda_n$ gives $\nu_1(\Lambda_n;t)$ from Eq. (31). Now, we use the integral representation of two-parameter Mittag–Leffler function $E_{\alpha,\mu}$ deduced from Ref. 45, this is

$$t^{\mu-1}E_{\alpha,\mu}(-xt^{\alpha})=\int_0^{\infty}e^{-xy}\mathscr{L}^{-1}\left[s^{\alpha-\mu}e^{-ys^{\alpha}};t\right]dy. \tag{D4}$$

Therefore, Eq. (D1) reads

$$\begin{aligned}t^{\alpha+\mu}E_{(\alpha,2\alpha),\alpha+\mu+1}\left(-\frac{a_2}{a_1}t^{\alpha},-\frac{a_3}{a_1}t^{2\alpha}\right)&=\frac{a_1}{\sqrt{a_2^2-4a_1a_3}}\times\int_0^t u^{\mu-1}\left[E_{\alpha,\mu}\left(-\frac{Y_-}{2a_1}u^{\alpha}\right)\right.\\&\quad\left.-E_{\alpha,\mu}\left(-\frac{Y_+}{2a_1}u^{\alpha}\right)\right]du,\end{aligned} \tag{D5}$$

where

$$Y_{\pm}=a_2\pm\sqrt{a_2^2-4a_1a_3}. \tag{D6}$$

REFERENCES

[1] G. Cookson, *The Cable: The Wire That Changed the World* (Tempus Publishing Limited, Gloucestershire, 2003).
[2] O. Heaviside, "On induction between parallel wires," J. Soc. Telegraph Eng. **9**(34), 427–458 (1880).
[3] L. Seccia, T. Ruggeri, and A. Muracchini, "Second sound and multiple shocks in superfluid helium," Z. Angen. Math. Phys. **60**, 1074–1094 (2009).
[4] W. Dai, H. Wang, P. M. Jordan, R. E. Mickens, and B. A., "A mathematical model for skin burn injury induced by radiation heating," Int. J. Heat Mass Transf. **51**, 5497–5510 (2008).
[5] Y. Zhang, "Generalized dual-phase lag bioheat equations based on nonequilibrium heat transfer in living biological tissues," Int. J. Heat Mass Transf. **52**, 4829–4834 (2009).
[6] Z. Ding, J. Zhou, B. Song, V. Chiloyan, M. Li, T. H. Liu, and G. Chen, "Phonon hydrodynamic heat conduction and Knudsen minimum in graphite," Nano Lett. **18**, 638–649 (2018).
[7] L. Lindsay, A. Katre, A. Cepellotti, and N. Mingo, "Perspective on *ab initio* phonon thermal transport," J. Appl. Phys. **126**, 050902 (2019).
[8] M. Simoncelli, N. Marzari, and A. Cepellotti, "Generalization of Fourier's law into viscous heat equations," Phys. Rev. X **10**, 011019 (2020).
[9] C. R. Cattaneo, "Sulla conduzione del calore," Atti Sem. Mat. Fis. Univ. Modena **3**, 83 (1948).
[10] C. R. Cattaneo, "Sur une forme de l'equation de la chaleur eliminant le paradoxe d'une propagation instantanee'," C. R. Acad. Sci. **247**, 431 (1958).
[11] P. Vernotte, "Les paradoxes de la théories continue de l'equation de la chaleur," C. R. Acad. Sci. Paris **246**, 3154–3155 (1958).
[12] S. Goldstein, "On diffusion by discontinuous movements, and on the telegraphers' equation," Q. J. Mech. Appl. Math. **4**(2), 129 (1951).
[13] M. Kac, "A stochastic model related to the telegrapher's equation," Rocky Mount. J. Math. **4**, 497 (1974).
[14] J. Masoliver, K. Lindenberg, and G. H. Weiss, "A continuous-time generalization of the persistent random walk," Physica A **157**, 891 (1989).
[15] G. H. Weiss, "Some applications of persistent random walks and the telegrapher's equation," Physica A **311**, 381 (2002).
[16] J. Masoliver and K. Lindenberg, "Continuous time persistent random walk: A review and some generalizations," Eur. Phys. J. B **90**, 107 (2017).
[17] K. Górska, A. Horzela, E. K. Lenzi, G. Pagnini, and T. Sandev, "Generalized Cattaneo (telegrapher's) equation in modeling anomalous diffusion phenomena," Phys. Rev. E **102**, 022128 (2020).
[18] A. Compte and R. Metzler, "The generalized Cattaneo equation for the description of anomalous transport processes," J. Phys. A: Math. Gen. **30**, 7277 (1997).
[19] E. Awad, "On the time-fractional Cattaneo equation of distributed order," Physica A **518**, 210 (2019).
[20] J. Masoliver, "Fractional telegrapher's equation from fractional persistent random walks," Phys. Rev. E **93**, 052107 (2016).
[21] E. Orsingher and L. Beghin, "Time-fractional telegraph equations and telegraph process with Brownian time," Probab. Theory Relat. Fields **128**, 141 (2024).
[22] Y. Povstenko, *Fractional Thermoelasticity* (Springer, Cham, 2024).
[23] T. Kosztołowicz, "Cattaneo-type subdiffusion-reaction equation," Phys. Rev. E **90**, 042151 (2014).
[24] K. D. Lewandowska and T. Kosztołowicz, "Application of generalized Cattaneo equation to model subdiffusion impedance," Acta Phys. Pol. B **39**(5), 1211 (2008).
[25] A. Madhukar, Y. Park, W. Kim, H. J. Sunaryanto, R. Berlin, L. P. Chamorro, J. Bentsman, and M. Ostoja-Starzewski, "Heat conduction in porcine muscle and blood: Experiments and time-fractional telegraphers' equation model," J. R. Soc. Interface **16**, 20190726 (2019).

[26] The solution of Eq. (1) depends on the kernel functions η and γ. However, if Eq. (6) is satisfied, these functions are related to each other, which enables us to simplify formulas we adopt for $u(\hat{\eta},\hat{\gamma};x,t)$ the notation $u(\hat{\gamma};x,t)$. The "hat" symbol refers to the Laplace transform.

[27]T. Pietrzak, A. Horzela, and K. Górska, "The generalized telegraph equation with moving harmonic source: Solvability using the integral decomposition technique and wave aspects," Int. J. Heat Mass Transf. **225**, 125373 (2024).

[28]Y. Povstenko and M. Ostoja-Starzewski, "Doppler effect described by the solutions of the Cattaneo telegraph equation," Acta Mech. **232**, 725–740 (2021).

[29]K. Górska, "Integral decomposition for the solutions of the generalized Cattaneo equation," Phys. Rev. E **104**, 024113 (2021).

[30]K. Górska and A. Horzela, "Subordination and memory dependent kinetics in diffusion and relaxation phenomena," Fract. Calcul. Appl. Anal. **26**, 480 (2023).

[31] The LF transform

$$\tilde{\hat{u}}(\hat{\gamma}; \kappa, s) = \int_{-\infty}^{\infty} e^{-i\kappa x} \left[\int_0^{\infty} u(\hat{\gamma}; x, t) e^{-st} dt \right] dx.$$

Notice that the order of taking the Fourier and Laplace transform is arbitrary because the coordinates x and t commute to each other.

[32]A. M. Efros, "The application of the operational calculus to the analysis," Mat. Sb. **42**, 699 (1935). in Russian.

[33]Ł. Włodarski, "Sur une formule de Efros," Stud. Math. **13**, 183 (1952).

[34]U. Graf, *Applied Laplace Transforms and z-Transforms for Sciences and Engineers* (Birkhäuser, Basel, 2004).

[35]A. Apelblat and F. Mainardi, "Application of the Efros theorem to the function represented by the inverse Laplace transform of $s^{-\mu}\exp(-s^{\nu})$," Symmetry **13**, 354 (2021).

[36]J. A. Stratton, *Electromagnetic Theory* (McGraw-Hill Book Co, New York, 1941).

[37]P. M. Morse and H. Feshbach, *Methods of Theoretical Physics* (McGraw-Hill Book Co, New York, 1953).

[38]H. Pollard, "The representation of $e^{-x^{\lambda}}$ as a Laplace integral," Bull. Am. Math. Soc. **52**, 908 (1946).

[39]J. Chen, F. Liu, and V. Anh, "Analytical solution for the time-fractional telegraphers' equation by the method of separating variables," J. Math. Anal. Appl. **338**, 1364–1377 (2008).

[40]Y. Luchko and R. Gorenflo, "An operational method for solving fractional differential equations with the Caputo derivatives," Acta Math. Vietnam **24**, 207–233 (1999).

[41] B. Boashash, *Time-Frequency Analysis: Theory and Applications* (Elsevier Science, 2003).

[42]Y. Povstenko and M. Ostoja-Starzewski, "Fractional telegraph equation under moving time-harmonic impact," Int. J. Heat Mass Transf. **182**, 121958 (2022).

[43]A. P. Prudnikov, Y. Brychkov, and O. Marichev, *Integrals and Series. Inverse Laplace Transforms* (Gordon and Breach, New York, 1992), Vol. 5.

[44]E. Bazhlekova, "Completely monotone multinomial Mittag-Leffler type functions and diffusion equations with multiple time-derivatives," Fract. Calcul. Appl. Anal. **24**, 88–111 (2021).

[45]K. Górska, A. Horzela, A. Lattanzi, and T. K. Pogány, "On complete monotonicity of three parameter Mittag–Leffler function," Appl. Anal. Discrete Math. **15**, 118–128 (2021).

Journal of Computational and Applied Mathematics 433 (2023) 115306

Contents lists available at ScienceDirect

Journal of Computational and Applied Mathematics

journal homepage: www.elsevier.com/locate/cam

Volterra-Prabhakar function of distributed order and some applications

K. Górska [a,*], T. Pietrzak [a], T. Sandev [b,c,d], Ž. Tomovski [e]

[a] H. Niewodniczański Institute of Nuclear Physics, Polish Academy of Sciences, ul.Eljasza-Radzikowskiego 152, PL 31342 Kraków, Poland
[b] Research Center for Computer Science and Information Technologies, Macedonian Academy of Sciences and Arts, Bul. Krste Misirkov 2, 1000 Skopje, Macedonia
[c] Institute of Physics, Faculty of Natural Sciences and Mathematics, Ss. Cyril and Methodius University, Arhimedova 3, 1000 Skopje, Macedonia
[d] Institute of Physics & Astronomy, University of Potsdam, D-14776 Potsdam-Golm, Germany
[e] University of Ostrava, Faculty of Sciences, Department of Mathematics, 30. Dubna 22701 03 Ostrava, Czech Republic

ARTICLE INFO

Article history:
Received 7 January 2023
Received in revised form 4 April 2023

Keywords:
Anomalous diffusion
Distributed order memory kernel
Distributed order Prabhakar function
Volterra-Prabhakar function of distributed order
Bernstein function

ABSTRACT

The paper studies the exact solution of two kinds of generalized Fokker–Planck equations in which the integral kernels are given either by the distributed order function $k_1(t) = \int_0^1 t^{-\mu}/\Gamma(1-\mu)\,\mathrm{d}\mu$ or the distributed order Prabhakar function $k_2(\alpha, \gamma; \lambda; t) = \int_0^1 e^{-\gamma}_{\alpha,1-\mu}(\lambda; t)\,\mathrm{d}\mu$, where the Prabhakar function is denoted as $e^{-\gamma}_{\alpha,1-\mu}(\lambda; t)$. Both of these integral kernels can be called the fading memory functions and are the Stieltjes functions. It is also shown that their Stieltjes character is enough to ensure the non-negativity of the mean square values and higher even moments. The odd moments vanish. Thus, the solution of generalized Fokker–Planck equations can be called the probability density functions. We introduce also the Volterra-Prabhakar function and its generalization which are involved in the definition of $k_2(\alpha, \gamma; \lambda; t)$ and generated by it the probability density function $p_2(x, t)$.

1. Introduction

The anomalous diffusion is characterized by the power-law mean square displacement (MSD), *i.e.*, $\langle x^2(t)\rangle \simeq t^{\mu}$. It encompasses the sub-diffusion ($\mu \in (0, 1)$) and super-diffusion ($\mu \in (1, 2)$). For $\mu = 1$ we have the normal diffusion and $\mu = 2$ it is the ballistic motion. It is known that the sub-diffusion character is obtained by investigating the anomalous diffusion, for example, either with fractional derivative in the Caputo sense or the Prabhakar derivative [1–5]. These both fractional derivatives can be presented as $\int_0^t k(t-\xi)\partial_\xi f(\xi)\,\mathrm{d}\xi$ in which $k(t)$ for the Caputo derivative reads

$$K_1(\mu; t) = \frac{t^{-\mu}}{\Gamma(1-\mu)} \qquad \text{and} \qquad \hat{K}_1(\mu; s) = s^{\mu-1}, \quad \mu \in (0, 1), \tag{1}$$

and for the Prabhakar derivative one has $k(t) = K_2(\alpha, \mu, \gamma; \lambda; t)$,

$$K_2(\alpha, \mu, \gamma; \lambda; t) = e^{-\gamma}_{\alpha,1-\mu}(\lambda; t) \qquad \text{and} \qquad \hat{K}_2(\alpha, \mu, \gamma; s) = \hat{K}_1(\mu; s)\left(1 + \frac{\lambda}{s^{\alpha}}\right)^{\gamma}, \tag{2}$$

* Corresponding author.
E-mail addresses: katarzyna.gorska@ifj.edu.pl (K. Górska), tobiasz.pietrzak@ifj.edu.pl (T. Pietrzak), trifce.sandev@manu.edu.mk (T. Sandev), zhivorad.tomovski@osu.cz (Ž. Tomovski).

https://doi.org/10.1016/j.cam.2023.115306

with $\lambda > 0$, $\mu \in (0, 1)$, and $\alpha \in (0, 1)$. The Prabhakar function $e^{\gamma}_{\alpha,\beta}(t; \lambda)$ is equal to

$$e^{\gamma}_{\alpha,\beta}(\lambda; t) = t^{\beta-1}E^{\gamma}_{\alpha,\beta}(-\lambda t^{\alpha}), \quad \text{where} \quad E^{\gamma}_{\alpha,\beta}(z) = \sum_{r=0}^{\infty} \frac{(\gamma)_r z^r}{r!\Gamma(\beta+\alpha r)} \tag{3}$$

is the three parameters Mittag-Leffler functions and $(\gamma)_r = \Gamma(\gamma + r)/\Gamma(\gamma)$ is the Pochhammer (raising) symbol. The symbol '$\wedge$' denotes the Laplace transform of $f(t)$, this is $\hat{f}(s) = \mathscr{L}[f(t); s]$, where the Laplace pairs are $s \div t$. From Eqs. (2) and (3) it follows that $K_2(\alpha, \mu, \gamma; \lambda; t)$ goes to $K_1(\mu; t)$ either for $\lambda = 0$ or $t \ll 1$ because $E^{\gamma}_{\alpha,1-\mu}(-\lambda t^{\alpha}) \simeq 1/\Gamma(1-\mu)$. For more information about the Mittag-Leffler function we refer to [6–11].

Despite the power-law MSD, in many experiments it is also observed a ultraslow-diffusion, for which MSD grows logarithmically with time, $\langle x^2(t)\rangle \simeq \ln^{\nu}(t)$. For instance, it is observed in the Sinai model [12] describing the one-dimensional thermal random motion of a particle in a random potential, which is also related to the random-field Ising models [13] and mechanical DNA unzipping [14,15], in the motion in aging environments [16,17], in iterated maps [18], as well as in annealed (renewal) continuous time random walks with logarithmic waiting time distribution [19], to name a few. It is generated by the distributed order memory kernels introduced in Refs. [20,21] and, next, considered in, e.g., [22,23], in which the authors took the integral over $\mu \in (0, 1)$ of Eq. (1),

$$k_1(t) = \int_0^1 \frac{t^{-\mu}}{\Gamma(1-\mu)}\,\mathrm{d}\,\mu \qquad \text{and} \qquad \hat{k}_1(s) = \int_0^1 s^{\mu-1}\,\mathrm{d}\,\mu = \frac{s-1}{s\ln s}. \tag{4}$$

We can also integrate Eq. (2) over $\mu \in (0, 1)$ and consider the so-called distributed order Prabhakar derivative [1,24]:

$$k_2(\alpha, \gamma; \lambda; t) = \int_0^1 e^{-\gamma}_{\alpha,1-\mu}(\lambda; t)\,\mathrm{d}\,\mu \qquad \text{and} \qquad \hat{k}_2(\alpha, \gamma; \lambda; s) = \hat{k}_1(s)\left(1 + \frac{\lambda}{s^{\alpha}}\right)^{\gamma}, \tag{5}$$

where $\alpha, \gamma \in (0, 1)$ and $\lambda > 0$. Notice that the integral in Eqs. (4) and (5) can be arbitrarily changed by setting $\beta = \mu + p$, $p \in \mathbb{N}$, which is used to determine the higher types of fractional derivatives. For instance, $p = 0$ was used in the anomalous diffusion with distributed order derivative [20,21,23] or in its Langevin pictures [25]. The special case with $p = 1$ is used in [24,26,27].

The memory kernel is involved in the generalized Fokker–Planck equation being the Volterra type equation,

$$\int_0^t k(t-\xi)\partial_{\xi}p(x, \xi)\,\mathrm{d}\,\xi = \partial_x^2[B(x, t)p(x, t)] - \partial_x[\lambda(x, t)p(x, t)], \tag{6}$$

where we assume that the diffusion $B(x, t)$ and the drift $\lambda(x, t)$ coefficients are independent on time. Moreover, we take $B(x, t)$ to be a positive constant B and $\lambda(x, t)$ is equal to zero. We recall that Eq. (6) for $k(t-\xi) = \delta(t-\xi)$ is the Fokker–Planck equation. The fundamental solution of Eq. (6) with $B > 0$ and without the drift term, i.e. $\lambda(x) = 0$, in the Fourier-Laplace space reads

$$\tilde{\hat{p}}(\kappa, s) = \frac{\hat{k}(s)}{s\hat{k}(s) + B\kappa^2} \tag{7}$$

and taking its inverse Fourier transform we get

$$\hat{p}(x, s) = \frac{1}{2s}\sqrt{\frac{s\hat{k}(s)}{B}}\; \mathrm{e}^{-|x|\sqrt{\frac{s\hat{k}(s)}{B}}}. \tag{8}$$

Due to the Bernstein theorem A we conclude that $p(x, t)$ is a probability density function (PDF) if $\hat{p}(x, s)$ is a completely monotonic function (CMF), *i.e.*, it is a non-negative function belonging to C^{∞} whose all derivative alternate. It is satisfied in twofold: either (a) for $[\hat{k}(s)/s]^{1/2}$ being CMF and $[s\hat{k}(s)]^{1/2}$ being the Bernstein function (BF) or (b) for $[s\hat{k}(s)]^{1/2}$ being the completely Bernstein function (CBF) [28].

Remark 1. From (b) and the property (a2) in Appendix A follows that $s\hat{k}(s) = \hat{\Psi}(s)$ is CBF, which implies that there exists conjugated with it a CBF function $\hat{\Phi}(s) = s/\hat{\Psi}(s) = 1/\hat{k}(s)$ [29, Proposition 7.1]. Moreover, from [29, Theory 7.3] it appears that $\hat{k}(s)$ is a Stieltjes function (SF) which with conjugated with it another SF $\hat{M}(s) = 1/\hat{\Phi}(s)$ forms the Sonnine pair [30,31] satisfying the Sonnine equation, e.g. [32]:

$$\hat{k}(s)\hat{M}(s) = s^{-1}. \tag{9}$$

Thus, Eq. (8) solves also

$$p(x, t) = p_0(x) + \int_0^t M(t-\xi)B\partial_x^2 p(x, \xi)\,\mathrm{d}\,\xi, \tag{10}$$

where $p_0(x) = p(x, 0)$ for the fundamental solution is the δ-Dirac distribution. Notice that Eq. (10) is the Sonnine partner of Eq. (6) and can be obtained by inserting Eq. (9) into Eq. (6), as is shown in [8].

The brief description of CMF, BF, CBF, and SF are presented in Appendix A.

Remark 2. We note that the generalized diffusion Eq. (6) can be obtained within the continuous time random walk theory, by parametrizing the random walk $x(t)$ in terms of the number of steps u via the following coupled Langevin equations [33], see also [11],

$$\begin{cases} \dot{x}(u) = \zeta(u), \\ \dot{t}(u) = \xi(u). \end{cases}$$

Here u is called the operational time, which is connected to the physical time by the total $t(u) = \int_0^u \xi(u')\,du'$ of the individual waiting times ξ for each step. Furthermore, $\zeta(u)$ is a white Gaussian noise ($\langle\zeta(u)\rangle = 0$ and $\langle\zeta(u)\zeta(u')\rangle = 2\delta(u-u')$), while $\xi(u)$ is a generalized stable Lévy noise with a characteristic function $\hat{L}(u,s) = \exp[-us\hat{k}(s)]$ and Lévy exponent $\hat{\Psi}(s) = s\hat{k}(s)$. This so-called subordination approach can also be used to show the non-negativity of the solution. Therefore, for the memory kernels (4) and (5) the corresponding Lévy exponents read as $\hat{\Psi}_1(s) = (s-1)/\ln s$ and $\hat{\Psi}_2(\alpha,\gamma;\lambda;s) = \hat{\Psi}_1(s)(1+\lambda s^{-\alpha})^{\gamma}$, respectively.

In this paper, we give the exact solution of the generalized Fokker–Planck equation with distributed order derivatives as well as calculate the exact form of its MSD. The paper is organized as follows. Section 2 is the mathematical background of further consideration. We introduce the Volterra-Prabhakar function and its generalization as well as we study their properties. In Section 3 it is shown that the Volterra-Prabhakar functions appear in the definition of memory kernels $k_1(t)$, $k_2(\alpha,\gamma;\lambda;t)$ and their Sonnie partners. The MSDs as well as the higher moments are calculated in Section 4 whereas the PDFs is found in Section 5. The paper is concluded in Section 6.

2. Volterra-Prabhakar function

Volterra's function is defined as follows [34,35]

$$\mu(t,\beta,\alpha) = \frac{1}{\Gamma(1+\beta)}\int_0^\infty \frac{t^{u+\alpha}\,u^{\beta}}{\Gamma(u+\alpha+1)}\,\mathrm{d}\,u, \qquad \mathfrak{Re}(\beta) > -1 \quad \text{and} \quad t>0, \tag{11}$$

whose particular cases are

$$\begin{aligned} \alpha=\beta=0: &\quad \nu(t) = \mu(t,0,0), \\ \alpha\neq 0,\ \beta=0: &\quad \nu(t,\alpha) = \mu(t,0,\alpha), \\ \alpha=0,\ \beta\neq 0: &\quad \mu(t,\beta) = \mu(t,\beta,0). \end{aligned}$$

The Laplace transform of the Volterra's function $\mu(t,\beta,\alpha)$ is given by [34]

$$\mathscr{L}[\mu(t,\beta,\alpha);s] = \frac{1}{s^{\alpha+1}\ln^{\beta+1}s}. \tag{12}$$

More information about Volterra's function can be found in Refs. [34,36–40]. Here, we present some properties of the Volterra's function, which are used in the paper.

Proposition 1. *For $t>0$, $\alpha>0$, and $p\in\mathbb{R}$ we have*

$$\int_0^t \xi^{\alpha-1}\nu(t-\xi,p)\,\mathrm{d}\,\xi = \Gamma(\alpha)\,\nu(t,\alpha+p) \tag{13}$$

and in particular

$$\int_0^t \xi^{\alpha-1}\nu(t-\xi,-\alpha)\,\mathrm{d}\,\xi = \Gamma(\alpha)\,\nu(t).$$

Proof. Proposition 1 can be proved by direct calculations in which we involve the definition of the Euler's Beta function $B(x,y) = \Gamma(x)\Gamma(y)/\Gamma(x+y)$. These calculations read

$$\begin{aligned} \int_0^t \xi^{\alpha-1}\nu(t-\xi,p)\,\mathrm{d}\,\xi &= \int_0^\infty \frac{1}{\Gamma(1+p+u)}\left[\int_0^t \xi^{\alpha-1}(t-\xi)^{u+p}\,\mathrm{d}\,\xi\right]\mathrm{d}\,u \\ &= \int_0^\infty \frac{t^{u+\alpha+p}}{\Gamma(1+p+u)}\,B(\alpha,1+p+u)\,\mathrm{d}\,u \\ &= \Gamma(\alpha)\int_0^\infty \frac{t^{u+\alpha+p}}{\Gamma(1+\alpha+p+u)}\,\mathrm{d}\,u. \end{aligned} \tag{14}$$

Using the definition of Volterra's ν function for the integral in Eq. (14) we complete the proof. □

Proposition 2. *For $t > 0$, $\alpha \in (0, 1)$, $\gamma \in \mathbb{R}$, and $p \in \mathbb{R}$ we get*

(a)

$$\int_0^t \nu(t-\xi, p)\, e^{\gamma}_{\alpha,0}(\lambda; \xi)\, \mathrm{d}\,\xi = \sum_{n=0}^{\infty} \frac{(-\lambda)^n}{n!} (\gamma)_n\, \nu(t, \alpha n + p), \tag{15}$$

(b)

$$\sum_{n=0}^{\infty} \frac{(-\lambda)^n}{n!} (\gamma)_n\, \nu(t, \alpha n + p) = \int_0^{\infty} e^{\gamma}_{\alpha, u+p+1}(t; \lambda)\, \mathrm{d}\, u \tag{16}$$

where the Pochhammer (raising) symbol $(\gamma)_n$ is defined with Eq. (3).

Proof. To prove Proposition 2(a) we use the series form of the Prabhakar functions (3) and change (in a legitimate way) the order of integral and series. Hence, we get

$$\int_0^t \nu(t-\xi, p) e^{\gamma}_{\alpha,0}(\lambda; \xi)\, \mathrm{d}\,\xi = \sum_{n=0}^{\infty} \frac{(-\lambda)^n}{n!\, \Gamma(\alpha n)} (\gamma)_n \int_0^t \xi^{\alpha n - 1} \nu(t-\xi, p)\, \mathrm{d}\,\xi.$$

The use of Eq. (13) allows one to obtain Eq. (15). Thereafter, representing the right-hand side (rhs) of Eq. (16) by the definition of Volterra's function and changing the order of series and integral we have

$$\sum_{n=0}^{\infty} \frac{(-\lambda)^n}{n!} (\gamma)_n\, \nu(t, \alpha n + p) = \int_0^{\infty} t^{u+p} \sum_{n=0}^{\infty} \frac{(\gamma)_n (-\lambda t^{\alpha})^n}{n!\, \Gamma(u + p + \alpha n + 1)}\, \mathrm{d}\, u,$$

where the series constitutes the three-parameter Mittag-Leffler function (3). In this way we proved Proposition 2(b). □

Let the function

$$\epsilon^{\gamma}_{\alpha,\, p}(\lambda; t) = \int_0^{\infty} e^{\gamma}_{\alpha, u+p+1}(\lambda; t)\, \mathrm{d}\, u \tag{17}$$

be called the Volterra-Prabhakar function which for $\gamma = 0$ and/or $\lambda = 0$ reduces to $\nu(t, p)$. It has the following properties: **(A)** Applying the Leibnitz rule for differentiation under the integral sign in (17), this is $\frac{\mathrm{d}^n}{\mathrm{d}\,t^n} e^{\gamma}_{\alpha,\beta}(\lambda; t) = e^{\gamma}_{\alpha,\beta-n}(\lambda; t)$ [6,10], we obtain the following recurrence relation:

$$\frac{\mathrm{d}^{\,n}}{\mathrm{d}\,t^n}[\epsilon^{\gamma}_{\alpha,\, p}(\lambda; t)] = \epsilon^{\gamma}_{\alpha,\, p-n}(\lambda; t) \quad \text{for} \quad n \in \mathbb{N}_0.$$

In particular, $\frac{\mathrm{d}^n}{\mathrm{d}\,t^n}[\epsilon^{\gamma}_{\alpha,\, n}(\lambda; t)] = \epsilon^{\gamma}_{\alpha,\, 0}(\lambda; t)$, $\frac{\mathrm{d}^n}{\mathrm{d}\,t^n}[\epsilon^{\gamma}_{\alpha,\, 2n}(\lambda; t)] = \epsilon^{\gamma}_{\alpha,\, n}(\lambda; t)$, $\frac{\mathrm{d}^n}{\mathrm{d}\,t^n}[\epsilon^{\gamma}_{\alpha,\, 3n}(\lambda; t)] = \epsilon^{\gamma}_{\alpha,\, 2n}(\lambda; t)$, etc., *i.e.*, by induction we obtain the general form

$$\frac{\mathrm{d}^{\,n}}{\mathrm{d}\,t^n}[\epsilon^{\gamma}_{\alpha,\, kn}(\lambda; t)] = \epsilon^{\gamma}_{\alpha,\, (k-1)n}(\lambda; t), \quad k \in \mathbb{N}.$$

(B) Next, we give a convolution relation between Volterra, Prabhakar, and Volterra-Prabhakar functions. Since,

$$\mathscr{L}\left[\epsilon^{\gamma}_{\alpha,\, p}(\lambda; t); s\right] \mathscr{L}\left[\mu(t, \beta-1, \alpha-1); s\right] = \mathscr{L}\left[e^{\gamma}_{\alpha,\, p}(\lambda; t); s\right] \mathscr{L}\left[\mu(t, \beta, \alpha); s\right],$$

by the convolution theorem of the Laplace transform, we obtain,

$$\epsilon^{\gamma}_{\alpha,\, p}(\lambda; t) \star \mu(t, \beta-1, \alpha-1) = e^{\gamma}_{\alpha,\, p}(\lambda; t) \star \mu(t, \beta, \alpha).$$

Furthermore, from

$$\mathscr{L}\left[\epsilon^{\gamma}_{\alpha,\, p}(\lambda; t); s\right] \mathscr{L}\left[\epsilon^{\gamma'}_{\alpha,\, p'}(\lambda; t); s\right] = \mathscr{L}\left[\epsilon^{\gamma+\gamma'}_{\alpha,\, p+p'}(\lambda; t); s\right] \mathscr{L}\left[\nu(t); s\right],$$

we get the convolution semigroup property

$$\epsilon^{\gamma}_{\alpha,\, p}(\lambda; t) \star \epsilon^{\gamma'}_{\alpha,\, p'}(\lambda; t) = \epsilon^{\gamma+\gamma'}_{\alpha,\, p+p'}(\lambda; t) \star \nu(t).$$

In particular,

$$\epsilon^{\gamma}_{\alpha,\, p}(\lambda; t) \star \epsilon^{-\gamma}_{\alpha,\, -p}(\lambda; t) = \mu(t, 1, 1).$$

In order to evaluate the integral representation of $\epsilon^{\gamma}_{\alpha,\, p}(\lambda; t)$ for $0 < \alpha < 1$, we consider the inverse Laplace transform of the Volterra-Prabhakar function.

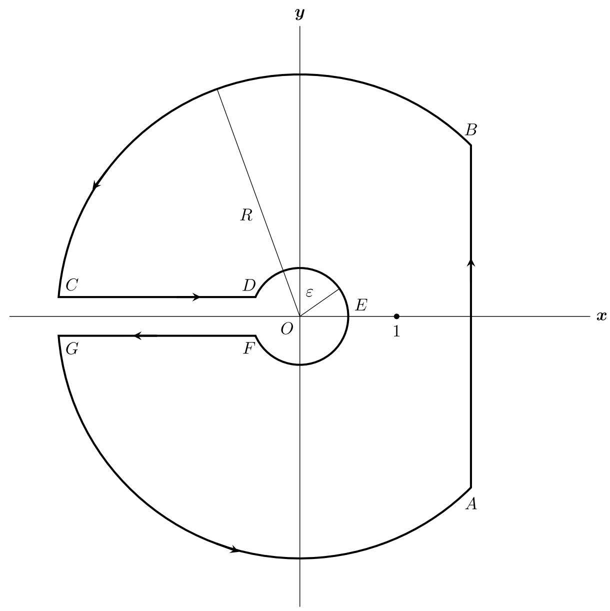

Fig. 1. The Bromwich contour.

Proposition 3. *The Laplace transform of the Volterra-Prabhakar function* $\epsilon^{\gamma}_{\alpha,\,p}(\lambda;\,t)$ *is given by*

$$\mathscr{L}\left[\epsilon^{\gamma}_{\alpha,\,p}(\lambda;\,t);\,s\right] = \frac{s^{\alpha\gamma-p-1}}{(s^{\alpha}+\lambda)^{\gamma}\ln s} = \mathscr{L}\left[e^{\gamma}_{\alpha,\,p}(\lambda;\,t)\star\nu(t);\,s\right]. \tag{18}$$

Proof. Notice that $\mathscr{L}[\epsilon^{\gamma}_{\alpha,\,p}(\lambda;\,t);\,s]$ contains two integrals: one of them is placed in the direct Laplace transform and another one is settled in the definition of the Volterra-Prabhakar function. Changing the order of these integrals the proof of Proposition 3 follows immediately. □

Notice that Eq. (18) can be also presented as

$$\mathscr{L}[\epsilon^{-\gamma}_{\alpha,\,p}(\lambda;\,t);\,s] = s^{-p}(s-1)^{-1}\hat{k}_2(\alpha,\gamma;\,\lambda;\,s).$$

The use of Eq. (5) in which by appropriate chose of the values of α, γ, and λ, enables us to write

$$\mathscr{L}[\epsilon^{-1}_{1,\,p}(-1;\,t);\,s] = s^{-p-1}\hat{k}_1(s).$$

By using the already established integral representation results and certain earlier investigations by Stanković, Tomovski et al. [41] in a lucid and transparent way, gave an elegant proof, that the function $e^{\gamma}_{\alpha,\beta}(\lambda;\,t)$ is CMF under the conditions $\alpha,\beta\in(0,1)$, $\gamma>0$ and $\alpha\gamma\le\beta$. Alternative proof can be obtained by taking the product of two CMFs, *i.e.*, $t^{\beta-1}$ and three parameters Mittag-Leffler function $E^{\gamma}_{\alpha,\beta}(-x)$. The mathematical rigorous proof, being the extension on Pollard's proof presented in [42], that $E^{\gamma}_{\alpha,\beta}(-x)$ is CMF can be found in [9].

Example 1. Using Bromwich integral for inverse Laplace transform of (17), we will find integral representation for Volterra-Prabhakar function with $\lambda=1$ and $0<\alpha\le1$. The complex integral can be evaluated by taking into account that the integrand has the branch point at $s=0$ and the pole at $s=1$. The point $s=\exp(\mathrm{i}\pi)=-1$, (for $\alpha=1$) is isolated singular point. For all non-integer values of α, the power s^{α} is given by $s^{\alpha}=|s|^{\alpha}e^{\mathrm{i}\,\alpha\,\arg(s)}$, where $|\arg(s)|<\pi$, that is, in the complex s-plane cut along the negative real axis. The Bromwich contour used in the integration is presented in Fig. 1. The contour consists of the straight line AB, a large semi-circle of radius R, a small circle about the origin, and a cut along the negative axis. According to the Jordan lemma, the integrals over the large semi-circle parts BC and GA vanish as $R\to\infty$. Thus contributions to the integral come only from the loop H, starting from CD, encircles the circular disk DEF and finishes to the lower side of the negative real half-axis, *i.e.*, FG parts of the contour and from the pole at $s=1$. The residue at this point is $\mathrm{e}^{t}/2^{\gamma}$. For $\alpha\gamma-p\ge0$ the integral over the small circle DEF vanishes when $\varepsilon\to0$ and therefore,

$$\epsilon^{\gamma}_{\alpha,\,p}(1;\,t)\equiv\epsilon^{\gamma}_{\alpha,\,p}(t) = \frac{1}{2\pi\mathrm{i}}\int_{c-\mathrm{i}\infty}^{c+\mathrm{i}\infty}\mathrm{e}^{st}\,\frac{s^{\alpha\gamma-p}}{(s^{\alpha}+1)^{\gamma}s\ln s}\,\mathrm{d}\,s = \frac{\mathrm{e}^{t}}{2^{\gamma}} + f^{\gamma}_{\alpha,p}(t),$$

where

$$f^{\gamma}_{\alpha,p}(t) = \frac{1}{2\pi\mathrm{i}}\int_{H}\mathrm{e}^{st}\,\frac{s^{\alpha\gamma-p}}{(s^{\alpha}+1)^{\gamma}s\ln s}\,\mathrm{d}\,s = \mathscr{L}\left[K^{\gamma}_{\alpha,\,p}(r);\,t\right].$$

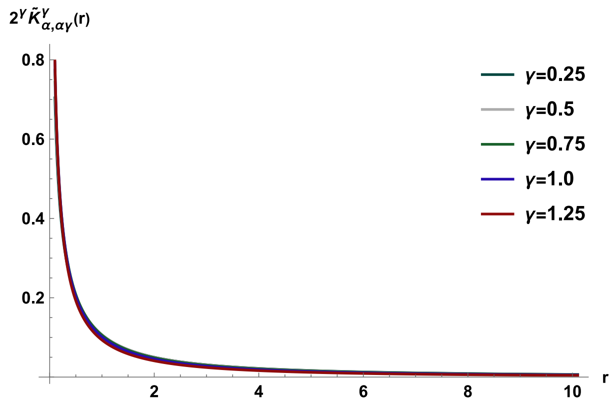

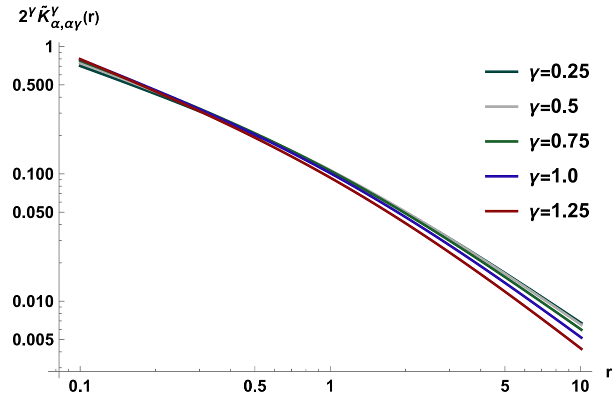

Fig. 2. Linear–linear (left) and log–log plot (right) of the function $2^\gamma \widetilde{K}^\gamma_{\alpha,\alpha\gamma}$ for $\alpha = 0.4$.

By applying the Titchmarsh formula [43, Eq.(11.6.5) on p. 316], it follows

$$K^\gamma_{\alpha,p}(r) = -\frac{1}{\pi}\mathfrak{Im}\left\{\frac{r^{\alpha\gamma-p}\,e^{i\pi(\alpha\gamma-p)}}{(r^\alpha\,e^{i\pi\alpha}+1)^\gamma(r\,e^{i\pi})\ln(r\,e^{i\pi})}\right\}$$
$$= -\frac{r^{\alpha\gamma-p-1}}{\pi}\mathfrak{Im}\left\{\frac{e^{i\pi(\alpha\gamma-p-1)}}{(r^\alpha\,e^{i\pi\alpha}+1)^\gamma(i\pi+\ln r)}\right\}.$$

Next, we remove the imaginary part from the denominator. To realize this purpose we multiply and divide Eq. 1 by $[r^\alpha \exp(-i\pi\alpha)+1]^\gamma = |z|^\gamma \exp[-i\gamma\theta_\alpha(r)]$ and $(-i\pi + \ln r)$. Thus, we get

$$K^\gamma_{\alpha,p}(r) = -\frac{r^{\alpha\gamma-p-1}}{\pi}\mathfrak{Im}\left\{\frac{e^{i\pi(\alpha\gamma-p-1)}\,|z|^\gamma\,e^{-i\gamma\theta_\alpha(r)}(-i\pi+\ln r)}{|z|^{2\gamma}(\pi^2+\ln^2 r)}\right\}$$

with

$$|z| = [r^{2\alpha} + 2r^\alpha\cos(\pi\alpha)+1]^{1/2} \qquad \text{and} \qquad \theta_\alpha(r) = \arctan\left[\frac{\sin(\pi\alpha)}{\cos(\pi\alpha)+r^{-\alpha}}\right].$$

Then, the spectral function kernel $K^\gamma_{\alpha,p}(r)$ can be written as

$$K^\gamma_{\alpha,p}(r) = \frac{r^{\alpha\gamma-p-1}}{\pi}\,\frac{(\ln r)\sin[\pi(\alpha\gamma-p)-\gamma\theta_\alpha(r)] - \pi\cos[\pi(\alpha\gamma-p)-\gamma\theta_\alpha(r)]}{[r^{2\alpha}+2r^\alpha\cos(\pi\alpha)+1]^{\gamma/2}(\pi^2+\ln^2 r)}.$$

Finally,

$$\epsilon^\gamma_{\alpha,\,p}(t) = \frac{e^t}{2^\gamma} - \int_0^\infty e^{-rt}\,\tilde{K}^\gamma_{\alpha,p}(r)\,d\,r, \tag{19}$$

where $\widetilde{K}^\gamma_{\alpha,p}(r) = -K^\gamma_{\alpha,p}(r)$. Since $\epsilon^\gamma_{\alpha,\,p}(0) = 0$ then from Eq. (19) we obtain the following result

$$\int_0^\infty \widetilde{K}^\gamma_{\alpha,p}(r)\,d\,r = \frac{1}{2^\gamma}.$$

We ask now, under which conditions on parameters, the kernel $K^\gamma_{\alpha,p}(r)$ is a negative function, *i.e.*, $\widetilde{K}^\gamma_{\alpha,p}(r)$ is positive in respect to r? Since $r^{2\alpha}+2r^\alpha\cos(\pi\alpha)+1 \geq r^{2\alpha}-2r^\alpha+1 = (r^\alpha-1)^2 > 0$ and $\pi^2+\ln^2 r > 0$, one option $K^\gamma_{\alpha,p}(r)$ to be negative is $\alpha \in (0, 1/2]$, $\gamma > 0$, and $\alpha\gamma = p$ or $\alpha\gamma - p = 2k$, where k is integer number. In this case, $2^\gamma\widetilde{K}^\gamma_{\alpha,p}(r) = 2^\gamma\widetilde{K}^\gamma_{\alpha,\alpha\gamma}(r) > 0$ or $2^\gamma\widetilde{K}^\gamma_{\alpha,p}(r) = 2^\gamma\widetilde{K}^\gamma_{\alpha,\alpha\gamma-k}(r) > 0$ are the densities of a probability measure concentrated on the positive real line (see Figs. 2, 3, and 4). If $p = 0$, $\gamma > 0$ then we will analyze the sign of the argument $\gamma[\pi\alpha - \theta_\alpha(r)]$ of sin and cos functions. So, if $\alpha \in (1/2, 1)$ and $0 < r < 1$ then

$$\tan(\pi\alpha) - \frac{\sin(\pi\alpha)}{\cos(\pi\alpha)+r^{-\alpha}} = \frac{r^{-\alpha}\tan(\pi\alpha)}{\cos(\pi\alpha)+r^{-\alpha}} < 0,$$

or $\tan(\pi\alpha) < \frac{\sin(\pi\alpha)}{\cos(\pi\alpha)+r^{-\alpha}}$, *i.e.*, $\pi\alpha < \theta_\alpha(r)$. Hence, $\gamma[\pi\alpha - \theta_\alpha(r)] < 0$, *i.e.*, $\widetilde{K}^\gamma_{\alpha,0}(r) > 0$. So, $2^\gamma\widetilde{K}^\gamma_{\alpha,0}(r)$ represents density function for $0 < r < 1$.

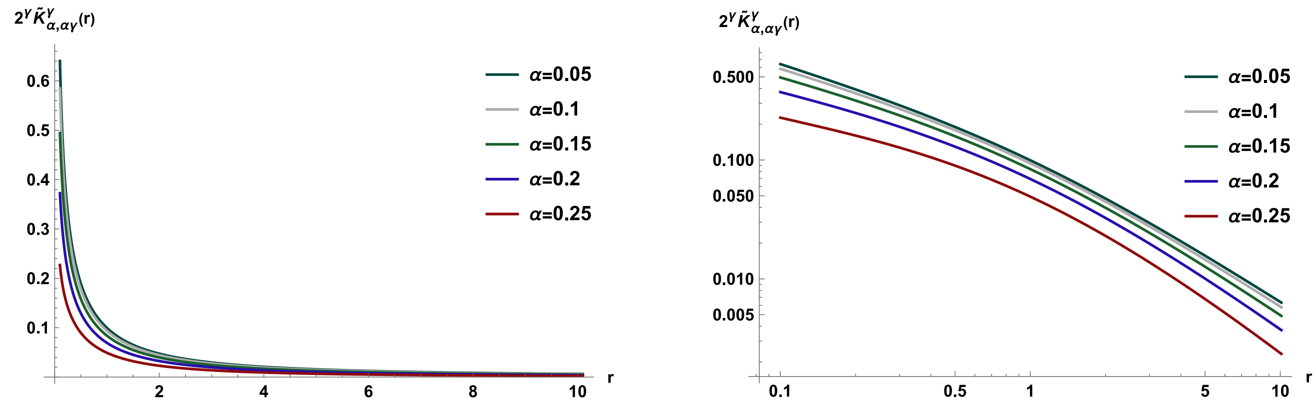

Fig. 3. Linear–linear (left) and log–log plot (right) of the function $2^\gamma \widetilde{K}^\gamma_{\alpha,\alpha\gamma}$ for $\gamma = 3.0$.

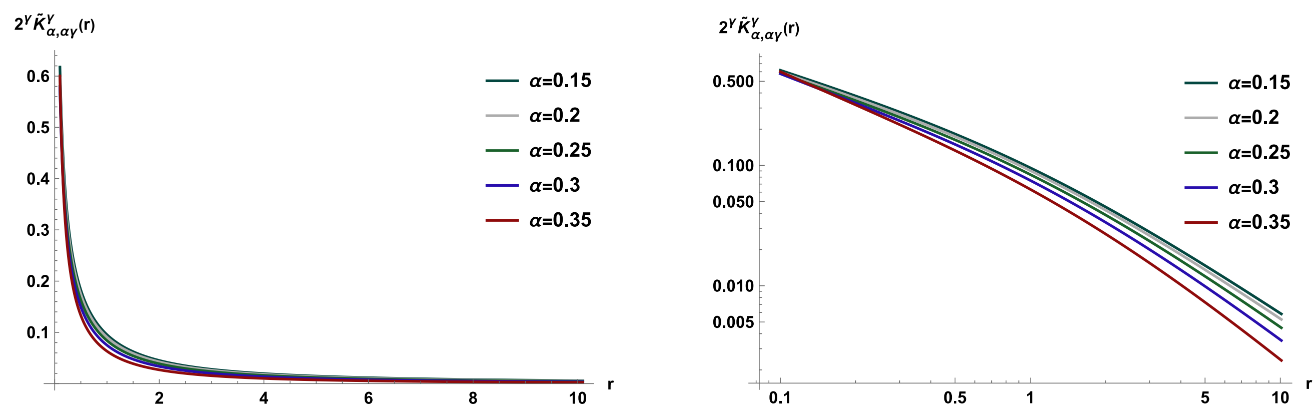

Fig. 4. Linear–linear (left) and log–log plot (right) of the function $2^\gamma \widetilde{K}^\gamma_{\alpha,\alpha\gamma}$ for $\gamma = 2.0$.

By applying the Bernstein theorem, we obtain the following results:

Proposition 4. *Let $\gamma > 0$. The following assertions hold true:*

(a) $\epsilon^\gamma_{\alpha,p}(t) - \frac{e^t}{2^\gamma}$ is CM on $(0, \infty)$ for $\alpha \in (0, 1/2]$ and $\alpha\gamma - p = 2k$, $k \in \mathbb{Z}$;
(b) $\epsilon^\gamma_{\alpha,\alpha\gamma}(t) - \frac{e^t}{2^\gamma}$ is CM on $(0, \infty)$ for $\alpha \in (0, 1/2]$;
(c) $\epsilon^\gamma_{\alpha,0}(t) - \frac{e^t}{2^\gamma}$ is CM on $(0, 1)$ for $\alpha \in (1/2, 1]$.

Consequently, under the same conditions, the functions of the previous proposition are log-convex, since every CM function is log-convex, see [44]. In particular, for $\gamma = 0$ we obtain the integral

$$\nu(t, p) = \epsilon^0_{\alpha,p}(t) = e^t - \frac{1}{\pi} \int_0^\infty \frac{\mathrm{e}^{-rt}}{r^{p+1}} \frac{(\ln r)\sin(\pi p) + \pi \cos(\pi p)}{\pi^2 + \ln^2 r}\, \mathrm{d}r.$$

Hence,

$$\int_0^\infty \frac{1}{\pi} r^{p+1} \frac{(\ln r)\sin(\pi p) + \pi \cos(\pi p)}{\pi^2 + \ln^2 r}\, \mathrm{d}r = 1.$$

For $p \in [0, 1/2]$ the integrand of the last integral is positive, so it represents a PDF. Furthermore, for $\gamma = p = 0$, we obtain the Ramanujan integral (see [38, Eq. (16.2.3) on p. 27])

$$\nu(t) = \epsilon^0_{\alpha,0}(t) = \mathrm{e}^t - \int_0^\infty \frac{e^{-rt}}{r} \frac{1}{\pi^2 + \ln^2 r}\, \mathrm{d}r.$$

Hence,

$$\int_0^\infty \frac{1}{r}\frac{1}{\pi^2+\ln^2 r}\,\mathrm{d}\,r = 1.$$

The integrand of the last integral is a positive function, so it represents a PDF.

Proposition 5. *The following assertions hold true:*

(a) The function $\mathrm{e}^t - \nu(t,p)$ *is CM and log-convex on* $(0,\infty)$*, for* $p \in [0, 1/2]$*;*
(b) The function $\mathrm{e}^t - \nu(t)$ *is CM and log-convex on* $(0,\infty)$*.*

The cases $1 < \alpha \le 2$ and $\gamma \in \mathbb{N}$ we leave for the reader. For an idea, we refer to Ref. [41].

A more general form of the Volterra-Prabhakar function, associated by (11) is

$$\epsilon^{\gamma}_{\alpha,\,\beta,\,p}(\lambda;t) = \int_0^\infty u^\beta e^{\gamma}_{\alpha,u+p+1}(\lambda;t)\,\mathrm{d}\,u, \tag{20}$$

which we will call Volterra-Prabhakar function of distributed order. In particular, $\epsilon^{\gamma}_{\alpha,\,0,\,p}(\lambda;t) = \epsilon^{\gamma}_{\alpha,\,p}(\lambda;t)$.

Without proof, we will present slight generalizations of Propositions 1 and 2.

Proposition 6. *For* $t > 0$, $\alpha, \beta > 0$, $\lambda, \gamma \in \mathbb{R}$ *we have*

(a)

$$\int_0^t \xi^{\alpha-1}\mu(t-\xi,\beta,\alpha)\,\mathrm{d}\,\xi = \Gamma(\alpha)\,\mu(t,\beta,2\alpha),$$

(b)

$$\int_0^t \mu(t-\xi,\beta,\alpha)\,e^{\gamma}_{\alpha,\beta}(\lambda;\xi)\,\mathrm{d}\,\xi = \sum_{n=0}^\infty \frac{(-\lambda)^n}{n!}(\gamma)_n\,\mu(t,\beta,\alpha n+\alpha+\beta),$$

(c)

$$\epsilon^{\gamma}_{\alpha,\,\beta,\,\alpha+\beta}(\lambda;t) = \sum_{n=0}^\infty \frac{(-\lambda)^n}{n!}(\gamma)_n\,\mu(t,\beta,\alpha n+\alpha+\beta).$$

Proposition 7. *The Laplace transform of* $\epsilon^{\gamma}_{\alpha,\,\beta,\,p}(\lambda;t)$ *for* $\mathfrak{Re}\,\beta > 0$ *reads*

$$\mathscr{L}[\epsilon^{\gamma}_{\alpha,\,\beta,\,p}(\lambda;t);s] = \Gamma(1+\beta)\frac{s^{\alpha\gamma-p-1}}{(s^\alpha+\lambda)^\gamma\,(\ln s)^{1+\beta}}.$$

Furthermore, the following convolution relation holds true,

$$\epsilon^{\gamma}_{\alpha,\,\beta,\,p}(\lambda;t) = e^{\gamma}_{\alpha,p}(\lambda;t)\star\mu(t,\beta,0).$$

Proof. The Proposition 7 can be proved by direct calculations in which we use Eq. (20) and change the order of integral with the integral defining the direct Laplace transform. Hence, we have

$$\begin{aligned}\mathscr{L}[\epsilon^{\gamma}_{\alpha,\,\beta,\,p}(\lambda;t);s] &= \int_0^\infty u^\beta\left[\int_0^\infty \mathrm{e}^{-st}\,e^{\gamma}_{\alpha,u+p+1}(\lambda;t)\,\mathrm{d}\,t\right]\mathrm{d}\,u\\ &= \frac{s^{\alpha\gamma-p-1}}{(s^\alpha+\lambda)^\gamma}\int_0^\infty u^\beta s^{-u}\,\mathrm{d}\,u.\end{aligned}$$

The use of $\int_0^\infty u^\beta s^{-u}\,\mathrm{d}\,u = \Gamma(1+\beta)(\ln s)^{-1-\beta}$ finishes the proof. □

Proposition 8. *For* $\alpha > 0,\ 0 < \mathfrak{Re}\,\beta < 1,\ 0 < \mathfrak{Re}\,s < \mathfrak{Re}\,\gamma \le 1 - \mathfrak{Re}\,\beta,\ p \in \mathbb{R}$ *the Mellin transform of* $\epsilon^{\gamma}_{\alpha,\,\beta,\,p}(t)$ *is given by*

$$\mathscr{M}[\epsilon^{\gamma}_{\alpha,\,\beta,\,p}(t);s] = \frac{-\alpha^\beta\pi}{[\sin(\pi\beta)]\,\Gamma(1-s)}\sum_{k=0}^\infty\binom{-\gamma}{k}[(\frac{p+s}{\alpha}+k)^\beta - (-\gamma+\frac{p+s}{\alpha}-k)^\beta].$$

Proof. Using the Mellin transform formula for Prabhakar function,

$$\mathscr{M}[E^{\gamma}_{\alpha,\alpha'}(-t); s] = \frac{1}{\Gamma(\gamma)} \frac{\Gamma(s)\Gamma(\gamma - s)}{\Gamma(\alpha' - \alpha s)} \quad (0 < \mathfrak{Re}\, s < \mathfrak{Re}\, \gamma),$$

we have

$$\begin{aligned}
\mathscr{M}[\epsilon^{\gamma}_{\alpha,\beta,p}(t); s] &= \int_0^\infty u^\beta \left[\int_0^\infty t^{s-1} e^{\gamma}_{\alpha,u+p+1}(t)\, \mathrm{d}\, t\right] \mathrm{d}\, u \\
&= \frac{1}{\alpha \Gamma(\gamma)\Gamma(1-s)} \int_0^\infty u^\beta \Gamma\left(\frac{u+p+s}{\alpha}\right) \Gamma\left(\gamma - \frac{u+p+s}{\alpha}\right) \mathrm{d}\, u \\
&= \frac{\alpha^\beta}{\Gamma(\gamma)\Gamma(1-s)} \int_0^\infty u^\beta \Gamma\left(u + \frac{p+s}{\alpha}\right) \Gamma\left(\gamma - u - \frac{p+s}{\alpha}\right) \mathrm{d}\, u.
\end{aligned}$$

Let us use $l = \frac{p+s}{\alpha}$ and apply the definition for the gamma function

$$\begin{aligned}
J &= \int_0^\infty u^\beta \left[\int_0^\infty \int_0^\infty \mathrm{e}^{-(x+y)} x^{u+l-1} y^{\gamma-u-l-1}\, \mathrm{d}\, x\, \mathrm{d}\, y\right] \mathrm{d}\, u \\
&= \int_0^\infty \int_0^\infty \mathrm{e}^{-(x+y)} x^{l-1} y^{\gamma-l-1}\, \mathrm{d}\, x\, \mathrm{d}\, y \int_0^\infty u^\beta \left(\frac{x}{y}\right)^u \mathrm{d}\, u \\
&= \Gamma(\beta+1) \int_0^\infty \int_0^\infty \mathrm{e}^{-(x+y)} x^{l-1} y^{\gamma-l-1} \left(\ln \frac{y}{x}\right)^{-(\beta+1)} \mathrm{d}\, x\, \mathrm{d}\, y.
\end{aligned}$$

Recently, Maryam Al-Kandari et al. [45] introduced the following integral operator

$$(T_\phi f)(x) = \int_0^\infty \int_0^\infty \mathrm{e}^{-(\tau_1+\tau_2)} \tau_1^{-\alpha} \tau_2^{\beta-1} f\left(\frac{x\tau_1^a}{\tau_2^b}\right) \mathrm{d}\, \tau_1\, \mathrm{d}\, \tau_2.$$

Taking $a = b = 1$, $x = 1$, $\alpha = 1 - l$, $\beta = \gamma - l$ and $f(\tau_1/\tau_2) = [\ln(\tau_2/\tau_1)]^{-(\beta+1)}$, we get

$$J = \Gamma(\beta+1)(T_\phi \ln^{-\beta-1})(1).$$

Substituting $x+y = v$ and $y/x = w$, we obtain $x = v/(1+w)$, $y = vw/(1+w)$ with Jacobi-determinant $\frac{\partial(x,y)}{\partial(v,w)} = v/(1+w)^2$, and

$$\begin{aligned}
J &= \Gamma(\beta+1)\Gamma(\gamma) \int_0^\infty w^{\gamma-l-1}(1+w)^{-\gamma}(\ln w)^{-(\beta+1)}\, \mathrm{d}\, w \\
&= \Gamma(\beta+1)\Gamma(\gamma)(J_1 + J_2),
\end{aligned}$$

where

$$J_1 = \int_0^1 w^{\gamma-l-1}(1+w)^{-\gamma}(\ln w)^{-(\beta+1)}\, \mathrm{d}\, w$$

and

$$J_2 = \int_1^\infty w^{\gamma-l-1}(1+w)^{-\gamma}(\ln w)^{-(\beta+1)}\, \mathrm{d}\, w.$$

To solve the last integrals, we will apply the integral 14, p.552 given in [46],

$$\int_0^1 \left(\ln \frac{1}{x}\right)^{r-1} \frac{x^{p-1}}{(1+x^q)^s}\, \mathrm{d}\, x = \Gamma(r) \sum_{k=0}^\infty \binom{-s}{k} \frac{1}{(p+kq)^r} \qquad (p \ge 0,\ q \ge 0,\ r \ge 0,\ 0 \le s \le r+2)$$

with $r = -\beta$, $p = l$, $q = 1$, $s = \gamma$. Namely,

$$J_2 = \int_0^1 \left(\ln \frac{1}{w}\right)^{-(\beta+1)} \frac{w^{l-1}}{(1+w)^\gamma}\, \mathrm{d}\, w = \Gamma(-\beta) \sum_{k=0}^\infty \binom{-\gamma}{k} (l+k)^\beta.$$

Analogously,

$$J_1 = (-1)^{\beta+1}\Gamma(-\beta) \sum_{k=0}^\infty \binom{-\gamma}{k} (\gamma - l + k)^\beta.$$

Then,

$$J_1 + J_2 = \Gamma(-\beta)\sum_{k=0}^{\infty}\binom{-\gamma}{k}[(l+k)^{\beta} - (-\gamma + l - k)^{\beta}]$$
$$(\mathfrak{Re}\ \beta > 0,\ 0 < \mathfrak{Re}\ \gamma \leq 1 - \mathfrak{Re}\ \beta). \quad \square$$

3. The distributed order prabhakar kernel and its sonnine partner

The distributed order kernel $\hat{k}_1(s)$ and distributed order Prabhakar kernel $\hat{k}_2(\alpha, \gamma; \lambda; s)$ fulfill Kochubei's limits given by [47, Eqs. (3.1) and (3.2)] from which it appears that $[s\hat{k}_1(s)]^{-1}$ and $[s\hat{k}_2(\alpha, \gamma; \lambda; s)]^{-1}$ vanishes at $s \gg 1$. Hence, both of them can be called the fading memory function [48,49].

In Ref. [24] it is shown that $\hat{k}_1(s)$ and $\hat{k}_2(\alpha, \gamma; \lambda; s)$ are SFs and they can be presented as $s\hat{k}_1(s)/s$ and $s\hat{k}_2(\alpha, \gamma; \lambda; s)/s$, where $s\hat{k}_1(s)$ and $s\hat{k}_2(\alpha, \gamma; \lambda; s)$ are CBFs (the property (a6) in Appendix A). It guarantees that Remark 1 is satisfied which means that exist the Sonnine partner of $\hat{k}_1(s)$ and $\hat{k}_2(\alpha, \gamma; \lambda; s)$. Namely

$$\hat{M}_1(s) = \frac{1}{s\hat{k}_1(s)} = \frac{\ln s}{s-1} \quad \text{and} \quad \hat{M}_2(\alpha, \gamma; \lambda; s) = \frac{1}{s\hat{k}_2(\alpha, \gamma; \lambda; s)} = \hat{M}_1(s)\left(1 + \frac{\lambda}{s^{\alpha}}\right)^{-\gamma}, \tag{21}$$

and $\alpha, \gamma \in (0, 1)$ with $\lambda > 0$.

The asymptotic behavior of $k_1(t)$, $k_2(\alpha, \gamma; \lambda; t)$ and their Sonnine partners at short time t can be found by applying the following Tauberian theorem [50].

Theorem 1. *For $\hat{f}(s) = \mathscr{L}[f(t); s]$ such that for $s \to 0$ it can be presented as*

$$\hat{f}(s) \simeq s^{-\rho}L\left(\frac{1}{s}\right), \quad \textit{for} \quad \rho > 0,$$

then

$$f(t) \simeq \frac{1}{\Gamma(\rho)}t^{\rho-1}L(t), \qquad t \to \infty$$

for $L(t)$ being a slowly varying function at infinity, i.e., $\lim_{t\to\infty}\frac{L(at)}{L(t)} = 1$ for any $a > 0$.

Proof. The proof of this theorem is presented in Ref. [50]. $\square$

Tauberian theorem is also valid if s and t are interchanges, that is $s \to \infty$ and $t \to 0$ [50].

Example 2. The asymptotics of $\hat{k}_1(s)$ and $\hat{k}_2(\alpha, \gamma; \lambda; s)$ at $s \to 0$ read

$$\hat{k}_1(s) \simeq \frac{1}{s\ln(1/s)} \qquad \text{and} \qquad \hat{k}_2(\alpha, \gamma; \lambda; s) \simeq \lambda^{\gamma}\frac{s^{-(1+\alpha\gamma)}}{\ln(1/s)},$$

for $\alpha, \gamma \in (0, 1)$ and $\lambda > 0$, which from Theorem 1 give

$$k_1(t) \simeq \frac{1}{\ln t} \qquad \text{and} \qquad k_2(\alpha, \gamma; \lambda; t) \simeq \frac{t^{\alpha\gamma}}{\Gamma(1+\alpha\gamma)}\frac{1}{\ln t}, \qquad \text{for} \quad t \to \infty.$$

We note that at $s \to \infty$ we cannot apply Theorem 1 since $\hat{k}_1(s)$ and $\hat{k}_2(\alpha, \gamma; s)$ can be only approximated by $(\ln s)^{-1}$ without any power function.

Example 3. The asymptotics of $\hat{M}_1(s)$ and $\hat{M}_2(\alpha, \gamma; \lambda; s)$ for small and large s read, respectively

$$\hat{M}_1(s) \simeq \ln(1/s) \quad \text{and} \quad \hat{M}_2(\alpha, \gamma; \lambda; s) \simeq s^{\alpha\gamma}\ln(1/s) \quad \text{for} \qquad s \to 0$$

as well as

$$\hat{M}_1(s) = \hat{M}_2(\alpha, \gamma; \lambda; s) \simeq s^{-1}\ln s \qquad \text{for} \qquad s \to \infty.$$

Then, we cannot apply Tauberian's theorem (Theorem 1) because $\rho = 0$ and/or, respectively, $\rho = -\alpha\gamma$ which for $\alpha, \gamma \in (0, 1)$ gives negative value. For $s \gg 1$ Theorem 1 gives

$$M_1(t) = M_2(\alpha, \gamma; \lambda; t) \simeq \ln\frac{1}{t}, \qquad \text{for} \quad t \to 0.$$

The use of the Laplace transform of convolution allows one to invert Eqs. (5) and (21), as well as express the distributed order Prabhakar kernel and its Sonnine partner in the forms which correspond to $\hat{k}_1(s)$ and $\hat{M}_1(s)$. Indeed, we have

$$k_2(\alpha,\gamma;\lambda;t)=\int_0^t k_1(t-\xi)\,e^{-\gamma}_{\alpha,0}(\lambda;\xi)\,\mathrm{d}\,\xi \tag{22}$$

and

$$M_2(\alpha,\gamma;\lambda;t)=\int_0^t M_1(t-\xi)\,e^{\gamma}_{\alpha,0}(\lambda;\xi)\,\mathrm{d}\,\xi. \tag{23}$$

Moreover, the inverse Laplace transform of $\hat{k}_1(s)$ gives

$$k_1(t)=\mathscr{L}^{-1}\left[\left(1-\frac{1}{s}\right)\frac{1}{\ln s};t\right]=\nu(t,-1)-\nu(t), \tag{24}$$

where $\nu(t,p)$ and $\nu(t)$, for $p\in\mathbb{Z}$ and $t>0$, belong to the family of Volterra's function presented in Section 2. For $M_1(t)=\mathscr{L}^{-1}[\hat{M}_1(s);t]$ we take the inverse Laplace transform and use [51, Eq. (2.5.2.2)]. That allows one to get

$$M_1(t)=\mathrm{e}^t\,\mathscr{L}^{-1}\left[\frac{\ln(s+1)}{s};t\right]=-\,\mathrm{e}^t\,\mathrm{Ei}(-t), \tag{25}$$

where $\mathrm{Ei}(-t)=-\int_t^\infty \exp(-u)/u\ \mathrm{d}\,u$ is the exponential integral. Next, we substitute Eqs. (24) and (25) into Eqs. (22) and (23), respectively. In the case of $k_2(\alpha,\gamma;t)$ Proposition 2 enable us to write

$$k_2(\alpha,\gamma;\lambda;t)=\sum_{n=0}^\infty\frac{(-\lambda)^n}{n!}(-\gamma)_n\left[\nu(t,\alpha n-1)-\nu(t,\alpha n)\right],$$

where $\nu(t,\cdot)$ is Volterra's function and $(\gamma)_n$ is a Pochhammer (raising) symbol. The same result we obtain by taking the inverse Laplace transform of $\hat{k}_2(\alpha,\gamma;s)$ in which we first present $(1+\lambda/s^\alpha)^\gamma$ as the series indexed by $n\in\mathbb{N}_0$. The crucial step consists on calculating $\mathscr{L}^{-1}\{s^{-\alpha n-j}[\ln(s)]^{-1};t\}$ with $j=0,1$. That can be done by employing Eq. (12). Moreover, Proposition 2b and Eq. (16) allow us to express $k_2(\alpha,\gamma;t)$ as the difference of Volterra-Prabhakar functions,

$$k_2(\alpha,\gamma;\lambda;t)=\epsilon^{-\gamma}_{\alpha,-2}(\lambda;t)-\epsilon^{-\gamma}_{\alpha,-1}(\lambda;t).$$

To get the exact form of $M_2(\alpha,\gamma;t)$ we will use Eq. (22) for which we substitute Eq. (25) and apply the series form of the three parameters Mittag-Leffler function given by Eq. (3). That gives

$$\begin{aligned}M_2(\alpha,\gamma;\lambda;t)&=-\int_0^t \mathrm{e}^\xi\,\mathrm{Ei}(-\xi)\sum_{r=0}^\infty\frac{(\gamma)_r\,(-\lambda)^r}{r!\,\Gamma(\alpha r)}(t-\xi)^{\alpha r-1}\,\mathrm{d}\,\xi\\&=-\sum_{r=0}^\infty\frac{(\gamma)_r\,(-\lambda)^r}{r!\,\Gamma(\alpha r)}\int_0^t \mathrm{e}^\xi\,\mathrm{Ei}(-\xi)(t-\xi)^{\alpha r-1}\,\mathrm{d}\,\xi,\end{aligned} \tag{26}$$

where we change (in a legitimate way) the order of sum and integral. The integral in Eq. (26) can be calculated by using [52, Eq. (2.5.1.7)] which implies

$$\int_0^t \mathrm{e}^\xi\,\mathrm{Ei}(-\xi)(t-\xi)^{\alpha r-1}\,\mathrm{d}\,\xi=\Gamma(\alpha r)\,\ln(t)\,e_{1,1+\alpha r}(t)-t^{\alpha r-1}\sum_{j=1}^\infty t^j\,\frac{\psi(j+\alpha r)}{(\alpha r)_j}, \tag{27}$$

where $\psi(z)=\frac{\mathrm{d}}{\mathrm{d}\,z}\ln\Gamma(z)$ is the digamma function such that $\psi(1)=-C\simeq-0.57721$ is equal to the Euler–Mascheroni constant taken with minus sign. Inserting it into Eq. (26) allows us to find the exact form of $M_2(\alpha,\gamma;t)$, namely

$$M_2(\alpha,\gamma;\lambda;t)=\ln\!\left(\frac{1}{t}\right)\sum_{r=0}^\infty\frac{(\gamma)_r}{r!}(-\lambda)^r e_{1,1+\alpha r}(t)+\sum_{r=0}^\infty\frac{(\gamma)_r(-\lambda t^\alpha)^r}{r!\,\Gamma(\alpha r)}\sum_{j=1}^\infty t^{j-1}\frac{\psi(j+\alpha r)}{(\alpha r)_j} \tag{28}$$

in which we employ the series form of three parameters Mittag-Leffler function and Prabhakar function. At short time $t\ll 1$ from the asymptotic of three parameters Mittag-Leffler function we have $e_{1,1+\alpha r}(t)\simeq t^{\alpha r}/\Gamma(1+\alpha r)$ [6]. That implies that the first term of Eq. (28) which contains the logarithmic function is proportional to $\ln(1/t)E^\gamma_{\alpha,1}(-\lambda t^\alpha)$ which for $t\ll 1$ gives $\ln(1/t)$. The second term with two series at short time vanishes because for $t\to 0$ the only term which can survive is for $r=0$ and $j=1$ that gives $\psi(1)/\Gamma(0)\sim 0$. As a conclusion we can say that Eq. (28) reconstructs the behavior of $M_2(\alpha,\gamma;\lambda;t)$ found with the help of Tauberian theorem (Theorem 1) at $t\ll 1$.

4. Mean square displacement and higher moments

The PDF $p_{\hat{k}}(x,t) = \mathscr{L}^{-1}[\hat{p}_{\hat{k}}(x,s);t]$, where $\hat{p}_{\hat{k}}(x,s)$ is given by Eq. (8), is symmetric function with respect to x. Thus, all its odd moments vanish and only the even ones are different from zero which for $n \in \mathbb{N}_0$ read

$$\begin{aligned} \langle x^{2n}(t)\rangle_{\hat{k}} &= \int_{\mathbb{R}} x^{2n} p_{\hat{k}}(x,t)\,\mathrm{d}x = \mathscr{L}^{-1}\left[\int_{\mathbb{R}} x^{2n}\hat{p}_{\hat{k}}(x,s)\,\mathrm{d}x;t\right] \\ &= \mathscr{L}^{-1}\left[(-1)^n \frac{\mathrm{d}^{2n}}{\mathrm{d}\kappa^{2n}}\int_{\mathbb{R}} \mathrm{e}^{-\mathrm{i}\kappa x}\,\hat{p}_{\hat{k}}(x,s)\,\mathrm{d}x;t\right]_{\kappa=0}, \end{aligned} \tag{29}$$

where we used $x^{2n}\exp(-\mathrm{i}\kappa x) = (-1)^n \frac{\mathrm{d}^{2n}}{\mathrm{d}\kappa^{2n}}\exp(-\mathrm{i}\kappa x)$. The integral in Eq. (29) is the Fourier transform of $\hat{p}_{\hat{k}}(x,s)$, so we can write

$$\langle x^{2n}(t)\rangle_{\hat{k}} = \mathscr{L}^{-1}\left[(-1)^n\frac{\mathrm{d}^{2n}}{\mathrm{d}\kappa^{2n}}\tilde{\hat{p}}_{\hat{k}}(\kappa,s);t\right]$$

with $\tilde{\hat{p}}_{\hat{k}}(\kappa,s)$ given by Eq. (7). Setting now $y = \mathrm{i}\kappa\sqrt{B/[s\hat{k}(s)]}$ we get

$$\begin{aligned} \frac{\mathrm{d}^{2n}}{\mathrm{d}\kappa^{2n}}\tilde{\hat{p}}_{\hat{k}}(\kappa,s) &= (-1)^n\left[\frac{B}{s\hat{k}(s)}\right]^n \frac{1}{s}\frac{\mathrm{d}^{2n}}{\mathrm{d}y^{2n}}\frac{1}{1-y^2} \\ &= (-1)^n\left[\frac{B}{s\hat{k}(s)}\right]^n \frac{1}{2s}\frac{\mathrm{d}^{2n}}{\mathrm{d}y^{2n}}\left\{\frac{1}{1-y}+\frac{1}{1+y}\right\} \\ &= (-1)^n\left[\frac{B}{s\hat{k}(s)}\right]^n \frac{(2n)!}{2s}\left\{\frac{1}{(1-y)^{2n+1}}+\frac{1}{(1+y)^{2n+1}}\right\}. \end{aligned}$$

Finally, at the limit of $y=0$, we obtain an extreme equal to 1.

$$\begin{aligned} \langle x^{2n}(t)\rangle_{\hat{k}} &= (2n)!\,B^n\mathscr{L}^{-1}\{s^{-1}[s\hat{k}(s)]^{-n};t\} = (2n)!\,B^n\mathscr{L}^{-1}[s^{-1}\hat{M}^n(s);t] \\ &= (2n)!B^n\int_0^t \mathscr{L}^{-1}[\hat{M}^n(s);u]\,\mathrm{d}u, \end{aligned} \tag{30}$$

where we apply the Sonnine Eq. (9).

All the moments $\langle x^{2n}(t)\rangle_{\hat{k}}$ for $\hat{k}(s) \equiv \hat{k}_1(s)$ and $\hat{k}(s) \equiv \hat{k}_2(\alpha,\gamma;\lambda;s)$ are non-negative which follows from the property (a1) given in Appendix A. Indeed, at the beginning of Section 3 it is shown that $s\hat{k}_1(s)$ and $s\hat{k}_2(\alpha,\gamma;\lambda;s)$ are CBF. Thus, due to the property (a3) it appears that $[s\hat{k}_1(s)]^{-n}$ as well as $[s\hat{k}_2(\alpha,\gamma;\lambda;s)]^{-n}$ are CMFs. Next, the use of the property (a1) finished the proof.

4.1. Mean square displacement

Taking $n=1$ in Eq. (30) we get the MSD

$$\langle x^2(t)\rangle_{\hat{k}} = 2B\mathscr{L}^{-1}\{[s^2\hat{k}(s)]^{-1};t\} = 2B\int_0^t M(u)\,\mathrm{d}u.$$

The first approach to calculate the MSD for $\hat{k}_1(s)$ and $\hat{k}_2(\alpha,\gamma;s)$ is to use Tauberian theorem, see Theorem 1.

Example 4. For $\langle x^2(t)\rangle_{\hat{k}_1} \equiv \langle x^2(t)\rangle_1$ we have

$$\mathscr{L}[\langle x^2(t)\rangle_1;s] = 2B[s^2\hat{k}_1(s)]^{-1} \simeq 2B\begin{cases} s^{-1}\ln(1/s), & \text{for} \quad s\to 0, \\ s^{-2}\ln s, & \text{for} \quad s\to\infty, \end{cases}$$

and respectively

$$\langle x^2(t)\rangle_1 \simeq 2B\begin{cases} \ln t, & \text{for} \quad t\to\infty, \\ t\ln(1/t), & \text{for} \quad t\to 0. \end{cases}$$

Example 5. In the case of $\langle x^2(t)\rangle_{\hat{k}_2} \equiv \langle x^2(t)\rangle_2$ we can approximate it as follows

$$\mathscr{L}[\langle x^2(t)\rangle_2;s] = 2B[s^2\hat{k}_2(\alpha,\gamma;s)]^{-1} \simeq 2B\begin{cases} \lambda^{-\gamma}s^{-(1-\alpha\gamma)}\ln(1/s), & \text{for} \quad s\to 0, \\ s^{-2}\ln s, & \text{for} \quad s\to\infty. \end{cases}$$

Because $\alpha\gamma \in (0, 1)$ then $1 - \alpha\gamma \in (0, 1)$ and we can apply the Tauberian theory which gives

$$\langle x^2(t)\rangle_2 \simeq 2B \begin{cases} \lambda^{-\gamma} \frac{t^{-\alpha\gamma}}{\Gamma(1-\alpha\gamma)} \ln t, & \text{for} \quad t \to \infty, \\ t \ln(1/t), & \text{for} \quad t \to 0. \end{cases} \tag{31}$$

In the next approach we calculate the exact form of $\langle x^2(t)\rangle_1$ and $\langle x^2(t)\rangle_2$. For $\langle x^2(t)\rangle_1$ we have

$$\begin{aligned} \langle x^2(t)\rangle_1 &= 2B \int_0^t M_1(u)\, \mathrm{d}\, u = -2B \int_0^t \mathrm{e}^u \,\mathrm{Ei}(-u)\, \mathrm{d}\, u \\ &= 2B \sum_{j=1}^{\infty} \frac{t^j}{j!} [\psi(1+j) - \ln t] \\ &= 2B \sum_{j=1}^{\infty} \frac{t^j}{j!} \psi(1+j) + 2B(\mathrm{e}^t - 1) \ln\left(\frac{1}{t}\right), \end{aligned} \tag{32}$$

where we employ [52, Eq. (2.5.1.7)]. The series in Eq. (32) is the exponential generating function which is given by [53, Eq. (4.2a)] and reads

$$\sum_{j=1}^{\infty} \frac{t^j}{j!} \psi(1+j) = C + \mathrm{e}^t [\ln(t) - \mathrm{Ei}(-t)]. \tag{33}$$

Eq. (33) enables us to express $\langle x^2(t)\rangle_1$ in the form

$$\langle x^2(t)\rangle_1 = 2B[C + \ln(t) - \mathrm{e}^t \,\mathrm{Ei}(-t)]. \tag{34}$$

Let us now consider its asymptotic behavior at short and long time t. At $t \ll 1$ we can approximate $E_1(t) = -\mathrm{Ei}(-t) \simeq -C - \ln(t) + t$ [54, Eq. (6.6.2)]. That reduces Eq. (34) into $\langle x^2(t)\rangle_1 \simeq 2B\left[\left(-C + \ln \frac{1}{t}\right)(\mathrm{e}^t - 1) + t\, \mathrm{e}^t\right]$. Next, notice that $\exp(t) \simeq 1 + t$ at short t we approximate it as

$$\langle x^2(t)\rangle_1 \simeq 2B(1 - C)t + 2Bt \ln \frac{1}{t} \simeq 2Bt \ln \frac{1}{t},$$

this is the asymptotics obtained from Theorem 1. At $t \gg 1$ the exponential integral behaves as $E_1(t) = -\mathrm{Ei}(-t) \simeq \exp(-t)/t$ [54, Eq. (6.12.1)]. It means that for $t \gg 1$ we have $\langle x^2(t)\rangle_1 \simeq 2B[C + \ln(t) - t^{-1}]$. The most important term there is equal to $2B \ln(t)$ which was indicated by Tauberian theorem (Theorem 1).

In the case of the MSD calculated for the distributed order Prabhakar derivative we proceed similarly as for $\langle x^2(t)\rangle_1$. Hence, we can write

$$\begin{aligned} \langle x^2(t)\rangle_2 &= 2B \int_0^t M_2(\alpha, \gamma; \lambda; u)\, \mathrm{d}\, u = 2B \int_0^t \left\{ \int_0^u M_1(\xi)\, e^{\gamma}_{\alpha,0}(\lambda; u - \xi)\, \mathrm{d}\, \xi \right\} \mathrm{d}\, u \\ &= -\sum_{r=0}^{\infty} \frac{(\gamma)_r (-\lambda)^r}{r! \Gamma(\alpha r)} \int_0^t \left[\int_0^u \mathrm{e}^{\xi} \,\mathrm{Ei}(-\xi)(u - \xi)^{\alpha r - 1}\, \mathrm{d}\, \xi \right] \mathrm{d}\, u, \end{aligned}$$

where in the first equality we apply Eq. (23). To get the next equality we employed the series form of three parameters Mittag-Leffler function (3). The integral over $\xi \in (0, u)$ inside the square braced is calculated in Eq. (27). That allows one to present $\langle x^2(t)\rangle_2$ as

$$\langle x^2(t)\rangle_2 = -2B \sum_{r=0}^{\infty} \frac{(\gamma)_r (-\lambda)^r}{r!} \left[\int_0^t \ln(u)\, e_{1,1+\alpha r}(1; u)\, \mathrm{d}\, u + \sum_{j \geq 1} \frac{\psi(j + \alpha r)}{\Gamma(j + \alpha t)} \int_0^t u^{\alpha r + j - 1}\, \mathrm{d}\, u \right]. \tag{35}$$

For calculation of the first integral in the square bracket we need the following Proposition 9.

Proposition 9. *For $a > 0$ and $t > 0$ we have*

$$\int_0^t \ln(u)\, e_{1,1+a}(1; u)\, \mathrm{d}\, u = \ln(t)\, e_{1,2+a}(t) - \frac{t^{1+a}}{1+a} \frac{1}{\Gamma(2+a)}\, {}_2F_2\left(\begin{matrix} 1, a+1 \\ a+2, a+2 \end{matrix}; t \right). \tag{36}$$

Proof. Let us employ the series form of the three parameters Mittag-Leffler function (3). Hence, we have

$$\begin{aligned}\int_0^t \ln(u)\, e_{1,1+a}(u)\,\mathrm{d}\,u &= \sum_{j=0}^{\infty} \frac{1}{\Gamma(1+j+a)} \int_0^t u^{a+j} \ln(u)\,\mathrm{d}\,u \\ &= \ln(t) \sum_{j=0}^{\infty} \frac{t^{1+j+a}}{\Gamma(2+j+a)} - t^{1+a} \sum_{j\geq 0} \frac{t^j}{(1+j+a)\Gamma(2+j+a)},\end{aligned} \tag{37}$$

where we used [55, Eq. (2.6.2.2.)] according to which

$$\int_0^t u^{a+1} \ln(u)\,\mathrm{d}\,u = \frac{t^{1+j+a}}{1+j+a}\Big[\ln(t) - (1+j+a)^{-1}\Big].$$

Thereafter, the first series in Eq. (37) due to Eq. (3) is the Prabhakar function. The second series there gives the generalized hypergeometric function of type ${}_2F_2$. That finishes the proof. □

The second integral in the square bracket reads

$$\int_0^t u^{\alpha r+j-1}\,\mathrm{d}\,u = \frac{t^{\alpha r+j}}{\alpha r+j}. \tag{38}$$

Finally, inserting Eqs. (36) and (38) into Eq. (35) we obtain

$$\begin{aligned}\langle x^2(t)\rangle_2 &= \ln\left(\frac{1}{t}\right) \sum_{r=0}^{\infty} \frac{(\gamma)_r\,(-\lambda)^r}{r!}\, e_{1,2+\alpha r}(1;t) \\ &\quad + t \sum_{r=0}^{\infty} \frac{(\gamma)_r\,(-\lambda t^{\alpha})^r}{(1+\alpha r) r!\,\Gamma(2+\alpha r)}\, {}_2F_2\left(\begin{matrix}1, 1+\alpha r\\ 2+\alpha r, 2+\alpha r\end{matrix}; t\right) \\ &\quad + \sum_{r=0}^{\infty} \frac{(\gamma)_r(-\lambda t^{\alpha})^r}{r!\,\Gamma(\alpha r)} \sum_{j=1}^{\infty} t^j\, \frac{\psi(j+\alpha r)}{(\alpha r)_j}.\end{aligned} \tag{39}$$

The latter sum in this equation, i.e. $\sum_{j=1}^{\infty} t^j\,\psi(j+\alpha r)/(\alpha r)_j$ is calculated as $\partial_a E_{a,\alpha r}(x)|_{a=1}$ [56]. In a short time, the second and third series in Eq. (39) can be neglected. At $t \ll 1$ we can approximate $e_{1,2+\alpha r}(1;t)$ as $t^{1+\alpha r}/\Gamma(2+\alpha r)$ and insert it into the first series. That gives $t\ln(1/t)E^{\gamma}_{\alpha,2}(-\lambda t^{\alpha})$ where $E^{\gamma}_{\alpha,2}(-\lambda t^{\alpha}) \sim 1/\Gamma(2) = 1$. Thus, $\langle x^2(t)\rangle_2$ at $t \ll 1$ is proportional to $t\ln(1/t)$. It means that we obtain the behavior indicated by Tauberian theorem (Theorem 1), see Eq. (31). In the opposite case, *i.e.*, at large t, the most important term is also the first series. From [6, Eq. (4.4.17)] appears that $e_{1,2+\alpha r}(1;t) \simeq -t^{\alpha r}/\Gamma(1+\alpha r)$ for $t \gg 1$. Hence, $\langle x^2(t)\rangle_2 \simeq \ln(t)E^{\gamma}_{\alpha,1}(-\lambda t)$, in which with the help of [57] we approximate $E^{\gamma}_{\alpha,1}(-\lambda t)$ as $\lambda^{-\gamma}t^{-\alpha\gamma}/\Gamma(1-\alpha\gamma)$. That leads us to the asymptotic behavior of $\langle x^2(t)\rangle_2$ at the large time given by Tauberian theorem, see Eq. (31).

4.2. Standard deviation, skewness, and kurtosis

Because the odd moments are equal to zero then the standard deviation reads

$$\sigma = \sqrt{\langle x^2(t)\rangle_{\hat{k}}}.$$

The MSD $\langle x^2(t)\rangle_{\hat{k}_1} \equiv \langle x^2(t)\rangle_1$ is given by Eq. (34) whereas $\langle x^2(t)\rangle_{\hat{k}_2} \equiv \langle x^2(t)\rangle_2$ is presented by Eq. (39). Moreover, the skewness $\mu_3 = \mathbb{E}[(x - \langle x\rangle)^3]/\sigma^3$ proportional to the odd moments vanishes which appears for symmetric PDF. The expectation operator is denoted by $\mathbb{E}$.

The kurtosis according to definition for symmetric PDF figures out

$$\mu_4 = \frac{\mathbb{E}[(x-\langle x\rangle_{\hat{k}})^4]}{\sigma^4} = \frac{\langle x^4\rangle_{\hat{k}}}{\langle x^2\rangle^2_{\hat{k}}}.$$

Eq. (30) for $n = 2$ gives the 4th moments which depends on the MSD. Indeed, we have

$$\begin{aligned}\langle x^4(t)\rangle_{\hat{k}} &= 24B^2 \int_0^t \mathscr{L}^{-1}[\hat{M}^2(s); u]\,\mathrm{d}\,u \\ &= 24B^2 \int_0^t \left[\int_0^u M(u-\xi)M(\xi)\,\mathrm{d}\,\xi\right]\mathrm{d}\,u \\ &= 24B^2 \int_0^t M(\xi)\left[\int_{\xi}^t M(u-\xi)\,\mathrm{d}\,u\right]\mathrm{d}\,\xi.\end{aligned} \tag{40}$$

Setting now $u - \xi = y$ we get that the integral in square bracket reads

$$\int_\xi^t M(u-\xi)\,\mathrm{d}\,u = \int_0^{t-\xi} M(y)\,\mathrm{d}\,y = (2B)^{-1}\langle x^2(t-\xi)\rangle_{\hat{k}}.$$

Substituting this results in Eq. (40) we obtain

$$\langle x^4(t)\rangle_{\hat{k}} = 12B\int_0^t M(\xi)\,\langle x^2(t-\xi)\rangle_{\hat{k}}\,\mathrm{d}\,\xi. \tag{41}$$

Proposition 10. *For $t > 0$ the following convolution integral formula holds true*

$$\int_0^t \mathrm{e}^{\xi}\,\mathrm{Ei}(-\xi)\ln(t-\xi)\,\mathrm{d}\,\xi = -C^2\,\mathrm{e}^t + \frac{\pi^2}{6}(1-\mathrm{e}^t) - (2C+\ln t)\,\mathrm{e}^t(\ln t) + (C+2\ln t)\,\mathrm{e}^t\,\mathrm{Ei}(-t)$$
$$- \;C(\ln t) - (\ln t)^2 + 2t\,\mathrm{e}^t\,\Phi^{\star(1,1)}_{1;1}(-t,3,1),$$

where $\Phi^{\star(1,1)}_{1;1}(-t,3,1) = {}_3F_3\left({1,1,1 \atop 2,2,2}; -t\right)$ is the generalized Hurwitz-Lerch function.

Proof. By Laplace transform method and convolution theorem, we have

$$\begin{aligned}\mathscr{L}\left[\int_0^t \mathrm{e}^{\xi}\,\mathrm{Ei}(-\xi)\ln(t-\xi)\,\mathrm{d}\,\xi; s\right] &= \mathscr{L}\left[\mathrm{e}^t\,\mathrm{Ei}(-t); s\right]\mathscr{L}\left[\ln(t); s\right]\\ &= -\mathscr{L}[\mathrm{Ei}(-t); s-1]\,\frac{1}{s}(C+\ln s)\\ &= \frac{\ln^2 s}{s(s-1)} + C\frac{\ln s}{s(s-1)},\end{aligned} \tag{42}$$

where we have used Eq. (25) and $\mathscr{L}[\ln t; s] = -(C+\ln s)/s$. The first inverse Laplace transform can be calculated by using [51, Eq. (1.1.1.13)], namely

$$\mathscr{L}^{-1}\left[\frac{F(s)}{s+a}; t\right] = \mathrm{e}^{-at}\int_0^t \mathscr{L}^{-1}[F(s); u]\,\mathrm{e}^{au}\,\mathrm{d}\,u.$$

Setting $a = -1$ and $F(s) = (\ln s)^2/s$, we have

$$\begin{aligned}\mathscr{L}^{-1}\left[\frac{\ln^2 s}{s(s-1)}; t\right] &= \mathrm{e}^t\int_0^t \mathrm{e}^u\,\mathscr{L}^{-1}\left[\frac{(\ln s)^2}{s}; u\right]\mathrm{d}\,u\\ &= \left(C^2 - \frac{\pi^2}{6}\right)\mathrm{e}^t\int_0^t \mathrm{e}^{-u}\,\mathrm{d}\,u + 2C\,\mathrm{e}^t\int_0^t \mathrm{e}^{-u}(\ln u)\,\mathrm{d}\,u + \mathrm{e}^t\int_0^t \mathrm{e}^{-u}(\ln u)^2\,\mathrm{d}\,u\\ &= \left(C^2 - \frac{\pi^2}{6}\right)(\mathrm{e}^t - 1) + 2C\,\mathrm{e}^t\int_0^t \mathrm{e}^{-u}(\ln u)\,\mathrm{d}\,u + \mathrm{e}^t\int_0^t \mathrm{e}^{-u}(\ln u)^2\,\mathrm{d}\,u,\end{aligned} \tag{43}$$

where according to [51, Eq. (2.5.1.7)], we have

$$\mathscr{L}^{-1}\left[\frac{\ln^2 s}{s}; t\right] = (C+\ln t)^2 - \frac{\pi^2}{6}. \tag{44}$$

To calculate the first integral given by Eq. (43) we can apply [55, Eq. (1.6.10.2)] which leads us to

$$\int_0^t \mathrm{e}^{-u}(\ln u)\,\mathrm{d}\,u = \mathrm{Ei}(-t) - C - \mathrm{e}^{-t}\ln t.$$

In the next integral we use the series form of exponential function and change (in legitimate way) the order of integration and series. That allows us to get

$$\begin{aligned}\int_0^t \mathrm{e}^{-u}(\ln u)^2\,\mathrm{d}\,u &= \sum_{r=0}^{\infty}\frac{(-1)^r}{r!}\int_0^t u^r(\ln u)^2\\ &= 2t\sum_{r=0}^{\infty}\frac{(-t)^r}{r!(1+r)^3} - 2t(\ln t)\sum_{r=0}^{\infty}\frac{(-t)^r}{r!(1+r)^2} - (\ln t)^2\sum_{r=0}^{\infty}\frac{(-t)^{1+r}}{(1+r)!}\\ &= 2t\,{}_3F_3\left({1,1,1 \atop 2,2,2}; -t\right) - 2t\,(\ln t)\,{}_2F_2\left({1,1 \atop 2,2}; -t\right) - (\ln t)^2(\mathrm{e}^{-t} - 1)\\ &= 2t\,{}_3F_3\left({1,1,1 \atop 2,2,2}; -t\right) - 2(\ln t)(C - \mathrm{Ei}(-t) + \ln t) - (\ln t)^2(\mathrm{e}^{-t} - 1),\end{aligned}$$

where ${}_2F_2\left({}^{1,1}_{2,2}; -t\right) = (C - \mathrm{Ei}(-t) + \ln t)/t$. From [58, Eq. (1.25)] we can obtain that ${}_3F_3\left({}^{1,1,1}_{2,2,2}; -t\right)$ is equal to the generalized Hurwitz–Lerch function $\Phi^{\star(1,1)}_{1;1}(-t, 3, 1)$. Finally, we have

$$\mathscr{L}^{-1}\left[\frac{\ln^2 s}{s(s-1)}; t\right] = -\left(C^2 + \frac{\pi^2}{6}\right) \mathrm{e}^t + 2t\,\mathrm{e}^t\,\Phi^{\star(1,1)}_{1;1}(-t, 3, 1) + 2(C + \ln t)\,\mathrm{e}^t\,\mathrm{Ei}(-t) \\ - (2C + \ln t)(\mathrm{e}^t + 1)(\ln t) - C^2 + \frac{\pi^2}{6}. \tag{45}$$

The latter inverse Laplace transform reads

$$\mathscr{L}^{-1}\left[\frac{\ln s}{s(s-1)}; t\right] = \int_0^t \mathscr{L}^{-1}\left[\frac{\ln s}{s-1}; u\right] \mathrm{d}\,u = \int_0^t M_1(u)\,\mathrm{d}\,u = \frac{\langle x^2(t)\rangle_1}{2B}, \tag{46}$$

where we employed Eqs. (25) and (32). Insertion of Eqs. (45) and (46) into the inverse Laplace transform of Eq. (42) finishes the proof. □

Example 6. From Eqs. (34) and (41), we obtain

$$\langle x^4(t)\rangle_1 = 24B^2 \int_0^t M_1(\xi)\big[C - \mathrm{e}^{t-\xi}\,\mathrm{Ei}(\xi - t) + \ln(t-\xi)\big]\,\mathrm{d}\,\xi \\ = 12BC\,\langle x^2(t)\rangle_1 + 24B^2\,\mathrm{e}^t \int_0^t \mathrm{Ei}(-\xi)\mathrm{Ei}(\xi - t)\,\mathrm{d}\,\xi - 24B^2 \int_0^t \mathrm{e}^{\xi}\,\mathrm{Ei}(-\xi)\ln(t-\xi)\,\mathrm{d}\,\xi. \tag{47}$$

The second term in Eq. (47) can be calculated by using [52, Eq. (2.5.11.6) p. 77] and it reads

$$\int_0^t \mathrm{Ei}(-\xi)\mathrm{Ei}(\xi - t)\,\mathrm{d}\,\xi = 2(C + \ln t)\,\mathrm{e}^{-t} - 2(1 - tC - t\ln t)\mathrm{Ei}(-t) - t\left[\frac{\pi^2}{6} + (C + \ln t)^2\right] \\ + 2\Phi^{\star(1,1)}_{1;1}(-t, 3, 1).$$

For the integral of the third term, we will apply the last Proposition 10. That allows us to obtain the exact form of $\langle x^4(t)\rangle_1$.

5. Probability density function $p_{\hat{k}}(x, t)$

We begin with finding the explicit form of the PDF $p_{\hat{k}}(x, t)$ for the memory kernels $k_1(t)$ and $k_2(\alpha, \gamma; \lambda; t)$ for which we have $p_{\hat{k}_1}(x, t) \equiv p_1(x, t)$ and $p_{\hat{k}_2}(x, t) \equiv p_2(x, t)$, respectively. For that purpose we are using the general form of PDF given by Eq. (8) in which we take $\hat{k}_1(s)$ from Eq. (4) and $\hat{k}_2(\alpha, \gamma; \lambda; s)$ from Eq. (5). Thus, we have

$$p_1(x, t) = \sum_{r=0}^{\infty} p_1(r; x, t) \quad \text{where} \quad p_1(r; x, t) = \frac{1}{2\sqrt{B}}\left(\frac{-|x|}{\sqrt{B}}\right)^r \frac{1}{r!\,\Gamma(b_r)}\,\epsilon^{-b_r}_{1, b_r - 1, -b_r}(t), \tag{48}$$

where $b_r = (r+1)/2$, as well as

$$p_2(x, t) = \sum_{r=0}^{\infty} \int_0^{\infty} p_1(r; x, t - \xi)\,e^{-\gamma b_r}_{1,0}(\lambda, \xi)\,\mathrm{d}\,\xi. \tag{49}$$

Proof of Eqs. (48) and (49). Without specifying the memory function $\hat{k}(s)$ we express Eq. (8) as

$$p_{\hat{k}}(x, t) = \frac{1}{2\sqrt{B}} \sum_{r=0}^{\infty} \frac{(-|x|/\sqrt{B})^r}{r!}\,\mathscr{L}^{-1}\left\{s^{b_r - 1}\,[\hat{k}(s)]^{b_r}; t\right\} \tag{50}$$

and we set $b_r = (r+1)/2$. Here, we assume that the inverse Laplace transform of the series is the same as the series of inverse Laplace transforms. Next, we express $[\hat{k}_1(s)]^{b_r}$ in the series form

$$[\hat{k}(s)]^{b_r} = (\ln s)^{-b_r}\left(1 - \frac{1}{s}\right)^{b_r} = (\ln s)^{-b_r} \sum_{j=0}^{\infty} \frac{s^{-j}}{j!}(-b_r)_j.$$

That allows one to calculate $\mathscr{L}^{-1}[s^{b_r-1}\,\hat{k}_1^{b_r}(s);t]$, namely

$$\begin{aligned}\mathscr{L}^{-1}[s^{b_r-1}\,\hat{k}_1^{b_r}(s);t] &= \sum_{j=0}^{\infty}\frac{(-b_r)_j}{j!}\mathscr{L}^{-1}\left[s^{b_r-j-1}(\ln s)^{-b_r};t\right]\\ &= \sum_{j=0}^{\infty}\frac{(-b_r)_j}{j!}\,\mu(t,b_r-1,j-b_r)\\ &= \frac{1}{\Gamma(b_r)}\epsilon_{1,b_r-1,-b_r}^{-b_r}(t),\end{aligned}\tag{51}$$

where we used Proposition 6. Inserting it into Eq. (50) we end up the proof of Eq. (48).

In the case of $p_2(x,t)$ using the memory function $k_2(\alpha,\gamma;\lambda;s)$ only the inverse Laplace transform in Eq. (50) will be changed. Employing Eq. (5) and the Laplace transform of convolution we have

$$\begin{aligned}\mathscr{L}^{-1}\{s^{b_r-1}[\hat{k}_2(\alpha,\gamma;\lambda;s)]^{b_r};t\} &= \mathscr{L}^{-1}\left[s^{b_r-1}\hat{k}_1^{b_r}(s)\left(1+\frac{\lambda}{s^{\alpha}}\right)^{\gamma b_r};t\right]\\ &= \int_0^{\infty}\mathscr{L}^{-1}[s^{b_r-1}\hat{k}_1^{b_r}(s),t-\xi]\,e_{\alpha,0}^{-\gamma b_r}(\lambda;\xi)\,\mathrm{d}\,\xi.\end{aligned}$$

Employing now Eq. (51), we finish the proof of Eq. (49). □

6. Conclusion

The paper presents the exact solution of the generalized Fokker–Planck equation whose integral kernel $k(t)$ informs on the form of smearing first-time derivative and it is called a memory function. With respect to the form of the memory function, we considered two examples of the generalized Fokker–Planck equation. In one of them, we take the distributed order kernel denoted by $k_1(t)$. In the next example, we studied the generalized Fokker–Planck equation with distributed order Prabhakar kernel $k_2(\alpha,\gamma;\lambda;t)$. We showed that $k_1(t)$ and $k_2(\alpha,\gamma;\lambda;t)$ can be expressed as the differences of Volterra functions or Volterra-Prabhakar functions, which was introduced in the present paper, respectively. Thereafter, we calculated the MSDs, 4th moments, and PDFs. The non-negativity of these functions is ensured by the Stieltjes character of $k_1(t)$ and $k_2(\alpha,\gamma;\lambda;t)$.

Data availability

No data was used for the research described in the article.

Acknowledgments

KG and TP research was supported by the NCN Research Grant Preludium Bis 2 No. UMO-2020/39/O/ST2/01563. TS acknowledges financial support by the German Science Foundation (DFG, Grant number ME 1535/12-1) and by the Alexander von Humboldt Foundation. ŽT was supported by the NAWA Program PROM No. PPI/PRO/2019/1/00016/U/00001 and the Department of Mathematics, Faculty of Sciences, University of Ostrava.

Appendix A. Completely monotone, Stieltjes, Bernstein, and completely Bernstein functions - a brief tutorial [11,29]

The completely monotone functions (CMFs) are a class of non-negative functions $G(s)$ of a non-negative argument whose all derivatives exist for $s>0$ and alternate, *i.e.*, $(-1)^n\,G^{(n)}(s)\geq 0$, $n\in\mathbb{N}_0$, where $G^{(n)}(s)=\mathrm{d}^n\,G(s)/\,\mathrm{d}\,s^n$. According to the Bernstein theorem [29] we can connect in a unique way the CMF and non-negative functions: $s\in[0,\infty)\to G(s)\in$ CMF iff

$$G(s)=\int_0^{\infty}\exp(-st)\,g(t)\mathrm{d}\,t\tag{A.1}$$

and if $g(t)\geq 0$ for all $t\in[0,\infty)$.

Among the important properties of CMFs we present the following.

(a1) The product of two CMFs is also CMF.

Note that Eq. (A.1) is the real-valued Laplace integral of a non-negative function $g(t)$ and in order to deal with the Laplace transform its argument has to be complex. Hence, $G(s)$ and the Laplace transform of $g(t)$, denoted as $\hat{g}(z)$ are different objects: the first of them is a real function of $s>0$ while the second is complex-valued and depends on $z\in\mathbb{C}\setminus\mathbb{R}_-$. Knowledge of analytic continuation of $G(s)\to\hat{g}(z)$ is important because these are special analytic properties of $\hat{g}(z)$ (known as Herglotz conditions, [59,60]) which determine, e.g., according to the Theorem 2.6 of Ref. [61] quoted as Theorem of Ref. [62], conditions under which $\hat{g}(z)$ is representable as the Laplace transform of a nonnegative measure defined on positive semi-axis. In the majority of probabilistic applications, we may restrict considerations to the real variable s and treat $\hat{g}(s)$ as the real function $G(s)$ but to find the inverse Laplace transform of $\hat{g}(z)$ we must have the variable z complex.

The next class of functions needed in our considerations is that of complete Bernstein functions (CBF) [11,29]: $c(s)$ is CBF, $s > 0$, if $c(s)/s$ is the Laplace transform of CMF restricted to the positive semiaxis, or, equivalently, in the same way restricted Stieltjes transform of a positive function named also as the Stieltjes function (SF). Note that all SFs are completely monotone, *i.e.*, SFs are a subclass of CMF.

The following properties of CBFs and connected to them SFs will be used:

(a2) The composition of CBFs is CBF;
(a3) The composition of CMF and CBF is another CMF;
(a4) The composition of SF and CBF as well as CBF and SF is another SF;
(a5) The algebraical inversion of SF is CBF and the algebraical inversion of CBF is SF;
(a6) If $c(s)$ is CBF then $c(s)/s$ is SF and if $c(s)$ is SF then $s/c(s)$ is CBF.

CBFs form a subclass of the Bernstein functions (BF). These are defined as non-negative functions whose derivative is CMF [11,29]: $h(s) > 0$ is BF if

$$(-1)^{n-1}\, h^{(n)}(s) \geq 0, \quad n = 1, 2, \ldots .$$

Appendix B. Proposition 10 for $t \ll 1$

For $t \ll 1$ the following convolution integral formula holds true

$$\int_0^t \mathrm{e}^{\xi}\, \mathrm{Ei}(-\xi) \ln(t-\xi)\, \mathrm{d}\,\xi = -\mathrm{e}^t (C + \ln t)^2 + C\, \mathrm{e}^t\, \mathrm{Ei}(-t) + 2(\ln t)\, \mathrm{e}^t\, \mathrm{Ei}(-t) - C(\ln t) - (\ln t)^2 \\ - \sum_{n=1}^{\infty} \frac{1}{(n+1)^2} \sum_{r=1}^{n} \frac{t^r}{r!} + \mathrm{e}^t \int_0^t \left\{ \frac{2}{u}\, \mathrm{Ein}(u) + \frac{\mathrm{e}^{-u}}{u}\, \mathrm{Ein}(-u) \right\} \mathrm{d}\,u,$$

where $\mathrm{Ein}(t) = \int_0^t (1 - \mathrm{e}^{-u})\, \mathrm{d}\,u/u$.

Proof. The inverse Laplace transform of the first term of (42) which contains the square of logarithmic function can be calculated by using [38, Eq. (19.5.2)]

$$\mathscr{L}^{-1}[s^{-\lambda-1} \ln^2 s; t] = \frac{t^{\lambda}}{\Gamma(\lambda+1)} \big\{ [\psi(\lambda+1) - \ln t]^2 - \psi'(\lambda+1) \big\}. \tag{B.1}$$

Namely,

$$\mathscr{L}^{-1}\left[\frac{\ln^2 s}{s-1}; t\right] = \mathscr{L}^{-1}\left[\frac{1}{s}\, \frac{\ln^2 s}{1 - 1/s}; t\right] = \mathscr{L}^{-1}\left[(\ln^2 s) \sum_{n=0}^{\infty} s^{-n-1}; t\right] \\ = \sum_{n=0}^{\infty} \mathscr{L}^{-1}\big[s^{-n-1} \ln^2 s; t\big] = \sum_{n=0}^{\infty} \{[\psi(n+1) - \ln t]^2 - \psi'(n+1)\} \frac{t^n}{n!}.$$

Hence,

$$\int_0^t \mathrm{e}^{\xi}\, \mathrm{Ei}(-\xi) \ln(t-\xi)\, \mathrm{d}\,\xi = \mathscr{L}^{-1}\left[\frac{\ln^2 s}{s-1}; t\right] - \mathscr{L}^{-1}\left[\frac{\ln^2 s}{s}; t\right] + C\, \mathscr{L}^{-1}\left[\frac{\ln s}{s(s-1)}; t\right].$$

Using the inverse Laplace transform we have $\mathscr{L}^{-1}\{(\ln s)/[s(s-1)]; t\} = \int_0^t \mathscr{L}^{-1}[(\ln s)/(s-1); u]\, \mathrm{d}\,u$, which from Eqs. (25) and (32) appears to be equal to $\int_0^t M_1(u)\, \mathrm{d}\,u = \langle x^2(t) \rangle_1/(2B)$. Now, from Eqs. (34) and (B.1) we obtain

$$\int_0^t \mathrm{e}^{\xi}\, \mathrm{Ei}(-\xi) \ln(t-\xi)\, \mathrm{d}\,\xi = \sum_{n=0}^{\infty} \{[\psi(n+1) - \ln t]^2 - \psi'(n+1)\} \frac{t^n}{n!} - (\ln t + C)^2 + \frac{\pi^2}{6} \\ - C\, \mathrm{e}^t\, \mathrm{Ei}(-t) + \gamma \ln t + C^2 \\ = \sum_{n=0}^{\infty} \{[\psi(n+1)]^2 - \psi'(n+1)\} \frac{t^n}{n!} - 2(\ln t) \sum_{n=0}^{\infty} \psi(n+1) \frac{t^n}{n!} \\ + \mathrm{e}^t \ln^2 t - (\ln t + C)^2 + \frac{\pi^2}{6} - C\, \mathrm{e}^t\, \mathrm{Ei}(-t) + C \ln t + C^2. \tag{B.2}$$

Let $H_n^{(s)} = \sum_{k=1}^n k^{-s}$, $s = \mathbb{N}$ is a sequence of harmonic power numbers, where $H_n^{(1)} = H_n$. Since, $\psi(n+1) = -C + H_n$ and $\psi'(n+1) = \pi^2/6 - \sum_{k=1}^n n^{-2} = \pi^2/6 - H_n^{(2)}$, (see [63,64]), we obtain,

$$[\psi(n+1)]^2 - \psi'(n+1) = C^2 - 2CH_n + (H_n)^2 - \frac{\pi^2}{6} + H_n^{(2)}$$
$$= -C^2 - 2C\,\psi(n+1) + (H_n)^2 - \frac{\pi^2}{6} + H_n^{(2)}.$$

That allows us to write

$$\begin{aligned}\sum_{n=0}^{\infty}\{[\psi(n+1)]^2 - \psi'(n+1)\}\frac{t^n}{n!} - 2(\ln t)\sum_{n=0}^{\infty}\psi(n+1)\frac{t^n}{n!} &= -\left(C^2+\frac{\pi^2}{6}\right)\sum_{n=0}^{\infty}\frac{t^n}{n!} \\ &- 2(C+\ln t)\sum_{n=0}^{\infty}\frac{t^n}{n!}\psi(1+n) + \sum_{n=0}^{\infty}(H_n)^2\frac{t^n}{n!} + \sum_{n=0}^{\infty}H_n^{(2)}\frac{t^n}{n!}.\end{aligned} \tag{B.3}$$

Usually it is assumed that $\psi(1) = -C$ which means that $H_0 = 0$. Then, Eq. (B.3) can be presented as

$$\text{LHS of Eq. (B.3)} = -\left(C^2 + \frac{\pi^2}{6}\right)\mathrm{e}^t + 2(C^2 + C\ln t) - 2(C+\ln t)\sum_{n=1}^{\infty}\frac{t^n}{n!}\psi(1+n)$$
$$+ \sum_{n=1}^{\infty}(H_n)^2\frac{t^n}{n!} + \sum_{n=1}^{\infty}H_n^{(2)}\frac{t^n}{n!}.$$

The abbreviation LHS means left-hand size. Next, we use Eq. (33) in which is calculated the generating function for the digamma function and apply results of Ref. [63]. By employing the umbral calculus the authors show

$$\sum_{n=1}^{\infty}H_n^{(2)}\frac{t^n}{n!} = \mathrm{e}^t - 1 + \sum_{n=1}^{\infty}\frac{1}{(n+1)^2}\left(\mathrm{e}^t - \sum_{r=0}^{n}\frac{t^r}{r!}\right) = \frac{\pi^2}{6}(\mathrm{e}^t - 1) - \sum_{n=1}^{\infty}\frac{1}{(n+1)^2}\sum_{r=1}^{n}\frac{t^r}{r!},$$
$$\sum_{n=1}^{\infty}(H_n)^2\frac{t^n}{n!} = \mathrm{e}^t\int_0^t\left[2\,\mathrm{Ein}(u) + \mathrm{e}^{-u}\,\mathrm{Ein}(-u)\right]\frac{\mathrm{d}u}{u}$$

where $\mathrm{Ein}(s)$ is defined in Proposition 10. Collecting all obtained in this proof results we get

$$\text{LHS of Eq. (B.3)} = -C^2\,\mathrm{e}^t + 2\,\mathrm{e}^t(C+\ln t)\left[\mathrm{Ei}(-t) - \ln t\right] - \frac{\pi^2}{6}$$
$$- \sum_{n=1}^{\infty}\frac{1}{(n+1)^2}\sum_{r=1}^{n}\frac{t^r}{r!} + \mathrm{e}^t\int_0^t\left[2\,\mathrm{Ein}(u) - \mathrm{e}^u\,\mathrm{Ein}(-u)\right]\frac{\mathrm{d}u}{u}.$$

Finally, by substituting the term of the right-hand side of the last equation in Eq. (B.2), the proof of the proposition is completed. □

References

[1] A. Fernandez, N. Rani, Ž. Tomovski, An operational calculus approach to Hilfer-Prabhakar fractional derivatives, Banach J. Math. Anal. 17 (2023) 33, http://dx.doi.org/10.1007/s43037-023-00258-1.

[2] R. Garra, R. Gorenflo, F. Polito, Ž. Tomovski, Hilfer–Prabhakar derivatives and some applications, Appl. Math. Comput. 242 (2014) 576–589, http://dx.doi.org/10.1016/j.amc.2014.05.129.

[3] A. Giusti, General fractional calculus and Prabhakar's theory, Commun. Nonlinear Sci. Numer. Simul. 83 (2020) 105114, http://dx.doi.org/10.1016/j.cnsns.2019.105114.

[4] A. Giusti, I. Colombaro, R. Garra, R. Garrappa, F. Polito, M. Popolizio, F. Mainardi, A practical guide to prabhakar fractional calculus, Fract. Calc. Appl. Anal. 23 (2020) 9–54, http://dx.doi.org/10.1515/fca-2020-0002.

[5] F. Polito, Ž. Tomovski, Some properties of Prabhakar-type fractional calculus operators, FDC 6 (1) (2016) 73–94, http://dx.doi.org/10.7153/fdc-06-05.

[6] R. Gorenflo, A.A. Kilbas, F. Mainardi, S. Rogosin, Mittag-Leffler Functions, Related Topics and Applications, second ed., Springer, Berlin, 2020.

[7] K. Górska, A. Horzela, A. Lattanzi, Composition law for the Cole-Cole relaxation and ensuing evolution equations, Phys. Lett. A 383 (2019) 1716–1721, http://dx.doi.org/10.1016/j.physleta.2019.03.008.

[8] K. Górska, A. Horzela, The Volterra type equations related to the non-Debye relaxation, Commun. Nonlinear Sci. Numer. Simul. 85 (2020) 105246, http://dx.doi.org/10.1016/j.cnsns.2020.105246.

[9] K. Górska, A. Horzela, A. Lattanzi, T.K. Pogány, On the complete monotonicity of the three parameter generalized Mittag-Leffler function $E^{\gamma}_{\alpha,\beta}(-x)$, Appl. Anal. Discrete Math. 15 (2021) 118–128, http://dx.doi.org/10.2298/AADM190226025G.

[10] H.J. Haubold, A.M. Mathai, R.K. Saxena, Mittag-Leffler functions and their applications, J. Anal. Math. 2011 (2011) 298628, http://dx.doi.org/10.1155/2011/298628.

[11] T. Sandev, Z. Tomovski, Fractional Equations and Models: Theory and Applications, Springer Nature, Cham, 2019.

[12] Y.G. Sinai, The limiting behavior of a one-dimensional random walk in a random medium, Theory Probab. Appl. 27 (1982) 256–268, http://dx.doi.org/10.1137/1127028.

[13] D.S. Fisher, P. Le Doussal, C. Monthus, Nonequilibrium dynamics of random field Ising spin chains: Exact results via real space renormalization group, Phys. Rev. E 64 (2001) 066107, http://dx.doi.org/10.1103/PhysRevE.64.066107.
[14] Y. Kafr, A. Polkovnikov, DNA unzipping and the unbinding of directed polymers in a random media, Phys. Rev. Lett. 97 (2006) 208104, http://dx.doi.org/10.1103/PhysRevLett.97.208104.
[15] J.-C. Waler, A. Ferrantini, E. Carlon, C. Vanderzande, Fractional Brownian motion and the critical dynamics of zipping polymers, Phys. Rev. E 85 (2012) 031120, http://dx.doi.org/10.1103/PhysRevE.85.031120.
[16] L. Laloux, P. Le Doussal, Aging and diffusion in low dimensional environments, Phys. Rev. E 57 (1998) 6296, http://dx.doi.org/10.1103/PhysRevE.57.6296.
[17] M.A. Lomholt, L. Lizana, R. Metzler, T. Ambjörnsson, Microscopic origin of the logarithmic time evolution of aging processes in complex systems, Phys. Rev. Lett. 110 (2013) 208301, http://dx.doi.org/10.1103/PhysRevLett.110.208301.
[18] J. Dräger, J. Klafter, Strong anomaly in diffusion generated by iterated maps, Phys. Rev. Lett. 84 (2000) 5998, http://dx.doi.org/10.1103/PhysRevLett.84.5998.
[19] A. Godec, A.V. Chechkin, E. Barkai, H. Kantz, R. Metzler, Localisation and universal fluctuations in ultraslow diffusion processes, J. Phys. A 47 (2014) 492002, http://dx.doi.org/10.1088/1751-8113/47/49/492002.
[20] A.V. Chechkin, R. Gorenflo, I.M. Sokolov, Retarding subdiffusion and accelerating superdiffusion governed by distributed-order fractional diffusion equation, Phys. Rev. E 66 (2002) 046129, http://dx.doi.org/10.1103/PhysRevE.66.046129.
[21] A.V. Chechkin, J. Klafter, I.M. Sokolov, Fractional Fokker–Planck equation for ultraslow kinetics, Europhys. Lett. 63 (2003) 326–332, http://dx.doi.org/10.1209/epl/i2003-00539-0.
[22] T. Sandev, A. Chechkin, H. Kantz, R. Metzler, Diffusion and Fokker–Planck-Smoluchowski equations with generalized memory kernel, Fract. Calc. Appl. Anal. 18 (2015) 1006–1038, http://dx.doi.org/10.1515/fca-2015-0059.
[23] T. Sandev, I.M. Sokolov, R. Metzler, A.V. Chechkin, Beyond monofractional kinetics, Chaos Solitons Fractals 102 (2017) 210–217, http://dx.doi.org/10.1016/j.chaos.2017.05.001.
[24] T. Sandev, Ž. Tomovski, J.L.A. Dubbeldam, A. Chechkin, Generalized diffusion-wave equation with memory kernel, J. Phys. A 52 (2019) 015201, http://dx.doi.org/10.1088/1751-8121/aaefa3, 22pp.
[25] T. Sandev, Ž. Tomovski, Langevin equation for a free particle driven by power law type of noises, Phys. Lett. A 378 (2014) 1–9, http://dx.doi.org/10.1016/j.physleta.2013.10.038.
[26] T.M. Atanackovic, S. Pilipovic, D. Zorica, Time distributed-order diffusion-wave equation. I. Volterra-type equation, Proc. R. Soc. Lond. Ser. A Math. Phys. Eng. Sci. 465 (2009) 1869–1891, http://dx.doi.org/10.1098/rspa.2008.0445.
[27] T.M. Atanackovic, S. Pilipovic, D. Zorica, Time distributed-order diffusion-wave equation. II. Applications of Laplace and Fourier transformations, Proc. R. Soc. Lond. Ser. A Math. Phys. Eng. Sci. 465 (2009) 1893–1917, http://dx.doi.org/10.1098/rspa.2008.0446.
[28] K. Górska, A. Horzela, E.K. Lenzi, G. Pagnini, T. Sandev, The generalized Cattaneo (telegrapher's) equation and corresponding random walks, Phys. Rev. E 102 (2020) 022128, http://dx.doi.org/10.1103/PhysRevE.102.022128.
[29] R. Schilling, R. Song, Z. Vondracek, Bernstein Functions. Theory and Applications, De Gruyter, Berlin/Boston, 2012.
[30] A. Hanyga, A comment on a controversial issue: A generalized fractional derivative cannot have a regular kernel, Fract. Calc. Appl. Anal. 23 (2020) 211–223, http://dx.doi.org/10.1515/fca-2020-0008.
[31] A. Hanyga, A remark on non-CM kernels of GFD and GFI, 2021, https://www.researchgate.net/profile/Andrzej-Hanyga/publication/353193556_A_remark_on_non-CM_kernels_of_GFD_and_GFI/links/60ec6cd90859317dbddb0127/A-remark-on-non-CM-kernels-of-GFD-and-GFI.pdf. (Accessed 2021).
[32] K. Górska, A. Horzela, Subordination and memory dependent kinetics in diffusion and relaxation phenomena, Fract. Calc. Appl. Anal. 26 (2023) 480–512, http://dx.doi.org/10.1007/s13540-023-00141-8
[33] H.C. Fogedby, Langevin equations for continuous time Léy flights, Phys. Rev. E 50 (1994) 1657, http://dx.doi.org/10.1103/PhysRevE.50.1657.
[34] H. Bateman, A. Erdélyi, Higher Transcendental Functions, Vol. 3, Robert E. Krieger Pub. Comp., Malabra, 1955.
[35] A. Ansari, On the Volterra μ- functions and M-Wright functions as kernels and eigenfunctions of Volterra type integral operators, Fract. Calc. Appl. Anal. 19 (2) (2016) 567–572, http://dx.doi.org/10.1515/fca-2016-0030.
[36] A. Ansari, On the Volterra μ-functions and the M-Wright functions as kernels and eigenfuncions of Volterra type integral operators, Fract. Calc. Appl. Anal. 19 (2) (2016) 567–572, http://dx.doi.org/10.1515/fca-2016-0030.
[37] A. Apelblat, Integral Transforms and Volterra Function, Nova Sci. Pub. Inc., New York, 2010.
[38] A. Apelblat, Volterra Functions, Nova Sci. Pub. Inc., New York, 2013.
[39] R. Garrappa, F. Mainardi, On volterra functions and ramanujan integrals, Analysis 36 (2016) 89–105, http://dx.doi.org/10.1515/anly-2015-5009.
[40] K. Mehrez, S.M. Sitnik, Monotonicity properties and functional inequalities for the Volterra and incomplete Volterra functions, Integral Transforms Spec. Funct. 29 (2018) 875–892, http://dx.doi.org/10.1080/10652469.2018.1512107.
[41] Ž. Tomovski, T.K. Pogány, H.M. Srivastava, Laplace type integral expressions for a certain three-parameter family of generalized Mittag-Leffler functions with applications involving complete monotonicity, J. Franklin 351 (2014) 5437–5454, http://dx.doi.org/10.1016/j.jfranklin.2014.09.007.
[42] H. Pollard, The completely monotonic character of the Mittag-Leffler function $E_\alpha(-x)$, Bull. Amer. Math. Soc. 54 (1948) 1115–1116.
[43] E.C. Titchmarsh, Introduction to the Theory of Fourier Integrals, Oxford University Press, Oxford, London, NewYork, 1937.
[44] D.V. Widder, The Laplace Transform, Princeton University Press, Princeton, 1941.
[45] M. Al-Kandari, L.A.-M. Hanna, Yu.F. Luchko, A convolution family in the dimovski sense for the composed Erdélyi-Kober fractional integrals, Integral Transforms Spec. Funct. 30 (2019) 400–417, http://dx.doi.org/10.1080/10652469.2019.1576037.
[46] I.S. Gradshtein, I.M. Ryzhik, Table of Integrals, Series and Products, seventh ed., Elsevier-Academic Press, 2007.
[47] A.N. Kochubei, General fractional calculus, evolution equations, and renewal processes, Integer. Equ. Oper. Theory 71 (2011) 583–600, http://dx.doi.org/10.1007/s00020-011-1918-8.
[48] E. Capelas de Oliveira, S. Jarosz, J. Vaz Jr., Fractional calculus via Laplace transform and its application in relaxation processes, Commun. Nonlinear Sci. Numer. Simul. 69 (2019) 58–72, http://dx.doi.org/10.1016/j.cnsns.2018.09.013.
[49] D. Zhao, HoangGuang Sun, Anomalous relaxation model based on the fractional derivative with a Prabhakar like kernel, Z. Angew. Math. Phys. 70 (2019) 42, http://dx.doi.org/10.1007/s00033-019-1086-2, 8pp.
[50] W. Feller, An Introduction to Probability Theory and Its Applications, Vol. 2, John Wiley and Sons, Inc, New York, 1971.
[51] A.P. Prudnikov, Yu.A. Brychkov, O.I. Marichev, Integrals and series, in: Inverse Laplace Transforms, Vol. 5, Gordon and Breach Sci. Publisher, New York, 1992.
[52] A.P. Prudnikov, Yu.A. Brychkov, O.I. Marichev, Integrals and series, in: More Special Functions, Vol. 2, Gordon and Breach Sci. Publisher, New York, 1998.
[53] A.R. Miller, Summations for certain series containing the digamma function, J. Phys. A: Math. Gen. 39 (2006) 3011–3020, http://dx.doi.org/10.1088/0305-4470/39/12/010.
[54] F.W.J. Olver, D.W. Lozier, R.F. Boisvert, Ch.W. Clark, NIST Handbook of Mathematical Functions, National Institute of Standards and Technology and Cambridge University Press, Cambridge, 2010, In chapter 6 we should pay attention that $E_1(t)$. (Chapter 6).

[55] A.P. Prudnikov, Yu.A. Brychkov, O.I. Marichev, Integrals and series, in: Elementary Functions, Vol. 1, Gordon and Breach Sci. Publisher, New York, 1998.
[56] A. Apelblat, J.L. González-Santander, Differentiation of integral Mittag-Leffler and integral Wright functions with respect to parameters, Fract. Calc. Appl. Anal. (2023) http://dx.doi.org/10.1007/s13540-023-00142-7.
[57] R. Garra, R. Garrappa, The prabhakar or three parameter Mittag–Leffler function: theory and application, Commun. Nonlinear Sci. Numer. Simul. 56 (2018) 314–329, http://dx.doi.org/10.1016/j.cnsns.2017.08.018.
[58] H.M. Srivastava, R.K. Saxena, T.K. Pogány, R. Saxena, Integral and computational representations of the extended Hurwitz-Lerch zeta function, Integral Transforms Spec. Funct. 22 (2013) 487–506, http://dx.doi.org/10.1080/10652469.2010.530128.
[59] N.I. Akhiezier, The Classical Moment Problem and Some Related Problems in Analysis, Oliver and Boyd, Edinburgh and London, 1965.
[60] Ch. Berg, Stieltjes-Pick-Bernstein-Schoenberg and their connection to complete monotonicity, in: J. Mateu, E. Porcu (Eds.), Positive Defined Functions: From Schoenberg to Space–Time Challenges, Dep. Math. of Univ. Jaume I, Castellon, 2008.
[61] G. Grippenberg, S.O. Londen, O.J. Staffans, Volterra Integral and Functional Equations, Cambridge University Press, Cambridge, 1990.
[62] E. Oliveira de Capelas, F. Mainardi, J. Vaz Jr., Models based on Mittag-Leffler functions for anomalous relaxation in dielectrics, Eur. Phys. J. Spec. Top. 193 (2011) (2011) 161–171, http://dx.doi.org/10.1140/epjst/e2011-01388-0.
[63] G. Datolli, S. Licciardi, E. Sabia, H.M. Srivastava, Some properties and generating functions of generalized harmonic numbers, Mathematics 7 (2019) 577, http://dx.doi.org/10.3390/math7070577.
[64] J. Choi, H.M. Srivastava, Some summation formulas involving harmonic numbers and generalized harmonic numbers, Math. Comput. Modelling 54 (2011) 2220–2234, http://dx.doi.org/10.1016/j.mcm.2011.05.032.

IOP Publishing Journal of Physics A: Mathematical and Theoretical
J. Phys. A: Math. Theor. **57** (2024) 235004 (27pp) https://doi.org/10.1088/1751-8121/ad4934

Anomalous and ultraslow diffusion of a particle driven by power-law-correlated and distributed-order noises

Z Tomovski[1], **K Górska**[2], **T Pietrzak**[2,7], **R Metzler**[3,4] and **T Sandev**[3,5,6,*]

[1] Department of Mathematical Analysis and Applications of Mathematics, Faculty of Science Palacký University Olomouc,17. listopadu 12, 771 46 Olomouc, Czech Republic
[2] Institute of Nuclear Physics, Polish Academy of Sciences, ul.Eljasza-Radzikowskiego 152, PL 31342 Krakow, Poland
[3] Institute of Physics & Astronomy, University of Potsdam, D-14476 Potsdam-Golm, Germany
[4] Asia Pacific Centre for Theoretical Physics, Pohang 37673, Republic of Korea
[5] Research Centre for Computer Science and Information Technologies, Macedonian Academy of Sciences and Arts, Bul. Krste Misirkov 2, 1000 Skopje, Macedonia
[6] Institute of Physics, Faculty of Natural Sciences and Mathematics, Ss Cyril and Methodius University, Arhimedova 3, 1000 Skopje, Macedonia
[7] Kraków Interdisciplinary Doctoral School ⟨KISD⟩, ul.Eljasza-Radzikowskiego 152, PL 31342 Kraków, Poland

E-mail: trifce.sandev@manu.edu.mk and sandev@uni-potsdam.de

Received 10 November 2023; revised 7 April 2024
Accepted for publication 9 May 2024
Published 28 May 2024

Abstract

We study the generalised Langevin equation (GLE) approach to anomalous diffusion for a harmonic oscillator and a free particle driven by different forms of internal noises, such as power-law-correlated and distributed-order noises that fulfil generalised versions of the fluctuation-dissipation theorem. The mean squared displacement and the normalised displacement correlation function are derived for the different forms of the friction memory kernel. The corresponding overdamped GLEs for these cases are also investigated. It is shown that such models can be used to describe anomalous diffusion in complex

[*] Author to whom any correspondence should be addressed.

media, giving rise to subdiffusion, superdiffusion, ultraslow diffusion, strong anomaly, and other complex diffusive behaviours.

Keywords: anomalous diffusion, generalized Langevin equation, mean squared displacement, correlation functions

1. Introduction

The behaviour of a test particle of mass m, that is coupled to a thermal bath of temperature, T, can be described by Newton's second law for a particle in the presence of a deterministic external potential $V(x)$ and a stochastically varying force $\xi(t)$. When the friction acting on the test particle is given by the constant value γ_0, the resulting dynamic is described by the standard Langevin equation for a Brownian particle [1–3],

$$m\ddot{x}(t) + m\gamma_0\dot{x}(t) + \frac{\mathrm{d}V(x)}{\mathrm{d}x} = \xi(t), \quad \dot{x}(t) = v(t), \tag{1}$$

where $x(t)$ is the particle displacement and $v(t)$ is its velocity. The stochastic force, i.e. the 'noise', $\xi(t)$ is Gaussian, has zero mean, and is white such that its autocovariance is δ-correlated, $\langle\xi(t+t')\xi(t)\rangle = mk_\mathrm{B}T\gamma_0\delta(t')$ with thermal energy $k_\mathrm{B}T$. The mean-squared displacement (MSD) encoded in the stochastic equation (1) scales quadratically ('ballistically') at short times, at which it is dominated by inertial effects, and then crosses over to a linear time dependence beyond the characteristic time scale $1/\gamma_0$.

In the following, we will consider generalisations of the stochastic equation (1) that include 'memory', by which we mean non-localities in time. A simple example giving rise to memory is the Brownian harmonic oscillator ('Ornstein-Uhlenbeck process')

$$\dot{x}(t) = v(t), \quad m\dot{v} = -m\omega^2 x(t) - m\gamma_0 v(t) + \xi_v(t), \tag{2}$$

where $\xi_v(t)$ is zero-mean white Gaussian noise. The subscript v denotes that this noise appears in the equation for $\dot{v}(t)$. On purpose, we here use the phase space notation explicitly keeping the velocity $v(t)$ in the second equation. Suppose that $v(0) = 0$, so that we can integrate the second equation from $t = 0$, yielding

$$v(t) = \int_0^t \mathrm{e}^{-\gamma_0(t-t')}\left(-\omega^2 x(t') + \xi_v(t')/m\right)\mathrm{d}t'. \tag{3}$$

Substituting this result back into the first equation in (2), we find

$$\dot{x}(t) = -\int_0^t K(t')\,x(t-t')\,\mathrm{d}t' + \xi_x(t), \tag{4}$$

where we defined the memory kernel $K(t)$ and the positional friction $\xi_x(t)$,

$$K(t) = \omega^2\mathrm{e}^{-\gamma_0 t}, \quad \xi_x(t) = \frac{1}{m}\int_0^t \mathrm{e}^{-\gamma_0 t'}\xi_v(t-t')\,\mathrm{d}t'. \tag{5}$$

At sufficiently long times $t \ll 1/\gamma_0$ (or when we start the process at $t = -\infty$) the Ornstein-Uhlenbeck process reaches equilibrium and satisfies the fluctuation–dissipation theorem $\langle\xi_x(t)\xi_x(t')\rangle \sim \langle x^2\rangle_\mathrm{eq}K(|t-t'|)$ with the thermal value $\langle x^2\rangle_\mathrm{eq} = k_\mathrm{B}T/(m\omega^2)$.

From our result (4), which is characterised by an exponential memory, one thus cannot conclude that the underlying Ornstein–Uhlenbeck process is non-Markovian. However, we showed a general property: namely, when integrating out Markovian degrees of freedom, memory effects in the resulting equation for the test particle of interest emerges [2]. Indeed, much more pronounced memories, such as power-law forms, can be affected by eliminating a quasi-continuum of Markovian degrees of freedom, see, e.g. [2, 4–6].

For a general friction memory kernel $\gamma(t)$ the dynamics of a stochastic process is described in terms of the generalised Langevin equation (GLE) [2]

$$m\ddot{x}(t) + m\int_0^t \gamma(t-t')\dot{x}(t')\,\mathrm{d}t' + \frac{\mathrm{d}V(x)}{\mathrm{d}x} = \xi(t), \quad \dot{x}(t) = v(t). \tag{6}$$

The second fluctuation-dissipation theorem (FDT) is then valid in a thermal bath of temperature T, where fluctuations and dissipation come from the same source. The FDT relates the friction memory kernel $\gamma(t)$ with the correlation function $\xi(t)$ of the random force [2, 7, 8]. The FDT allows one to write

$$\langle \xi(t+t')\xi(t')\rangle = C(t) = k_\mathrm{B}T\gamma(t). \tag{7}$$

Here the friction memory kernel is assumed to satisfy [9]

$$\lim_{t\to\infty}\gamma(t) = \lim_{s\to 0} s\hat{\gamma}(s) = 0, \tag{8}$$

where the hat denotes the Laplace transform of $\gamma(t)$, i.e. $\hat{\gamma}(s) = \mathscr{L}\{\gamma(t);s\} = \int_0^\infty \gamma(t)\mathrm{e}^{-st}\mathrm{d}t$. We note that when the noise is external in the sense of Klimontovich [10], i.e. the noise is not provided by a heat bath in a non-equilibrium systems, the relation (7) does not hold and $\langle\xi(t)\xi(t')\rangle = C(t-t')$ is used instead. When we again consider the harmonic oscillator and use the unit mass $m=1$ (i.e. $V(x) = \omega^2x^2/2$), then (6) can rewritten in the form [11]

$$x(t) = \langle x(t)\rangle + \int_0^t G(t-t')\xi(t')\,\mathrm{d}t', \quad v(t) = \langle v(t)\rangle + \int_0^t g(t-t')\xi(t')\,\mathrm{d}t', \tag{9}$$

where

$$\langle x(t)\rangle = x_0\left[1-\omega^2 I(t)\right] + v_0 G(t), \quad \langle v(t)\rangle = v_0 g(t) - \omega^2 x_0 G(t) \tag{10}$$

are the average particle displacement velocity, respectively, given the initial conditions $x_0 = x(0)$ and $v_0 = v(0)$. Moreover, we introduced the so-called relaxation functions $G(t)$, $I(t) = \int_0^t G(\xi)\mathrm{d}\xi$ and $g(t) = \frac{\mathrm{d}G(t)}{\mathrm{d}t}$, which in the Laplace space read

$$\hat{G}(s) = \frac{1}{s^2 + s\hat{\gamma}(s) + \omega^2}, \quad \hat{g}(s) = s\hat{G}(s), \quad \text{and} \quad \hat{I}(s) = s^{-1}\hat{G}(s). \tag{11}$$

These functions are used to calculate the following four fundamental quantities:

(i) the MSD [9]

$$\langle x^2(t)\rangle = 2k_\mathrm{B}TI(t) = 2k_\mathrm{B}T\int_0^t G(\xi)\,\mathrm{d}\xi; \tag{12}$$

(ii) the diffusion coefficient $\mathcal{D}(t) = \frac{1}{2}\frac{\mathrm{d}\langle x^2(t)\rangle}{\mathrm{d}t}$ that, due to relation (12) can be expressed as

$$\mathcal{D}(t) = k_\mathrm{B}TG(t) = k_\mathrm{B}T\frac{\mathrm{d}I(t)}{\mathrm{d}t}, \tag{13}$$

compare the proof of relation (13) for the GLE in the free-force case in [8, 12];

(iii) the normalised displacement autocorrelation function (DACF), that can be experimentally measured which under the initial conditions $\langle x_0^2\rangle = k_B T/\omega^2$, $\langle x_0 v_0\rangle = 0$, and $\langle \xi(t) x_0\rangle = 0$, can be represented as [13, 14]

$$C_X = \frac{\langle x(t) x_0\rangle}{\langle x_0^2\rangle} = 1 - \omega^2 I(t) = 1 - \omega^2 \int_0^t G(\xi)\,\mathrm{d}\xi. \tag{14}$$

Different DACFs for fractional GLE are studied in [14];

(iv) the normalised velocity autocorrelation function (VACF) [9]

$$C_V(t) = \frac{\langle v(t) v_0\rangle}{\langle v_0^2\rangle} = g(t) = \frac{\mathrm{d}G(t)}{\mathrm{d}t} = \frac{\mathrm{d}^2 I(t)}{\mathrm{d}t^2}. \tag{15}$$

In the large friction limit, we neglect the inertial term $m\ddot{x}(t)$, and the resulting overdamped GLE (6) has the form

$$\int_0^t \gamma(t-t')\dot{x}(t')\,\mathrm{d}t' + \frac{\mathrm{d}V(x)}{\mathrm{d}x} = \xi(t), \quad \dot{x}(t) = v(t). \tag{16}$$

The solution of this overdamped equation is of particular interest due to its application in modelling the anomalous dynamics of colloidal (micron-sized) test particles or the longer-time internal motion of proteins. Large friction, which appears due to the liquid environment means that the acceleration $\ddot{x}(t)$ is negligible in comparison to the effect of the friction term. Single-particle tracking of colloidal particles in an optical tweezers trap [15–19] or the internal motion of proteins can be considered as the effective motion in an harmonic potential [20, 21], the motion is described by the GLE

$$\int_0^t \gamma(t-t')\dot{x}(t')\,\mathrm{d}t' + m\omega^2 x(t) = \xi(t), \quad \dot{x}(t) = v(t). \tag{17}$$

The relaxation functions in the overdamped limit read

$$G_o(t) = \mathscr{L}^{-1}\left[\frac{1}{s\hat{\gamma}(s)+\omega^2};t\right],\ g_o(t) = \mathscr{L}^{-1}\left[\frac{s}{s\hat{\gamma}(s)+\omega^2};t\right], \text{and}$$
$$I_o(t) = \mathscr{L}^{-1}\left[\frac{s^{-1}}{s\hat{\gamma}(s)+\omega^2};t\right]. \tag{18}$$

For the case of a white Gaussian form for the noise $\xi(t)$ the GLE (6) corresponds to the classical overdamped Ornstein-Uhlenbeck process with friction coefficient γ_0. In the force-free case this further reduces to the Langevin equation (1) for a force-free Brownian particle. At times $t \gg 1/\gamma_0$ the MSD is then given by $\langle x^2(t)\rangle \sim 2[k_B T/(\gamma_0 m)]t$, and thus the diffusion coefficient becomes $\mathcal{D} = \lim_{t\to\infty}\langle x^2(t)\rangle/(2t) = k_B T/(m\gamma_0)$, whose physical dimensions are $[\mathcal{D}] = \text{length}^2\,\text{time}^{-1}$. The latter result for the diffusion coefficient of a Brownian particle in fact represents the Einstein-Smoluchowski-Sutherland relation [22–25].

Different forms for the friction memory kernel, particularly power-law forms [8, 9, 26–29] and Mittag–Leffler (ML) forms [11, 13, 14, 30, 31] have been introduced to model anomalous diffusion, for which the MSD scales non-linearly in time,

$$\langle x^2(t)\rangle = \frac{2\mathcal{D}_\mu}{\Gamma(1+\mu)} t^\mu, \tag{19}$$

where $\mathcal{D}_\mu$ is the generalised diffusion coefficient with physical dimension $[\mathcal{D}_\mu] = \text{length}^2\,\text{time}^{-\mu}$, and where α is the anomalous diffusion exponent. We distinguish the cases of subdiffusion ($0 < \mu < 1$) and superdiffusion ($1 < \mu$) [32]. Anomalous diffusion of this power-law form occurs in a multitude of systems across many scales [33–38] and it is non-universal in the sense that the MSD (19) for a given μ may emerge from a range of different anomalous stochastic processes [39–44]. We also mention that anomalous diffusion based on the GLE with crossovers to a different μ exponent or normal diffusion can be modelled in terms of tempered power-law kernels as introduced in [45] and applied to the anomalous diffusion of lipids in bilayer membranes [46]. Similar crossovers can be achieved in terms of formulations with distributed-order kernels as discussed below. We also note that non-Gaussian processes with power-law correlated noise was shown to emerge from a superstatistical approach based on the GLE [47, 48] and interactions of GLE dynamics with reflecting boundaries were analysed in [49].

In previous work [29] we considered the GLE for a free particle driven by a mixture of N independent internal white Gaussian noises

$$\xi(t) = \sum_{i=1}^{N} \alpha_i \xi_i(t), \tag{20}$$

such that each has zero mean, $\langle \xi_i(t)\xi_j(t')\rangle = 0$ and correlation

$$\langle \xi_i(t)\xi_i(t')\rangle = \delta_{ij}\zeta_i(t'-t), \tag{21}$$

where δ_{ij} is the Kronecker-δ. The correlation function of the additive noise $\xi(t)$ is then [29], see also [50],

$$\langle \xi(t)\xi(t')\rangle = \left\langle \sum_{i=1}^{N} \alpha_i \xi_i(t) \sum_{j=1}^{N} \alpha_j \xi_j(t') \right\rangle = \sum_{i=1}^{N} \alpha_i^2 \langle \xi_i(t)\xi_i(t')\rangle. \tag{22}$$

From the second FDT (7) we thus see that the noise fulfils

$$\sum_{i=1}^{N} \alpha_i^2 \zeta_i(t) = k_B T \gamma(t), \tag{23}$$

where $\gamma(t)$ is the associated friction memory kernel. In [29] the GLE with internal noises of Dirac-δ, power-law and ML types were analysed, and various different diffusive regimes obtained. Moreover, it was shown that friction memory kernels of distributed order can be used to describe ultraslow diffusion with a logarithmic time dependence of the MSD. In what follows we consider a stochastic harmonic oscillator driven by a mixture of internal noises, from which we recover the results for a free particle in the limit of vanishing force constant. The purpose of introducing a mixture of different noises is due to some experimental observations, showing that two types of noise are needed to model the motion of a tracked particle in intracellular transport in biological cells [16, 51, 52].

Here we analyse the MSD and DACF for different forms of the friction memory kernel. In section 2 we specify the GLE approach to anomalous diffusion. We analyse the relaxation functions, MSD, and DACF for Dirac-δ, power-law, and combinations friction kernels. The corresponding overdamped limits are analysed and the force-free limit recovered. Distributed-order friction memory kernels are considered in section 3. It is shown that such kernels yield ultraslow diffusion, strong anomaly, and other complex behaviours. The overdamped motion of a harmonic oscillator driven by distributed-order noises is investigated in detail. A summary is presented in section 5.

2. GLE in presence of white and power-law noises

We study the GLE for both white and power-law noises and their combinations. At the end of this section, we also derive the overdamped limit.

2.1. Additive white noises

The simplest case of the GLE is obtained for a test particle connected to a thermal bath of temperature T effecting N additive internal white Gaussian and zero-mean noises, equation (20), in which each component fulfils $\zeta_i(t) = \delta(t)$ (i.e. $\hat{\zeta}_i(s) = 1$). Physically such a joint noise may stem from an environment with different components. As we assume that the noise is internal, from the second FDT we conclude that the friction memory kernel is given by

$$\hat{\gamma}(s) = \sum_{i=1}^{N} \frac{\alpha_i^2}{k_{\mathrm{B}}T} \tag{24}$$

in Laplace space. From relation (11), we obtain the relaxation function $G(t)$ in the form

$$\begin{aligned} G(t) &= \mathscr{L}^{-1}\left\{\frac{1}{s^2+\kappa s+\omega^2};t\right\} \\ &= \frac{2}{\sqrt{\kappa^2-4\omega^2}}\exp\left(-\frac{\kappa t}{2}\right)\sinh\left(\frac{t}{2}\sqrt{\kappa^2-4\omega^2}\right), \end{aligned} \tag{25}$$

where $\kappa = \sum_{i=1}^{N} \alpha_i^2/(k_{\mathrm{B}}T) > 2\omega$. The limit $\omega = 0$ leads to the known result $G(t) = [1-\exp(-\kappa t)]/\kappa$ [29], i.e. a constant diffusion coefficient in the linear time dependence of the MSD on time in the long time limit ($t \to \infty$),

$$\langle x^2(t)\rangle \sim 2\mathcal{D}t, \quad \text{where} \quad \mathcal{D} = \frac{(k_{\mathrm{B}}T)^2}{\sum_{i=1}^{N}\alpha_i^2}. \tag{26}$$

We note that in the short time limit $G(t) \sim t$, leading to $\langle x^2(t)\rangle \sim t^2$, which means ballistic motion. Writing $\kappa = 2\omega_c$ in terms of the compound frequency $\omega_c = \sum_{i=1}^{N}\alpha_i^2/(2k_{\mathrm{B}}T)$, then $\mathcal{D}(t) = t\exp(-\omega_c t)$, and the MSD is given by

$$\langle x^2(t)\rangle = \omega_c^{-2}\left[1-(1+\omega_c t)\,\mathrm{e}^{-\omega_c t}\right]. \tag{27}$$

Therefore, the relaxation function $I(t)$ from (14) with $I(t) = \omega^{-2}[1-C_X(t)]$ is defined in terms of

$$C_X(t) = \mathrm{e}^{-\kappa t/2}\left[\cosh\left(\frac{t}{2}\sqrt{\kappa^2-4\omega^2}\right) + \frac{\kappa}{\sqrt{\kappa^2-4\omega^2}}\sinh\left(\frac{t}{2}\sqrt{\kappa^2-4\omega^2}\right)\right]. \tag{28}$$

With our notation $\kappa = 2\omega_c$ it is given by $C_X(t) = (1+\omega_c t)\mathrm{e}^{-\omega_c t}$. The case $\kappa < 2\omega$, i.e. the case of underdamped motion, yields in the form

$$C_X(t) = \mathrm{e}^{-\kappa t/2}\left[\cos\left(\frac{t}{2}\sqrt{4\omega^2-\kappa^2}\right) + \frac{\kappa}{\sqrt{4\omega^2-\kappa^2}}\sin\left(\frac{t}{2}\sqrt{4\omega^2-\kappa^2}\right)\right]. \tag{29}$$

Thus, the MSD in the long time limit approaches the equilibrium value $\langle x^2(t)\rangle_{\mathrm{eq}} = 2k_{\mathrm{B}}T/\omega^2$. A graphical representation of the NDCF $C_X(t)$ is given in figure 1. From panel (a) we conclude that in the overdamped case, the NDCF shows a monotonic decay to zero, without zero crossings. The underdamped case shows oscillatory behaviour of $C_X(t)$ with zero crossings (panels (b) and (c)), where oscillations become more pronounced for increasing oscillator frequency.

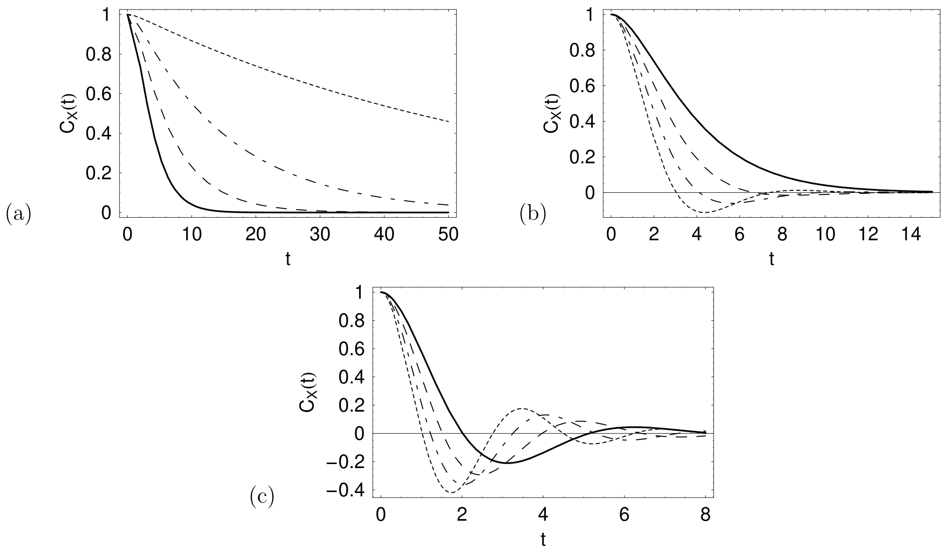

Figure 1. Normalised displacement correlation function for $\kappa = 1$: (a) overdamped motion $\kappa > 2\omega$ (28), $\omega = \omega_c = 1/2$ (solid line), $\omega = 3/8$ (dashed line); $\omega = 1/4$ (dot-dashed line); $\omega = 1/8$ (dotted line); (b) underdamped motion (29), $\omega = \omega_c = 1/2$ (solid line), $\omega = 5/8$ (dashed line); $\omega = 3/4$ (dot-dashed line); $\omega = 7/8$ (dotted line); (c) underdamped motion (29), $\omega = \omega_c = 9/8$ (solid line), $\omega = 11/8$ (dashed line); $\omega = 13/8$ (dot-dashed line); $\omega = 15/8$ (dotted line).

Remark 1. Let us analyse the diffusion coefficient in this case somewhat further. We see that if we consider a single internal white noise the diffusion coefficient is $\mathcal{D}_i = (k_{\mathrm{B}}T)^2/\alpha_i^2$, for $i = 1, 2, \ldots, N$. From relation (26), by using the relation between harmonic and arithmetic mean, we obtain

$$\mathcal{D} = \frac{1}{\sum_{i=1}^{N} \frac{1}{\mathcal{D}_i}} \leqslant \frac{\sum_{i=1}^{N} \mathcal{D}_i}{N^2}. \tag{30}$$

So we see that if the particular diffusion coefficients $\mathcal{D}_i$ are identical and equal to $\bar{\mathcal{D}}$, the diffusion coefficient for N independent internal white Gaussian noise terms scales inversely to N, $\mathcal{D} = \bar{\mathcal{D}}/N$.

If we write $\mathcal{D}_i = a^2/(2\tau_i)$ in a random walk-like notation, where a^2 represents the squared lattice constant or the variance of the jump length PDF [39, 40, 53], we rewrite the compound diffusion coefficient as

$$\mathcal{D} = \frac{1}{\sum_{i=1}^{N} \frac{2\tau_i}{a^2}} = \frac{a^2}{2\sum_{i=1}^{N} \tau_i} = \frac{a^2}{2N\langle\tau\rangle} = \frac{\overline{\mathcal{D}}}{N}. \tag{31}$$

In this sense the equality in (30) always holds. We note that the mean time $\langle\tau\rangle$ may be a misrepresentation of the largest time scale $\tau_m \max_i\{\tau_i\}$, depending on the underlying set $\{\tau_i\}$.

2.2. *Different power-law noises*

We now turn to generalising the results of [29], where the authors studied the GLE for free particles and N independent internal noises, by using a harmonic potential, corresponding to the Hookean force $F(x) = -m\omega^2 x$, in the GLE (6). To this end we first recall the considerations in [28], where the authors study the GLE for a harmonic potential and one internal noise, and then generalise these results. We mention that in [28] complementary polynomials are used to analyse the overdamped, underdamped, and critical behaviours of the oscillator. Here, our investigation is based on multinomial Prabhakar-type functions, $\mathcal{E}_{(\vec{\mu}),\beta}(s;\vec{a})$ (see [54] and appendix A). Despite the somewhat complicated notation, their definition and use in analytic calculations are in fact quite straightforward.

2.2.1. Power-law noises. We first consider the single-term internal power-law noise with correlation function $\zeta_1(t) = t^{-\lambda_1}/\Gamma(1-\lambda_1)$ (i.e. $\hat{\zeta}_1(s) = s^{\lambda_1 - 1}$) for $\lambda_1 \in (0,1)$. Thus, the friction memory kernel due to the second FDT (23) is given by $\gamma_1(t) = \alpha_1^2 \zeta_1(t)/(k_\mathrm{B}T)$. Then the GLE (6) reads (using unit mass)

$$\ddot{x}(t) + \frac{\alpha_1^2}{k_\mathrm{B}T}\, {}^{C}D_t^{\lambda_1} x(t) + \omega^2 x(t) = \xi(t), \qquad \dot{x}(t) = v(t). \tag{32}$$

Due to the power-law friction memory, the friction terms can be compactly written in terms of the fractional Caputo derivative (${}^{C}D_t^{\lambda_1}$, and the GLE (32) is often referred to as the fractional Langevin equation [27, 40]. The Caputo operator for $\lambda_1 \in (0,1)$ is defined via ${}^{C}D_t^{\lambda_1} x(t) = \int_0^t \dot{x}(t')(t-t')^{-\lambda_1}\mathrm{d}t'/\Gamma(1-\lambda_1)$, see for example [50, 55]. The relaxation functions $G_1(t)$, $I_1(t)$, and $g_1(t)$ are obtained by inverting the Laplace transform (11). They are given in terms of the multinomial Prabhakar-type functions $\mathcal{E}_{(\vec{\mu}),\beta}(s;\vec{a}) = t^{\beta-1}E_{(\vec{\mu}),\beta}(-a_1 t^{\mu_1}, \ldots, -a_N t_N^{\mu})$ where $\vec{\mu} = \mu_1, \ldots \mu_N$ and $\vec{a} = a_1, \ldots, a_N$ (see [54] and appendix A) as

$$G_1(t) = \mathscr{L}^{-1}\left\{\left(s^2 + A_1 s^{\lambda_1} + \omega^2\right)^{-1}; t\right\} = \mathcal{E}_{(2,2-\lambda_1),2}\left(t;\omega^2, A_1\right), \tag{33}$$

and

$$I_1(t) = \mathcal{E}_{(2,2-\lambda_1),3}\left(t;\omega^2, A_1\right), \quad g_1(t) = \mathcal{E}_{(2,2-\lambda_1),1}\left(t;\omega^2, A_1\right), \tag{34}$$

where $A_1 = \alpha_1^2/(k_\mathrm{B}T)$. For $t \gg 1$ these functions are estimated by the two-parameter ML function, see (A.8), whose asymptotic behaviours follow from equation (A.10), such that

$$G_1(t) \sim_{t\to\infty} A_1^{-1} t^{\lambda_1 - 1} E_{\lambda_1,\lambda_1}\left(-\omega^2 t^{\lambda_1}/A_1\right) \sim_{t\to\infty} -\frac{A_1}{\omega^4}\frac{t^{-\lambda_1-1}}{\Gamma(-\lambda_1)} = \frac{A_1\lambda_1}{\omega^4}\frac{t^{-\lambda_1-1}}{\Gamma(1-\lambda_1)}, \tag{35}$$

$$I_1(t) \sim_{t\to\infty} A_1^{-1} t^{\lambda_1} E_{\lambda_1,\lambda_1+1}\left(-\omega^2 t^{\lambda_1}/A_1\right) \sim_{t\to\infty} \frac{1}{\omega^2}\left[1 - \frac{A_1}{\omega^2}\frac{t^{-\lambda_1}}{\Gamma(1-\lambda_1)}\right], \tag{36}$$

and

$$g_1(t) \sim_{t\to\infty} A_1^{-1} t^{\lambda_1 - 2} E_{\lambda_1,\lambda_1-1}\left(-\omega^2 t^{\lambda_1}/A_1\right) \sim_{t\to\infty} -\frac{A_1}{\omega^4}\frac{t^{-\lambda_1-2}}{\Gamma(-1-\lambda_1)}. \tag{37}$$

The same results can be obtained by calculating the appropriate overdamped relaxation functions such that we have $\lim_{t\to\infty} G_1(t) = G_{o;1}(t)$, $\lim_{t\to\infty} I_1(t) = I_{o;1}(t)$, and $\lim_{t\to\infty} g_1(t) = g_{o;1}(t)$. From the result for the relaxation function $I_1(t)$ we conclude that the MSD in the long time limit approaches the equilibrium (thermal) value $\langle x^2(t)\rangle_\mathrm{eq} = 2k_\mathrm{B}T/\omega^2$ via a power-law decay, i.e.

$$\langle x^2(t)\rangle \sim_{t\to\infty} \langle x^2(t)\rangle_\mathrm{eq}\left[1 - \frac{A_1}{\omega^2}\frac{t^{-\lambda_1}}{\Gamma(1-\lambda_1)}\right]. \tag{38}$$

By asymptotic analysis in the short time limit ballistic motion is also observed since the MSD behaves as $\langle x^2(t)\rangle \sim \frac{t^2}{2} - A_1 \frac{t^{4-\lambda_1}}{\Gamma(5-\lambda_1)}$.

For the force-free case ($\omega = 0$) the MSD becomes

$$\begin{aligned}\langle x^2(t)\rangle &= 2k_B T \mathcal{L}^{-1}\left[\frac{s^{-1-\lambda_1}}{s^{2-\lambda_1}+A_1}\right] \\ &= 2k_B T t^2 E_{2-\lambda_1,3}\left(-A_1 t^{2-\lambda_1}\right) \sim \begin{cases} t^2 - A_1 \frac{t^{4-\lambda_1}}{\Gamma(5-\lambda_1)}, & t\to 0, \\ t^{\lambda_1}, & t\to\infty, \end{cases}\end{aligned} \tag{39}$$

from which we conclude that from ballistic motion in the short time limit, the particle turns to subdiffusion in the long time limit [29].

2.2.2. N power-law noises. The compound fractional Langevin equation, i.e. the GLE in which we use N independent internal noises, for $m = 1$ reads

$$\ddot{x}(t) + \sum_{r=1}^{N} A_r\, {}^{C}D_t^{\lambda_r} x(t) + \omega^2 x(t) = \xi(t). \tag{40}$$

The friction memory kernel $\gamma_N(t)$ becomes $\sum_{r=1}^{N}\gamma_r(t)$, where $\gamma_r(t)$ is defined analogously to $\gamma_1(t)$ above, but instead of a single internal noise we now have N. Here, we assume that $0 < \lambda_1 < \cdots < \lambda_N < 1$. Using short-hand notation we denote the relaxation functions $g_N(t)$, $G_N(t)$, and $I_N(t)$ by the function $F_{N;j}(t)$ indexed by $j = 1,2,3$ such that $F_{N;1}(t) = g_N(t)$ is obtained for $j = 1$, $F_{N;2}(t) = G_N(t)$ for $j = 2$, and $F_{N;3}(t) = I_N(t)$ for $j = 3$. The auxiliary functions $F_{N;j}(t)$ read

$$F_{N;j}(t) = \mathcal{E}_{(2,2-\lambda_1,\ldots,2-\lambda_N),j}\left(t;\omega^2,A_1,\ldots,A_N\right) \tag{41}$$

in terms of the Prabakhar-type function. Following [54] we check the behaviour of $F_{N;j}(t)$ in (41) at long t. In this case we obtain that $F_{N;j}(t)$ tends to the relaxation function for $N = 1$, i.e.

$$F_{N;j}(t) \sim_{t\to\infty} A_1^{-1} t^{\lambda_1+j-3} E_{\lambda_1,\lambda_1+j-2}\left(-\omega^2 t^{\lambda_1}/A_1\right). \tag{42}$$

Their further asymptotics in the long-time limit $t\to\infty$ depend on the value of j, such that for $j = 1,2,3$ we get equations (35)–(37), respectively. Making use of equation (42) we calculate the quantities (i) to (iv) defined in the introductory section is necessary to describe the time evolution of stochastic systems coupled to a thermal bath.

Based on these results the MSD can be shown to be given by the expression

$$\langle x^2(t)\rangle_N = 2k_B T \mathcal{E}_{(2,2-\lambda_1,\ldots,2-\lambda_N),3}\left(t;\omega^2,A_1,\ldots,A_N\right). \tag{43}$$

Thus, by asymptotic analysis, in the long time limit, we find the behaviour

$$\langle x^2(t)\rangle_N \sim_{t\to\infty} \langle x^2(t)\rangle_{\mathrm{eq}}\left[1 - \frac{A_1}{\omega^2}\frac{t^{-\lambda_1}}{\Gamma(1-\lambda_1)}\right]. \tag{44}$$

The MSD approaches the equilibrium (thermal) value $\langle x^2(t)\rangle_{\mathrm{eq}} = 2k_B T/\omega^2$ in power-law fashion, instead of the exponentially fast relaxation for the normal Ornstein-Uhlenbeck process. Note that similar power-law relaxations are known from subdiffusive continuous time random walks [32, 56] and from the time-averaged MSD of the fractional Langevin equation [17, 57] in an external harmonic potential. From equation (44) we see that the noise with the smaller exponent λ_1 has the dominant contribution to the oscillator behaviour in the long time limit. We also note that the same result for the MSD in the long time limit can be obtained by Tauberian theorems (see appendix B) if we analyse the behaviour of $\hat{I}_N(s)$ in the limit $s \to 0$ [58]. The short time limit $t \to 0$ yields $I_N(t) \simeq t^2/2 - A_N t^{4-\lambda_N}/\Gamma(5-\lambda_N)$, so we conclude that the noise with the largest exponent λ_N dominates the dynamic in the short time limit.

For the force-free case ($\omega = 0$), we recover the result for the MSD obtained in [29], which in the short time limit behaves as $\langle x^2(t)\rangle_N \sim t^2 - A_1 \frac{t^{4-\lambda_N}}{\Gamma(5-\lambda_N)}$, while in the long time limit we find $\langle x^2(t)\rangle_N \sim t^{\lambda_1}$. Thus, the highest exponent is the dominant contribution in the short time limit, while the lowest exponent has the analogous role in the long time limit.

The DACF (14) in the case of thermal initial conditions $\langle x_0^2\rangle = k_{\mathrm{B}}T/\omega^2$, $\langle x_0 v_0\rangle = 0$, and $\langle \xi(t) x_0\rangle = 0$, from equations (14) and (41), we obtain

$$C_X(t) = 1 - \omega^2 \mathcal{E}_{(2,2-\lambda_1,\ldots,2-\lambda_N),3}\left(t;\omega^2,A_1,\ldots,A_N\right). \tag{45}$$

Its asymptotic behaviour in the long time limit via equation (36) reads

$$C_X(t) \sim_{t\to\infty} 1 - \frac{\omega^2}{A_1} t^{\lambda_1} E_{\lambda_1,\lambda_1+1}\left(-\frac{\omega^2}{A_1} t^{\lambda_1}\right) = E_{\lambda_1}\left(-\frac{\omega^2}{A_1} t^{\lambda_1}\right) \sim_{t\to\infty} \frac{A_1}{\omega^2} \frac{t^{-\lambda_1}}{\Gamma(1-\lambda_1)}. \tag{46}$$

Thus we obtain a power-law decay, approaching the zero line from positive values for $\lambda_1 \in (0,1)$, and from negative values for $\lambda_1 \in (1,2)$, if we consider a memory kernel defined in Laplace space as $\hat{\gamma}(s) = \sum_{i=1}^{N} s^{\lambda_i - 1}$, $1 < \lambda_i < 2$. Since $E_\alpha(-x)$ is a completely monotone function for $\alpha \in (0,1)$ [59–62], we conclude that the normalised displacement correlation function is completely monotone in the long time limit for $\lambda_1 \in (0,1)$. A more detailed analysis of $C_X(t)$ is provided in section 2.4 for the case of high damping, which has more practical application in the theory of anomalous dynamics in single particle tracking and protein dynamics. We mention that the equality in equation (46) was proven in [63] and [64, remark 3].

2.3. Combinations of white and power-law noises

In the same way, as for the power-law noises, we can analyse the relaxation functions for a mixture of δ- and power-law distributed noises. The approach given in [29] can be applied in the case of a harmonic oscillator driven by P white noises and Q power-law noises ($P + Q = N$) as well. Here we consider the special case $\gamma(t) = B_1\delta(t) + B_2 t^{-\lambda}/\Gamma(1-\lambda)$ where $B_1 = \alpha^2/(k_{\mathrm{B}}T)$, $B_2 = \beta^2/(k_{\mathrm{B}}T)$, and $0 < \lambda < 1$ [29, 65].

With the help of equation (A.2) we see that

$$G(t) = \mathcal{E}_{(2,2-\lambda,1),2}\left(t;\omega^2,B_2,B_1\right). \tag{47}$$

From equations (A.3) and (A.4) we can calculate the associated integral and derivative which, respectively, lead to $I(t)$ and $g(t)$. Then, the MSD obtained from equation (12) reads

$$\langle x^2(t)\rangle = 2k_{\mathrm{B}}T\,\mathcal{E}_{(2,2-\lambda,1),3}\left(t;\omega^2,B_2,B_1\right). \tag{48}$$

Notice that equation (48) in the force-free case $\omega = 0$, after applying equation (A.15), can be recognised as [29, equation (27) for $\lambda_1 = \lambda$, $\lambda_2 = 1$], namely,

$$\langle x^2(t)\rangle = 2k_{\mathrm{B}}T \sum_{n=0}^{\infty} (-B_2)^n t^{(2-\lambda)n+2} E_{1,(2-\lambda)n+3}^{n+1}(-B_1 t). \tag{49}$$

The asymptotic of the MSD at short and long times are calculated from equations (A.5) and (A.6), yielding

$$\langle x^2(t)\rangle \sim_{t\to 0} \frac{t^2}{2} - \frac{t^3}{3!} - \frac{t^4}{4!} - \frac{t^{4-\lambda}}{\Gamma(5-\lambda)} \tag{50}$$

for $t\to 0$, and for $t \gg 1$ we have

$$\langle x^2(t)\rangle \sim_{t\to\infty} \frac{2k_\mathrm{B}T}{B_2} t^\lambda E_{\lambda,1+\lambda}\left(-\frac{\omega^2}{B_2}t^\lambda\right) \sim_{t\to\infty} \frac{2k_\mathrm{B}T}{\omega^2}\left[1 - \frac{B_2}{\omega^2}\frac{t^{-\lambda}}{\Gamma(1-\lambda)}\right], \tag{51}$$

which means that the MSD has a power-law decay to the equilibrium value $\langle x^2(t)\rangle_\mathrm{eq} = 2k_\mathrm{B}T/\omega^2$. We conclude that the power-law noise is dominant in the long time limit, and the white noise in the short time limit, as naively expected. We note that in the force-free case ($\omega = 0$), in the long time limit the particle shows anomalous diffusion of the form $\langle x^2(t)\rangle \sim t^\lambda$, while in the short time limit ballistic motion is observed. This means that the fractional exponent has a dominant contribution in the long time limit [29].

For the DACF $C_X(t)$, we obtain from relation (14) that

$$C_X(t) = 1 - \omega^2\,\mathcal{E}_{(2,2-\lambda,1),3}\left(t;\omega^2,B_2,B_1\right), \tag{52}$$

from where the long time limit follows,

$$C_X(t) \sim_{t\to\infty} 1 - \frac{\omega^2}{B_2}t^\lambda E_{\lambda,1+\lambda}\left(-\frac{\omega^2}{B_2}t^\lambda\right) \sim_{t\to\infty} \frac{B_2}{\omega^2}\frac{t^{-\lambda}}{\Gamma(1-\lambda)}. \tag{53}$$

We conclude that $C_X(t)$ in the long time limit is a completely monotone function since $0 < \lambda < 1$, showing a power-law decay to zero.

Following the same procedure one may consider mixtures of white noises, power-law noises, and ML type noises. The calculation of the relaxation function can be represented in terms of multinomial Prabhakar functions [29, 54].

2.4. Overdamped limit

Next, we analyse the high-damping limit, in which the inertial term $m\ddot{x}(t)$ can be neglected. Then, the relaxation functions are defined by equation (18).

The case of a mixture of N internal white noises considered in section 2.1, for the MSD $\langle x^2(t)\rangle_\mathrm{o} = 2k_\mathrm{B}TI_\mathrm{o}(t)$ and the DACF $C_{X,\mathrm{o}}(t)$ yields

$$\langle x^2(t)\rangle_\mathrm{o} = 2k_\mathrm{B}T\mathscr{L}^{-1}\left\{\frac{s^{-1}}{\kappa s+\omega^2};t\right\} = \frac{2k_\mathrm{B}T}{\omega^2}\left[1-\exp\left(-\frac{\omega^2}{\kappa}t\right)\right], \tag{54}$$

$$C_{X,\mathrm{o}}(t) = \exp\left(-\frac{\omega^2}{\kappa}t\right) = \exp\left(-\frac{\mathcal{D}\omega^2}{k_\mathrm{B}T}t\right), \tag{55}$$

where κ is given below equation (25) and $\mathcal{D}$ is defined in equation (26). We find that $C_{X,o}(t)$ has a monotonic exponential decay, as expected. In the short time limit the MSD has a linear dependence on time, $\langle x^2(t)\rangle_\mathrm{o} \sim t$, as it is expected.

For the case of N power-law noises, it follows from relation (12) in the overdamped case that

$$\langle x^2(t)\rangle_\mathrm{o} = \frac{2k_\mathrm{B}T}{A_N}\mathcal{E}_{(\lambda_N,\lambda_N-\lambda_1,\ldots,\lambda_N-\lambda_{N-1});\lambda_N+1}\left(t,\frac{\omega^2}{A_N},\frac{A_1}{A_N},\ldots,\frac{A_{N-1}}{A_N}\right), \tag{56}$$

$$C_{X,\mathrm{o}}(t) = 1 - \frac{\omega^2}{A_N}\mathcal{E}_{(\lambda_N,\lambda_N-\lambda_1,\ldots,\lambda_N-\lambda_{N-1});\lambda_N+1}\left(t, \frac{\omega^2}{A_N}, \frac{A_1}{A_N}, \ldots, \frac{A_{N-1}}{A_N}\right). \quad (57)$$

In the long time limit the particle shows a power-law decay of the MSD to the equilibrium value of the form (44), which means that the lowest fractional exponent has a dominant contribution, while in the short time limit anomalous diffusion of the form $\langle x^2(t)\rangle_\mathrm{o} \sim t^{\lambda_N}$ is observed, i.e. the highest fractional exponent has the dominant contribution at short times. For the force-free case ($\omega = 0$) the MSD shows characteristic crossover from $\langle x^2(t)\rangle_\mathrm{o} \sim t^{\lambda_N}$ for short times to $\langle x^2(t)\rangle_\mathrm{o} \sim t^{\lambda_1}$ for long times, i.e. decelerating subdiffusion.

The DACF shows an asymptotic power-law decay in the long time limit, i.e.

$$C_{X,\mathrm{o}}(t) \sim_{t\to\infty} E_{\lambda_1}\left(-\frac{\omega^2}{A_1}t^{\lambda_1}\right) \sim_{t\to\infty} \frac{A_1}{\omega^2}\frac{t^{-\lambda_1}}{\Gamma(1-\lambda_1)}. \quad (58)$$

Thus, we can use equation (16) in the overdamped limit case, which is simpler instead of the GLE (6), to analyse the asymptotic behaviour of the harmonic oscillator in the long time limit.

A graphical representation of the DACF is presented in figure 2. From panel (a) we see that by changing the values of the parameters λ_1 and λ_2 for fixed frequency ω there appears a non-monotonic decay of $C_{X,o}(t)$ without zero crossings, approaching the zero line at infinity (see solid line), a monotonic decay without zero crossings to zero at infinity (dashed line), a non-monotonic decay without zero crossings approaching zero at a finite time instant and at infinity (dot-dashed line), or a non-monotonic decay with zero crossings approaching zero at infinity (dotted line). All long-time decays of the DACF are of power-law form to zero, as it can be anticipated from relation (58). The behaviour of $C_X(t)$ for different values of the frequency ω and fixed values of λ_1 and λ_2 is shown in figures 2(b) and (c). We see that there are different critical frequencies, i.e. the frequency at which $C_{X,o}(t)$ changes its behaviour, for instance, from non-monotonic to monotonic decay without zero crossings, or the frequency at which $C_{X,o}(t)$ crosses the zero line. Such different types of critical frequencies were discussed in [28].

Figure 3 depicts the MSD for unconfined and confined motion. For free motion the MSD may have monotonic, non-monotonic, and oscillatory behaviour, turning into a power-law form in the long time limit. For the confined case the MSD has different behaviours at intermediate times, and in the long-time limit, the MSD has a power-law approach to the equilibrium value $\langle x^2(t)\rangle_\mathrm{eq} = 2k_\mathrm{B}T/\omega^2$.

In the same way as above, we obtain the following DACF for the case of a mixture of a white noise a and power-law noise (see results 2.3),

$$C_{X,\mathrm{o}}(t) = \sum_{n=0}^{\infty}\left(-\frac{\omega^2}{B_1}\right)^n t^n E_{1-\lambda,n+1}^{n}\left(-\frac{B_2}{B_1}t^{1-\lambda}\right), \quad (59)$$

for $0 < \lambda < 1$, and

$$C_{X,\mathrm{o}}(t) = \sum_{n=0}^{\infty}\left(-\frac{\omega^2}{B_2}\right)^n t^{\lambda n} E_{\lambda-1,\lambda n+1}^{n}\left(-\frac{B_1}{B_2}t^{\lambda-1}\right), \quad (60)$$

for $1 < \lambda < 2$, where B_1 and B_2 are given at the beginning of section 2.3. These results are equivalent to those obtained in section 2.3 in the long time limit for the GLE when the inertial term is not neglected, as it should be.

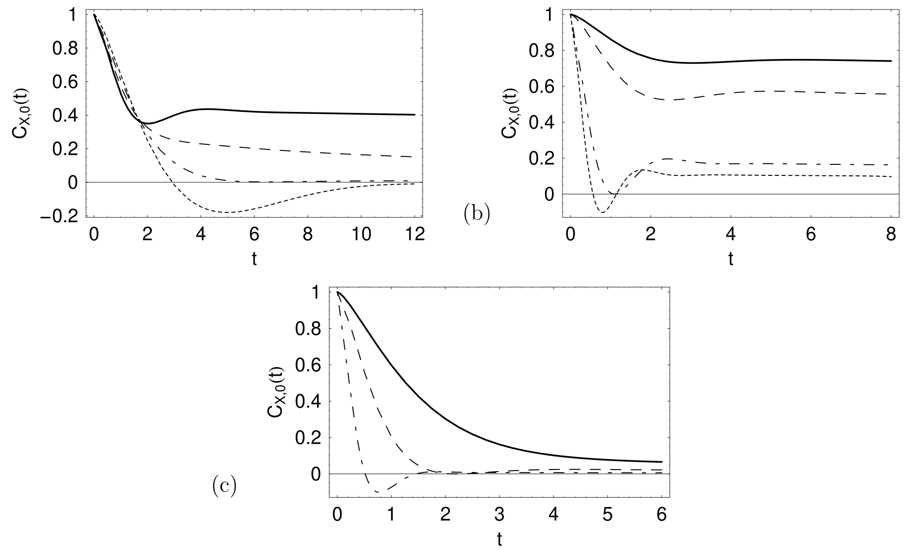

Figure 2. Normalised displacement correlation function (57) for the following cases for $N = 2$: (a) $\omega = 1$, $\lambda_2 = 3/2$, $\lambda_1 = 1/8$, (solid line), $\lambda_1 = 1/2$ (dashed line), $\lambda_1 = 7/8$ (dot-dashed line), $\lambda_1 = 5/4$ (dotted line); (b) $\lambda_1 = 1/8$, $\lambda_2 = 3/4$, $\omega = 0.5$ (solid line), $\omega = 0.75$ (dashed line), $\omega = 1.8959706$ (dot-dashed line), $\omega = 2.5$ (dotted line); (c) $\lambda_1 = 3/4$, $\lambda_2 = 3/2$, $\omega = 1$ (solid line), $\omega = 1.617$ (dashed line), $\omega = 3$ (dot-dashed line).

3. Distributed-order Langevin equations

It has been shown that the distributed-order differential equations are suitable tools for modelling ultraslow relaxation and diffusion processes [29, 55, 66–70]. In the case of distributed order differential equations, one uses the following memory kernel (see for example [70])

$$\gamma(t) = (k_B T)^{-1} \int_0^1 p(\lambda) \frac{t^{-\lambda}}{\Gamma(1-\lambda)} \mathrm{d}\lambda, \tag{61}$$

where $p(\lambda)$ is a dimensionless, non-negative weight function with $\int_0^1 p(\lambda)\mathrm{d}\lambda = c$, where c is a constant. When $c = 1$, $p(\lambda)$ is normalised. The distributed order memory kernel mixes fractional exponents from 0 to 1, and is obtained when the summation in the memory kernel in case of N fractional power-law functions turns to integration. If we substitute the distributed-order memory kernel in the GLE (6) we transform it to the following distributed-order Langevin equation

$$\ddot{x}(t) + \frac{1}{k_B T} \int_0^1 p(\lambda)\, {}^C D_t^{\lambda} x(t)\, \mathrm{d}\lambda + \frac{\mathrm{d}V(x)}{\mathrm{d}x} = \xi(t), \quad \dot{x}(t) = v(t). \tag{62}$$

Here we note that assumption (8) is satisfied for distributed-order Langevin equations since $\lim_{s\to 0} s\hat{\gamma}(s) \sim \lim_{s\to 0} \int_0^1 p(\lambda) s^{\lambda} \mathrm{d}\lambda = 0$. Thus we can use the representations of MSD, VACF, time-dependent diffusion coefficient and DACFs in terms of the relaxation functions.

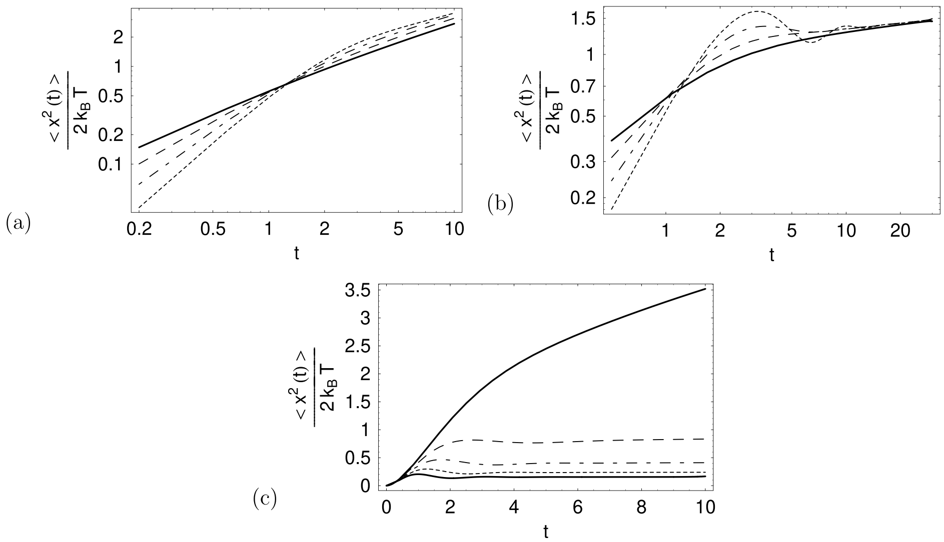

Figure 3. MSD (56) for the following cases for $N=2$: (a) $\omega=0$, $\lambda_1=1/2$, $\lambda_2=1$, (solid line), $\lambda_2=5/4$ (dashed line), $\lambda_2=3/2$ (dot-dashed line), $\lambda_2=7/4$ (dotted line); (b) $\omega=0$, $\lambda_1=0.1$, $\lambda_2=1$, (solid line), $\lambda_2=5/4$ (dashed line), $\lambda_2=3/2$ (dot-dashed line), $\lambda_2=7/4$ (dotted line); (c) $\lambda_1=1/2$, $\lambda_2=7/4$, $\omega=0$ (upper solid line), $\omega=1$ (dashed line), $\omega=1.5$ (dot-dashed line), $\omega=2$ (dotted line), $\omega=2.5$ (lower solid line).

We now consider the distributed-order Langevin equation (62) in the presence of the constant external force F. Then we have

$$\ddot{x}(t)+\frac{1}{k_{\mathrm{B}}T}\int_0^1 p(\lambda)\,{}^{C}D_t^{\lambda}x(t)\,\mathrm{d}\lambda-F=\xi(t),\quad \dot{x}(t)=v(t), \tag{63}$$

from which, by the Laplace transform method, we obtain

$$x(t)=\langle x(t)\rangle_F+\int_0^t G(t-t')\,\xi(t')\,\mathrm{d}t', \tag{64}$$

where $\langle x(t)\rangle_F=FI(t)$ and $\hat{\gamma}(s)$ is given by equation (61), and where

$$G(t)=\mathscr{L}^{-1}\left\{\frac{1}{s^2+s\hat{\gamma}(s)};t\right\}\quad \text{and}\quad I(t)=\mathscr{L}^{-1}\left\{\frac{s^{-1}}{s^2+s\hat{\gamma}(s)};t\right\}. \tag{65}$$

The latter expression corresponds to (11) for a free particle ($\omega=0$). Thus, we conclude that the generalised Einstein relation $\langle x^2(t)\rangle_F=[F/(2k_{\mathrm{B}}T)]\langle x^2(t)\rangle_{F=0}$ is satisfied for the distributed-order Langevin equation (62), where $\langle x^2(t)\rangle_{F=0}=2k_{\mathrm{B}}T\mathscr{L}^{-1}\{s^{-1}[s^2+s\hat{\gamma}(s)]^{-1};t\}$ is the MSD for the case of a free particle.

3.1. Force-free case

We first consider the distributed-order Langevin equation for a free particle with $\omega=0$. Note that a weight function of the form $p(\lambda)=\sum_{i=1}^{N}\alpha_i^2\,\delta(\lambda-\lambda_i)$ yields the fractional Langevin equation and we have the compound white Gaussian noise, see section 2.2.2. For $p(\lambda)=\alpha^2$ we obtain the uniformly distributed noise [69]

$$k_{\mathrm{B}}T\gamma(t)=\alpha^2\int_0^1\frac{t^{-\lambda}}{\Gamma(1-\lambda)}\mathrm{d}\lambda, \tag{66}$$

which was used by Kochubei in the theory of evolution equations. In [29] we analysed the GLE for a free particle with friction memory kernel of distributed order (66) and showed that the MSD in the long time limit is given by

$$\langle x^2(t)\rangle\sim_{t\to\infty}\frac{2(k_{\mathrm{B}}T)^2}{\alpha^2}\left[C+\log t+\mathrm{e}^t\mathrm{E}_1(t)\right], \tag{67}$$

where $C=0.577\,216$ is the Euler-Mascheroni (or Euler's) constant, $\mathrm{Ei}(-t)=-\int_t^\infty(\mathrm{e}^{-x}/x)\mathrm{d}x$ is the exponential integral [71], and $\mathrm{E}_1(t)=-\mathrm{Ei}(-t)$. From the asymptotic expansion $\mathrm{E}_1(t)\sim_{t\to\infty}t^{-1}\mathrm{e}^{-t}\sum_{k=0}^{n-1}(-1)^k k!t^{-k}$ [55], which has an error of order $\mathcal{O}(n!t^{-n})$, we obtained that the particle shows ultraslow diffusion, i.e. $\langle x^2(t)\rangle\sim_{t\to\infty}[2(k_{\mathrm{B}}T)^2/\alpha^2](C+\log t)$ [29]. In the short time limit, again ballistic motion is observed.

Consider now the power-law case $p(\lambda)=\alpha^2\beta\lambda^{\beta-1}$, where $\beta>0$. Then the friction memory kernel becomes

$$k_{\mathrm{B}}T\gamma(t)=\alpha^2\int_0^1\beta\lambda^{\beta-1}\frac{t^{-\lambda}}{\Gamma(1-\lambda)}\mathrm{d}\lambda. \tag{68}$$

For the MSD in the long time limit, we obtain (see (65) based on Tauberian theorems)

$$\langle x^2(t)\rangle\sim_{t\to\infty}\frac{2(k_{\mathrm{B}}T)^2}{\alpha^2}\frac{\log^\beta t}{\Gamma(1+\beta)}. \tag{69}$$

From this result, we conclude that this power-law model leads to ultraslow diffusion (for $\beta=1$) or a strong anomaly. In [72] a strong anomaly means the behaviour of form $\langle x^2(t)\rangle\sim\log^\nu t$, which for $\nu=4$ has the same form as the MSD of the Sinai diffusion model in a random force field [73, 74], compare also to the discussion in [75]. We also note that the Sinai diffusion here occurs due to the friction memory kernel, while in a quenched disorder landscape the Sinai diffusion occurs due to the thermal random motion of a particle in a random potential [76, 77]. Thus the physics of the logarithmic anomalous diffusion is different in both cases. However, as demonstrated in [73], the statistical behaviour in terms of the MSD and PDF are strikingly similar. Result (69) for the MSD is equivalent to the one obtained by Eab and Lim [68], since the long time limit considered here corresponds to the case of the overdamped limit (the inertial term $\ddot{x}(t)$ is neglected) studied in [68]. The same result for the MSD can be obtained from the distributed-order diffusion equation [67] in which the weight function corresponds to the one considered in the memory kernel (68).

Next we consider the weight function $p(\lambda)=\alpha^2/(\lambda_2-\lambda_1)$ for $0\leqslant\lambda_1<\lambda<\lambda_2\leqslant1$, and $p(\lambda)=0$ otherwise [66]. With the help of relation (65) the MSD yields in the form

$$\begin{aligned}\langle x^2(t)\rangle=2k_{\mathrm{B}}T\Bigg[\frac{t^2}{2}+\sum_{n=1}^\infty\left(-\frac{\alpha^2}{k_{\mathrm{B}}T}\right)^n\frac{1}{(\lambda_2-\lambda_1)^n}\sum_{k=0}^n\binom{n}{k}(-1)^k\\ \times\mu\left(t,n-1,(2-\lambda_2)n+(\lambda_2-\lambda_1)k+2\right)\Bigg],\end{aligned} \tag{70}$$

which in the long time limit becomes (use the Tauberian theorem in equation (65))

$$\begin{aligned}\langle x^2(t)\rangle\sim_{t\to\infty}\frac{2(k_{\mathrm{B}}T)^2}{\alpha^2}\sum_{n=1}^\infty\frac{t^{\lambda_2-(\lambda_2-\lambda_1)n}}{\Gamma(\lambda_2-(\lambda_2-\lambda_1)n+1)}\\ \times\left[\ln t^{\lambda_2-\lambda_1}-(\lambda_2-\lambda_1)\psi(\lambda_2-(\lambda_2-\lambda_1)n+1)\right],\end{aligned} \tag{71}$$

where we used the Volterra function $\mu(t,\beta,\alpha)$ defined in appendix C, and $\psi = \frac{\Gamma'}{\Gamma}$ is the digamma function. Thus, we conclude that in the long time limit the MSD has the ultraslow form

$$\langle x^2(t)\rangle \sim_{t\to\infty} \frac{2(k_{\mathrm{B}}T)^2}{\alpha^2}\frac{\lambda_2-\lambda_1}{\Gamma(1+\lambda_1)}t^{\lambda_1}\ln t.$$

For $\lambda_1 = 0$ and $\lambda_2 = 1$ we arrive at the result (66) obtained for uniformly distributed noise with a logarithmic MSD dependence on time. In the short time limit the particle performs ballistic motion, as well.

Such relaxation patterns of logarithmic form and ultraslow diffusion have been observed in the analysis of distributed-order relaxation and diffusion equations by Kochubei [69, 78–80] as well as by Mainardi *et al* [55, 70].

3.2. Harmonic oscillator: overdamped limit

We now move on to consider the distributed-order GLE for a harmonic oscillator with different weight functions in the overdamped limit. For the uniformly distributed noise (66) we obtain the following form of the MSD

$$\langle x^2(t)\rangle_{\mathrm{o}} = 2k_{\mathrm{B}}T\mathscr{L}^{-1}\left\{\frac{s^{-1}}{\frac{\alpha^2}{k_{\mathrm{B}}T}\frac{s-1}{\log s}+\omega^2};t\right\} = 2k_{\mathrm{B}}T\mathscr{L}^{-1}\left\{\frac{s^{-1}\log s}{\omega^2\log s+As-A};t\right\}, \tag{72}$$

where $A = \alpha^2/(k_{\mathrm{B}}T)$. From Tauberian theorems (see appendix B) we analyse the asymptotic behaviour in the long and short time limits. At long times ($t\to\infty$, equivalent to $s\to 0$) it follows that

$$\begin{aligned}\langle x^2(t)\rangle_{\mathrm{o}} &\sim_{t\to\infty} \frac{2k_{\mathrm{B}}T}{\omega^2}\mathscr{L}^{-1}\left\{\frac{s^{-1}}{1-\frac{A}{\omega^2\log s}};t\right\} \sim_{t\to\infty} \frac{2k_{\mathrm{B}}T}{\omega^2}\mathscr{L}^{-1}\left\{\frac{1}{s}+\frac{\frac{A}{\omega^2}}{s\log s};t\right\}\\ &= \frac{2k_{\mathrm{B}}T}{\omega^2}\left[1+\frac{A}{\omega^2}\nu(t)\right],\end{aligned} \tag{73}$$

where $\nu(t)$ is the Volterra function, see appendix C. Thus, the DACF in the long time limit becomes

$$C_{X,\mathrm{o}}(t) \sim_{t\to\infty} -\frac{A}{\omega^2}\nu(t). \tag{74}$$

At short times ($t\to 0$, or $s\to\infty$), we find for the MSD and DACF that

$$\langle x^2(t)\rangle_{\mathrm{o}} \sim_{t\to 0} \frac{2k_{\mathrm{B}}T}{A}\mathscr{L}^{-1}\left\{\frac{\log s}{s^2};t\right\} = \frac{2k_{\mathrm{B}}T}{A}t\left(\log\frac{1}{t}+1-\gamma\right), \tag{75}$$

and

$$C_{X,\mathrm{o}}(t) \sim_{t\to 0} 1-\frac{\omega^2}{A}t\left(\log\frac{1}{t}+1-\gamma\right), \tag{76}$$

respectively.

Now consider the distributed-order noise (68). From the relaxation function $I_o(t)$ the MSD becomes

$$\langle x^2(t)\rangle_{\mathrm{o}} = \frac{2k_{\mathrm{B}}T}{\omega^2}\mathscr{L}^{-1}\left\{\frac{s^{-1}}{\frac{A}{\omega^2}\nu\left(\log\frac{1}{s}\right)^{-\nu}\gamma(\nu,-\log s)+1};t\right\}, \tag{77}$$

where $\gamma(a,\sigma) = \int_0^\sigma t^{a-1} \mathrm{e}^{-t} \mathrm{d}t$ is the lower incomplete Gamma function. Taking the long time limit yields

$$\begin{aligned}\left\langle x^2(t)\right\rangle_{\mathrm{o}} &\sim_{t\to\infty} \frac{2k_{\mathrm{B}}T}{\omega^2}\left\{1-\frac{A}{\omega^2}\Gamma(1+\nu)\mathscr{L}^{-1}\left\{\frac{1}{s}\left(\log\frac{1}{s}\right)^{-\nu};t\right]\right\}\\ &\sim_{t\to\infty} \frac{2k_{\mathrm{B}}T}{\omega^2}\left[1-\frac{A}{\omega^2}\frac{\Gamma(1+\nu)}{\log^{\nu}t};t\right],\end{aligned} \tag{78}$$

from which we obtain the asymptotic behaviour of the DACF,

$$C_{X,\mathrm{o}}(t) \sim_{t\to\infty} \frac{2k_{\mathrm{B}}T}{\omega^2}\frac{A}{\omega^2}\frac{\Gamma(1+\nu)}{\log^{\nu}t}. \tag{79}$$

In the short time limit, we find

$$\left\langle x^2(t)\right\rangle_{\mathrm{o}} \sim_{t\to 0} \frac{2k_{\mathrm{B}}T}{A}\frac{\log^{\nu}\frac{1}{t}}{\Gamma(1+\nu)} \tag{80}$$

and

$$C_{X,\mathrm{o}}(t) \sim_{t\to 0} 1-\frac{\omega^2}{A}\frac{\log^{\nu}\frac{1}{t}}{\Gamma(1+\nu)}. \tag{81}$$

Similarly, we obtain for the distributed-order noise (61) with weight function $p(\lambda) = \alpha^2/(\lambda_2-\lambda_1)$ ($0 \leqslant \lambda_1 < \lambda < \lambda_2 \leqslant 1$, and $p(\lambda) = 0$ otherwise) the asymptotic forms of the MSD:

$$\left\langle x^2(t)\right\rangle_{\mathrm{o}} \sim_{t\to\infty} \frac{2k_{\mathrm{B}}T}{\omega^2}\left\{1-\frac{A/\omega^2}{(\lambda_2-\lambda_1)}\left[\nu(t,-\lambda_2)-\nu(t,-\lambda_1)\right]\right\}, \tag{82}$$

in the long time limit, and

$$\begin{aligned}\left\langle x^2(t)\right\rangle_{\mathrm{o}} &\sim_{t\to 0} \frac{2k_{\mathrm{B}}T}{A}\sum_{n=0}^{\infty}\frac{t^{(\lambda_2-\lambda_1)n+\lambda_2}}{\Gamma\left[(\lambda_2-\lambda_1)n+\lambda_2+1\right]}\\ &\quad\times\left[\log t^{-(\lambda_2-\lambda_1)}-(\lambda_2-\lambda_1)\psi\left((\lambda_2-\lambda_1)n+\lambda_2+1\right)\right]\end{aligned} \tag{83}$$

in the short time limit. From here we can easily find the DACF.

From these results, we conclude that the distributed-order GLE may be used to model various anomalous diffusive behaviours, such as ultraslow diffusion, strong anomaly, and other complex diffusive regimes.

4. Further generalisations

4.1. LE with power-logarithmic distributed order noises

Let us consider the Langevin equation (6) with the logarithmically distributed-order friction kernel

$$\gamma(t) = (k_{\mathrm{B}}T)^{-1}\int_0^1 \Gamma(3/2-\lambda)\frac{\log^{\lambda-1}t}{\sqrt{t}}\mathrm{d}\lambda \quad \text{with} \quad \hat{\gamma}(s) = \frac{\pi}{k_{\mathrm{B}}T}\frac{s-1}{\sqrt{s}\log s}, \tag{84}$$

which satisfies the condition (8). The relaxation function $I(t)$ defined by equation (11) assumes the form

$$I(t) = \mathscr{L}^{-1}\left\{\frac{s^{-1}}{s^2 + \frac{\pi}{k_\mathrm{B}T}\frac{s(s-1)}{\sqrt{s}\log s} + \omega^2}; t\right\}. \tag{85}$$

As it is challenging to calculate the exact form of equation (85) for general $t > 0$ we concentrate on the asymptotic behaviour for small $s \ll 1$, yielding

$$\hat{I}(s) \sim_{s\to 0} \frac{s^{-1}}{\omega^2}\frac{1}{1 - \frac{\pi}{k_\mathrm{B}T\omega^2}\frac{s(1-s)}{\sqrt{s}\log s}} \simeq \frac{1}{\omega^2}\left[s^{-1} + \frac{\pi}{k_BT\omega^2}\frac{1}{\sqrt{s}\log s} - \frac{\pi}{k_\mathrm{B}T\omega^2}\frac{\sqrt{s}}{\log s}\right],$$

where we take the zeroth and first-order terms of the series expansion. If s tends zero then the term $\sqrt{s}/\log s$ can be neglected. Thus, we have

$$\hat{I}(s) \sim_{s\to 0} \frac{1}{\omega^2}\left[s^{-1} + \frac{\pi}{k_\mathrm{B}T\omega^2}\frac{1}{\sqrt{s}\log s}\right] \quad \text{and} \quad I(t) \sim_{t\to\infty} \frac{1}{\omega^2}\left[1 + \frac{\pi}{k_\mathrm{B}T\omega^2}\nu(t,-1/2)\right]. \tag{86}$$

This allows us to find the MSD and DACF for $t \to \infty$,

$$\langle x^2(t)\rangle \sim_{t\to\infty} \frac{2k_\mathrm{B}T}{\omega^2} + \frac{2\pi}{\omega^4}\nu(t,-1/2) \quad \text{and} \quad C_X(t) \sim_{t\to\infty} -\frac{\pi}{k_\mathrm{B}T\omega^2}\nu(t,-1/2).$$

Note that for $\omega = 0$ we get

$$\begin{aligned}\langle x^2(t)\rangle &= 2k_\mathrm{B}T\mathscr{L}^{-1}\left\{\frac{s^{-1}}{s^2 + \frac{\pi}{k_\mathrm{B}T}\frac{s(s-1)}{\sqrt{s}\log s}}; t\right\} \sim_{t\to\infty} 2k_\mathrm{B}T\mathscr{L}^{-1}\left\{\frac{s^{-1}}{\frac{\pi}{k_\mathrm{B}T}\frac{s(s-1)}{\sqrt{s}\log s}}; t\right\} \\ &\sim_{t\to\infty} \frac{2(k_\mathrm{B}T)^2}{\pi}\mathscr{L}^{-1}\left\{\frac{\log s}{s^{3/2}(s-1)}; t\right\} \sim_{t\to\infty} \frac{2(k_\mathrm{B}T)^2}{\pi}\mathscr{L}^{-1}\left\{\frac{\log\frac{1}{s}}{s^{3/2}}; t\right\} \\ &\sim_{t\to\infty} \frac{2(k_\mathrm{B}T)^2}{\pi}\frac{1}{\Gamma(3/2)}t^{1/2}\log t = \frac{4(k_\mathrm{B}T)^2}{\pi^{3/2}}t^{1/2}\log t.\end{aligned} \tag{87}$$

We note that in the short time limit ballistic motion is observed, as well, due to the effect of the inertial term.

4.2. Langevin equation with distributed-order Mittag–Leffler noise

In the next example, we study the GLE for a harmonic oscillator with the ML friction memory kernel

$$\gamma(t) = \frac{1}{k_\mathrm{B}T}\int_0^1 E_\lambda\left(-t^\lambda\right)\mathrm{d}\lambda \quad \left(\hat{\gamma}(s) = \frac{1}{k_\mathrm{B}T}\frac{\log\frac{s+1}{2}}{s\log s}\right), \tag{88}$$

which satisfies the condition (8). The long-time asymptotic of the relaxation function $I(t)$ involved in the MSD and the DACF can be calculated by use of the Tauberian theorem (appendix B) in which we consider the limit $s \to 0$ of $\hat{I}(s)$. Thus, we have

$$I(t) = \mathscr{L}^{-1}\left\{\frac{s^{-1}}{s^2 + \frac{1}{k_\mathrm{B}T}\frac{\log\frac{s+1}{2}}{\log s} + \omega^2}; t\right\} \sim_{t\to\infty} \frac{1}{\omega^2}\mathscr{L}^{-1}\left\{\frac{1}{s} - \frac{1}{k_\mathrm{B}T\omega^2}\frac{\log 2}{s\log s}; t\right\}$$
$$= \frac{1}{\omega^2}\left[1 - \frac{\log 2}{k_\mathrm{B}T\omega^2}\nu(t)\right]. \tag{89}$$

In the force-free case with $\omega = 0$ we observe ultraslow diffusion, since the relaxation function $I(t)$ has a logarithmic time dependence,

$$I(t) \sim_{t\to\infty} \frac{k_\mathrm{B}T}{\log 2}\mathscr{L}^{-1}\left\{\frac{\log\frac{1}{s}}{s}; t\right\} = \frac{k_\mathrm{B}T}{\log 2}\log t = k_\mathrm{B}T\log_2 t. \tag{90}$$

In the short time limit the relaxation function behaves as $I(t) \sim t^2$.

4.3. Distributed-order Langevin equation with Caputo-Prabhakar derivative

In this part, we now consider the GLE (6) for a harmonic oscillator with the choice of the distributed-order Prabhakar friction memory kernel

$$\gamma(t) = \frac{1}{k_\mathrm{B}T}\int_0^1 t^{-\lambda}E^{\delta}_{\rho,1-\lambda}(-t^{\rho})\,\mathrm{d}\lambda \quad \text{with} \quad \hat{\gamma}(s) = \frac{1}{k_\mathrm{B}T}\frac{s-1}{s\log s}\left(1+s^{-\rho}\right)^{-\delta}. \tag{91}$$

We consider two cases, the first one for $0 < \rho, \delta < 1$ and the second one for $-1 < \rho, \delta < 0$. In both cases the condition (8) is satisfied. If we substitute the distributed-order Prabhakar friction memory kernel in the GLE (6) we arrive to the following generalised Langevin equation

$$\ddot{x}(t) + \frac{1}{k_\mathrm{B}T}\int_0^1 \left({}_\mathrm{C}\mathcal{D}^{\delta,\lambda}_{\rho,1,0+}x\right)(t)\,\mathrm{d}\lambda + \frac{\mathrm{d}V(x)}{\mathrm{d}x} = \xi(t), \quad \dot{x}(t) = v(t), \tag{92}$$

with regularised fractional derivative

$$\left({}_\mathrm{C}\mathcal{D}^{\delta,\lambda}_{\rho,\omega,0+}f\right)(t) = \int_0^t (t-t')^{-\lambda}E^{\delta}_{\rho,1-\lambda}\left(-\omega[t-t']^{\rho}\right)\frac{\mathrm{d}}{\mathrm{d}t'}f(t')\,\mathrm{d}t'.$$

Using the Tauberian theorem we calculate the asymptotics of the relaxation function $I(t)$. **(i)** In the case $0 < \rho, \delta < 1$ and for $t \to \infty$ we have

$$I(t) \sim_{t\to\infty} \mathscr{L}^{-1}\left\{\frac{s^{-1}}{\omega^2 + \frac{1}{k_\mathrm{B}T}\frac{s-1}{\log s}\left(1+s^{-\rho}\right)^{-\delta}}; t\right\} \sim_{t\to\infty} \mathscr{L}^{-1}\left\{\frac{s^{-1}}{\omega^2 + \frac{1}{k_\mathrm{B}T}\frac{s-1}{\log s}s^{\rho\delta}}; t\right\}$$
$$\sim_{t\to\infty} \frac{1}{\omega^2}\mathscr{L}^{-1}\left\{\frac{s^{-1}}{1 + \frac{1}{k_\mathrm{B}T\omega^2}\frac{s^{\rho\delta}}{\log\frac{1}{s}}}; t\right\} \sim_{t\to\infty} \frac{1}{\omega^2}\mathscr{L}^{-1}\left\{\frac{1}{s} - \frac{1}{k_\mathrm{B}T\omega^2}\frac{s^{-1+\rho\delta}}{\log\frac{1}{s}}; t\right\}$$
$$\sim_{t\to\infty} \frac{1}{\omega^2}\left[1 - \frac{1}{k_\mathrm{B}T\omega^2\Gamma(1-\rho\delta)}\frac{t^{-\rho\delta}}{\log t}\right]. \tag{93}$$

From the asymptotic form of $I(t)$ we obtain the long time behaviours of the MSD and DACF,

$$\langle x^2(t)\rangle \sim_{t\to\infty} \frac{2k_\mathrm{B}T}{\omega^2} - \frac{1}{\omega^4\Gamma(1-\rho\delta)}\frac{t^{-\rho\delta}}{\log t} \tag{94}$$

and

$$C_X(t) \sim_{t\to\infty} \frac{1}{k_\mathrm{B}T\omega^2\Gamma(1-\rho\delta)}\frac{t^{-\rho\delta}}{\log t}. \tag{95}$$

In addition, note that in the free particle case ($\omega = 0$) the long-time limit (or for the over-damped case when we neglect the term with s^2) becomes

$$I(t) \sim_{t\to\infty} k_{\mathrm{B}}T\mathscr{L}^{-1}\left\{\frac{s^{-1}\left(1+s^{-\rho}\right)^{\delta}\log s}{s-1};t\right\} \sim_{t\to\infty} k_{\mathrm{B}}T\mathscr{L}^{-1}\left\{\frac{\log s}{s^{1+\rho\delta}\left(s-1\right)};t\right\}$$
$$\sim_{t\to\infty} k_{\mathrm{B}}T\mathscr{L}^{-1}\left\{s^{-1-\rho\delta}\log\frac{1}{s};t\right\} \sim_{t\to\infty} k_{\mathrm{B}}T\frac{t^{\rho\delta}}{\Gamma\left(1+\rho\delta\right)}\log t. \tag{96}$$

(ii) Replacing ρ by $-\rho$ and δ by $-\delta$ in equations (91) and (92) we find

$$\gamma(t) = \frac{1}{k_{\mathrm{B}}T}\int_0^1 t^{-\lambda}E_{-\rho,1-\lambda}^{-\delta}\left(-t^{-\rho}\right)\mathrm{d}\lambda \quad \text{and} \quad \hat{\gamma}(s) = \frac{1}{k_{\mathrm{B}}T}\frac{s-1}{s\log s}\left(1+s^{\rho}\right)^{\delta}, \tag{97}$$

where $0 < \rho, \delta < 1$. The relaxation function $I(t)$ for $\omega \neq 0$ reads

$$I(t) \sim_{t\to\infty} \mathscr{L}^{-1}\left\{\frac{s^{-1}}{\frac{1}{k_{\mathrm{B}}T}\frac{s-1}{\log s}\left(1+s^{\rho}\right)^{\delta}+\omega^2};t\right\} \sim_{t\to\infty} \mathscr{L}^{-1}\left\{\frac{s^{-1}}{\frac{1}{k_{\mathrm{B}}T}\frac{s-1}{\log s}+\omega^2};t\right\}$$
$$= \frac{1}{\omega^2}\mathscr{L}^{-1}\left\{\frac{s^{-1}}{1-\frac{1}{k_{\mathrm{B}}T\omega^2}\frac{1-s}{\log s}};t\right\} \sim_{t\to\infty} \frac{1}{\omega^2}\mathscr{L}^{-1}\left\{\frac{1}{s}+\frac{1}{k_{\mathrm{B}}T\omega^2}\frac{1}{s\log s};t\right\}$$
$$= \frac{1}{\omega^2}\left[1+\frac{\nu(t)}{k_{\mathrm{B}}T\omega^2}\right]. \tag{98}$$

For $\omega = 0$ the long time asymptotic of $I(t)$ is equal to

$$I(t) = k_{\mathrm{B}}T\mathscr{L}^{-1}\left\{\frac{s^{-1}}{\frac{s-1}{\log s}\left(1+s^{\rho}\right)^{\delta}};t\right\} \sim_{t\to\infty} k_{\mathrm{B}}T\mathscr{L}^{-1}\left\{\frac{\log s}{s\left(s-1\right)};t\right\}$$
$$= k_{\mathrm{B}}T\left[C+\log t+\mathrm{e}^{t}E_1(t)\right]. \tag{99}$$

Note that the relevant MSD is the same as obtained for the force-free case by using the distributed-order fractional derivative, i.e. equation (67) for $\alpha = 1$.

4.4. Langevin equation with distributed-order Volterra function

We consider the GLE for which the friction kernel is based on the Volterra functions $\nu(t, -\alpha)$ and $\mu(t, -\beta)$ for $0 < \alpha, \beta < 1$, see appendix C. In the first case the friction memory kernel in t and s reads

$$\gamma_1(t) = \frac{1}{k_{\mathrm{B}}T}\int_0^1 \nu(t,-\alpha)\,\mathrm{d}\alpha \quad \text{and} \quad \hat{\gamma}_1(s) = \frac{1}{k_{\mathrm{B}}T}\frac{s-1}{s\log^2 s}, \tag{100}$$

thus satisfying condition (8). For the GLE for the stochastic harmonic oscillator ($\omega \neq 0$) the long time limit ($t \to \infty$) of the relaxation function $I_1(t)$ yields in the form

$$I_1(t) = \mathscr{L}^{-1}\left\{\frac{s^{-1}}{s^2+\frac{1}{k_{\mathrm{B}}T}\frac{s-1}{\log^2 s}+\omega^2};t\right\} \sim_{t\to\infty} \frac{1}{\omega^2}\mathscr{L}^{-1}\left\{\frac{1}{s}+\frac{1}{k_{\mathrm{B}}T\omega^2}\frac{1}{s\log^2 s};t\right\}$$
$$= \frac{1}{\omega^2}\left[1+\frac{\mu(t,1)}{k_{\mathrm{B}}T\omega^2}\right]. \tag{101}$$

In the force-free case ($\omega = 0$) we obtain [60, equation (45)]

$$I_1(t) = \mathscr{L}^{-1}\left\{\frac{s^{-1}}{s^2 + \frac{1}{k_B T}\frac{s-1}{\log^2 s}};t\right\} \sim_{t\to\infty} k_B T \mathscr{L}^{-1}\left\{\frac{\log^2 s}{s(s-1)};t\right\}$$
$$= k_B T\Bigg[-\left(C^2+\pi^2/6\right)\mathrm{e}^t + 2t\mathrm{e}^t \Phi^{\star,(1,1)}_{1;1}(-t,3,1) - 2(C+\log t)\mathrm{e}^t E_1(t)$$
$$-(2C+\log t)(\mathrm{e}^t+1)(\log t) - C^2 + \pi^2/6\Bigg]. \tag{102}$$

Here $\Phi^{\star,(1,1)}_{1;1}$ is the Hurwitz–Lerch function, see [81].

In the second case, the friction in t and s spaces turns out to be

$$\gamma_2(t) = \frac{1}{k_B T}\int_0^1 \mu(t,-\beta)\,\mathrm{d}\beta \quad \text{and} \quad \hat{\gamma}_2(s) = \frac{1}{k_B T}\frac{\log s - 1}{s(\log s)(\log\log s)}. \tag{103}$$

Here we consider only the force-free case, i.e. $\omega = 0$. In that case we find the asymptotic of $I_2(t)$ at long times. Using that $\log\log s$ is a slowly varying function, by Tauberian theorems we find that

$$I_2(t) \sim_{t\to\infty} k_B T \mathscr{L}^{-1}\left\{\frac{(\log s)(\log\log s)}{s(\log s - 1)};t\right\} = k_B T \mathscr{L}^{-1}\left\{\frac{\log\log s}{s\left(1-\frac{1}{\log s}\right)};t\right\}$$
$$\sim_{t\to\infty} k_B T \mathscr{L}^{-1}\left\{\frac{1}{s}\log\log\frac{1}{s^{-1}};t\right\} = k_B T \log\log\frac{1}{t}. \tag{104}$$

Finally, we consider a memory kernel of distributed order in respect to both parameters in the Volterra μ function:

$$\gamma_3(t) = \frac{1}{k_B T}\int_0^1\int_0^1 \mu(t,\beta,\alpha-1)\,\mathrm{d}\beta\mathrm{d}\alpha \tag{105}$$

and

$$\hat{\gamma}_3(s) = \frac{1}{k_B T}\int_0^1 \frac{\mathrm{d}\alpha}{s^\alpha}\int_0^1 \frac{\mathrm{d}\beta}{\log^{\beta+1} s} = \frac{1}{k_B T}\frac{(s-1)(\log s - 1)}{s\left(\log^3 s\right)(\log\log s)}. \tag{106}$$

For $\omega \neq 0$ the long time limit of the relaxation function $I_3(t)$ yields

$$I_3(t) = \mathscr{L}^{-1}\left\{\frac{s^{-1}}{s^2 + \frac{1}{k_B T}\frac{(s-1)(\log s-1)}{s\left(\log^3 s\right)(\log\log s)} + \omega^2};t\right\}$$
$$\sim_{t\to\infty} \frac{1}{\omega^2}\mathscr{L}^{-1}\left\{\frac{s^{-1}}{1 - \frac{1}{k_B T\omega^2}\frac{(1-s)(\log s-1)}{s\left(\log^3 s\right)(\log\log s)}};t\right\}$$
$$\sim_{t\to\infty} \frac{1}{\omega^2}\mathscr{L}^{-1}\left\{\frac{1}{s} + \frac{1}{k_B T\omega^2}\frac{1}{s^2\left(\log^2 s\right)(\log\log s)};t\right\}$$

$$\sim_{t\to\infty} \frac{1}{\omega^2}\mathscr{L}^{-1}\left\{\frac{1}{s}+\frac{1}{k_\mathrm{B}T\omega^2}\frac{1}{s^2\left(\log^2\frac{1}{s}\right)\left(\log\log\frac{1}{s^{-1}}\right)};t\right\}$$
$$\sim_{t\to\infty} \frac{1}{\omega^2}\left\{1+\frac{1}{k_\mathrm{B}T\omega^2}\frac{t}{\left(\log^2 t\right)\left(\log\log\frac{1}{t}\right)}\right\}. \tag{107}$$

5. Summary

We studied the GLE for an external harmonic potential and the free particle limit for various cases of the friction memory kernel. In particular, we derived the associated MSD and DACF for the different chosen forms for the friction memory kernel of Dirac delta, power-law, and distributed-order forms. Various anomalous diffusive behaviours, such as subdiffusion, superdiffusion, ultraslow diffusion, and strong anomaly, are observed. Special attention was paid to distributed-order GLEs and distributed-order diffusion-type equation. For different forms of the weight functions, we obtained ultraslow diffusion, strong anomaly, and other complex diffusive behaviours.

It will be interesting to compare the results obtained here for the GLE to the case for external noise [10], i.e. when the second FDT is not satisfied. In both cases, superstatistical and stochastic variations of the diffusion coefficient and anomalous scaling exponent (Hurst exponent) have been analysed recently [47, 82–86]. Studying such concepts in the frameworks developed here will significantly enlarge our current range of stochastic models for disordered systems. We also note potential generalisations with respect to subordinated GLE models such as those studied in [87, 88], fractional GLE [14, 31], as well as the presence of stochastic resetting [89] in the system, including resetting in the memory kernel [90, 91].

Data availability statement

All data that support the findings of this study are included within the article (and any supplementary files).

Acknowledgments

R M and T S acknowledge financial support by the German Science Foundation (DFG, Grant Number ME 1535/12-1). T S is supported by the Alliance of International Science Organizations (Project No. ANSO-CR-PP-2022-05). T S is also supported by the Alexander von Humboldt Foundation. K G and T P acknowledge the financial support provided by the NCN Grant Preludium Bis 2 No. UMO-2020/39/O/ST2/01563. Z T, K G and T S acknowledge the hospitality and support from the Lorentz Center in Leiden.

Appendix A. Multinomial Prabhakar type functions $\mathcal{E}_{(\vec{\mu}),\beta}(t;\vec{a})$

The multinomial Prabhakar function $\mathcal{E}_{(\vec{\mu}),\beta}(t;\vec{a})$ with $\mu_1>\mu_2>\cdots>\mu_m>0$, see [54], is related to the multinomial ML function $E_{(\vec{\mu}),\beta}(-a_1t^{\mu_1},\ldots,-a_mt^{\mu_m})$ as follows

$$\mathcal{E}_{(\vec{\mu}),\beta}\left(t;\vec{a}\right)=t^{\beta-1}E_{(\vec{\mu}),\beta}\left(-a_1t^{\mu_1},\ldots,-a_mt^{\mu_m}\right). \tag{A.1}$$

Its Laplace transform reads

$$\mathscr{L}\left\{\mathcal{E}_{(\vec{\mu}),\beta}\left(t;\vec{a}\right);s\right\} = \frac{s^{\mu_1-\beta}}{s^{\mu_1}+a_m s^{\mu_1-\mu_m}+\ldots+a_2 s^{\mu_1-\mu_2}+a_1}. \tag{A.2}$$

Theorem 2.3 from [54] implies that the following identities hold true:

$$\int_0^t \mathcal{E}_{(\vec{\mu}),\beta}\left(\xi;\vec{a}\right)\mathrm{d}\xi = \mathcal{E}_{(\vec{\mu}),\beta+1}\left(t;\vec{a}\right), \tag{A.3}$$

$$\frac{\mathrm{d}}{\mathrm{d}t}\mathcal{E}_{(\vec{\mu}),\beta}\left(t;\vec{a}\right) = \mathcal{E}_{(\vec{\mu}),\beta-1}\left(t;\vec{a}\right), \qquad \beta>1. \tag{A.4}$$

The asymptotic behaviours of the multinomial Prabhakar function for $t \ll 1$ and $t \gg 1$ are equal to

$$\mathcal{E}_{(\vec{\mu}),\beta}\left(t;\vec{a}\right) \sim_{t\to 0} \frac{t^{\beta-1}}{\Gamma(\beta)} - \sum_{j=1}^{m}\frac{t^{\beta-1+\mu_j}}{\Gamma(\beta+\mu_j)}, \tag{A.5}$$

$$\mathcal{E}_{(\vec{\mu}),\beta}\left(t;\vec{a}\right) \sim_{t\to\infty} a_2^{-1}t^{\beta-\mu_2-1}E_{\mu_1-\mu_2,\beta-\mu_2}\left(-a_1a_2^{-1}t^{\mu_1-\mu_2}\right), \tag{A.6}$$

respectively. Equation (A.1) implies the series representation of $\mathcal{E}_{(\vec{\mu}),\beta}(s;\vec{a})$, that is

$$\mathcal{E}_{(\vec{\mu}),\beta}\left(t;\vec{a}\right) = \sum_{k=0}^{\infty}\sum_{\substack{k_1+\ldots+k_m=k\\ k_1,\ldots,k_m\geqslant 0}}\frac{(-1)^k\,k!}{k_1!\ldots k_m!}\frac{\prod_{j=1}^m a_j^{k_j}t^{\beta-1+\sum_{j=0}^m\mu_jk_j}}{\Gamma\left(\beta+\sum_{j=1}^m\mu_jk_j\right)} \tag{A.7}$$

from which it appears that we can represent the multinomial Prabhakar function by the sums of the three-parameter ML function [92], i.e.

$$E_{\mu,\beta}^{\delta}\left(-\lambda t^{\mu}\right) = \frac{1}{\Gamma(\delta)}\sum_{r=0}^{\infty}\frac{\Gamma(\delta+r)\left(-\lambda t^{\mu}\right)^r}{r!\Gamma(\beta+\mu r)}, \tag{A.8}$$

whose the Laplace transform reads

$$\mathscr{L}\left\{t^{\beta-1}E_{\mu,\beta}^{\delta}\left(-\lambda t^{\mu}\right);s\right\} = \frac{s^{\mu\delta-\beta}}{\left(\lambda+s^{\mu}\right)^{\delta}}. \tag{A.9}$$

For $\delta=1$ the three-parameter ML function becomes a two-parameter ML function, while for $\beta=\delta=1$ it becomes one parameter ML function. The asymptotic expansion of the three-parameter ML function follows from the expression [93, 94]

$$E_{\rho,\beta}^{\delta}(-z) = \frac{z^{-\delta}}{\Gamma(\delta)}\sum_{n=0}^{\infty}\frac{\Gamma(\delta+n)}{\Gamma(\beta-\rho(\delta+n))}\frac{(-z)^{-n}}{n!}, \tag{A.10}$$

with $z>1$, and $0<\rho<2$.

For example, for $m=2$, we have

$$\mathcal{E}_{(\mu_1,\mu_2),\beta}\left(t;a_1,a_2\right) = \sum_{j=0}^{\infty}(-a_2)^j t^{\beta+\mu_2 j-1}E_{\mu_1,\beta+\mu_2 j}^{1+j}\left(-a_1t^{\mu_1}\right) \tag{A.11}$$

$$= \sum_{j=0}^{\infty}(-a_1)^j t^{\beta+\mu_1 j-1}E_{\mu_2,\beta+\mu_1 j}^{1+j}\left(-a_2t^{\mu_2}\right). \tag{A.12}$$

Moreover, equation (A.2) for $m = 2$ under condition $|a_1 s^{-\mu_1} + a_2 s^{-\mu_2}| > 1$ gives

$$\mathcal{E}_{(\mu_1,\mu_2),\beta}(t;a_1,a_2) = \sum_{r=0}^{\infty} \frac{(-1)^r}{a_1^{r+1}} t^{\beta-\mu_2(r+1)-1} E^{r+1}_{\mu_1-\mu_2,\beta-\mu_2(r+1)}\left(-\frac{a_2}{a_1} t^{\mu_1-\mu_2}\right) \tag{A.13}$$

$$= \sum_{r=0}^{\infty} \frac{(-1)^r}{a_2^{r+1}} t^{\beta-\mu_1(r+1)-1} E^{r+1}_{\mu_2-\mu_1,\beta-\mu_1(r+1)}\left(-\frac{a_1}{a_2} t^{\mu_2-\mu_1}\right). \tag{A.14}$$

From equation (A.7) for $m = 3$ after some laborious calculation can be derived, e.g. following formula which is used in our manuscript

$$\begin{aligned}\mathcal{E}_{(\mu_1,\mu_2,\mu_3),\beta}(t;a_1,a_2,a_3) = &\sum_{j=0}^{\infty} \frac{(-a_3)^j}{j!} \sum_{k=0}^{\infty} \frac{(-a_1)^k}{k!} (k+j)! \\ &\times t^{\beta-1+\mu_1 k+\mu_3 j} E^{j+k+1}_{\mu_2,\beta+\mu_1 k+\mu_3 j}\left(-a_2 t^{\mu_2}\right).\end{aligned} \tag{A.15}$$

Appendix B. Tauberian theorems [95]

If the Laplace transform pair $\hat{r}(s)$ of the function $r(t)$ behaves like

$$\hat{r}(s) \sim s^{-\rho} L\left(s^{-1}\right), \quad s \to 0, \quad \rho > 0, \tag{B.1}$$

where $L(t)$ is a slowly varying function at infinity, then $r(t)$ has the following asymptotic behaviour [95]

$$r(t) \sim \frac{1}{\Gamma(\rho)} t^{\rho-1} L(t), \quad t \to \infty. \tag{B.2}$$

A slowly varying function at infinity means that

$$\lim_{t\to\infty} \frac{L(at)}{L(t)} = 1, \quad a > 0. \tag{B.3}$$

The Tauberian theorem works also for the opposite asymptotic, i.e. for $t \to 0$.

Appendix C. The Volterra family functions

Volterra's function is defined as follows [96–98]

$$\mu(t,\beta,\alpha) = \frac{1}{\Gamma(1+\beta)} \int_0^{\infty} \frac{t^{u+\alpha} u^{\beta}}{\Gamma(u+\alpha+1)} \mathrm{d}u, \quad \Re(\beta) > -1 \quad \text{and} \quad t > 0, \tag{C.1}$$

whose particular cases are

$$\begin{aligned} \alpha = \beta = 0: &\qquad \nu(t) = \mu(t,0,0), \\ \alpha \neq 0, \beta = 0: &\qquad \nu(t,\alpha) = \mu(t,0,\alpha), \\ \alpha = 0, \beta \neq 0: &\qquad \mu(t,\beta) = \mu(t,\beta,0). \end{aligned}$$

The Laplace transform of the Volterra's function $\mu(t,\beta,\alpha)$ is given by [98]

$$\mathscr{L}\{\mu(t,\beta,\alpha);s\} = \frac{1}{s^{\alpha+1}\log^{\beta+1} s}. \tag{C.2}$$

Appendix D. Derivation of equation (84)

Since,

$$\begin{aligned}\int_0^\infty \mathrm{e}^{-st} t^a \left(\log^{\lambda-1} t\right) \mathrm{d}t &= \frac{\partial^{\lambda-1}}{\partial a^{\lambda-1}} \int_0^\infty \mathrm{e}^{-st} t^a \mathrm{d}t = \frac{\partial^{\lambda-1}}{\partial a^{\lambda-1}} \left\{\frac{\Gamma(a+1)}{s^{a+1}}\right\} = I_0^{1-\lambda}\left\{\frac{\Gamma(a+1)}{s^{a+1}}\right\} \\ &= \frac{\Gamma(a+1)}{\Gamma(1-\lambda)} \int_0^s (s-t)^{-\lambda} t^{-a-1} \mathrm{d}t = \frac{\Gamma(a+1)\Gamma(-a)}{s^{\lambda+a}\Gamma(1-\lambda-a)},\end{aligned} \tag{D.1}$$

for $a = -1/2$, we get

$$\int_0^\infty \mathrm{e}^{-st} t^{-1/2} \left(\log^{\lambda-1} t\right) \mathrm{d}t = \frac{\pi}{s^{\lambda-1/2}\Gamma(3/2-\lambda)}, \quad 0 < \lambda < 1. \tag{D.2}$$

Here $I_0^{1-\lambda}$ denotes the Riemann–Liouville (fractional) integral, defined by [50, 55]

$$\left(I_a^\mu f\right)(t) = \frac{1}{\Gamma(\mu)} \int_a^t \frac{f(\tau)}{(t-\tau)^{1-\mu}} \mathrm{d}\tau, \quad t > a, \quad \Re(\mu) > 0. \tag{D.3}$$

Then,

$$\begin{aligned}k_\mathrm{B} T \hat{\gamma}(s) &= \int_0^1 \Gamma(3/2-\lambda)\,\mathrm{d}\lambda \left[\int_0^\infty \mathrm{e}^{-st} t^{-1/2} \left(\log^{\lambda-1} t\right) \mathrm{d}t\right] \\ &= \pi\sqrt{s} \int_0^1 \frac{\mathrm{d}\lambda}{s^\lambda} = \pi \frac{s-1}{\sqrt{s}\log s}.\end{aligned} \tag{D.4}$$

ORCID iDs

Z Tomovski https://orcid.org/0000-0003-4745-9460
K Górska https://orcid.org/0000-0003-4798-9146
R Metzler https://orcid.org/0000-0002-6013-7020
T Sandev https://orcid.org/0000-0001-9120-3847

References

[1] Langevin P 1908 *C. R.* **146** 530
[2] Zwanzig R 2001 *Nonequilibrium Statistical Mechanics* (Oxford University Press)
[3] Coffey W T and Kalmykov Y P 2012 *The Langevin Equation* (World Scientific)
[4] Kupferman R 2004 *J. Stat. Phys.* **114** 291
[5] Goychuk I 2012 *Adv. Chem. Phys.* **150** 187 (available at: www.physik.uni-augsburg.de/theo1/hanggi/History/Langevin1908.pdf)
[6] Lizana L, Ambjörnsson T, Taloni A, Barkai E and Lomholt M L 2010 *Phys. Rev.* E **81** 051118
[7] Kubo R 1966 *Rep. Prog. Phys.* **29** 255
[8] Mainardi F and Pironi P 1996 *Extr. Math.* **10** 140
[9] Despósito M A and Viñales A D 2008 *Phys. Rev.* E **77** 031123
Despósito M A and Viñales A D 2009 *Phys. Rev.* E **80** 021111
[10] Klimontovich Y L 1991 *Turbulent Motion and the Structure of Chaos* (Kluwer)
[11] Viñales A D and Despósito M A 2007 *Phys. Rev.* E **75** 042102
Viñales A D, Wang K G and Despósito M A 2009 *Phys. Rev.* E **80** 011101
Viñales A D and Despósito M A 2006 *Phys. Rev.* E **73** 016111

[12] Pottier N 2003 *Physica* A **317** 371
Pottier N and Mauger A 2000 *Physica* A **282** 77
[13] Sandev T 2012 *Phys. Macedonica* **61** 59
[14] Sandev T, Metzler R and Tomovski Ž 2014 *J. Math. Phys.* **55** 023301
[15] Franosch T, Grimm M, Belushkin M, Mor F M, Foffi G, Forro L and Jeney S 2011 *Nature* **478** 7367
[16] Jeon J -H, Tejedor V, Burov S, Barkai E, Selhuber-Unkel C, Berg-Sørensen K, Oddershede L and Metzler R 2011 *Phys. Rev. Lett.* **106** 048103
[17] Jeon J -H, Leijnse N, Oddershede L B and Metzler R 2013 *New J. Phys.* **15** 045011
[18] Nørregaard K, Metzler R, Ritter C, Berg-Sørensen K and Oddershede L 2017 *Chem. Rev.* **117** 4342
[19] Selhuber-Unkel C, Weiss M, Scott S, Barooji Y F, Sabri A, Erler J T, Metzler R and Oddershede L B 2023 *Phys. Chem. Chem. Phys.* **25** 1513
[20] Kou S C and Xie X S 2004 *Phys. Rev. Lett.* **93** 180603
[21] Yang H, Luo G, Karnchanaphanurach P, Louie T-M, Reich I, Cova S, Xun L and Xie X S 2003 *Science* **302** 262
[22] Einstein A 1905 *Ann. Phys., Lpz.* **322** 549
[23] von Smoluchowski M 1906 *Ann. Phys., Lpz.* **21** 756
[24] Spiechowicz J, Marchenko I G, Hänggi P and Łczka J 2022 *Entropy* **25** 42
[25] Sutherland W 1905 *Phil. Mag.* **9** 781
[26] Wang K G 1992 *Phys. Rev.* A **45** 833
Wang K G and Tokuyama M 1999 *Physica* A **265** 341
[27] Lutz E 2001 *Phys. Rev.* E **64** 051106
[28] Burov S and Barkai E 2008 *Phys. Rev.* E **78** 031112
Burov S and Barkai E 2008 *Phys. Rev. Lett.* **100** 070601
[29] Sandev T and Tomovski Ž 2014 *Phys. Lett.* A **378** 1
[30] Sandev T, Tomovski Ž and Dubbeldam J L A 2011 *Physica* A **390** 3627
[31] Sandev T, Metzler R and Tomovski Ž 2012 *Fract. Calc. Appl. Anal.* **15** 426
[32] Metzler R and Klafter J 2000 *Phys. Rep.* **339** 1
Metzler R and Klafter J 2004 *J. Phys. A: Math. Gen.* **37** R161
[33] Barkai E, Garini Y and Metzler R 2012 *Phys. Today* **65** 29
[34] Castiglione P, Mazzino A, Muratore-Ginanneschi P and Vulpiani A 1999 *Physica* D **134** 75
[35] Höfling F and Franosch T 2013 *Rep. Progr. Phys.* **76** 046602
[36] Krapf D and Metzler R 2019 *Phys. Today* **72** 48
[37] Klafter J and Sokolov I M 2005 *Phys. World* **18** 29
[38] Vilk O *et al* 2022 *Phys. Rev. Res.* **4** 033055
[39] Burov S, Jeon J -H, Metzler R and Barkai E 2011 *Phys. Chem. Chem. Phys.* **13** 1800
[40] Metzler R, Jeon J -H, Cherstvy A G and Barkai E 2014 *Phys. Chem. Chem. Phys.* **16** 24128
[41] Muñoz-Gil G *et al* 2021 *Nat. Commun.* **12** 6253
[42] Riascos A P and Mateos J L 2014 *Phys. Rev.* E **90** 032809
Riascos A P and Mateos J L 2015 *J. Stat. Mech.* P 07015
Michelitsch T M, Collet B A, Riascos A P, Nowakowski A F and Nicolleau F C G A 2017 *J. Phys. A: Math. Theor.* **50** 055003
Michelitsch T M, Collet B A, Riascos A P, Nowakowski A F and Nicolleau F 2017 *J. Phys. A: Math. Theor.* **50** 505004
Michelitsch T, Riascos A P, Collet B, Nowakowski A and Nicolleau F 2019 *Fractional Dynamics on Networks and Lattices* (Wiley)
[43] Seckler H and Metzler R 2022 *Nat. Commun.* **13** 6717
[44] Sokolov I M 2012 *Soft Matter* **8** 9043
[45] Molina-Garcia D, Sandev T, Safdari H, Pagnini G, Chechkin A and Metzler R 2018 *New J. Phys.* **20** 103027
[46] Jeon J -H, Martinez-Seara Monne H, Javanainen M and Metzler R 2012 *Phys. Rev. Lett.* **109** 188103
[47] Ślęzak J, Metzler R and Magdziarz M 2018 *New J. Phys.* **20** 023026
[48] van der Straeten E and Beck C 2011 *Physica* A **390** 951
[49] Vojta T, Skinner S and Metzler R 2019 *Phys. Rev.* E **100** 042142
[50] Sandev T and Tomovski Ž 2019 *Fractional Equations and Models: Theory and Applications* (Springer Nature)
[51] Tabei S M A, Burov S, Kim H Y, Kuznetsov A, Huynh T, Jureller J, Philipson L H, Dinner A R and Scherer N F 2013 *Proc. Natl Acad. Sci. USA* **110** 4911
[52] Weigel A V, Simon B, Tamkun M M and Krapf D 2011 *Proc. Natl Acad. Sci. USA* **108** 6438

[53] He Y, Burov S, Metzler R and Barkai E 2008 *Phys. Rev. Lett.* **101** 058101
[54] Bazhlekova E 2021 *Fract. Calc. Appl. Anal.* **24** 88
[55] Mainardi F 2010 *Fractional Calculus and Waves in Linear Viscoelesticity: An Introduction to Mathematical Models* (Imperial College Press)
[56] Metzler R, Barkai E and Klafter J 1999 *Phys. Rev. Lett.* **82** 3563
[57] Jeon J -H and Metzler R 2012 *Phys. Rev.* E **85** 021147
[58] Gorenflo R and Mainardi F 2005 *J. Phys.: Conf. Ser.* **7** 1
[59] Capelas de Oliveira E, Mainardi F and Vaz Jr J 2011 *Eur. Phys. J.* **193** 161–71
[60] Górska K, Pietrzak T, Sandev T and Tomovski Ž 2023 *J. Comput. Appl. Math.* **433** 115306
[61] Mainardi F 2014 *Discrete Contin. Dyn. Syst.* B **19** 2267
[62] Pollard H 1948 *Bull. Am. Math. Soc.* **54** 1115
[63] Górska K, Horzela A, Bratek L, Dattoli G and Penson K A 2018 *J. Phys. A: Math. Theor.* **51** 135202
[64] Górska K, Horzela A and Penson K A 2023 *J. Phys. A: Math. Theor.* **56** 313001
[65] Tateishi A A, Lenzi E K, da Silva L R, Ribeiro H V, Picoli S and Mendes R S 2012 *Phys. Rev.* E **85** 011147
[66] Chechkin A V, Gorenflo R and Sokolov I M 2002 *Phys. Rev.* E **66** 046129
[67] Chechkin A V, Klafter J and Sokolov I M 2003 *Europhys. Lett.* **63** 326
[68] Eab C H and Lim S C 2011 *Phys. Rev.* E **83** 031136
[69] Kochubei A N 2011 *Integr. Equ. Oper. Theory* **71** 583
[70] Mainardi F, Mura A, Gorenflo R and Stojanovic M 2007 *J. Vib. Control* **13** 1249
[71] Erdelyi A, Magnus W, Oberhettinger F and Tricomi F G 1955 *Higher Transcedential Functions* vol 3 (McGraw-Hill)
[72] Dräger J and Klafter J 2000 *Phys. Rev. Lett.* **84** 5998
[73] Godec A, Chechkin A V, Barkai E, Kantz H and Metzler R 2014 *J. Phys. A: Math. Theor.* **47** 492002
[74] Sinai Y G 1982 *Theor. Probab. Appl.* **27** 256
[75] Goychuk I, Kharchenko V I and Metzler R 2017 *Phys. Rev.* E **96** 052134
[76] Bouchaud J P and Georges A 1990 *Phys. Rep.* **195** 127
Bouchaud J P, Comtet A, Georges A and Le Doussal P 1990 *Ann. Phys.* **201** 285
[77] Padash A, Aghion E, Schulz A, Barkai E, Chechkin A V, Metzler R and Kantz H 2022 *New J. Phys.* **24** 073026
[78] Kochubei A N 2008 *J. Math Anal. Appl.* **340** 252
[79] Kochubei A N 2008 *Ukranian Math. J.* **60** 551
[80] Kochubei A N 2009 *J. Phys. A: Math. Theor* **42** 315203
[81] Lin S -D and Srivastava H M 2004 *Appl. Math. Comput.* **154** 725
[82] Balcerek M, Wylomańska A, Burnecki K, Metzler R and Krapf D 2023 *New J. Phys.* **25** 103031
[83] Balcerek M, Burnecki K, Thapa S, Wylomańska A and Chechkin A 2022 *Chaos* **32** 093114
[84] Han D, Korabel N, Chen R, Johnston M, Gavrilova A, Allan V J, Fedotov S and Waigh T A 2020 *eLife* **9** e52224
[85] Ślęzak J and Metzler R 2023 *J. Phys. A: Math. Theor.* A **56** 35LT01
[86] Wang W, Balcerek M, Burnecki K, Chechkin A V, Janušonis S, Slezak J, Vojta T, Wylomańska A and Metzler R 2023 *Phys. Rev. Res.* **5** L032025
[87] Fox Z R, Barkai E and Krapf D 2021 *Nat. Commun.* **12** 6162
[88] Liang Y, Wang W and Metzler R 2023 *Phys. Rev.* E **108** 024143
[89] Evans M R and Majumdar S N 2011 *Phys. Rev. Lett.* **106** 160601
Evans M R, Majumdar S N and Schehr G 2020 *J. Phys. A: Math. Theor.* **53** 193001
[90] Petreska I, Pejov L, Sandev T, Kocarev L and Metzler R 2022 *Fractal Fract.* **6** 88
[91] Sandev T and Iomin A 2022 *Special Functions of Fractional Calculus: Applications to Diffusion and Random Search Processes* (World Scientific)
[92] Prabhakar T R 1971 *Yokohama Math. J.* **19** 7
[93] Garra R and Garrappa R 2018 *Commun. Nonlinear Sci. Numer. Sim.* **56** 314
[94] Giusti A, Colombaro I, Garra R, Garrappa R, Polito F, Popolizio M and Mainardi F 2020 *Frac. Calc. Appl. Anal.* **23** 9
[95] Feller W 1968 *An Introduction to Probability Theory and Its Applications* vol II (Wiley)
[96] Apelblat A 2010 *Integral Transforms and Volterra Function* (Nova Sci. Pub., Inc.)
[97] Apelblat A 2013 *Volterra Functions* (Nova Sci. Pub., Inc.)
[98] Bateman H and Erdélyi A 1955 *Higher Transcendental Functions* vol 3 (Robert E. Krieger Pub. Comp)